# REDUCED RANK ADAPTIVE FILTERING APPLIED TO INTERFERENCE MITIGATION IN WIDEBAND CDMA SYSTEMS

By

Seema Sud

SUBMITTED TO THE DEPARTMENT OF
ELECTRICAL AND COMPUTER ENGINEERING
IN PARTIAL FULFILLMENT OF THE
REQUIREMENTS FOR THE DEGREE OF
DOCTOR OF PHILOSOPHY
AT
VIRGINIA POLYTECHNIC INSTITUTE AND STATE UNIVERSITY
FALLS CHURCH, VA USA
MARCH 14, 2002

Supervisor:

Dr. Timothy Pratt

Readers:

Dr. A. Annamalai

Dr. Luiz Da Silva

Dr. Scott Goldstein

Dr. Terry Herdman

Dr. Michael Zoltowski



Keywords: CDMA, reduced rank, multistage Wiener filter, interference mitigation, multiuser detection

# Abstract

REDUCED RANK ADAPTIVE FILTERING APPLIED TO INTERFERENCE MITIGATION IN WIDEBAND CDMA SYSTEMS

By

Seema Sud

The research presented in this dissertation is on the development and application of advanced reduced rank adaptive signal processing techniques for high data rate wireless code division multiple access (CDMA) communications systems. This is an important area of research in the field of wireless communications. Current systems are moving towards the use of multiple simultaneous users in a given channel to increase system capacity as well as spatial and/or temporal diversity for improved performance in the presence of multipath and fading channels. Furthermore, to accommodate the demand for higher data rates, fast signal processing algorithms are required, which often translate into blind signal detection and estimation and the desire for optimal, low complexity detection techniques. The research presented here shows how minimum mean square error (MMSE) receivers implemented via the multistage Wiener filter (MWF) can be employed at the receiving end of a CDMA system to perform multiuser detection (MUD) or interference suppression (IS) with no loss in performance and significant signal subspace compression better than any previous reduced rank techniques have shown. This is important for optimizing performance because it implies a reduction in the number of required samples, so it lessens the requirement that the channel be stationary for a time duration long enough to obtain

enough samples for an accurate MMSE estimate. The structure of these receivers is derived for synchronous and asynchronous systems for a multipath environment, and then it is shown that implementation of the receiver in a reduced rank subspace results in no loss in performance over full rank methods. It is also shown in some instances that reduced rank exceeds full rank performance. Multiuser detectors are also studied, and the optimal reduced rank detector is shown to be equivalent to a bank of parallel single user detectors performing interference suppression (IS). The performance as a function of rank for parallel and joint multiuser detectors are compared. The research is then extended to include joint space-code (i.e. a joint multiuser detector) and joint space-time processing algorithms which employ receiver diversity for low complexity diversity gain. Non-linear techniques, namely serial interference cancellation (SIC) and parallel interference cancellation (PIC), will also be studied. The conventional matched filter correlator will be replaced by the MWF, thereby incorporating IS at each stage of the interference canceller for improved performance. A closed form expression is derived for the probability of error, and performance gains are evaluated. It will be further shown how the receiver structure can be extended when space-time codes are employed at the transmitter for additional diversity gain with minimal impact on complexity. The MMSE solution is derived and implemented via the MWF with some examples. It is believed that these new techniques will have a significant impact on the design of fourth generation (4G) and beyond cellular CDMA systems.

*This dissertation is dedicated to the memory of my grandparents, Mr. Kedar Nath Mago and Mrs. Lajja Vati Mago.*

# Table of Contents

# List of Tables

# List of Figures

# List of Acronyms and Abbreviations

| | |
|---|---|
| AM | Analytical Model |
| AMPS | Advanced Mobile Phone System |
| AWGN | Additive White Gaussian Noise |
| BER | Bit Error Rate |
| BPSK | Binary Phase Shift Keying |
| CDMA | Code Division Multiple Access |
| cdma2000 | The U.S. Third Generation (3G) CDMA system |
| cdmaOne | The CDMA Development Body for EIA IS-95 and successors |
| CPM | Continuous Phase Modulation |
| CS | Cross-Spectral |
| CSA | Correlation Subtraction Architecture |
| CSFB | Cyclically Shifted Filter Bank |
| CTP | Code-Time Processing |
| D/A | Digital-to-Analog |
| dB | Decibel |
| DF | Decision Feedback |
| DS | Direct Sequence |
| $E_b/N_0$ | Bit Energy-to-Noise Power Spectral Density |
| EIA | Electronics Industries Association |
| FEC | Forward Error Control |

| | |
|---|---|
| FDMA | Frequency Division Multiple Access |
| FL | Forward Link |
| GSC | Generalized Sidelobe Canceller |
| GSM | Global System for Mobile Communications |
| IMT | International Mobile Telecommunications |
| IS | Interference Suppression |
| IS-95 | EIA Interim Standard for U.S. CDMA |
| ISI | Intersymbol Interference |
| ITU | International Telecommunications Union |
| LS | Least Squares |
| MAI | Multiple Access Interference |
| MC | Monte Carlo |
| Mcps | Megachips per second |
| MF | Matched Filter |
| MIL | Matrix Inversion Lemma |
| ML | Maximum Likelihood |
| MLRT | Maximum Likelihood Ratio Test |
| MLSE | Maximum Likelihood Sequence Estimation |
| MWF | Multistage Wiener Filter |
| MMSE | Minimum Mean Square Error |
| MSE | Mean Square Error |
| MUD | Multiuser Detection |
| PC | Principal Components |
| PCS | Personal Communications Services |
| PDF | Probability Density Function |
| $P_e$ | Probability of Error |
| PIC | Parallel Interference Cancellation |
| PN | Pseudo-random |
| PSD | Power Spectral Density |

| | |
|---|---|
| QAM | Quadrature Amplitude Modulation |
| QPSK | Quadrature Phase Shift Keying |
| RCC | Recursive Convolutional Encoder |
| RL | Reverse Link |
| RMB | Reed-Mallett-Brennan |
| Rx. | Receiver |
| SIC | Serial Interference Cancellation |
| SINR | Signal-to-Interference Plus Noise Ratio |
| SNR | Signal-to-Noise Ratio |
| SS | Spread Spectrum |
| STC | Space-Time Coding |
| STCP | Space-Time-Code Processing |
| STP | Space-Time Processing |
| SU | Single User |
| SVD | Singular Value Decomposition |
| TDL | Tapped-Delay Line |
| TDMA | Time Division Multiple Access |
| TIA | Telecommunications Industry Association |
| Tx. | Transmitter |
| UMTS | Universal Mobile Telephone System |
| UTRA | UMTS Terrestrial Radio Access |
| WCDMA | Wideband Code Division Multiple Access |
| WH | Wiener-Hopf |
| WSS | Wide-Sense Stationary |

# Acknowledgments

I express deep gratitude to my primary advisors, with whom I was most fortunate to work. First, I thank Dr. Timothy Pratt, for providing much invaluable guidance and advice. I am also deeply grateful for the time and effort he put forth to help me develop and improve my research and writing abilities. Second, I thank my co-advisor Dr. J. Scott Goldstein for allowing me to pursue my research interests and patience in helping me learn. Dr. Goldstein is also co-inventor of the multistage Wiener filter on which much of this research is based. I thank Dr. Michael Zoltowski at Purdue University for providing numerous thoughtful ideas and suggestions. I also thank the other members of my dissertation committee, Dr. A. Annamalai, Dr. Luiz Da Silva, and Dr. Terry Herdman, for insightful comments that greatly improved the quality of this dissertation.

I thank Dr. Wil Myrick, for many technical discussions that contributed to this dissertation. I acknowledge the technical guidance of Dr. Michael Honig at Northwestern University. I thank Dr. Vijay Garg at the University of Illinois, Chicago, for patiently answering my numerous questions about CDMA systems. I also thank Dr. Jeremy Allnutt and Dr. B.-P. Paris of George Mason University for providing much advice and technical support.

I am grateful to my mother Dr. Indu Sud and to my father Dr. Yogesh Sud, who have always guided me in my educational pursuits. I thank my sister and brother-in-law, Anu and Gregg Baron, for their support. I thank my grandparents, Ram and Shanti Sud.

I thank Shellie Camp, the graduate student advisor at Virginia Tech, for help with administrative matters on many occasions. I thank Jim Murphy and Carl Zitzmann for their assistance with the VTEL equipment at the Northern Virginia Center. I also thank the staff of the interlibrary loan service at Virginia Tech for assistance in obtaining many reference materials.

# Chapter 1

# Introduction

The second generation of wireless cellular communications systems, e.g. IS-95 in the United States, uses code division multiple access (CDMA) to allow multiple users to share the same bandwidth. CDMA enables an increase in system capacity over other multiple access techniques such as time division multiple access (TDMA) or frequency division multiple access (FDMA) ([63] and [96]), by as much as a factor of four or more. CDMA also offers other advantages, making it the preferred multiple access (MA) technique for future cellular systems. For instance, the impact of frequency selective multipath fading can be greatly reduced, since the CDMA spread spectrum (SS) signal is spread over a large bandwidth, assuming the bandwidth is larger than the coherence length of the channel [68]. CDMA systems have a soft capacity limit, unlike TDMA and FDMA. This means that the number of users may be increased without limit, and the resulting performance will begin to degrade linearly as the noise floor increases [68].

Designers of such emerging wireless communications systems must contend with a significant amount of interference. This interference arises from the very nature of the system, which must often accommodate multiple users transmitting simultaneously

through a common physical channel. The interference could also arise from multiple users sharing a common bandwidth for different services. Interference in such systems arises because of the non-orthogonal multiplexing of signals that results from the multipath induced by the channel, producing intersymbol interference (ISI). This type of interference occurs in cellular environments due to the reflections of signals off local surroundings, such as buildings, cars, terrain, trees, etc. Systems such as IS-95 employ traditional methods for combating the problem of multipath interference, namely the rake receiver developed by Price and Green [64]. While successful in mitigating multipath, this technique fails in the context of a highly loaded CDMA system. This occurs because the rake receiver treats the interfering users as noise and does not attempt to mitigate the induced interference. For the third generation, wireless systems, i.e. CDMA2000 (United States) and WCDMA (Europe and Asia) because of the high demand for access, and the need for high reliability and high throughput, more robust interference mitigation techniques are required.

The study of interference suppression techniques has been an active area of research for the past few years and will continue to grow in preparation for third generation wireless communications systems and beyond. Several such techniques exist, some requiring decision directed training to adapt, others requiring fewer sample support than the optimal full rank minimum mean square error (MMSE) method. The most recent research in interference suppression has focused on data aided or blind MMSE receivers, which are suboptimal in multipath channels. The results presented in this dissertation differ from those in [71], which considers an MMSE/rake solution that incorporates multipath but operates in a full rank environment. In [85], a

spatial domain rake receiver, operating in a full-rank space, is used to combat frequency selective fading while simultaneously realizing path diversity gain. In [32], a reduced rank asynchronous CDMA system is considered but without the presence of multipath. In [49], a cyclically shifted filter bank (CSFB) of lower complexity than a full rank MMSE filter is presented. It is shown that the CSFB performs better than the conventional matched filter (MF), although it is suboptimal compared to the MMSE detector. Finally, [35] discusses the reduced rank multistage Wiener filter for suppressing interference induced in asynchronous, direct sequence (DS) CDMA systems but does not include any additional processing to combat multipath.

Furthermore, since many systems operate under time-varying conditions, due to time-varying channel characteristics and user mobility, these techniques must be adaptive [34]. Current work in the field of adaptive interference suppression for CDMA systems is concerned with optimizing performance in time-varying, fast fading, multipath channels. A blind multiuser detector which converges to the MMSE detector with no more knowledge than the traditional single user detector is presented in [33]. A chip-level MMSE solution is shown to perform better than MMSE and the rake receiver for combating multipath on the forward link in [7], [42],and [105]. A two-dimensional angle of arrival estimator that could be extended to a two-dimensional rake receiver for joint time/space processing of the received signal is examined in [28]. Another joint adaptive MMSE/rake receiver is described in [71]. Joint space-time code diversity is also being investigated, e.g. [55], [88], and [89]. A low complexity MMSE/rake receiver, which performs optimally in the presence of multipath, and low complexity joint space-time coding techniques will be presented in this dissertation. The results are shown to apply for both the forward, base station (BS) to mobile, and reverse,

mobile to base station, links of a CDMA system, and can thus be utilized for single user (SU) detection or multiuser detection (MUD). These techniques all prove promising, but the research in this field is ongoing.

All of the techniques described above apply linear methods for interference suppression. Clearly, if the received signal is distorted by non-linearities, this is a suboptimal solution. However, extension to adaptive non-linear algorithms is still in the early stages of investigation. Two nonlinear receivers are serial interference cancellation (SIC) and parallel interference cancellation (PIC). However, decoding schemes relying on MMSE are far too complex for such systems. In this dissertation, a SIC and PIC employing a low complexity MMSE detector in place of the conventional matched filter detector are analyzed.

A novel diversity scheme known as space-time coding has been developed in recent years. This scheme improves performance in the presence of interference and fading by employing multiple antennas at the transmitter using a coding scheme which transmits the coded symbols on spatially separated antennas (see e.g. [1], [55], [86], [88], [89]). In this dissertation, the study of reduced rank techniques in the context of space-time coded systems is also performed.

## 1.1 Overview of Current and Next Generation CDMA Systems

Signal processing algorithms for CDMA systems are presented in this dissertation. In this section, an overview of these systems is presented and for brevity, attention is restricted to the second generation (2G) and third generation (3G) systems in the United States and Europe, to be deployed in the timeframe 2002-2004, although the

algorithms described herein are applicable and extendable to other systems.

Table 1.1 shows a comparison between the major forward and reverse traffic channel parameters for the current (2G) CDMA system, known as IS-95 in the United States. Note that in the forward link, where data is transmitted synchronously, Hadamard codes, to be described later, are used to distinguish users. This is possible because these codes have the desirable property that each code is orthogonal to every other code in the set. In the reverse link, however, where users are asynchronous, pseudo-random (PN) codes are used to distinguish users. PN codes are used because Hadamard codes have poor auto-correlation and cross-correlation properties. PN codes have good auto-correlation properties, but poor cross-correlation properties. Thus, while they will perform better in asynchronous transmission, capacity of the system will still be limited by the multiuser interference. For next generation systems, codes with good orthogonality, auto-correlation, and cross-correlation properties are desirable. In this dissertation, a set of codes called Gold codes will be shown to have all these properties and will be shown to perform well in the multiuser CDMA environment in conjunction with the new interference mitigation techniques to be presented.

In CDMA systems, traffic channels are used to send speech data via multiple channels separated in frequency. A good speech link must have bit error rates (BERs) prior to digital-to-analog (D/A) conversion of about $10^{-3}$. Throughout this dissertation, performance results will be analyzed to determine the conditions under which this error rate is achieved. As shown in Table 1.1, coding, interleaving, and symbol repetition are common techniques employed to improve BER. When necessary, these techniques will be discussed. Spreading code lengths in the same range as those

| | Forward Link | Reverse Link |
|---|---|---|
| Coding | Convolutional, Rate 1/2 | Convolutional, Rate 1/3 |
| Long Pseudo-random (PN) Codes | Spreading gain | Distinguish users |
| Hadamard Codes | Distinguish users | Provide modulation |
| Modulation Scheme | Quadrature Phase Shift Keying (QPSK) | Offset Quadrature Phase Shift Keying (O-QPSK) |
| Typical PN chips/symbol | 64 | 42.67 |

Table 1.1: Second Generation (2G) CDMA System (IS-95) Forward and Reverse Link Traffic Channel Comparison

shown for the current system are used in simulations.

Table 1.2 shows the evolution of the 2G systems to the 3G systems that have been proposed to satisfy the International Mobile Telecommunications (IMT) year 2000 requirements as presented by the International Telecommunications Union (ITU) [17]. The reason for the evolution of 3G systems is to meet the demand on mobile wireless communications systems to increase user accessibility and data access. Another vision is to enable the adaptability of handsets that can support global roaming and multiple air interface environments. Note the requirement for advanced signal processing techniques for 3G systems (shown in the shaded region) due to the requirements for higher capacity and for the support of multiple services in the same frequency band. Addressing this requirement will be the focus of the dissertation. Applications of 3G

systems include high speed and high quality voice services (e.g. CD quality), interactive imaging and video, video conferencing, data transmission, internet browsing capability, and geo-location.

| First Generation | Second Generation | Third Generation |
|---|---|---|
| Mobile Telephone Service | Advanced Wireless Telephone Services | Integrated Voice/Data |
| | Wireless Data Services | Multimedia Services |
| Analog Cellular Systems | Digital Cellular Systems | Emergency Location |
| | Picocellular Technology | Higher Data Rates with High Spectrum Efficiency |
| Macrocellular Systems | Wireless Intelligent Network | Advanced Networks |
| | | Advanced Coding & Signal Processing Techniques |
| | | Advanced Antennas |
| *1980s* | *1990s* | *Year 2000+* |
| *Analog AMPS* | *GSM*<br>*IS-95(cdmaOne)* | *W-CDMA*<br>*cdma2000* |

***AMPS: Advanced Mobile Phone System***
***GSM: Global System for Mobile Communications***
***IS-95 (cdmaOne): Interim standard for U.S. CDMA systems***
***W-CDMA: Wideband CDMA; third generation CDMA standard in Europe***
***cdma2000: Third generation CDMA system in the U.S.***

Table 1.2: Global Wireless and Network Services Evolution

A summary of the general differences between the 2G and 3G system services and parameters is shown in Table 1.3 [17]. The main requirement difference between these systems that fuels the research presented here is the requirement for higher data rates, which in turn places more stringent requirements on efficient signal processing algorithms with reliable performance in real-time applications.

| | 2G System | 3G System |
|---|---|---|
| Designed for | Voice services | High quality voice and internet/intranet services |
| Bit Rate | 16 kbps | 144 kbps (outdoor) and 2 Mbps (indoor) |
| Digital Technology | For modulation, speech, channel coding, control channels and data channels | Software radio, high order modulation, and improved channel coding |
| Environments | Optimized for specific (indoor, outdoor) environment | Multiple environments |
| Frequency Bands | 800 & 900 MHz; 1.5, 1.8, & 1.9 GHz | Use of common global frequency band (2 GHz) |
| Data Services | Up to 64 kbps | Up to 144 kbps outdoor and 2 Mbps indoor<br><br>Multimedia services |
| Roaming | Generally limited to specific regions | Global roaming due to global frequency coordination, availability of global satellite coverage |

Table 1.3: Second Generation (2G) vs. Third Generation (3G) Services

A summary of the main differences between the North American 2G and 3G systems is shown in Table 1.4 ([16], [17], and [90]). Note that the chip rate is now up to 12 times faster, but the rate of power control is the same. Thus, for an increase in capacity, the interference suppression will need to be more reliable. A summary of the main features of the wideband CDMA UMTS (Universal Mobile Telephone System) Terrestrial Radio Access (UTRA) system in Europe versus those of CDMA2000 in the United States is shown in Table 1.5. The asynchronism in the European system brings forth the requirement for better interference suppression (IS) mechanisms since this results in non-orthogonal multiplexing. In CDMA2000, IS should be used with fast power control for suppression of intracell/intercell interference.

| | cdmaOne (2G) | cdma2000 (3G) |
|---|---|---|
| Chip Rate (Mcps) | 1.2288 | F x 1.2288<br>F =1, 3, 6, 9, 12 |
| Frame Length (ms) | 20 | 5, 20 |
| Carrier Spacing (MHz) | 1.25 | 1.25, 5, 10, 15, 20 |
| Inter BS Synchronization | Synchronous | Synchronous |
| Coherent Detection | RL: no pilot channel<br>FL: common pilot channel | RL: pilot symbols multiplexed with power control bits<br>FL: common pilotchannel and auxiliary pilot channel |
| Power Control | Fast on RL (800 Hz), slow on FL | Fast (800 Hz) |

***cdmaOne: Second generation (2G) CDMA system in the U.S.***
***cdma2000: Third generation (3G) CDMA system in the U.S.***

***F = Spreading code factor***
***BS = Base station***
***RL = Reverse link***
***FL = Forward link***

Table 1.4: North American Second Generation (2G) vs. Third Generation (3G) Systems

## 1.2 Conventional Detection of CDMA Signals

One popular modern detection technique is the rake receiver ([44] and [64]). The idea behind the rake is that multipath components that are separated by delays greater than $1/W$, where $W$ is the correlation bandwidth of the incoming signal, can be resolved and are delayed and summed appropriately at its output. The gain obtained at the output is known as the rake diversity gain. The rake receiver performs well provided the number of interfering users is small. Thus, this type of detection scheme alone will result in an interference limited system and is not suitable for future

| | W-CDMA (Europe/Japan) | cdma2000 (U.S.) |
|---|---|---|
| Chip Rate (Mcps) | 1.024*/3.84/8.192/16.384 | F x 1.2288<br>F = 1, 3, 6, 9, 12 |
| Carrier Spacing (MHz) | 1.25*, 5, 10, 20 | 1.25, 5, 10, 15, 20 |
| Frame Length (ms) | 10 | 5, 20 |
| Inter BS Synchronization | Asynchronous;<br>Could be synchronous | Synchronous |
| Power Control | Fast (1500 Hz) | Fast (800 Hz) |
| Coherent Detection | User dedicated pilot (FL and RL), and common pilot in FL | RL: pilot symbols multiplexed with power control bits<br>FL: common pilot channel and auxiliary pilot channel |

*** Japan only**

***W-CDMA: Wideband CDMA; third generation CDMA standard in Europe***
***cdma2000: Third generation CDMA system in the U.S.***

***F = Length of spreading code***
***BS = Base station***
***RL = Reverse link***
***FL = Forward link***

Table 1.5: North American vs. European Third Generation (3G) Systems

generation systems.

Conventional detection techniques for CDMA signals also include interference rejection methods. For example, on the forward link in IS-95, long pseudo-random (PN) codes with different phase offsets are used by different base stations to help the mobile handset reject interference from other base stations [44]. Furthermore, on the reverse link, different mobile users are distinguished by different phases of a 42 stage long PN code. This is considered a long code because at the chip rate of 1.2288 Mcps, one period of the sequence lasts nearly six weeks. As mentioned before, these rejection techniques will have limitations because the cross-correlation peaks of PN

codes can be high.

## 1.3 Dissertation Overview

Throughout this dissertation, attention is restricted to binary data so that the bits are taken from the binary alphabet $(-1, +1)$. Thus, a system employing binary phase shift keying (BPSK) is assumed. Extending the work to quadrature phase shift keying (QPSK) and other modulation schemes is left for future research. Modulation is ignored for simplicity and baseband equivalent representations are used. In Chapter 2, the model of the CDMA system to be used throughout the dissertation is described. The optimal receiver is derived for the case of the the additive white Gaussian noise (AWGN) channel. It is shown that the optimal receiver is the minimum mean square error (MMSE) receiver, which is implemented by the classical Wiener filter. The analytical model (AM) and Monte Carlo (MC) method to be used in validating the theory are then briefly described. In Chapter 3, the eigenvector-based reduced rank signal processing algorithms, namely principal components (PC) and the cross-spectral (CS) method, are described. The reduced rank multistage Wiener filter (MWF) that has been shown in many different applications to meet or exceed the performance of the classical Wiener filter at a significantly lower rank is introduced. Structures for further improving the efficiency of MWF implementation are also provided; specifically, the correlation subtraction architecture (CSA) of the MWF is presented.

In Chapter 4, two reduced rank MMSE receivers implemented by the MWF are derived to combat interference and the multipath channel. The first is the MMSE/rake

receiver which optimally combines the multipath. The second is a suboptimal structure that employs an MMSE receiver at each rake finger to suppress interference followed by multipath combining. It will be shown that this solution is slightly suboptimal to the full rank solution, but can be implemented as a "plug-and-play" fix to the rake receiver in existing systems. Monte Carlo and analytical simulation results will be provided and compared to show the validity of the algorithms and the MC model for future simulations.

In Chapter 5, the multiuser detector is derived. It is shown that this detector can be implemented in matrix form or via a bank of parallel detectors without loss in performance. The tremendous complexity reduction using the CSA-MWF is demonstrated for the parallel implementation. The matrix implementation, equivalent to a joint code-time detection scheme, is analyzed in Chapter 6. Performance using a joint space-time detection scheme, which employs multiple receiver antennas is also explored. A new spreading code required by this structure will be derived. Chapter 7 extends use of the MWF to non-linear interference cancellation. Probability of error ($P_e$) is derived for the SIC and PIC. A simple two user example is used to compare the $P_e$ to the MC model, and then MC results are shown and analyzed. Chapter 8 extends the joint detection schemes to space-time codes in which symbols are coded and then transmitted over multiple antennas and multiple time slots. In this chapter, systems with multiple transmit and receive antennas are considered.

# Chapter 2

# Code Division Multiple Access (CDMA) System Model

In this chapter, the model of the code division multiple access (CDMA) system that will be used throughout the dissertation is described. An overall block diagram of the system architecture is presented first. The transmitter, channel, and optimum receiver are then described in detail. In the last section, a description of the simulation models that will be used is provided.

## 2.1 System and Signal Structure

A CDMA system with $K$ users is assumed. The diagram in Figure 2.1 illustrates the overall physical layer model of the communication system. This model is similar to the architecture for next generation CDMA systems proposed in [103]. The binary data, $b_k$ for $k = 1, 2, ..., K$ can be encoded using a space-time code and spread via a spreading code (or chip sequence) $\mathbf{s}_k$. The encoded data is then transmitted using $L_t$ transmitter (Tx.) antenna elements. This part of the system will not be discussed until Chapter 8. The signals propagate through the atmospheric channel and are captured by multiple receiver (Rx.) antennas. Multiuser detection (MUD),

or interference suppression (IS), is performed on the received data via the multistage Wiener filter (MWF) followed by spatial or temporal diversity processing, and then hard decisions are made to obtain the bit estimates, $\tilde{b_k}$. The topics of MUD and IS using the MWF and space-time processing/coding are discussed separately in this dissertation. In [103], the proposed system also includes a Turbo encoder at the front end of the transmitter and a Turbo decoder at the back end of the receiver for robustness in the presence of deep fading multipath channels. See [2] and [3] for a discussion of Turbo codes.

The notation used to describe the signal structure is similar to that used by Honig, et al., in [32] and [34]. User $k$ transmits a baseband signal given by

$$x_k(t) = \sum_i A_k b_k(i) s_k(t - iT - \tau_k), \tag{2.1}$$

where $b_k(i)$ is the symbol transmitted by user $k$ at time $i$, $s_k(t)$ is the spreading code associated with user $k$, and $A_k$ and $\tau_k$ are the amplitude and delay, respectively. Binary signaling is assumed, so that the symbols $b_k(i) \in$ (-1,+1). The spreading sequence can be written as

$$s_k(t) = \sum_{i=1}^{N-1} a_k[i] \Psi(t - iT_c), \tag{2.2}$$

where $a_k[i] \in (\frac{+1}{\sqrt{N}}, \frac{-1}{\sqrt{N}})$ is a normalization factor for the spreading code required to maintain unity energy in the spread bit. The processing gain of the CDMA system, or equivalently the bandwidth spreading factor, is given by $N = \frac{T}{T_c}$. Here, $T_c$ is the chip period, and $T$ is the symbol period. The spreading code is assumed to be a square wave sequence with no pulse shaping, i.e. direct sequence (DS) CDMA, so that the chip sequence $\Psi(t)$ is a constant. Short codes which span the duration

of a bit interval are assumed, so that joint multiuser detection (MUD) can be performed [46]. Future systems based on short codes have been proposed for personal communications services (PCS) because of their suitability for MUD ([48] and [57]).

Define the sampled transmitted signal $\mathbf{y}(i)$ as the N-vector composed of asynchronous combinations of the data for each user multiplied with its respective spreading sequence. Assume also, without loss of generality, that user one is the desired user, and that the receiver has timing information to synchronize to its spreading code. The transmitted signal may then be written in the form

$$\mathbf{y}(i) = b_1(i)\mathbf{s}_1 + \sum_{k=2}^{K} A_k[b_k(i)\mathbf{s}_k^+ + b_k(i-1)\mathbf{s}_k^-]. \tag{2.3}$$

Here, $\mathbf{s}_1$ is the spreading sequence of user one, and $\mathbf{s}_k^+$ and $\mathbf{s}_k^-$ are the $N \times 1$ vectors of spreading codes associated with each of the $K-1$ interfering users. Due to the asynchronous transmission, as is inherent to the reverse link of a cellular system, at time $i$ both the current bit of user $k$, denoted $b_k(i)$, and the previous bit of user $k$, denoted $b_k(i-1)$, multiplied with the respective portions of the spreading code, interfere with the current bit of user one. This is depicted pictorially in Figure 2.2.

## 2.2 Channel Models

### 2.2.1 Additive White Gaussian Noise (AWGN) Channel

In an additive white Gaussian noise (AWGN) channel, discrete noise samples denoted by $n_k$, are added to the transmitted signal, producing a received signal that is the sum of the two. AWGN has the desirable property that noise samples are uncorrelated from one time instance to the next; that is, the auto-correlation function of the noise process is given by $\Re\tau = \frac{N_O}{2}\delta(\tau)$. Furthermore, the double-sided power spectral

density (PSD), given by $S_n(f) = \frac{N_O}{2}$ in units of Watts/Hz, is a constant at all frequencies. Performance curves for most modulation schemes in the presence of AWGN are readily available in the literature (e.g. [15], [75], and [101]). Attention is restricted to zero mean AWGN processes.

When the channel is an AWGN channel, the sampled received signal is an $N$ vector containing samples at the output of a chip-matched filter at each symbol $i$, represented by

$$\mathbf{r}(i) = \mathbf{y}(i) + \mathbf{n}(i). \tag{2.4}$$

Substituting Eq. (2.3) for $\mathbf{y}(i)$, one can write

$$\mathbf{r}(i) = b_1(i)\mathbf{s_1} + \sum_{k=2}^{K} A_k[b_k(i)\mathbf{s_k^+} + b_k(i-1)\mathbf{s_k^-}] + \mathbf{n}(i). \tag{2.5}$$

To simplify the notation and to make the mathematical analysis easier, one can rewrite Eq. (2.3) in matrix form as

$$\mathbf{y}(i) = \mathbf{S}^+\mathbf{A}\mathbf{b}(i) + \mathbf{S}^-\mathbf{A}\mathbf{b}(i-1), \tag{2.6}$$

where $\mathbf{S}^+ = (\mathbf{s}_1^+ \ \mathbf{s}_2^+ \ ... \ \mathbf{s}_K^+)$, $\mathbf{S}^- = (\mathbf{s}_1^- \ \mathbf{s}_2^- \ ... \ \mathbf{s}_K^-)$, $\mathbf{A} = diag(A_1, A_2, ..., A_K)$, and $\mathbf{b}(i) = (b_1(i), b_2(i), ..., b_K(i))^T$. Here, $\mathbf{S}^+$ and $\mathbf{S}^-$ are $N \times K$ matrices, $\mathbf{A}$ is a $K \times K$ matrix in which the signal amplitudes are the diagonal components, and $\mathbf{b}(i)$ is a $K \times 1$ vector. Substituting for $\mathbf{y}$ using Eq. (2.6), one can rewrite the received signal in Eq. (2.5) in matrix form as

$$\mathbf{r}(i) = \mathbf{S}^+\mathbf{A}\mathbf{b}(i) + \mathbf{S}^-\mathbf{A}\mathbf{b}(i-1) + \mathbf{n}(i). \tag{2.7}$$

### 2.2.2 Multipath Channel

Now consider the case of a multipath channel, also termed a frequency selective fading channel, modelled in discrete time by an L-tap tapped-delay line whose coefficients

are denoted $\mathbf{h} = [h_1, h_2, ..., h_L]$. The parameter L, when viewed in units of time, is known as the delay spread of the channel and is typically on the order of 5 to 10 microseconds [78]. The received signal in a multipath channel can now be written as

$$\hat{\mathbf{r}}(i) = \hat{\mathbf{y}}(i) + \mathbf{n}(i), \tag{2.8}$$

where $\hat{\mathbf{y}} = \mathbf{y} * \mathbf{h}$ and $*$ denotes convolution [58]. Figure 2.3 shows the discrete-time representation of the multipath channel model in which $T_c$ is the chip period. The parameters $h_l$, for $l = 1, 2, ..., L$, are random variables whose amplitude is assumed to be taken from a Rayleigh distributed probability density function (pdf), defined as

$$p_R(\alpha) = \frac{\alpha}{\sigma^2} e^{-\alpha^2/(2\sigma^2)}, \tag{2.9}$$

where $\alpha$ is the Rayleigh fading parameter [44] and $\sigma$ is increased for successive $h_l$. The Rayleigh pdf is as shown in Figure 2.4. Substituting for $\mathbf{y}$ using Eq. (2.3), one can write the received signal explicitly as

$$\hat{\mathbf{r}}(i) = b_1(i)\hat{\mathbf{s}}_1 + \sum_{k=2}^{K} A_k[b_k(i)\hat{\mathbf{s}}_k^+ + b_k(i-1)\hat{\mathbf{s}}_k^-] + \mathbf{n}(i), \tag{2.10}$$

where $\hat{(\cdot)}$ will be used to denote convolution of the operand $(\cdot)$ with the channel vector $\mathbf{h}$ throughout the dissertation.

Using the matrix notation defined in Eq. (2.6), one can also write the received signal in Eq. (2.10) in matrix form as

$$\hat{\mathbf{r}}(i) = \hat{\mathbf{S}}^+\mathbf{A}\mathbf{b}(i) + \hat{\mathbf{S}}^-\mathbf{A}\mathbf{b}(i-1) + \mathbf{n}(i). \tag{2.11}$$

Note that the synchronous form is obtained by setting $\hat{\mathbf{s}}_k^+ = \hat{\mathbf{s}}_k$ or setting $\hat{\mathbf{S}}^+ = \hat{\mathbf{S}}$ in Eqs. (2.5)and (2.11), respectively (with $\hat{\mathbf{s}}_k^- = 0$ and $\hat{\mathbf{S}}^- = 0$), yielding

$$\hat{\mathbf{r}}(i) = \hat{\mathbf{S}}\mathbf{A}\mathbf{b}(i) + \mathbf{n}(i). \tag{2.12}$$

The AWGN form is obtained by further setting $\hat{\mathbf{S}} = \mathbf{S}$ or setting $\hat{\mathbf{s}}_k = \mathbf{s}_k$.

## 2.3 Optimum Receiver

For the single user detector, the goal is to extract the desired information, i.e., the bits transmitted by user one ($b_1$) while suppressing the interference represented by the term in the summation of Eq. (2.3) or Eq. (2.10). Ideally, it would be desirable to subtract out the interference term and then multiply by the spreading code of user one, $\mathbf{s}_1$, to extract $b_1$ from the received signal. This is not possible in practice because the interference is unknown and embedded in the received signal, and the channel will further distort the transmitted signal. Thus, attention is now focused on optimum linear detection techniques. In this section, the optimum linear receiver, in terms of minimum probability of bit error ($P_e$), is derived. It is shown that this optimum receiver is the minimum mean squared error (MMSE) receiver which can be implemented by the classical Wiener filter.

### 2.3.1 Maximum Likelihood (ML) Receiver

An optimum technique for estimating input sequences from a received signal that has been corrupted by a dispersive channel and AWGN is maximum likelihood sequence estimation (MLSE). In MLSE, the input sequence selected is that which maximizes the probability density function of the received signal with respect to all possible input sequences. MLSE is based on the Maximum Likelihood Ratio Test (MLRT) where at some arbitrary time instant, the estimate of the transmitted bit, $\tilde{b}$, is chosen to be that which maximizes $Pr(\mathbf{r}|b)$ where $\mathbf{r}$ denotes the received signal. In the case of binary signalling, there are two hypotheses under which the received vector $\mathbf{r}$ is

observed. These are

$$H_0 \ : \ \mathbf{r} = \mathbf{y} + \mathbf{n} \tag{2.13}$$

$$H_1 \ : \ \mathbf{r} = -\mathbf{y} + \mathbf{n} \tag{2.14}$$

where $\mathbf{y}$ represents the transmitted signal vector and $\mathbf{n}$ is the AWGN vector. Note from Eq. (2.5) that under these conditions, $\mathbf{y}$ is simply $\mathbf{s}_1$ and $\mathbf{n}$ contains the interference plus white noise terms. The noise is assumed AWGN for the purposes of this derivation, so the multivariate Gaussian probability density function of $\mathbf{r}$ can be easily obtained [61] and is given by

$$f(\mathbf{r}|H_0) = \frac{1}{(\pi)^N det(\mathbf{R_n})} e^{[-(\mathbf{r}-\mathbf{y})^H \mathbf{R_n}^{-1}(\mathbf{r}-\mathbf{y})]} \tag{2.15}$$

and

$$f(\mathbf{r}|H_1) = \frac{1}{(\pi)^N det(\mathbf{R_n})} e^{[-(\mathbf{r}+\mathbf{y})^H \mathbf{R_n}^{-1}(\mathbf{r}+\mathbf{y})]}, \tag{2.16}$$

where $\mathbf{R}_n$ is the covariance matrix of the interference plus the noise [43] and $(\cdot)^H$ represents the Hermitian (complex conjugate transpose) operator. The likelihood ratio test is then written as

$$\Lambda(\mathbf{r}) = \frac{f(\mathbf{r}|H_1)}{f(\mathbf{r}|H_0)} = \frac{e^{[-(\mathbf{r}+\mathbf{y})^H \mathbf{R_n}^{-1}(\mathbf{r}+\mathbf{y})]}}{e^{[-(\mathbf{r}-\mathbf{y})^H \mathbf{R_n}^{-1}(\mathbf{r}-\mathbf{y})]}}. \tag{2.17}$$

Using the monotonic property of the exponential function to take the natural logarithm and cancelling common terms, one obtains the log-likelihood ratio, given by

$$\Lambda_L(\mathbf{r}) \triangleq ln[\Lambda(\mathbf{r})] = 2(\mathbf{y}^H \mathbf{R_n}^{-1}\mathbf{r} + \mathbf{r}^H \mathbf{R_n}^{-1}\mathbf{y}) \tag{2.18}$$

which can be further simplified and written as

$$\Lambda_L(\mathbf{r}) = 4\Re e(\mathbf{y}^H \mathbf{R_n}^{-1}\mathbf{r}), \tag{2.19}$$

where $\Re e(\cdot)$ denotes "real part of". Thus, the MLRT becomes

$$\Re e(\mathbf{y}^H \mathbf{R_n}^{-1} \mathbf{r}) \gtrless_{H_0}^{H_1} 0. \tag{2.20}$$

Note from Eq. (2.20) that the final test is based on the inner product of the received vector $\mathbf{r}$ and the linear filter given by $\mathbf{R}_n^{-1}\mathbf{s}_1$ where $\mathbf{y}$ has been replaced with its equivalent $\mathbf{s}_1$ for the problem under consideration. This is a test that maximizes the output signal-to-interference plus noise ratio (SINR) [5].

In general, it can be shown that if the transmitted bits are equally likely, the ML decoder is equivalent to a maximum a posteriori (MAP) decoder [98]. It can further be shown, [78] and [98], that the MAP receiver is equivalent to a minimum $P_e$ receiver. Thus, the MLRT solution in (2.20) is the minimum probability of error solution. In the next section, it is shown that the MMSE solution, which can be implemented by the classical Wiener filter, gives the same result.

### 2.3.2 Minimum Mean Square Error (MMSE): The Wiener Filter

For the MMSE receiver, the coefficient vector $\mathbf{c}$ is chosen to minimize the mean square error (MSE) between the transmitted bit and its estimate, given by

$$MSE = E[|b_1(i) - \mathbf{c}^H \mathbf{r}(i)|^2], \tag{2.21}$$

where $E[\cdot]$ denotes the expected value operator. The bit estimate can be written directly as

$$\tilde{b}_1(i) = \mathbf{c}^H \mathbf{r}(i). \tag{2.22}$$

Solving Eq. (2.21) [34] yields

$$\mathbf{c}_{MMSE} = \mathbf{R}^{-1}\mathbf{p_1}, \tag{2.23}$$

where $\mathbf{R}$ is the well-known covariance matrix of the received signal, given by $E[\mathbf{r}(i)\mathbf{r}(i)^H]$, and has dimension $N \times N$. The quantity $\mathbf{p}_1$ is given by $\mathbf{r}(i)b_1(i)$ when the MMSE receiver operates in training mode. When it operates in blind mode, in which case the received bit $b_1(i)$ is unknown, $\mathbf{p}_1$ is given by $\mathbf{s}_1$, the spreading code of the desired user. Throughout the dissertation, simulation results are shown for blind mode only. The trend for future generation systems is to eliminate training requirements as this reduces system throughput. However, pilot channels will be continuously transmitted in near term future systems, so training data is available. With the low complexity implementation provided by the MWF, throughput may not be an issue. Performance in training mode will be significantly better than in blind mode.

The original Wiener filter structure is based on the problem of obtaining an $N$ dimensional filter of coefficients $\mathbf{w}_x$ to approximate a desired scalar signal $d_0(i)$ given an observed vector $\mathbf{x}_0(i)$ of dimension $N$ by minimizing the mean square error [22]. This is depicted pictorially in Figure 2.5. In other words, one chooses $\mathbf{w}_x$ to minimize

$$MSE_{WF} = E[|d_0(i) - \mathbf{w_x}^H \mathbf{x_0}(i)|^2], \tag{2.24}$$

in the same way as in Eq. (2.21) with the MMSE solution. Thus, the classical Wiener filtering problem has the same solution in accordance with Eq. (2.23) for the MMSE. As shown in [5], Eq. (2.23) also maximizes the output SINR, and is therefore equivalent to the MLRT solution given in Eq. (2.20). Thus, both solutions are equivalent to each other and also to the minimum probability of error solution. For a detailed treatment of the Wiener filtering problem, see [30] and [92].

### 2.3.3 Motivation for Reduced Rank Signal Processing

From Eq. (2.23), the MMSE solution, implemented by the Wiener filter, requires inversion of an $N \times N$ statistical covariance matrix $\mathbf{R}$. Recall that $N$ represents the processing gain of the CDMA system. A rule of thumb known as the RMB Rule (standing for Reed, Mallett, Brennan who initially discovered it) is that at least $2N$ statistically independent samples of a Gaussian random process are required to come within 3 dB of the optimal Wiener solution [69]. Also, the computational complexity associated with the matrix inversions is on the order of $N^3$ operations. Furthermore, in a rapidly varying channel or signal environment [59], the covariance matrix must also be updated rapidly, thereby increasing the computational burden. In some cases, the hardware may not be able to perform the calculations required to keep up with the rapidly varying environmental conditions or enough samples may not be available to converge to the optimum Wiener solution. In the next chapter, attention is focused on efficient methods of implementing the Wiener filter. Early reduced rank, subspace based approaches such as principal components and cross-spectral method, [25] and [97], have been presented to mitigate the aforementioned problems. It is shown that the computational burden associated with the multistage Wiener filter is far less than that of the other techniques and has the additional advantage that the reduced rank is not dependent on the number of signals present in the system.

## 2.4 Simulation Models

For validation of the analysis, many of the numerical results presented in this dissertation are based both on Monte Carlo (MC) methods and an analytical model (AM). In this section it is described how these models are developed. Simulations

are developed in MatLab®, and [50] and [66] are programming guides.

### 2.4.1 Monte Carlo Method and Bit Error Rate (BER)

Curves of $E_b/N_0$ vs. bit error rate (BER) will be obtained by varying the $E_b/N_0$ via the variance of the noise samples $\mathbf{n}(i)$. The parameter $E_b/N_0$ is a common figure of merit in communications and denotes bit energy $E_b$ divided by single-sided noise PSD $N_0$. It is equivalent to the signal-to-noise ratio (SNR) for BPSK if the data rate is equal to the noise bandwidth. Assume a sampling rate of one sample per bit or chip, so that $E_b/N_0$ for BPSK is defined by

$$E_b/N_0 = \mu^2/2\sigma^2, \tag{2.25}$$

where $\mu$ is the mean signal value at the receiver input, and $\sigma^2$ is the variance of the AWGN. Since the modulator produces output symbols $\epsilon$ $(-1, +1)$, $\mu^2$ is always one. Therefore, the $E_b/N_0$ will be adjusted via the noise variance alone. The number of users can be adjusted via the parameter $K$. It is also assumed that all the bits and spreading codes are real, so that the received signal will also be real. Hadamard codes or Gold codes, which are obtained by modulo two addition of PN codes, are chosen for spreading.

Hadamard codes are orthogonal [44] to one another and are therefore well-behaved in synchronous channels. Gold codes, first described in [18], have better cross-correlation properties than the corresponding PN sequences from which they are obtained [44] but are not strictly orthogonal. When important, a distinction will be made as to which code is used. For simplicity, modulation is ignored and simulations are performed using real, baseband data. For MMSE, Eq. (2.23) is used to compute $\mathbf{c}_{MMSE}$ which is then applied to Eq. (2.22) to compute the bit estimate. The method

for obtaining the bit estimate for the MWF is described in the next chapter. Errors will be counted to generate the BER.

### 2.4.2 Analytical Model and Probability of Error ($P_e$)

In the analytical model, curves of $E_b/N_0$ vs. $P_e$ are obtained by first computing an estimate of the SINR, defined as the ratio of the signal power to the noise plus interference power. The noise power for an AWGN process, $P_N$, is the area under the PSD curve. Since the mean of the process is assumed to be zero, the noise power is simply equal to its variance, i.e. $P_N = \sigma^2$, and since the sampling rate is normalized to one, the signal power is $P_S = E_b$. Furthermore (see Figure 2.6), the noise variance is $\sigma^2 = N_0/2$, which denotes the double-sided PSD. Thus, the SINR can be written as

$$SINR = \frac{E_b}{\sigma^2} = \frac{E_b}{N_0/2}. \tag{2.26}$$

The $P_e$ using the Gaussian relation for BPSK is [65]

$$P_e = Q(\sqrt{2E_b/N_0}). \tag{2.27}$$

So, in terms of the SINR, the $P_e$ becomes

$$P_e = Q(\sqrt{SINR}), \tag{2.28}$$

where $Q(\cdot)$ is the Marcum Q function and is defined by [101]

$$Q(x) = \int_x^\infty \frac{1}{\sqrt{2\pi}}\, e^{-t^2/2} dt. \tag{2.29}$$

The general formulation of the analytical SINR for the full rank MMSE receiver and the MWF can be expressed in terms of the covariance matrix $\mathbf{R}$, the spreading codes, $\mathbf{s}_k$, $k = 1, 2, ..., K$, and the weight vectors which are denoted $\mathbf{c}_{MMSE}$ and $\mathbf{c}_{MWF}$,

respectively. The expression for $\mathbf{c}_{MMSE}$ is given in Eq. (2.23), with $\mathbf{R}$ replaced by $\hat{\mathbf{R}}$ in multipath, and a detailed description on how to form $\mathbf{c}_{MWF}$ from the orthogonal decomposition of the MWF is provided in [21] and will be summarized in the following chapter. The analytical covariance matrix in multipath, expanded in terms of the received signal $\hat{\mathbf{r}}(i)$ in Eq. (2.11), is given as

$$\hat{\mathbf{R}} = E[\hat{\mathbf{r}}(i)\hat{\mathbf{r}}(i)^H] = \hat{\mathbf{S}}\mathbf{A}^2\hat{\mathbf{S}}^H + \sigma^2\mathbf{I} \tag{2.30}$$

for the synchronous case and

$$\hat{\mathbf{R}} = E[\hat{\mathbf{r}}(i)\hat{\mathbf{r}}(i)^H] = \hat{\mathbf{S}}^+\mathbf{A}^2\hat{\mathbf{S}}^{+H} + \hat{\mathbf{S}}^-\mathbf{A}^2\hat{\mathbf{S}}^{-H} + \sigma^2\mathbf{I} \tag{2.31}$$

for the asynchronous case. Even though in the presence of multipath, $\hat{\mathbf{S}}^+$ and $\hat{\mathbf{S}}^-$ are not orthogonal, the independence of the bits, specifically the current bit $\mathbf{b}(i)$ and previous bit $\mathbf{b}(i-1)$, forces the expectation of the cross-terms to zero. This equation is similar to Eq. (10) of [32], which is shown for the AWGN case. It is also important to note that for synchronous or asynchronous users in multipath, the length of the window used to represent the data $\hat{\mathbf{S}}^+$ and $\hat{\mathbf{S}}^-$ must span the entire channel length in bit duration, given by [76]

$$L_b = \ulcorner \frac{L+N-1}{N} \urcorner, \tag{2.32}$$

where $\ulcorner(x)\urcorner$ represents the smallest integer greater than or equal to $x$. Setting user one as the desired user, the analytical SINR can be written as [76]

$$SINR_{MMSE} = \frac{\mathbf{c}_{MMSE}^H \hat{\mathbf{s_1}}^+ A_1 A_1^H \hat{\mathbf{s_1}}^{+H} \mathbf{c}_{MMSE}}{\mathbf{c}_{MMSE}^H (\hat{\mathbf{R}} - \hat{\mathbf{s_1}}^+ A_1 A_1^H \hat{\mathbf{s_1}}^{+H}) \mathbf{c}_{MMSE}} \tag{2.33}$$

for the MMSE and similarly,

$$SINR_{MWF} = \frac{\mathbf{c}_{MWF}^H \hat{\mathbf{s_1}}^+ A_1 A_1^H \hat{\mathbf{s_1}}^{+H} \mathbf{c}_{MWF}}{\mathbf{c}_{MWF}^H (\hat{\mathbf{R}} - \hat{\mathbf{s_1}}^+ A_1 A_1^H \hat{\mathbf{s_1}}^{+H}) \mathbf{c}_{MWF}} \tag{2.34}$$

for the MWF. Then, the probability of error can be obtained using Eq. (2.28).

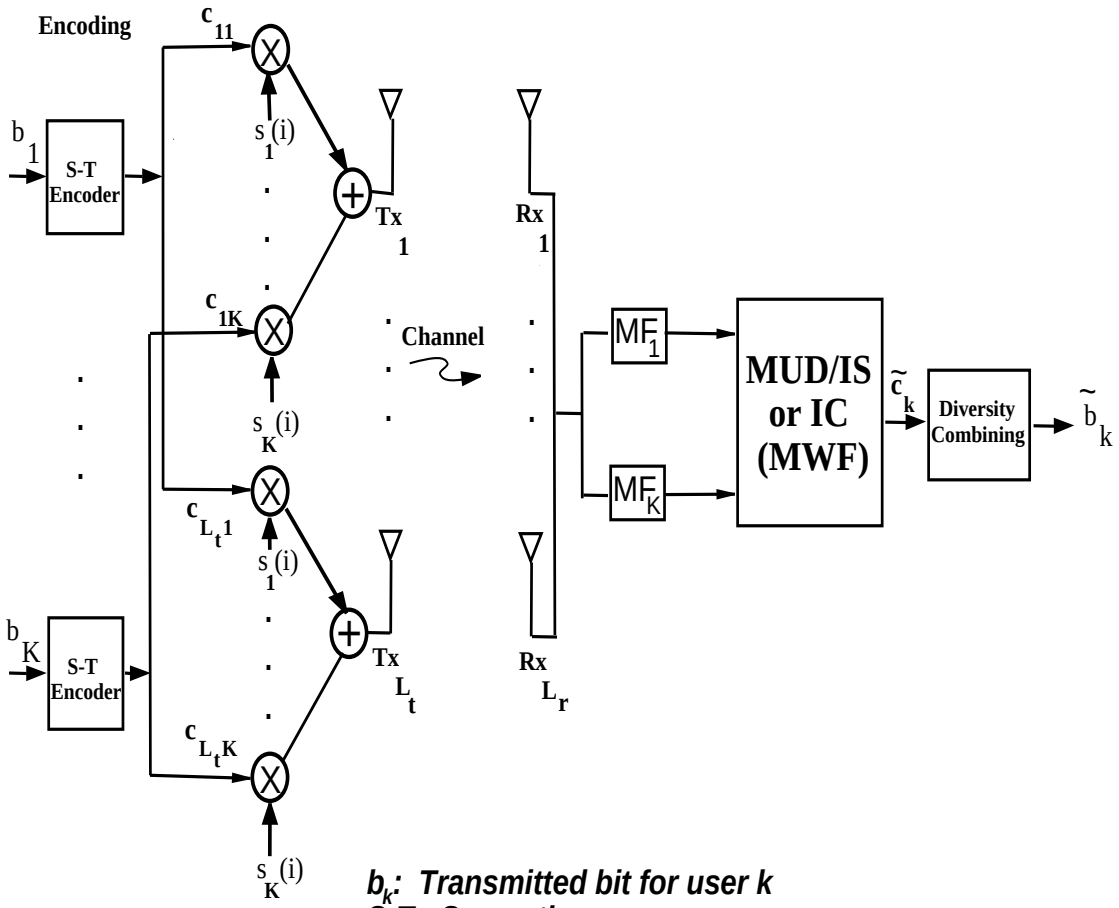


$b_k$: Transmitted bit for user k
S-T: Space-time
$c_{l,k}$: Code symbol at transmit antenna l for user k
$s_k$: Spreading code for user k
MF: Matched filter
MUD: Multiuser detection
IS: Interference suppression
IC: Interference cancellation
MWF: Multistage Wiener filter
K: The number of users
$L_t$: The number of transmit antennas
$L_r$: The number of receive antennas
$\tilde{c}_k$: Estimated code symbol for user k
$\tilde{b}_k$: Estimated bit for user k

Figure 2.1: Overall Code Division Multiple Access (CDMA) System Block Diagram

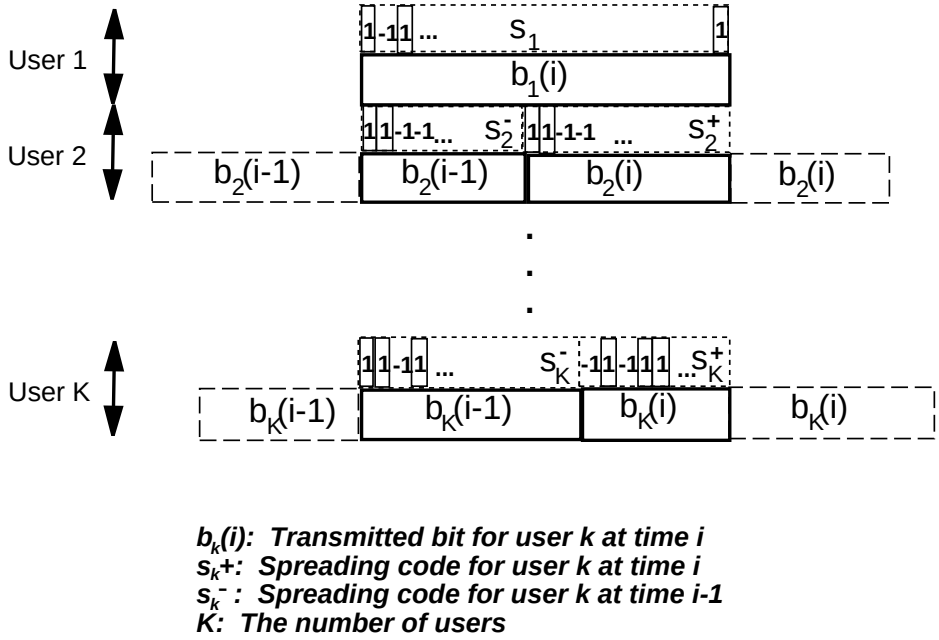


Figure 2.2: Asynchronous Code Division Multiple Access (CDMA) Signal Structure

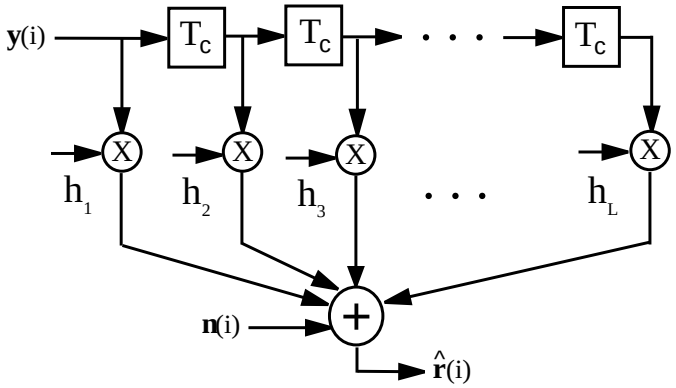


***y(i): Transmitted signal at time i***
***$h_l$: Channel coefficient l, l = 1, 2, ..., L***
***L: Channel delay spread***
***n(i): Additive white Gaussian noise (AWGN) at time i***
***$T_c$: Chip delay***
***$\hat{r}$(i): Received signal at time i***

Figure 2.3: Multipath Channel Model using Tapped-Delay Line (TDL)

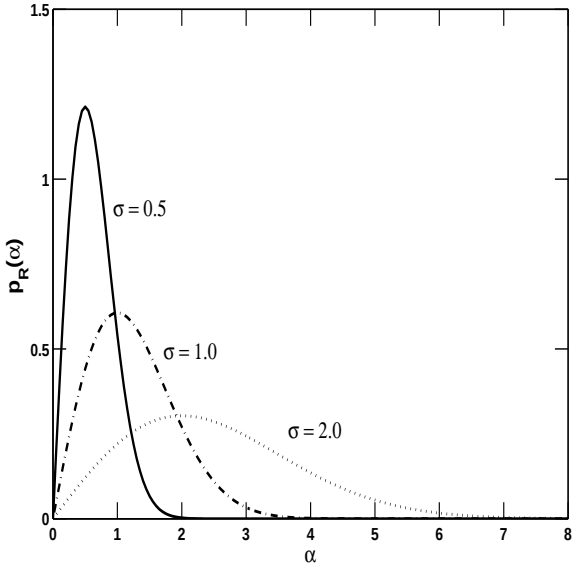


Figure 2.4: Rayleigh Probability Density Function (PDF)

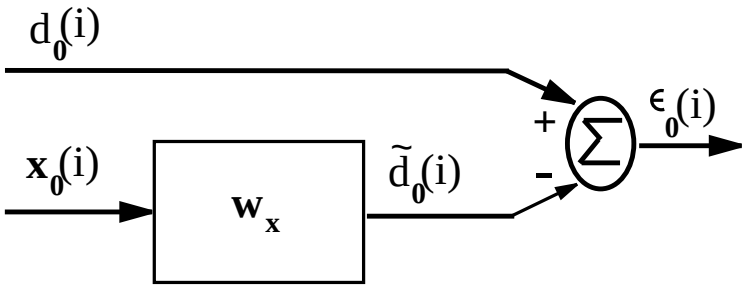


Figure 2.5: Classical Wiener Filter; $d_0(i)$=desired signal; $\mathbf{x}_0(i)$=observed signal; $\mathbf{w}_x$=Wiener filter coefficient vector; $\tilde{d}_0(i)$=estimate of desired signal; $\epsilon_0(i)$=error signal

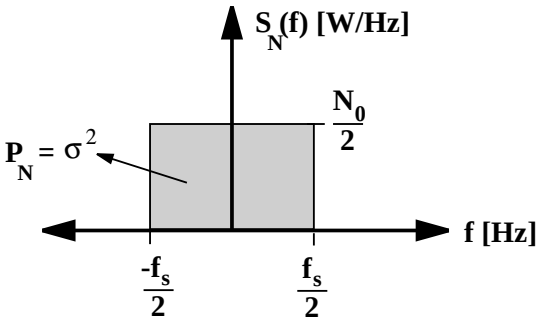


Figure 2.6: Additive White Gaussian Noise (AWGN) Double-Sided Power Spectral Density (PSD) $S_N(f)$; $P_N$=Total noise power; $\sigma^2$=Noise variance; $f_s$=Sampling frequency

# Chapter 3

# Reduced Rank Statistical Signal Processing Algorithms

Recall that computation of the minimum mean square error (MMSE) solution to the interference mitigation problem for CDMA requires inversion of the $N \times N$ covariance matrix $\mathbf{R}$, which can be quite computationally intense and may not even be possible in real-time for a high data rate system. Also, if the channel or signals are changing in time, then the sample covariance matrix estimated from the data does not depict the true non-stationary signal environment. Thus, it is desirable to find alternate solutions that approach, or better yet, exceed the performance of the MMSE receiver but require much fewer computations and can adapt rapidly. These conditions have motivated much of the research in the area of interference suppression and led to the development of the principal components method, the cross-spectral method, and the multistage Wiener filter (MWF). The multistage Wiener filter has demonstrated the ability operate successfully at a much lower rank than any other reduced rank method (e.g., see [22] and [32]). These techniques are described next.

## 3.1 Principal Components (PC)

The method of principal components is a popular reduced rank technique (introduced in [14] and [37] and applied in e.g., [35] and [91]) based on an eigen-decomposition of the covariance matrix $\mathbf{R}$ of the received signal vector $\mathbf{r}$. Specifically, let

$$\mathbf{R} = \mathbf{V}\mathbf{\Lambda}\mathbf{V}^H, \tag{3.1}$$

where $\mathbf{V}$ is the matrix whose columns consist of the eigenvectors of $\mathbf{R}$, and $\mathbf{\Lambda}$ is a diagonal matrix whose elements are the corresponding eigenvalues; $\mathbf{V}$ and $\mathbf{\Lambda}$ are $N \times N$ matrices. Given this decomposition, $\mathbf{R}$ can now be projected using only $D$ columns of the $N$ columns of $V$, where $D < N$. The columns that are chosen are those $D$ columns corresponding to the $D$ largest eigenvalues of $\mathbf{R}$. To see this explicitly, write $\mathbf{R}$ as

$$\mathbf{R} = \sum_{i=1}^{D} \lambda_i \mathbf{V}_i \mathbf{V}_i^H \tag{3.2}$$

where $\lambda_i$ is the $i^{th}$ diagonal element of $\mathbf{\Lambda}$ and $\mathbf{V}_i$ is the $i^{th}$ column of $\mathbf{V}$. Note here that if $D \geq K$, where $K$ is the number of users in the system, then the reduced rank subspace contains the signal subspace, so that full rank minimum mean square error performance can still be attained. If, however, $D < K$, i.e. if the number of users is unknown or changing, then performance can degrade quite rapidly as the number of users increases. This occurs because now the reduced rank subspace may no longer span the subspace containing the signal components. Another disadvantage to this method is the computational complexity associated with the eigen-decomposition, especially in a rapid time-varying environment.

## 3.2 Cross-Spectral (CS) Method

A technique that is closely related to the method of principal components is the cross-spectral (CS) method, which also uses the eigenvectors and eigenvalues in a way such as to reduce the rank of the signal subspace ([24] and [25]). Suppose a received data matrix $\mathbf{X}$ is formed, which can be assumed to be formed from many observations of the received vector $\mathbf{r}$. Thus, $\mathbf{X}$ has dimension $M \times N$, where $M$ is the number of observations of the sampled statistical process. One can compute the singular value decomposition (SVD) of the observation matrix $\mathbf{X}$ from [77]

$$\mathbf{X} = \mathbf{U}\mathbf{Z}\mathbf{V}^H, \tag{3.3}$$

where $\mathbf{U}$, $\mathbf{Z}$, and $\mathbf{V}$ are $M \times N$ left singular, $N \times N$ diagonal singular, and $N \times N$ right singular matrices of $\mathbf{X}$, respectively. The matrix $\mathbf{V}$ consists of the eigenvectors of $\mathbf{R} = \mathbf{X}^H\mathbf{X}$, the covariance matrix of $\mathbf{X}$. The column vectors of $\mathbf{U}$ form an orthonormal basis of $\mathbf{R}$. To solve the reduced rank problem one can choose a subset $D$, $D < N$, of these vectors to minimize the mean square error for the least squares (LS) problem, given by

$$MSE_{LS} = |\mathbf{d_0} - \mathbf{X}\mathbf{w_{LS}}|^2, \tag{3.4}$$

where $\mathbf{d}_0$ is some desired $M$ dimensional vector and $\mathbf{w}_{LS}$ is the LS weight vector to be determined. Note that the minimization of the MSE given in Eq. (3.4) is equivalent to maximization the norm of the estimate $\mathbf{X}\mathbf{w}_{LS}$, which can be written as

$$E_y = \|\mathbf{X}\mathbf{w}_{LS}\|^2. \tag{3.5}$$

Expanding $E_y$ in terms of the covariance matrix $\mathbf{R}$, one can write

$$E_y = \mathbf{r_{xd}}^H\mathbf{R}^{-1}\mathbf{r_{xd}} = \mathbf{r_{xd}}^H\mathbf{V}\Lambda^{-1}\mathbf{V}^H\mathbf{r_{xd}}, \tag{3.6}$$

where $\mathbf{r}_{xd} = \mathbf{X}^H\mathbf{d}$; i.e. the cross-correlation vector between the observed data matrix and the desired signal. Introducing the cross-correlation vector, defined by

$$\rho = \mathbf{V}^H\mathbf{r_{xd}}, \tag{3.7}$$

one can write

$$E_y = \sum_{j=1}^{N} \frac{\rho_k^2}{\lambda_k}, \tag{3.8}$$

where $\lambda_k$ is the $k^{th}$ eigenvalue of $\mathbf{R}$, alternatively the $k^{th}$ diagonal element of $\Lambda$, and $\rho_k$ is the $k^{th}$ element of $\rho$ for $k = 1, 2, ..., N$. To maximize the norm of the estimate, i.e. its energy, those eigenvectors that correspond to a large cross-correlation vector should be retained. Thus, the term in the summation above, $\frac{\rho_k^2}{\lambda_k}$, is a measure of the energy projected along the $k^{th}$ basis vector of $\mathbf{R}$ and is termed the cross-spectral energy. Note that the full rank LS solution is easily computed by solving the MMSE problem and is written as

$$\mathbf{w}_{LS} = \mathbf{R}^{-1}\mathbf{r_{xd}}, \tag{3.9}$$

Thus, by choosing a set of $D$ basis vectors that correspond to the $D$ largest values of the CS energy, a reduced rank subspace is formed. However, while this algorithm generally performs slightly better than principal components because it is not as sensitive to the number of users being less than or equal to the rank of the subspace, it too suffers from computational complexity issues [31]. More importantly, the CS metric is also dependent on eigen-decomposition and estimation of the covariance matrix.

## 3.3 The Multistage Wiener Filter (MWF)

It is important to point out that the eigen-based subspace approaches presented in the previous sections require calculation of the covariance matrix $\mathbf{R}$. This drives the required sample support and immediate degradation occurs if signals are non-stationary over the large intervals typically required to compute $\mathbf{R}$. In this section, a different approach is introduced which enables low complexity processing by avoiding calculation of the covariance matrix $\mathbf{R}$.

### 3.3.1 MWF Decomposition using Orthogonal Projections

The multistage Wiener filter was first introduced in [20], [22], [23], and [24] and is a pioneering breakthrough in reduced rank algorithms in that it meets or exceeds MMSE performance but does not require any matrix inversions nor computationally complex eigen-decompositions. This new representation of the Wiener filter can be obtained by performing multistage decompositions based on maximizing the cross-correlation between the desired signal and the observed signal. This results in two subspaces, one in the direction of the cross-correlation and one orthogonal to it. Note that this approach naturally creates signal subspaces at successive stages that are orthogonal to those of the previous stage. The multistage structure is obtained by repeated correlations of the signal that lies in the orthogonal subspace at the previous stage and thus is also termed the residual correlation algorithm [32]. It is shown in [21] that the mean square error obtained with this multistage structure is the same as with the classical multi-dimensional, single stage Wiener filter when all stages are retained, the covariance matrix exists (stationarity exists), and the covariance matrix can be estimated (sufficient sample support can be utilized). Thus, the full rank MWF is

also equivalent to the MMSE solution.

A block diagram showing the nested chain of scalar Wiener filters in a multistage implementation for $D = 4$ stages is shown in Figure 3.1. The notation used closely follows that of [21]. This structure requires that all input signals are wide-sense stationary (WSS) and this is assumed to be true in the system model. As shown in the figure, $\mathbf{x}_0(i)$ represents an $N \times 1$ data vector, which contains the outputs of a chip-matched filter. In training mode, $d_0(i)$ represents the desired signal, which is set equal to the training bit. The scalars $\epsilon_j(i)$, $j = 1, 2, ..., D-1$, denote the errors at each successive stage, and are given by

$$\epsilon_j = d_j(i) - w_{j+1}\epsilon_j(i) \tag{3.10}$$

This is analogous to the error signal of the multi-dimensional Wiener filter, represented by the term in brackets in Eq. (2.24). Note that $\epsilon_D(i) = d_D(i)$. The output, $\epsilon_0(i)$ denotes the error signal, which is the difference between the desired signal $d_0(i)$ and the final estimate of the signal produced by the filter and given by $\tilde{b}_1(i) = w_1\epsilon_1(i)$.

The vectors $\mathbf{h}_j$ for $j = 1, 2, ..., D$ represent the normalized cross-correlation vector between the corresponding input signal at that stage, $\mathbf{x}_{j-1}(i)$ and the desired signal for that stage, $\mathbf{d}_{j-1}(i)$. The matrices $\mathbf{B}_j$ for j=1, 2, ..., $D$ represent blocking matrices, which are orthogonal to $\mathbf{h}_j$ so that $\mathbf{B}_j\mathbf{h}_j = 0$, and whose rows are orthonormal. Therefore, all signal components in the same direction as $\mathbf{h}_j$ are eliminated at the next stage of the filter. One method for obtaining appropriate blocking matrices can be found in [21]. A simple blocking matrix is $\mathbf{B}_j = \mathbf{I} - \mathbf{h}_j\mathbf{h}_j^H$, and the orthogonality between $\mathbf{B}_j$ and $\mathbf{h}_j$ here can be easily verified. The scalars $w_j$, j = 1, 2, ..., $D$, are the new scalar Wiener weights, computed from the Wiener-Hopf (WH) equation [30]. Note that this multistage Wiener filter structure does not require an

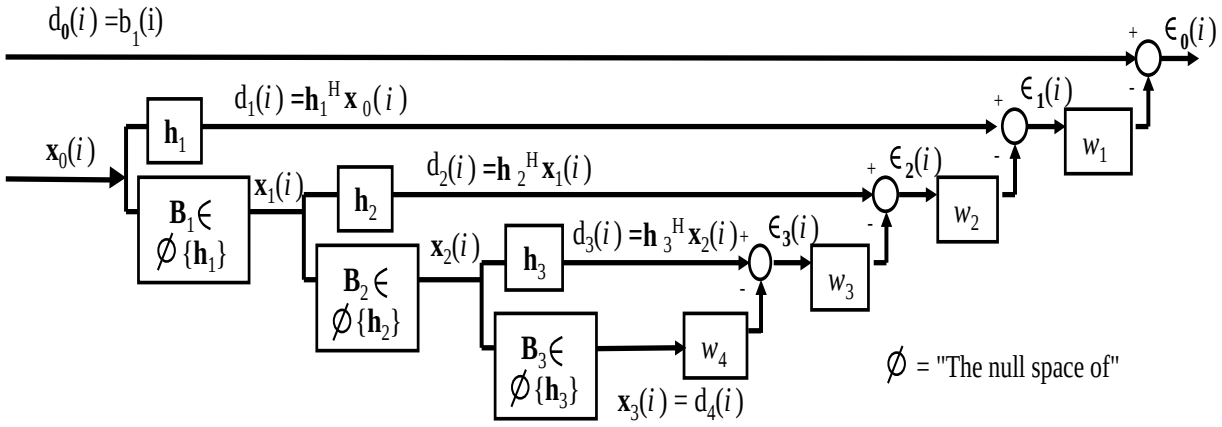


Figure 3.1: Multistage Wiener Filter (MWF) in Training Mode, $D = 4$ Stages; $d_0(i)$=desired signal at time $i$; $b_1(i)$=transmitted bit for user one; $\mathbf{x}_0(i)$=observed signal; $\epsilon_0(i)$=error signal

inverse of the covariance matrix of the input sequence, given by $\mathbf{R}_{x_0} = E[\mathbf{x}_0(i)\mathbf{x}_0^H(i)]$ as is required for the MMSE technique and for the classical multi-dimensional Wiener filter [22].

The multistage Wiener filter structure can be summarized by a set of recursive relationships. The forward and backward recursion equations, summarized below in Table 3.1, are identical to those used to implement the block residual correlation algorithm ([21] and [32]). The parameter $\Omega$ denotes the region of sample support used to compute the sample statistics. In training mode, $d_0(i) = b_1(i)$ and $\mathbf{x_0}(i) = \mathbf{r}(i)$.

In blind mode, when $b_1(i)$ is unknown, its estimate can be obtained via the matched filter (MF). Here, this is simply the spreading code, $\mathbf{s}_1$ of user one, more generically denoted a steering vector. So, one simply inserts $\mathbf{s}_1$ at the front end of the filter, so that now $d_0(i) = \mathbf{s}_1^H\mathbf{r}(i)$, and set $\mathbf{x}_0(i) = \mathbf{B}_0\mathbf{r}(i)$, where $\mathbf{B}_0$ is the blocking matrix which is orthogonal to the spreading code $\mathbf{s}_1$. The filter structure

Table 3.1: Recursion Equations for the Multistage Wiener Filter (MWF)

| |
|---|
| Initialization: $d_0(i)$ and $\mathbf{x}_0(i)$ |
| Forward Recursion: For $j = 1, 2, ..., D$: $\mathbf{h}_j = \frac{\sum_\Omega \{d^*_{j-1}(i)\mathbf{x}_{j-1}(i)\}}{\|\sum_\Omega \{d^*_{j-1}(i)\mathbf{x}_{j-1}(i)\}\|}$ $d_j(i) = \mathbf{h}_j^H \mathbf{x}_{j-1}(i)$ $\mathbf{x}_j(i) = \mathbf{B}_j \mathbf{x}_{j-1}(i)$ |
| Backward Recursion: For $j = D, D-1, ..., 1$ $e_D(i) = d_D(i)$ $w_j = \frac{\sum_\Omega \{d^*_{j-1}(i)e_j(i)\}}{\sum_\Omega \{\|e_j(i)\|^2\}}$ $e_{j-1}(i) = d_{j-1}(i) - w_j^* e_j(i)$ |

for blind mode operation is shown in Figure 3.2. Now, $d_0(i)$ is just the matched filter output and produces the best initial estimate of the bits in the absence of their prior knowledge. Note that in blind mode the Wiener filter eliminates signals that lie in the space orthogonal to $\mathbf{s}_1$, namely the interference. Thus, $\epsilon_0(i)$ is not an error signal but is the estimate of the transmitted information after the interference has been subtracted out. Thus, the bit estimate used in the Monte Carlo simulations is $\tilde{b}_1(i) = \epsilon_0(i)$. Performance results of the MWF for asynchronous CDMA in AWGN can be found in [32] and [43].

For the Monte Carlo simulations, the data in the Wiener filter is processed in blocks of $M$ bits at a time. In training mode, the $N \times 1$ vector $\mathbf{x_0}(i)$ is replaced with an $N \times M$ matrix $\mathbf{X_0}(i) = [\mathbf{x_0}(i)\ \mathbf{x_0}(i+1)\ ...\ \mathbf{x_0}(i+M-1)]$. Also, the scalar $d_0(i)$ is replaced by an $1 \times M$ vector of bits given by $\mathbf{d_0}(i) = [b_1(i)\ b_1(i+1)\ ...\ b_1(i+M-1)]$. The

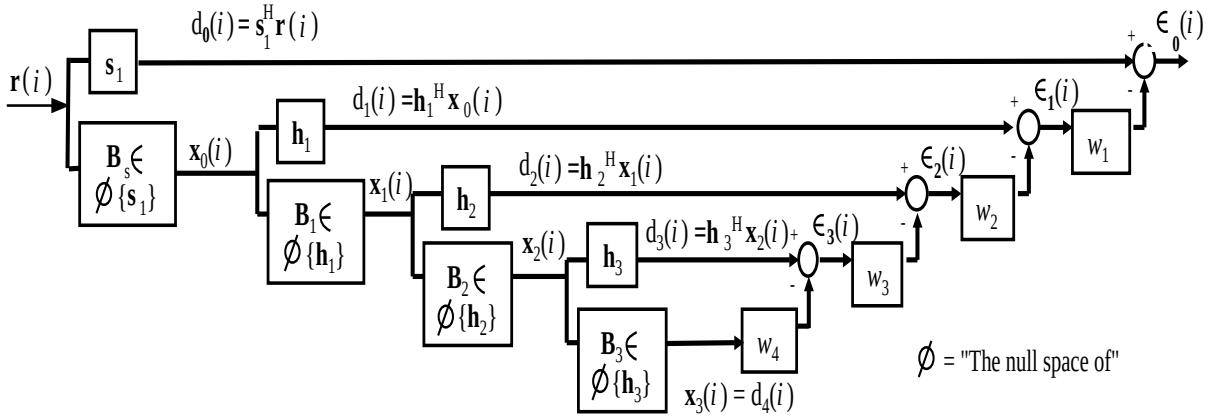


Figure 3.2: Multistage Wiener Filter (MWF) in Blind Mode, $D = 4$ Stages; $\mathbf{r}(i)$=received signal at time $i$; $\mathbf{s}_1$=spreading code for user one; $\epsilon_0(i)$=bit estimate for user one

same is true for the received vector $\mathbf{r}(i)$ in blind mode. So, estimates are also produced one block at a time and are given by $\tilde{\mathbf{b}}_1(i) = \omega_1 \epsilon_{\mathbf{1}}(i)$ in training mode or $\tilde{\mathbf{b}}_1(i) = \epsilon_{\mathbf{0}}(i)$ in blind mode. As mentioned earlier, typically $M \geq 2N$ data bits are required for reliable processing according to the Reed-Mallett-Brennan (RMB) rule.

In Figure 3.3, the Gram-Schmidt interpretation of the MWF is shown [21]. Combining this form and Figure 3.1, the MWF can be written in compact matrix form. In the figure, the MWF is represented by a combination of an analysis filterbank and a synthesis filterbank [21]. The filterbanks, $\mathbf{L}_N$ and $\mathbf{U}_N$, are given by

$$\mathbf{L}_N = \begin{bmatrix} \mathbf{h}_1^H \\ \mathbf{h}_2^H \mathbf{B}_1 \\ \vdots \\ \mathbf{h}_{N-1}^H \prod_{i=N-2}^{1} \mathbf{B}_i \\ \mathbf{h}_N^H \prod_{i=N-1}^{1} \mathbf{B}_i \end{bmatrix} \tag{3.11}$$

and

$$\mathbf{U}_N = \begin{bmatrix} 1 & -w_2^* & w_2^* w_3^* & \cdots & (-1)^N \prod_{i=2}^{N-1} w_i^* & (-1)^{N+1} \prod_{i=2}^{N} w_i^* \\ 0 & 1 & -w_3^* & \cdots & (-1)^{N-1} \prod_{i=3}^{N-1} w_i^* & (-1)^N \prod_{i=3}^{N} w_i^* \\ \vdots & & & \ddots & & \vdots \\ 0 & 0 & 0 & \cdots & 1 & -w_N^* \\ 0 & 0 & 0 & \cdots & 0 & 1 \end{bmatrix} \tag{3.12}$$

where $w_i$ is the scalar Wiener weight in the multistage decomposition at stage $i$ as depicted in Figure 3.1. From Figure 3.3, it is seen that the $(N+1) \times (N+1)$ output error vector $\epsilon(i) = [\epsilon_0(i)\ \epsilon_1(i)\ ...\ \epsilon_N(i)]^H$ can be written as

$$\epsilon(i) = \mathbf{U}_{N+1} \mathbf{L}_{N+1} \begin{bmatrix} d_0(i) \\ \mathbf{x}_0(i) \end{bmatrix}, \tag{3.13}$$

where the quantities $\mathbf{U}_{N+1}$ and $\mathbf{L}_{N+1}$ are defined by

$$\mathbf{L_{N+1}} = \begin{bmatrix} 1 & 0 \\ 0 & \mathbf{L_N} \end{bmatrix} \tag{3.14}$$

and

$$\mathbf{U_{N+1}} = \begin{bmatrix} 1 & -w_{z_1}^H \\ 0 & \mathbf{U_N} \end{bmatrix}, \tag{3.15}$$

respectively, and $w_{z_1}$ is given by

$$w_{z_1} = \begin{bmatrix} w_1^* & -w_1^* w_2^* & ... & (-1)^{N+1} \prod_{i=1}^{N} w_i^* \end{bmatrix}^H. \tag{3.16}$$

From this representation, the multistage Wiener filter can be written in compact vector form using

$$\mathbf{c}_{MWF} = \mathbf{U}_{N+1} \mathbf{L}_{N+1}, \tag{3.17}$$

which is the equation used to compute $\mathbf{c}_{MWF}$ in the analytical model.

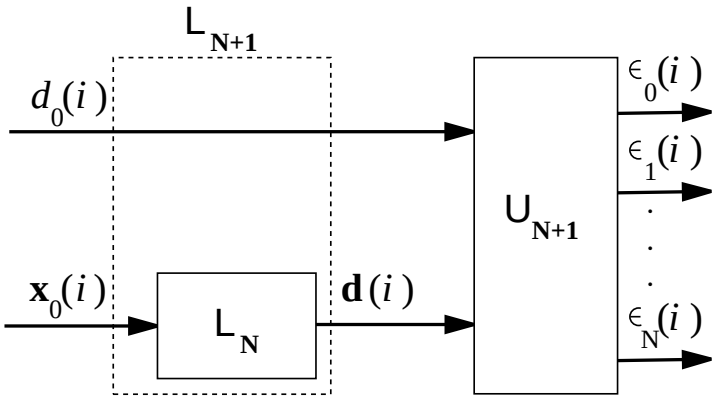


Figure 3.3: Gram-Schmidt Multistage Wiener Filter (MWF) Decomposition; $d_0(i)$=desired signal; $b_1(i)$=bits for user one; $\mathbf{x}_0(i)$=observed signal; $\epsilon_n(i)$=error signal at stage $n$

### 3.3.2 Reduced Rank MWF

Recall that the space spanned by the columns of the covariance matrix of the received signal is of rank $N$. Rank reduction for the classical Wiener filtering problem can be accomplished by filtering the input sequence by an $N \times D$ matrix, whose columns now span a space of rank $D$. This would result in a new covariance matrix of size $D \times D$, where clearly $D < N$. Rank reduction for the Wiener filter in the multistage structure can be accomplished easily by truncating the multistage filter at stage $D$, thereby discarding the last $N - D$ stages of the decomposition [21].

It is important to emphasize the superb ability of the MWF to compress the received signal space into a subspace composing the desired information in only a few stages by maximizing the mutual information between the desired data with the received signal at each stage. This enables significant rank reduction that is not attainable with either the principal components (PC) or cross-spectral (CS) reduced

rank techniques, which require the rank to equal or exceed the number of users present in the system for successful rank reduction. This implies that exact knowledge of the number of users must always be available. In many CDMA systems, this is not practical because the number of users is constantly changing.

### 3.3.3 Efficient Implementation Structures

In this section, two efficient structures that further reduce the computational complexity associated with the implementation of the MWF are presented.

**Correlation Subtraction Architecture (CSA)**

A new structure of the multistage Wiener filter, based on a correlation subtraction architecture (CSA) is described in [72]. The equations that perform the forward recursion are modified with the CSA by recognizing that the blocking matrix calculation is no longer required. By substituting the equation for the blocking matrix, $\mathbf{B}_j = (\mathbf{I} - \mathbf{h}_j\mathbf{h}_j^H)$ into $\mathbf{x}_j(i) = \mathbf{B}_j\mathbf{x}_{j-1}(i)$, and recognizing that $d_j(i) = \mathbf{h}_j^H\mathbf{x}_{j-1}(i)$, one can write the output at each stage $j$ simply as

$$\mathbf{x}_j(i) = \mathbf{x}_{j-1}(i) - \mathbf{h}_j d_j(i). \tag{3.18}$$

The multistage decomposition using the CSA for $D = 2$ stages is shown in Figure 3.4. As with the original MWF, for blind mode processing, $\mathbf{h}_0 = \mathbf{s}_1$, the spreading code of the desired user, and $\mathbf{d}_0(i) = \mathbf{s}_1^H\mathbf{x}_0(i)$. The filter in Figure 3.4 demonstrates the low complexity of this implementation of the MWF and the fact that the computation of signal blocking matrices are no longer necessary for any subspace partitioning such as that required for constrained adaptation. Again, with the CSA-MWF, data is typically processed in blocks of $M$ bits, rather than one bit at a time.

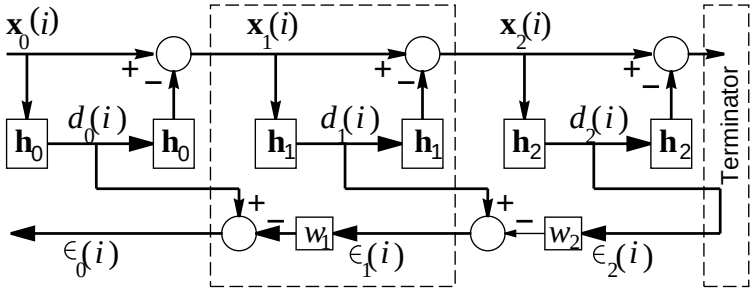


Figure 3.4: Correlation Subtraction Architecture of the Multistage Wiener Filter (CSA-MWF); $d_0(i)$=desired signal; $\mathbf{x}_0(i)$=observed signal; $\mathbf{h}_0 = \mathbf{s}_1$, the spreading code of user one; $\epsilon_0(i)$=bit estimate for user one

### Householder Transformation

The Householder transformation ([38] and [39]) is a matrix transformation which projects a vector $\mathbf{s}$ onto a hyperplane that spans the subspace orthogonal to another vector $\mathbf{u}$. To describe this transformation in more detail, assume that $\mathbf{u}$ is an $N \times 1$ vector and define the $N \times N$ Householder transformation matrix by [30]

$$\mathbf{H} = \mathbf{I} - \frac{2\mathbf{u}\mathbf{u}^H}{\|\mathbf{u}\|^2}. \tag{3.19}$$

Now post-multiply $\mathbf{H}$ by another $N \times 1$ vector $\mathbf{s}$ to obtain

$$\mathbf{H}\mathbf{s} = \mathbf{s} - \frac{2\mathbf{u}^H\mathbf{s}}{\|\mathbf{u}\|^2}\mathbf{u}. \tag{3.20}$$

By definition [30], the second term in the above expression without the scale factor is defined as the projection of $\mathbf{s}$ onto $\mathbf{u}$ and can be written as

$$\mathbf{P}_{\mathbf{u}}(\mathbf{s}) = \frac{\mathbf{u}^H\mathbf{s}}{\|\mathbf{u}\|^2}\mathbf{u}. \tag{3.21}$$

This operation is illustrated in Figure 3.5. Note from the figure that the product $\mathbf{H}\mathbf{s}$ is the reflection of $\mathbf{s}$ about the hyperplane $\mathbf{u}^{\perp}$, which is the plane orthogonal to the plane spanned by vector $\mathbf{u}$.

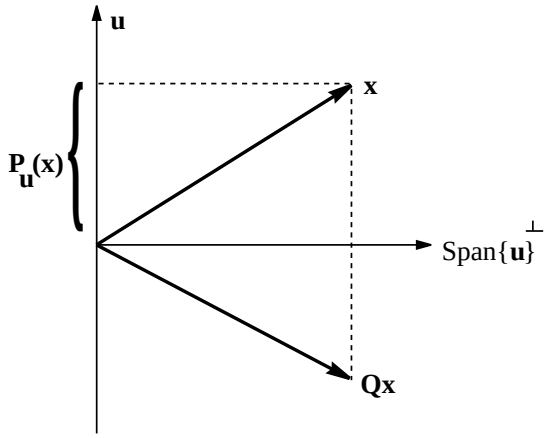


Figure 3.5: Geometric Interpretation of Householder Transformation

Suppose now that $\mathbf{H}$ is assumed to be composed of a spreading code vector $\mathbf{s}$ and a blocking matrix $\mathbf{B_s}$ orthogonal to $\mathbf{s}$. Then $\mathbf{Hs}$ can be written as

$$\mathbf{Hs} = \begin{bmatrix} \mathbf{s}^H \\ \mathbf{I} - \mathbf{s}\mathbf{s}^H \end{bmatrix} \mathbf{s} = \begin{bmatrix} 1 \\ 0 \\ 0 \\ \vdots \\ 0 \end{bmatrix} \tag{3.22}$$

It is seen that this interpretation of $\mathbf{H}$ obeys Property 6 of the Householder transformation [30]. Note here that the number of rows of $\mathbf{B_s}$ is now $N - 1$. Thus, at each stage the number of rows in the matrix decreases by one. This interpretation allows one to compute the decomposition at each stage in the Wiener filter using one matrix in place of a vector and a matrix.

### 3.3.4 Computational Cost and Memory Requirements

In this section, approximate formulas for the computational savings and memory requirements for the reduced rank MWF, the full rank MMSE, and the conventional MF are compared. These are important criteria to determine the actual implementation complexity reduction attainable with the MWF over the MMSE for real-time operation. Recall for this discussion that $N$ is the length of the spreading code, $D$ is the number of stages in the MWF, and $M$ is the number of bits per block.

**Computational Cost**

In the matched filter, $N$ multiplications and $N-1$ additions are required for each bit of data, equivalently approximately $N$ floating point operations (or flops) are required. For a block of data, $O(NM)$ flops are needed, where $O$ denotes 'on the order of'. The zeroth stage of the MWF is the matched filter, requiring $N$ operations per block. Next, the output is re-spread with the spreading code and subtracted from the received signal, requiring another $N$ flops. This is the dominant term in the computations, and for $D$ stages and $M$ blocks, the result is a requirement of $O(2DNM)$ flops. Finally, for the MMSE, the dominant term is the $N \times N$ matrix inversion, which requires $O(N^3)$ operations per block or a total of $O(N^3M)$ operations. Thus, the MF, MWF, and MMSE require $O(NM)$, $O(2DNM)$, and $O(N^3M)$ flops, respectively.

As an example, let $N = 32$, $D = 5$, and $M = 100$. The computational costs associated with the MF, MWF, and MMSE are $3,200$, $32,000$, and $3,276,800$ flops, respectively. Note that the MWF has an increase in complexity by a factor of only 10 over the MF, but reduces in complexity by a factor of 1024 over MMSE. This minimal

complexity increase of the MWF over the MF is outweighed by the performance increase. Furthermore, there also exists a huge complexity reduction over MMSE without the occurrence of any performance loss. In some cases, as will be shown in later chapters, there is actually a performance gain over the full rank receiver.

**Memory Requirements**

The memory requirement for the MF is simply a buffer of size $N$ needed to store the spreading code. For the MWF, $N$ elements are also needed for the MF stage, plus at each additional stage, storage space is required for $\mathbf{h}_j$ for j=1, 2, ..., $D$. Since each of these vectors is of length $N$, a total of $(D+1)N$ storage elements are necessary. This requirement is not a function of $M$ because the storage space can be overwritten for each subsequent block of data. Finally, the MMSE requires $2N^2+N$ storage elements to store the $N \times N$ covariance matrix, its inverse, and the dimension $N$ spreading code. Using the same example as above, the memory requirements associated with the MF, MWF, and MMSE are 32, 192, and $2,080$, respectively. While the storage requirement of the MWF is greater than the MF, it is again significantly less than the MMSE. Furthermore, as long as storage space is available on the desired implementation hardware, the MWF can be accommodated. These equations are summarized in Table 3.2 below.

Table 3.2: Computational Cost and Memory Requirements: Matched Filter (MF), Multistage Wiener Filter (MWF), and Minimum Mean Square Error (MMSE); $N$=length of spreading code; $D$=rank of MWF; $M$=block size

| | Computational Cost | Memory Requirements |
|---|---|---|
| MF | $NM$ | $N$ |
| MWF | $2DNM$ | $(D+1)N$ |
| MMSE | $N^3M$ | $2N^2+N$ |

# Chapter 4

# Minimum Mean Square Error (MMSE)/Rake Receivers

The rake receiver is the conventional processing method for handling multipath in a code division multiple access (CDMA) system by estimating the path amplitudes and delays and combining them at the receiver. However, the rake receiver fails in the presence of a large amount of interference. In this chapter, a minimum mean square error (MMSE) solution for interference suppression and signal detection in the presence of multipath is derived. This is termed the MMSE/rake receiver because it incorporates an MMSE-type solution in conjunction with a rake-type solution. It will be shown via simulation that implementation of this solution using the efficient, reduced rank correlation subtraction architecture (CSA) of the multistage Wiener filter (MWF) ([20], [22], and [21]) meets the full rank MMSE/rake performance at a low rank. Performance results of the standalone rake receiver will be shown for comparison.

The purpose of the MMSE/rake receiver implemented via the CSA-MWF is to perform interference suppression (IS) in the presence of multipath but without the covariance matrix inversion required by MMSE. In designing next generation CDMA

systems, as mentioned in Chapter 1, higher capacity and higher data rates fuel the need for sophisticated signal processing algorithms. For example, new personal communication systems (PCS) may employ short codes, so performance as a function of the code length (N) will be shown. Capacity improvements are shown in terms of the number of users (K) that can be supported. The rank (D) will be shown to be nearly independent of the number of users, thereby enabling a system design in which the number of users does not need to be continuously estimated. This is especially important on the forward link of a CDMA system, where the mobile typically does not have this information. An additional benefit of the MWF implementation is that the mobile does not need to know the spreading codes of the other users to optimally detect its own signal, in the MMSE sense; this is important because it implies that joint detection does not need to be performed for the mobile to detect its signal, but rather a single user detector is sufficient. The low rank and low implementation complexity further imply that the mobile can process the incoming data quickly, enabling higher data rates and the ability to adapt more quickly to rapidly changing channels. Perhaps more remarkably, at lower sample support (M) than required by full rank MMSE, the MWF implementation can actually exceed full rank performance.

Following the derivation of the receiver in Section 4.2, simulation results will be shown. In order to determine performance of the receiver in terms of bit error rate (BER) and its robustness to rank selection, the following parameters are varied: (1) the length of the spreading code ($N$); (2) the signal-to-noise ratio ($E_b/N_0$); (3) the number of bits per block that are processed ($M$); (4) the number of users ($K$); (5) the delay spread of the multipath channel ($L$); and, (6) synchronism vs. asynchronism among the users. In most of the simulations, the user of interest is at $\Delta P = 6$ dB less

power than the interferers. The rank ($D$) can be maintained at a maximum constant value without any loss in performance, independent of the number of users. The simulation parameters of the results presented in the next section are summarized in Table 4.1.

Table 4.1: Minimum Mean Square Error (MMSE)/Rake Receiver Simulation Parameters: $N$=length of spreading code, $E_b/N_0$=Bit energy divided by single-sided noise power spectral density (PSD), $M$=block size, $K$=number of users, $D$=rank of multistage Wiener filter (MWF), $L$=channel delay spread, $\Delta P$=power of interfering users/power of desired user

| | $N$ | $E_b/N_0$ [dB] | $M$ | $K$ | $D$ | $L$ | $\Delta P[dB]$ | Synchronism |
|---|---|---|---|---|---|---|---|---|
| Fig. 4.2 | 32 | 15 | 5000 | 12 | N/A | 5 | 6 | Asynchronous |
| Fig. 4.3 | 32 | N/A | 5000 | 15 | 7 | 5 | 6 | Asynchronous |
| Fig. 4.4 | 32 | 15 | 5000 | N/A | 7 | 5 | 6 | Asynchronous |
| Fig. 4.5 | 32 | 12 | 5000 | N/A | 7 | 5 | 6 | Asynchronous |
| Fig. 4.6 | 32 | 15 | 5000 | 12 | N/A | 5 | 6 | Synchronous |
| Fig. 4.7 | 32 | N/A | 5000 | 15 | 7 | 5 | 6 | Synchronous |
| Fig. 4.8 | 32 | 15 | 5000 | N/A | 7 | 5 | 6 | Synchronous |
| Fig. 4.9 | 32 | 15 | N/A | 15 | 3 | 5 | 0 | Asynchronous |
| Fig. 4.10 | 32 | N/A | 5000 | 15 | 7 | 12 | 6 | Synchronous |
| Fig. 4.11 | 128 | 15 | 5000 | 50 | N/A | 5 | 6 | Asynchronous |

A second receiver which employs an MMSE correlator to improve performance of the conventional rake receiver is described in the following section. This type of receiver could be an easy plug-and-play solution to improve the capacity and performance of existing systems, e.g. IS-95, that employ only rake receivers. This can be done because the receiver is modular in structure, consisting of an MMSE processor to perform interference suppression on each rake 'finger', followed by multipath combining as done by the conventional rake. Performance is shown to be sub-optimal to the

MMSE/rake because the processing spans only one bit and does not include the channel delay spread as the MMSE/rake does. Although this receiver is sub-optimal to the MMSE/rake solution, performance improvement over the rake is significant. The parameters used in simulations in that section are summarized in Table 4.2. First, a brief description of the rake receiver is provided.

Table 4.2: Minimum Mean Square Error (MMSE) Correlator Based Rake Receiver Simulation Parameters: $N$=length of spreading code, $E_b/N_0$=Bit energy divided by single-sided noise power spectral density (PSD), $M$=block size, $K$=number of users, $D$=rank of multistage Wiener filter (MWF), $L$=channel delay spread, $\Delta P$=power of interfering users/power of desired user

| | $N$ | $E_b/N_0$ [dB] | $M$ | $K$ | $D$ | $L$ | $\Delta P[dB]$ | Synchronism |
|---|---|---|---|---|---|---|---|---|
| Fig. 4.13 | 16 | N/A | 5000 | 15 | 7 | 3 | 0 | Synchronous |
| Fig. 4.14 | 16 | 12 | 5000 | N/A | 7 | 3 | 0 | Synchronous |
| Fig. 4.15 | 32 | N/A | 5000 | 30 | 7 | 3 | 0 | Synchronous |

## 4.1 The Rake Receiver

The conventional technique for mitigating multipath effects is the rake receiver [44], introduced in Chapter 1. The rake receiver operates by estimating the channel amplitudes and delays from each of the multiple paths of a transmitted signal in order to coherently combine them. The rake receiver structure is shown in Figure 4.1, where $W$ represents the correlation bandwidth of the received signal. Multipath components that are separated by delays greater than $1/W$ can be resolved by the rake receiver and are thus combined at the output of this tapped-delay line (TDL) to obtain improved performance, known also as the rake diversity gain. The variables $\hat{c}_l$, $l = 1, 2, ..., L$, represent the estimates of the channel coefficients. The parameter L,

also known as the delay spread of the channel, is the total number of paths that are received. While the rake receiver performs well when the number of users is small, its performance degrades significantly for highly loaded systems (i.e. it is interference limited). This occurs because the rake treats the interfering users in the system as additive white Gaussian noise (AWGN), and does not perform any interference rejection. Thus this detection technique is not suitable to meet the increasing capacity requirements on next generation systems.

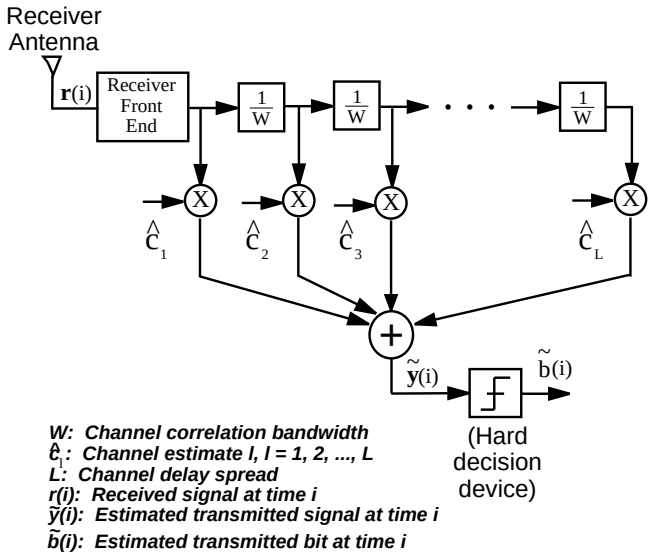


Figure 4.1: Rake Receiver

## 4.2 Optimal MMSE Receiver in Multipath

### 4.2.1 Derivation

Consider an asynchronous CDMA system with $K$ users transmitting. Eq. (2.10) gives the expression for the received signal in the presence of multipath, which for

convenience is rewritten here as [83]

$$\hat{\mathbf{r}}(i) = b_1(i)\hat{\mathbf{s}}_\mathbf{1} + \sum_{k=2}^{K} A_k[b_k(i)\hat{\mathbf{s}}_\mathbf{k}^+ + b_k(i-1)\hat{\mathbf{s}}_\mathbf{k}^-] + \mathbf{n}(i). \tag{4.1}$$

where $\mathbf{s}_1$ is the $N \times 1$ spreading code associated with user one, and $\mathbf{s}_k^+$ and $\mathbf{s}_k^-$ are the $N \times 1$ vectors of spreading codes associated with each of the $K-1$ interfering users. The terms $b_k(i)$ and $b_k(i-1)$ are the current bit and previous bit of user $k$ at time $i$, respectively. Since the general case of asynchronous transmission is assumed, portions of both bits, multiplied with the respective portions of the spreading codes, interfere with the desired user's bit, $b_1(i)$. The notation $\hat{(\cdot)}$ denotes convolution of the operand with the channel coefficients, and $\mathbf{n}(i)$ are AWGN samples.

It is assumed that the channel vector is known, or that it can be accurately estimated by some means, e.g. a training sequence, which can be assumed to be the pilot channel for CDMA systems. Using the analogy between Eq. (2.5) for the AWGN channel and Eq. (2.10) for the multipath channel, the MMSE solution in the presence of multipath can now be written directly from the AWGN solution in Eq. (2.23), or

$$\hat{\mathbf{c}}_{MMSE} = \hat{\mathbf{R}}^{-1}\hat{\mathbf{s}}_\mathbf{1} = E[\hat{\mathbf{r}}\hat{\mathbf{r}}^H]^{-1}\hat{\mathbf{s}}_\mathbf{1}. \tag{4.2}$$

By definition, $\hat{\mathbf{R}}$ is the covariance matrix of the received signal $\hat{\mathbf{r}}$ in multipath. The MWF implementation of this solution can be obtained similarly, by setting $\mathbf{h_0} = \hat{\mathbf{s}}_\mathbf{1}$ in the blind MWF filter shown in Figure 3.2. This solution is similar to the MMSE solution in AWGN, but with the matched filter replaced with a channel matched filter, exactly as the rake receiver. Thus, it is termed the MMSE/rake. Note that the rake solution, which only incorporates the effects of the multipath and neglects

the interference, can be written simply as

$$\mathbf{c}_{rake} = \hat{\mathbf{s}}_{\mathbf{1}}. \tag{4.3}$$

This interpretation of the rake receiver will be justified by an alternate method in the next section. In the presence of only AWGN, this further reduces to the matched filter (MF) solution, $\mathbf{c}_{MF} = \mathbf{s}_{\mathbf{1}}$. The equations above provide a simple and elegant way of representing the rake, MWF, and MMSE filter coefficients when multipath is present. Note that these receivers now span a duration greater than one symbol length of $N$ samples; they now span $N+L-1$ samples, where $L$ was defined previously as the channel delay spread. Validation of these equations is provided using analytical and Monte Carlo simulations in the next section. The analytical expression for the rake receiver is obtained by simply replacing $\mathbf{c}_{MMSE}$ or $\mathbf{c}_{MWF}$ by $\mathbf{c}_{rake}$ in the analytical model and by using $\tilde{b}_1(i) = \hat{\mathbf{s}}_1^H \mathbf{r}(i)$ in the Monte Carlo model.

### 4.2.2 Numerical Results

In this section, simulation results of the linear, reduced rank MMSE/rake receiver using the CSA-MWF are compared with the corresponding full rank MMSE receiver and rake receiver. Results from both the Monte Carlo simulation model and the analytical model are shown for comparison. Unless otherwise indicated, Hadamard codes with a processing gain of $N = 32$ are used. A random, $L$=5 tap Rayleigh distributed channel is used to simulate the multipath, using one tap per chip. The power of the interfering users is set to 6 dB greater than that of the desired user to determine performance in a near-far situation. For this and all subsequent runs, the number of bits per block in the Monte Carlo simulation and the number of blocks is chosen to be large enough to produce enough errors to obtain a valid statistical bit

error rate estimate (typically 10 to 100 errors). At least 10 runs are averaged in the analytical simulations as well, since there is randomness in the spreading codes and their relative shifts (for the asynchronous case). In these plots, Monte Carlo results are indicated with (MC) and analytical results with (AM).

The simulation results are as follows: the first three plots show rank ($D$), $E_b/N_0$, and number of users ($K$) vs. BER for asynchronous CDMA, respectively. The next plot shows the effect of increasing the span of the receiver from 2 bits to 3 bits for asynchronous users via the AM. The next three plots repeat the results from the first three for synchronous CDMA. Then, the effect of block size (M) on the performance of the CSA-MWF vs. the MMSE using the MC model is shown. Finally, for completeness in the analysis, plots of BER for larger $L$ and $N/K$ are provided.

Figure 4.2 shows a plot of rank of the multistage Wiener filter versus the bit error rate (BER) from the Monte Carlo model and $P_e$ from the analytical model. Observe the close agreement between the Monte Carlo and analytical models, as desired. The variation in BER for the MMSE and rake methods is due to the nature of the Monte Carlo simulation, since their performance is independent of rank. Note that for a rank as low as eight, the CSA-MWF performs as well as the full rank MMSE and maintains this performance as rank increases. The performance of the MWF does not significantly degrade until the rank is reduced below five. The MWF performance at full rank exactly matches the full rank MMSE for both models, as expected. Both the MWF and MMSE consistently perform significantly better than the rake receiver, which cannot combat the large number of interfering users. Note that the convergence at rank eight is less than the number of users, $K = 12$, and is significantly less than the full rank of $N = 32$.

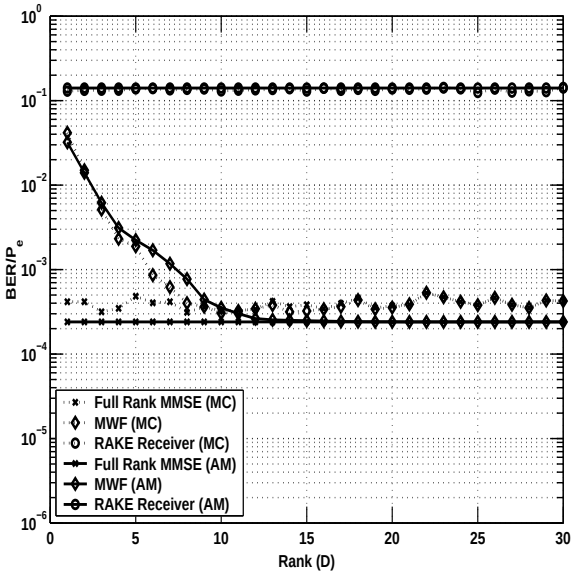


Figure 4.2: Minimum Mean Square Error (MMSE)/Rake Receiver, Multistage Wiener Filter (MWF) Implementation: Rank (D) of the MWF vs. BER; asynchronous CDMA; spreading code length, $N = 32$ (Hadamard Codes); $E_b/N_0 = 15$ dB; number of users, $K = 12$; channel delay spread, $L = 5$; power of interfering users/power of desired user, $\Delta P = 6$ dB (MC=Monte Carlo, AM=Analytical Model).

Figure 4.3 shows a plot of $E_b/N_0$ versus BER. In this case, the rank of the CSA-MWF is seven. It is seen here that the MWF performs as well as the MMSE receiver and significantly better than the rake receiver. Note that there is about a 6 dB degradation in performance from the ideal BPSK curve. This degradation is directly related to the desired user having 6 dB less power relative to the interferers. To a lesser extent, it is also caused by the system's being asynchronous and the environment, including the multipath channel. The performance here could be improved using decision feedback, coding, or power control. Note that the BER has degraded at $E_b/N_0 = 15$ dB from $3 \cdot 10^{-4}$ to about $10^{-3}$ from the preceding case because of the presence of three additional users. However, convergence to full rank MMSE is still

maintained at rank seven, demonstrating the rank robustness of the MWF.

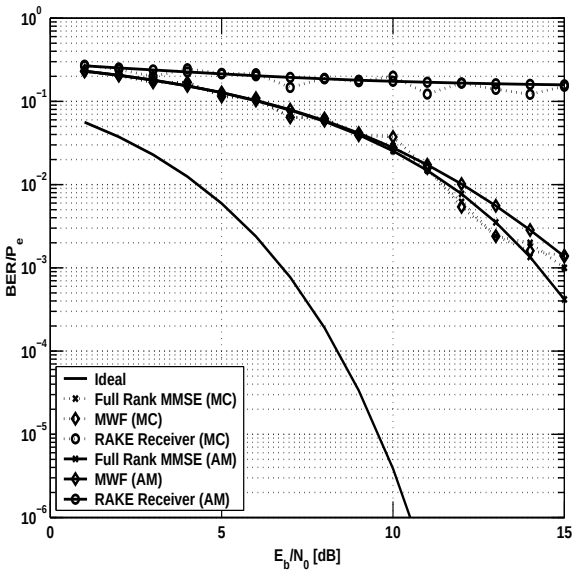


Figure 4.3: Minimum Mean Square Error (MMSE)/Rake Receiver, Multistage Wiener Filter (MWF) Implementation: $E_b/N_0$ [dB] vs. BER; asynchronous CDMA; spreading code length, $N = 32$ (Hadamard Codes); number of users, $K = 15$; rank of MWF, $D = 7$; channel delay spread, $L = 5$; power of interfering users/power of desired user, $\Delta P = 6$ dB (MC=Monte Carlo, AM=Analytical Model).

Next, Figure 4.4 shows a plot of the number of users ($K$) versus BER. Here, the $E_b/N_0$ is 15 dB, and the rank of the multistage Wiener filter is again seven. The number of users varies from 1 to 25. It is seen here that for a lightly loaded system, the rake receiver performs reasonably well, but its error rate degrades rapidly as the load is increased. As before, the MWF meets MMSE performance over the entire range of loading. Note that MWF and MMSE performance does not degrade much as the number of users is increased up to $N/2$. But, when the number of users increases beyond $N/2$, the performance degrades substantially. This occurs because the CDMA signals are asynchronous but the $N + L - 1$ taps of the MC receiver and the 2 bit

taps of the AM receiver in each case span just over the delay spread [48]. To correct this problem, a receiver with taps that span multiple symbols would be required. A sample plot showing the performance difference for the same parameters when the receiver spans two and three symbols is shown in Figure 4.5 using the analytical model. Ths plot shows that increasing the receiver span from two to three symbols improves the BER for $K \geq N/2$ by a factor of 5 to 10. Another possible way to mitigate this problem would be to increase the sampling rate, which is equivalent to increasing the number of taps per bit. Then, the asynchronism would have less of an impact. Of course, coding could also alleviate this problem.

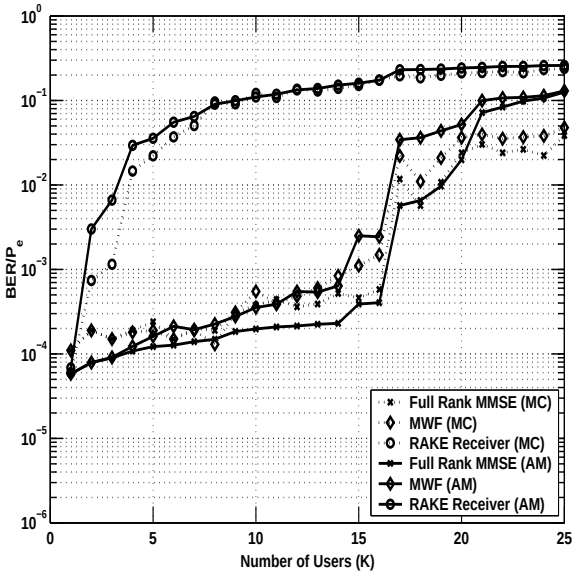


Figure 4.4: Minimum Mean Square Error (MMSE)/Rake Receiver, Multistage Wiener Filter (MWF) Implementation: Number of Users (K) vs. BER; asynchronous CDMA; spreading code length, $N = 32$ (Hadamard Codes); $E_b/N_0 = 15$ dB; rank of MWF, $D = 7$; channel delay spread, $L = 5$; power of interfering users/power of desired user, $\Delta P = 6$ dB (MC=Monte Carlo, AM=Analytical Model).

Figures 4.6-4.8 shows the results for synchronous signals. Note from Figure 4.8

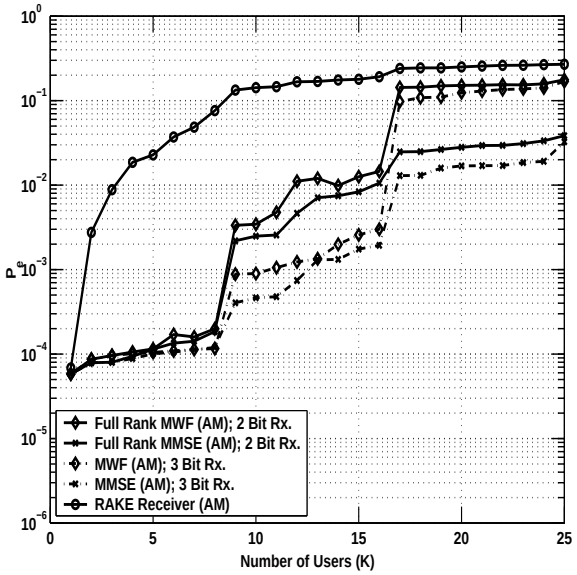


Figure 4.5: Minimum Mean Square Error (MMSE)/Rake Receiver, multistage Wiener filter (MWF) Implementation: Number of Users (K) vs. BER; Asynchronous CDMA; spreading code length, $N = 32$ (Hadamard Codes); $E_b/N_0 = 12$ dB; rank of MWF, $D = 7$; channel delay spread, $L = 5$; power of interfering users/power of desired user, $\Delta P = 6$ dB; 2 Bit Receiver (Rx.) vs. 3 Bit Receiver (AM=Analytical Model).

that the performance does not suffer degradation at $K \geq N/2$ as with asynchronous codes. In fact, performance is maintained with only slight linear degradation versus the number of users. This result shows the promise of the CSA-MWF to accommodate high capacity systems. There is also some improvement, as expected, over the asynchronous data, as the orthogonality among the codes is maintained more precisely. Again, the Monte Carlo model agrees well with the analytical model, as desired.

Figure 4.9 is a curve showing the number of bits per block versus BER. For this result, the $E_b/N_0$ is 15 dB, $K = 15$, and the rank of the CSA-MWF is three. The

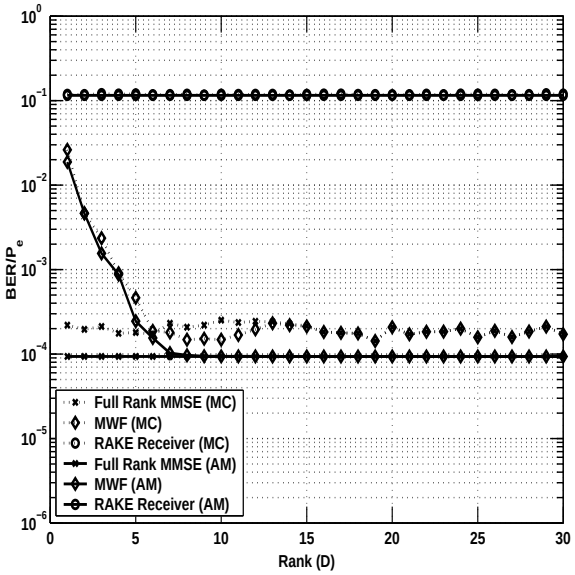


Figure 4.6: Minimum Mean Square Error (MMSE)/Rake Receiver, multistage Wiener filter (MWF) Implementation: Rank (D) of the MWF vs. BER; synchronous CDMA; spreading code length, $N = 32$ (Hadamard Codes); Bit energy divided by single-sided noise power spectral density (PSD), $E_b/N_0 = 15$ dB; number of users, $K = 12$; channel delay spread, $L = 5$; power of interfering users/power of desired user, $\Delta P = 6$ dB (MC=Monte Carlo, AM=Analytical Model).

true BER is shown with a dashed horizontal line. Note that the MMSE curve requires about 2000 samples to converge to the true bit error rate of about $5 \cdot 10^{-4}$. However, the MWF requires only about 1000 samples per block to converge to the same error rate. Thus, the MWF is less sensitive to sample support than the full rank MMSE. This in turn implies that the MWF can track changes in signals that are varying in time faster than MMSE, which is an important advantage of the reduced rank processing provided by the MWF. In addition, the MMSE solution requires inversion of an $N \times N$ covariance matrix, but the MWF does not. This illustrates the twofold benefit in computational savings that can be obtained by employing the

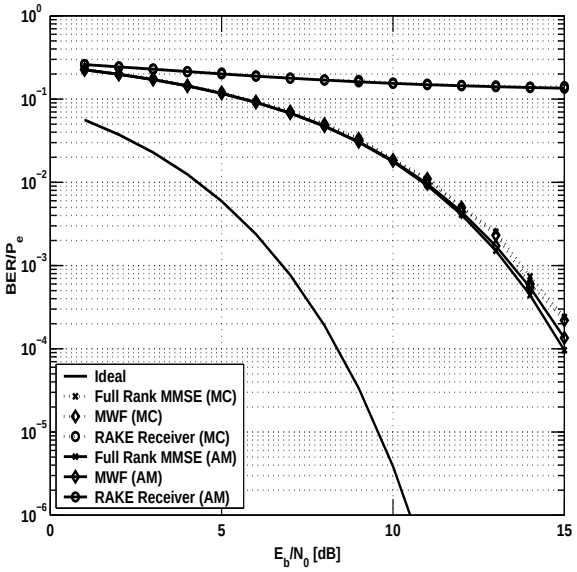


Figure 4.7: Minimum Mean Square Error (MMSE)/Rake Receiver, multistage Wiener filter (MWF) Implementation: $E_b/N_0$ [dB] vs. BER; synchronous CDMA; spreading code length, $N = 32$ (Hadamard Codes); number of users, $K = 15$; rank of MWF, $D = 7$; channel delay spread, $L = 5$; power of interfering users/power of desired user, $\Delta P = 6$ dB (MC=Monte Carlo, AM=Analytical Model).

reduced rank MWF, which yields the same performance as full rank MMSE. Note also that the MWF outperforms full rank for small block sizes. This is another distinguishing feature of the MWF, in that at low sample support and at low rank, it will meet or exceed full rank performance. That is, it simultaneously achieves a convergence speed-up substantially better than other reduced rank techniques **and** at a dramatically reduced computational burden. As before, the rake receiver does significantly worse, achieving at best an error rate forty times worse.

The curve in Figure 4.10 displays $E_b/N_0$ versus BER for synchronous users and a multipath channel tap length of $L = 10$. At a chip rate of 1.2288 Mcps, a delay spread of 8 $\mu$s, which is typical is urban cellular areas, will produce a multipath chip

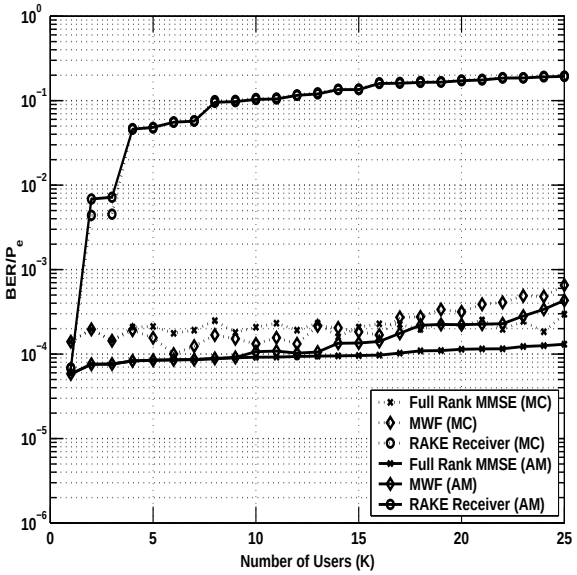


Figure 4.8: Minimum Mean Square Error (MMSE)/Rake Receiver, Multistage Wiener Filter (MWF) Implementation: Number of Users (K) vs. BER; synchronous CDMA; spreading code length, $N = 32$ (Hadamard Codes); $E_b/N_0 = 15$ dB; rank of MWF, $D = 7$; channel delay spread, $L = 5$; power of interfering users/power of desired user, $\Delta P = 6$ dB (MC=Monte Carlo, AM=Analytical Model).

spread of about 10 chips. Therefore, to test the reliability of the MWF in a realistic channel, $L = 10$ is simulated. Note that with $N = 32$, this is equal to a delay of about $\frac{1}{3}$ of a bit. While there is some degradation over the $L = 5$ case, performance of the reduced rank MMSE/rake receiver is maintained. Finally, the plot in Figure 4.11 shows rank vs. BER for asynchronous users with a processing gain of $N = 128$ with $K = 50$ users. Performance is maintained at $10^{-3}$ for large processing gains and large numbers of users.

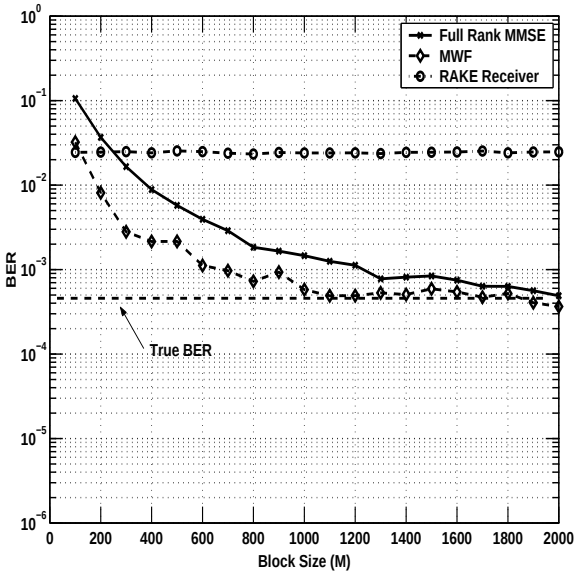


Figure 4.9: Minimum Mean Square Error (MMSE)/Rake Receiver, Multistage Wiener Filter (MWF) Implementation: Block Size (M) vs. BER; asynchronous CDMA; spreading code length, $N = 32$ (Hadamard Codes); $E_b/N_0 = 15$ dB; number of users, $K = 15$; rank of MWF, $D = 3$; channel delay spread, $L = 5$; power of interfering users/power of desired user, $\Delta P = 0$ dB (MC=Monte Carlo).

## 4.3 MMSE Correlator Based Rake Receiver

### 4.3.1 Coherent Rake Receiver

In this section, it is shown how the conventional rake receiver can be modified such that its performance is comparable to the MMSE/rake receiver as derived in the preceding section [54]. It is then shown how to implement this new structure using the MWF. In obtaining the result, it is also proved that the rake receiver can be written compactly in terms of Eq. (4.3).

Recall that the performance of the rake receiver is limited in the presence of multiple access interference (MAI). Assume without loss of generality that the user

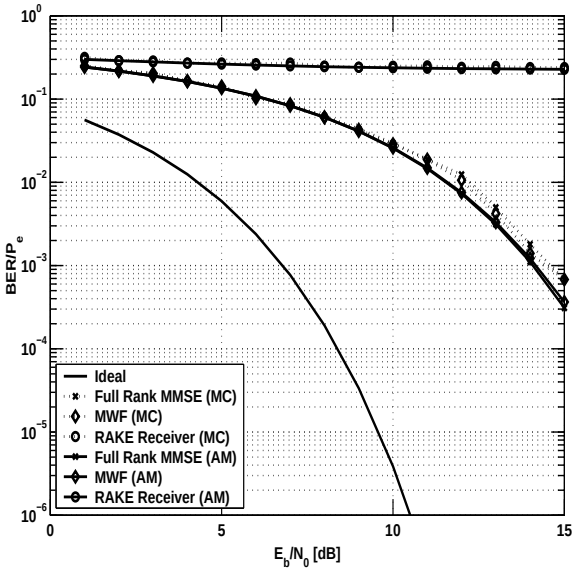


Figure 4.10: Minimum Mean Square Error (MMSE)/Rake Receiver, Multistage Wiener Filter (MWF) Implementation: $E_b/N_0$ vs. BER; synchronous CDMA; spreading code length, $N = 32$ (Hadamard Codes); number of users, $K = 15$; rank of MWF, $D = 7$; channel delay spread, $L = 10$; power of interfering users/power of desired user, $\Delta P = 6$ [dB] (MC=Monte Carlo, AM=Analytical Model).

of interest is user one. To provide insight on how it may be possible to improve the performance of the rake receiver to account for MAI, observe (see Figure 4.1) that the decision variable of the output of the rake receiver configured to detect user one can be written using the convolution integral as

$$\tilde{y} = \sum_{l=1}^{L} \int_0^T s_1^*(t - l/W)\hat{c}_l(t)r(t)dt. \tag{4.4}$$

If it is assumed that the channel is slowly fading, then the channel coefficients can be regarded as remaining constant over several chip periods. In this situation, Eq. (4.4) can be written as

$$\tilde{y} = \sum_{l=1}^{L} \hat{c}_l \int_0^T s_1^*(t - l/W)r(t)dt. \tag{4.5}$$

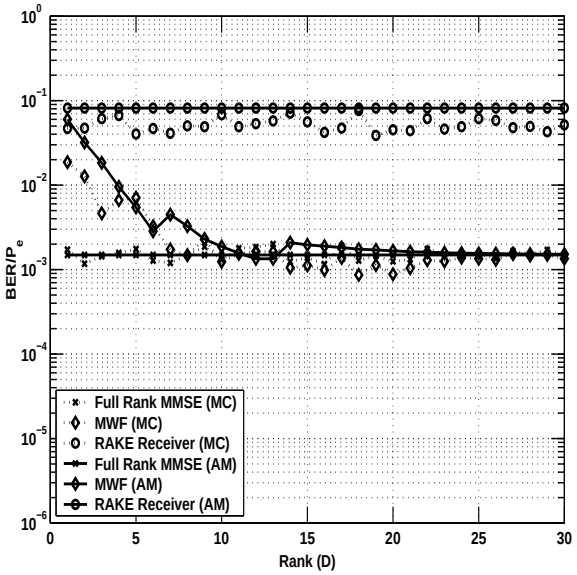


Figure 4.11: Minimum Mean Square Error (MMSE)/Rake Receiver, Multistage Wiener Filter (MWF) Implementation: Rank (D) vs. BER; asynchronous CDMA; spreading code length, $N = 128$ (Hadamard Codes); $E_b/N_0 = 15$ dB; number of users, $K = 50$; channel delay spread, $L = 5$; power of interfering users/power of desired user, $\Delta P = 6$ [dB] (MC=Monte Carlo, AM=Analytical Model).

Eq. (4.5) can be written in discrete form by exploiting the equivalent definition of inner product for discrete time vectors, so that

$$\int_0^T s_1^*(t - l/W)r(t)dt = \langle \bar{\mathbf{s}}_1, \mathbf{r} \rangle = \bar{\mathbf{s}}_1^H \mathbf{r}, \tag{4.6}$$

where $\bar{\mathbf{s}}_1$ are shifted versions of the spreading code for user one in a time interval that span multiple symbols and form the columns of a convolution matrix. So, now, Eq. (4.5) can be written as

$$\tilde{y} = \sum_{l=1}^{L} \hat{c}_l \bar{\mathbf{s}}_1^H \mathbf{r}. \tag{4.7}$$

Now, define $\hat{\mathbf{c}} = [\hat{c}_1, \hat{c}_2, ..., \hat{c}_L]^T$ and $\beta = [\bar{\mathbf{s}}_{1,0}^H \mathbf{r}, \bar{\mathbf{s}}_{1,1}^H \mathbf{r}, ..., \bar{\mathbf{s}}_{1,L-1}^H \mathbf{r}]^T$ where the second subscript denotes the number of samples by which the code has been shifted. The

columns of $\beta$ form the outputs at each "finger" of the rake. One can further write $\beta$ in term of the convolution matrix of the spreading code. That is,

$$\beta = \mathbf{C}_{\bar{s}_1}^H \mathbf{r}, \tag{4.8}$$

where the $N + L - 1 \times L$ matrix $\mathbf{C}_{\bar{s}_1}$ is given by

$$\mathbf{C}_{\bar{s}_1} = \begin{bmatrix} s_1(1) & ... & 0 \\ s_1(2) & ... & 0 \\ \vdots & \ddots & \vdots \\ s_1(N) & ... & s_1(N-2) \\ 0 & ... & s_1(N-1) \\ 0 & ... & s_1(N) \end{bmatrix}. \tag{4.9}$$

With this notation, Eq. (4.7) can be written as

$$\tilde{y} = \hat{\mathbf{c}}^H \mathbf{C}_{\bar{s}_1}^H \mathbf{r}. \tag{4.10}$$

One can further rewrite Eq. (4.10) as

$$\tilde{y} = \mathbf{s}_1^H \mathbf{C}_c^H \mathbf{r} = (\mathbf{C}_c \mathbf{s}_1)^H \mathbf{r}, \tag{4.11}$$

where $\mathbf{C}_c$ is the channel convolution matrix defined analogously to the spreading code convolution matrix. From the last equation, it is easy to recognize that the rake receiver can now be expressed simply as

$$\mathbf{c}_{rake} = \mathbf{C}_c \mathbf{s}_1. \tag{4.12}$$

The equality between this solution and that of Eq. (4.3) is clear, and thus the former is validated.

### 4.3.2 Derivation of MMSE Correlator

From Eq. (4.12), the standard rake receiver can be interpreted as a linear filter defined by a matrix multiplication (or convolution) of the channel coefficients with the desired user's spreading code, i.e. a channel matched filter. It is desirable to utilize an MMSE correlator in place of the matched filter $\mathbf{s}_k$ to suppress the multiple access interference (MAI) to improve upon the rake receiver's performance. Using similar notation as in the preceding section, the MMSE solution that combines multipath and is given in Eq. (4.2) can be rewritten as

$$\mathbf{c}_{MMSE} = \hat{\mathbf{R}}^{-1}\mathbf{C}_c\mathbf{s}. \tag{4.13}$$

To derive the MMSE based correlator, first rewrite $\beta$ from the preceding subsection as

$$\beta = [\mathbf{r}_1^H\mathbf{s}_1, \mathbf{r}_2^H\mathbf{s}_1, ..., \mathbf{r}_L^H\mathbf{s}_1]^H, \tag{4.14}$$

where now the received signal has been time delayed according to each of the $L$ diversity paths. So, now, one can suppress the MAI for each delayed symbol along each path of the rake receiver. To see this, apply MMSE to each delayed component and rewrite Eq. (4.14) as

$$\beta_{MMSE} = [(\mathbf{R}_1^{-1}\mathbf{r}_1)^H\mathbf{s}_1, (\mathbf{R}_2^{-1}\mathbf{r}_2)^H\mathbf{s}_1, ..., (\mathbf{R}_L^{-1}\mathbf{r}_L)^H\mathbf{s}_1]^H \tag{4.15}$$

or

$$\beta_{MMSE} = [\mathbf{r}_1^H\mathbf{R}_1^{-1}\mathbf{s}_1, \mathbf{r}_2^H\mathbf{R}_2^{-1}\mathbf{s}_1, ..., \mathbf{r}_L^H\mathbf{R}_L^{-1}\mathbf{s}_1]^H, \tag{4.16}$$

where $\mathbf{R}_l = E[\mathbf{r}_l\mathbf{r}_l^H]$ denotes the $N \times N$ covariance matrix windowed to the data symbol corresponding to the $l^{th}$ diversity path, and $l = 1, 2, ..., L$. The desired MMSE correlator can thus be defined as

$$\mathbf{s}_{MMSE_l} = \mathbf{R}_l^{-1}\mathbf{s}_1. \tag{4.17}$$

Note that this correlator will be sub-optimal relative to the MMSE/rake receiver described in the preceding section because the data window for suppressing the MAI is now smaller than the convolved channel window.

### 4.3.3 Implementation Using MWF

It is now shown how the MMSE based correlator can be efficiently implemented using the CSA-MWF. From the analogy between Eq. (4.2) and Eq. (4.17), it can easily be seen that the MMSE correlator based rake can be implemented with the structure shown in Figure 4.12. Here, $L = 3$ paths are assumed, so that the received signal is delayed by 3 samples. The MWF applies the MMSE solution to each delayed path, forming the MMSE solution in $\beta_{MMSE}$, and then the delayed paths are combined according to Eq. (4.7). A hard decision on the output $\tilde{\mathbf{y}}(i)$ is used to obtain the bit estimate. Note that this receiver implements the MMSE solution first, followed by the rake, whereas the previously described MMSE/rake receiver reversed the order of the operations.

### 4.3.4 Numerical Results

Figures 4.13, 4.14, and 4.14 are plots of $E_b/N_0$ number of users (K) vs. BER. The first two plots show $E_b/N_0$ and number of users ($K$) versus BER for $N = 16$, respectively, and the third plot shows a highly loaded $N = 32$ system. As expected, this implementation of the CSA-MWF is slightly sub-optimal compared to the full rank MMSE solution and MMSE/rake solution described previously. Note that the sub-optimum performance is less prevalent in the low $E_b/N_0$ regime, where the noise dominates the errors. However, performance is close to optimal because in this case

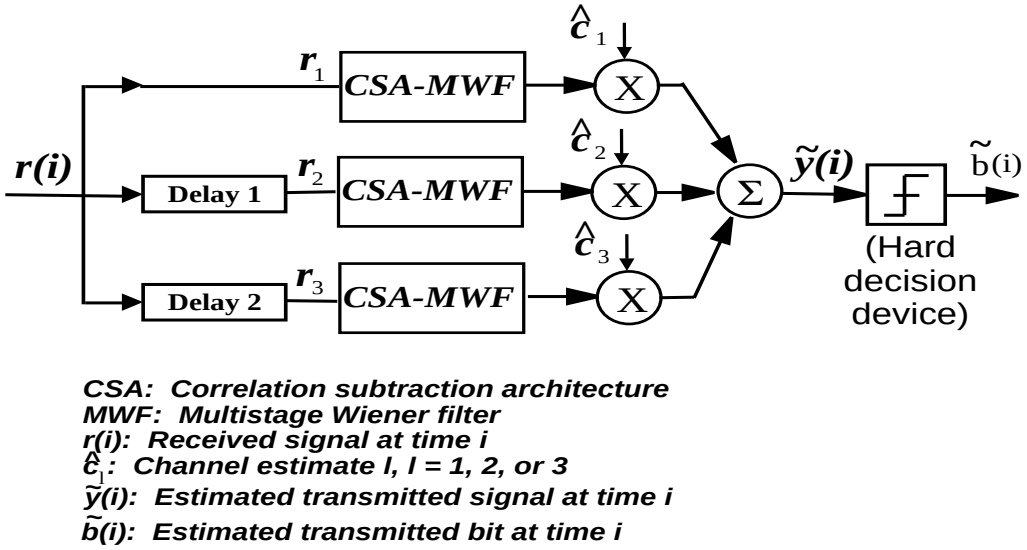


Figure 4.12: Minimum Mean Square Error (MMSE) Correlator Based Rake Receiver Example; channel length, $L = 3$)

the delay spread ($L$) of the channel is much less than the symbol period. In general, as the ratio $L/N$ increases, the degradation of the MMSE correlator based rake relative to the full rank MMSE will increase.

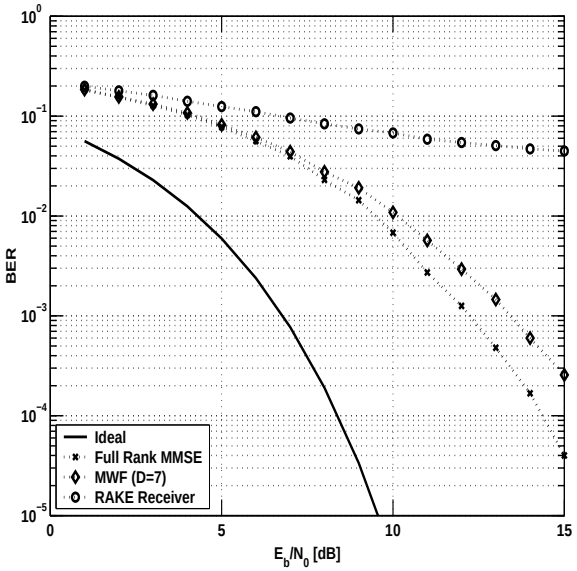


Figure 4.13: Minimum Mean Square Error (MMSE) Correlator Based Rake Receiver, Multistage Wiener Filter (MWF) Implementation: $E_b/N_0$ [dB] vs. BER; synchronous CDMA; spreading code length, $N = 16$ (Hadamard Codes); number of users, $K = 15$; rank of MWF, $D = 7$; channel delay spread, $L = 3$; power of interfering users/power of desired user, $\Delta P = 0$ dB

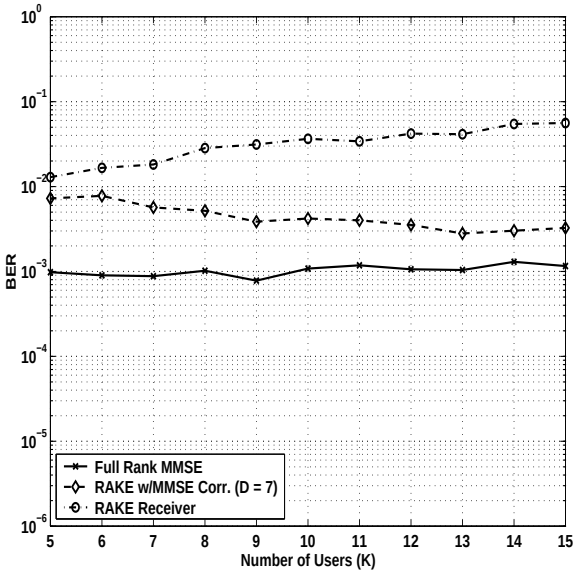


Figure 4.14: Minimum Mean Square Error (MMSE) Correlator Based Rake Receiver, Multistage Wiener Filter (MWF) Implementation: Number of Users (K) vs. BER; synchronous CDMA; spreading code length, $N = 16$ (Hadamard Codes); $E_b/N_0 =$ 12 dB; rank of MWF, $D = 7$; channel delay spread, $L = 3$; power of interfering users/power of desired user, $\Delta P = 0$ dB

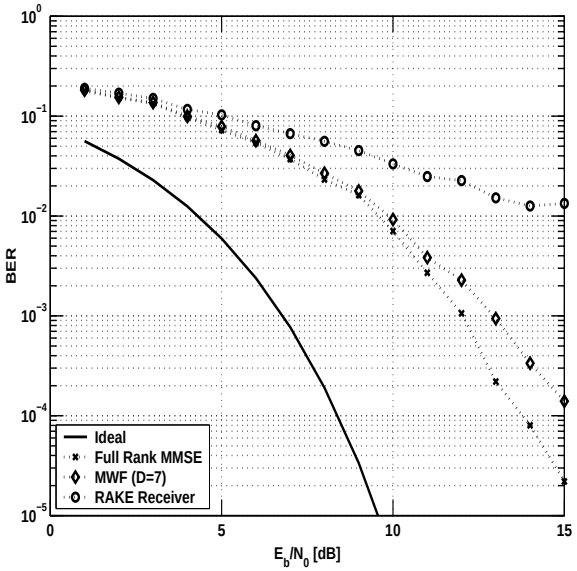


Figure 4.15: Minimum Mean Square Error (MMSE) Correlator Based Rake Receiver, Multistage Wiener Filter (MWF) Implementation: $E_b/N_0$ [dB] vs. BER; synchronous CDMA; spreading code length, $N = 32$ (Hadamard Codes); number of users, $K = 30$; rank of MWF, $D = 7$; channel delay spread, $L = 3$; power of interfering users/power of desired user, $\Delta P = 0$ dB

# Chapter 5

# Reduced Rank Multiuser Detection (MUD) and Interference Suppression (IS)

In this chapter, the multiuser solution for asynchronous users in multipath is derived and its implementation using the correlation subtraction architecture of the multistage Wiener filter (CSA-MWF) is presented. It is shown that the multiuser detector can be implemented in joint form or as a bank of parallel single user detectors, each performing interference suppression (IS), with no loss in performance. In joint form, the matched filter portion is a matrix of spreading codes, whereas in parallel form the single user spreading codes are used. The relationship between the parallel multiuser detector and the single user detector performing IS, as explained in the preceding chapter, is provided. Analysis of the joint detector is discussed in Chapter 6. The parallel MUD solution is compared to other full rank MUD solutions that exist in the literature, e.g. in [35] and [95]. MUD is also explored in [10], [33], [36], [84], [97], and [103].

A performance analysis is provided to determine the conditions under which the multiuser detector implemented by the CSA-MWF performs optimally. It will be

shown that the multiuser detector performs best when the cross-correlation between the spreading codes is low, e.g. as with Gold codes, versus when the cross-correlation is high, e.g. as with Hadamard codes. It will be shown that Gold codes will provide much better performance than Hadamard codes in real channels in which perfect orthogonality cannot be maintained, either due to the asynchronism among the users or the spreading of the codes induced by multipath, thus underscoring the importance of code choice for future generation systems. It is further shown that performance that can be achieved with Gold codes by employing the reduced rank CSA-MWF is often an order of magnitude or more better than with full rank MMSE. The parallel implementation also does not require knowledge of the spreading codes of the interfering users, and is therefore useful for forward link operation when the mobile does not have this information. Simulation parameters are summarized in Table 5.1.

Table 5.1: Multiuser Detector Simulation Parameters: $N$=length of spreading code, $E_b/N_0$=Bit energy divided by single-sided noise power spectral density (PSD), $M$=block size, $K$=number of users, $D$=rank of multistage Wiener filter (MWF), $L$=channel delay spread, $\Delta P$=power of interfering users/power of desired user

| | $N$ | $E_b/N_0$ [dB] | $M$ | $K$ | $D$ | $L$ | $\Delta P[dB]$ | Synchronism |
|---|---|---|---|---|---|---|---|---|
| Fig. 5.4 | 32 | 12 | 5000 | N/A | N/A | 5 | 0 | Synchronous |
| Fig. 5.6 | 32 | 12 | 5000 | N/A | N/A | 5 | 0 | Asynchronous |
| Fig. 5.7 | 31 | 12 | 5000 | N/A | N/A | 5 | 0 | Synchronous |
| Fig. 5.8 | 31 | 12 | 5000 | N/A | N/A | 5 | 0 | Asynchronous |

## 5.1 Derivation of Multiuser Detector

Recall that for the single user (SU) minimum mean square error (MMSE) receiver, the receiver filter coefficients in multipath, denoted in vector form by $\hat{\mathbf{c}}$, are chosen

to minimize the MSE between the transmitted bit and its estimate, given by

$$MSE_{SU} = E[|b_1(i) - \hat{\mathbf{c}}^H \hat{\mathbf{r}}(i)|^2], \tag{5.1}$$

where $E[\cdot]$ denotes the expected value operator and $(\cdot)^H$ represents the Hermitian transpose operator. The subscript SU (for single user) will be used to distinguish this solution from the multiuser solution. The MMSE solution in the presence of multipath was shown to be given by Eq. (4.2), repeated here for convenience as

$$\hat{\mathbf{c}}_{MMSE} = \hat{\mathbf{R}}^{-1}\hat{\mathbf{s}}_{\mathbf{1}} = E[\hat{\mathbf{r}}\hat{\mathbf{r}}^H]^{-1}\hat{\mathbf{s}}_{\mathbf{1}}. \tag{5.2}$$

For the MUD problem, the goal is to choose the receiver filter coefficients, denoted now in matrix form by $\hat{\mathbf{C}}$, to minimize the mean square error (MSE) between the vector of transmitted bits, $\mathbf{b}(i) = (b_1(i)\ b_2(i)\ ...\ b_K(i))$ and their estimates $\tilde{\mathbf{b}}(i) = (\tilde{b}_1(i)\ \tilde{b}_2(i)\ ...\ \tilde{b}_K(i))$ for all $k = 1, 2, ..., K$ users. This can be written as

$$MSE_{MUD} = E[||\mathbf{b}(i) - \tilde{\mathbf{b}}(i)||^2], \tag{5.3}$$

where

$$\tilde{\mathbf{b}}(i) = \hat{\mathbf{C}}^H \hat{\mathbf{r}}(i). \tag{5.4}$$

To obtain the MMSE solution, the above quantity must be minimized [81]. First, using the identity $||\mathbf{x}||^2 = trace(\mathbf{x}\mathbf{x}^H)$, where $trace(\mathbf{X})$ is the sum of the diagonal elements of matrix $\mathbf{X}$, write

$$\min_{\hat{\mathbf{C}}} E[trace((\mathbf{b}(i) - \hat{\mathbf{C}}^H \hat{\mathbf{r}}(i))(\mathbf{b}(i) - \hat{\mathbf{C}}^H \hat{\mathbf{r}}(i))^H)]. \tag{5.5}$$

Since the trace of the covariance of a vector quantity is always non-negative, the trace operation can be ignored. Expanding the quantity in brackets, one obtains

$$\min_{\hat{\mathbf{C}}} E[\mathbf{b}(i)\mathbf{b}(i)^H - \mathbf{b}(i)\hat{\mathbf{r}}(i)^H\hat{\mathbf{C}} - \hat{\mathbf{C}}^H\hat{\mathbf{r}}(i)\mathbf{b}(i)^H - \hat{\mathbf{C}}^H\hat{\mathbf{r}}\hat{\mathbf{r}}^H\hat{\mathbf{C}}]. \tag{5.6}$$

Next, from the linearity property of the $E[\cdot]$ operation, consider separately each of the terms in the brackets:

- $E[\mathbf{b}(i)\mathbf{b}(i)^H] = \mathbf{I}$
- $E[\mathbf{b}(i)\hat{\mathbf{r}}(i)^H\hat{\mathbf{C}}]$
  $= E[\mathbf{b}(i)(\mathbf{b}(i)^H\mathbf{A}\hat{\mathbf{S}}^{+H} + \mathbf{b}(i-1)^H\mathbf{A}\hat{\mathbf{S}}^{-H} + \mathbf{n}(i))]\hat{\mathbf{C}}$
  $= \mathbf{A}\hat{\mathbf{S}}^{+H}\hat{\mathbf{C}}$
- $E[\hat{\mathbf{C}}^H\hat{\mathbf{r}}(i)\mathbf{b}(i)^H]$
  $= \hat{\mathbf{C}}^H E[(\hat{\mathbf{S}}^{+}\mathbf{A}\mathbf{b}(i) + \hat{\mathbf{S}}^{-}\mathbf{A}\mathbf{b}(i-1) + \mathbf{n}(i))\mathbf{b}(i)^H]$
  $= \hat{\mathbf{C}}^H\hat{\mathbf{S}}^{+}\mathbf{A}$
- $E[\hat{\mathbf{C}}^H\hat{\mathbf{r}}\hat{\mathbf{r}}^H\hat{\mathbf{C}}] = \hat{\mathbf{C}}^H E[\hat{\mathbf{r}}\hat{\mathbf{r}}^H]\hat{\mathbf{C}} = \hat{\mathbf{C}}^H\hat{\mathbf{R}}\hat{\mathbf{C}}$.

In the second and third expression above, the fact that $\mathbf{b}(i)$ and $\mathbf{b}(i-1)$ are independent, identically distributed random variables so that their expected value is zero has been used. The fact that $\mathbf{A}$ is a real, diagonal matrix so that $\mathbf{A}^H = \mathbf{A}$ is employed. Furthermore, since the noise $\mathbf{n}(i)$ is additive white Gaussian noise (AWGN), its samples are uncorrelated with the data, so the expected value of their product is zero as well. The definition of the covariance matrix $\hat{\mathbf{R}}$ from Eq. (4.2) has been applied to the last term. Substituting these expressions into Eq. (5.6), the MSE can be written as

$$\min_{\hat{\mathbf{C}}}[\mathbf{I} - \mathbf{A}\hat{\mathbf{S}}^{+H}\hat{\mathbf{C}} - \hat{\mathbf{C}}^H\hat{\mathbf{S}}^{+}\mathbf{A} + \hat{\mathbf{C}}^H\hat{\mathbf{R}}\hat{\mathbf{C}}]. \tag{5.7}$$

To solve Eq. (5.7), take its gradient with respect to the minimization parameter $\hat{\mathbf{C}}$ and set the result equal to zero. This yields

$$-\mathbf{A}\hat{\mathbf{S}}^{+H} - \mathbf{A}\hat{\mathbf{S}}^{+H} + \hat{\mathbf{C}}^H\hat{\mathbf{R}}^H + \hat{\mathbf{C}}^H\hat{\mathbf{R}} = \mathbf{0}. \tag{5.8}$$

Now, using the property that the covariance matrix of a stationary discrete time random process is Hermitian, or $\hat{\mathbf{R}}^H$=$\hat{\mathbf{R}}$ [30], the final solution is given by

$$\hat{\mathbf{C}}_{MMSE} = \hat{\mathbf{R}}^{-1}\hat{\mathbf{S}}^{+}\mathbf{A}. \tag{5.9}$$

Before proceeding to the implementation of this solution, a few important observations are discussed. First, note that the solution for the $k^{th}$ user can be written individually by simply extracting the $k^{th}$ columns of $\hat{\mathbf{S}}^{+}$ and of $\mathbf{A}$. That is, the MUD solution may be written as

$$\hat{\mathbf{C}}_{MMSE} = [\hat{\mathbf{c}}_{1/MMSE},\ \hat{\mathbf{c}}_{2/MMSE},\ ...,\ \hat{\mathbf{c}}_{K/MMSE}], \tag{5.10}$$

where

$$\hat{\mathbf{c}}_{k/MMSE} = \hat{\mathbf{R}}^{-1}\hat{\mathbf{s}}_k^{+}A_k \tag{5.11}$$

for the $k^{th}$ user. Thus, the matrix form of the MUD solution can be implemented in vector form using parallel single user detectors. This agrees with the results stated in [35]. Note the similarity between the MUD solution in Eqs. (5.9) and (5.11) and the single user solution given in Eq. (4.2). Second, note that the synchronous solution is obtained by setting $\hat{\mathbf{S}}^{+} = \hat{\mathbf{S}}$ or setting $\hat{\mathbf{s}}_k^{+} = \hat{\mathbf{s}}_k$ in Eqs. (5.9)and (5.11), respectively (with $\hat{\mathbf{S}}^{-} = 0$ and $\hat{\mathbf{s}}_k^{-} = 0$). Also, recall from Eq. (2.31) that the covariance matrix, if expanded in terms of the received signal $\hat{\mathbf{r}}(i)$ in Eq. (2.10), is given by

$$\hat{\mathbf{R}} = \hat{\mathbf{S}}^{+}\mathbf{A}^2\hat{\mathbf{S}}^{+H} + \hat{\mathbf{S}}^{-}\mathbf{A}^2\hat{\mathbf{S}}^{-H} + \sigma^2\mathbf{I}. \tag{5.12}$$

Even though in the presence of multipath, $\hat{\mathbf{S}}^{+}$ and $\hat{\mathbf{S}}^{-}$ are not orthogonal, the independence of the current bit $\mathbf{b}(i)$ and previous bit $\mathbf{b}(i-1)$ forces the expectation of the cross-terms to zero. This equation is similar to Eq. (10) of [32], which is shown for the AWGN case.

## 5.2 Implementation of Multiuser Detector using the Multistage Wiener Filter (MWF)

For the multiuser detection (MUD) problem, the solution of Eqs. (5.9) or (5.11) show that the MUD implementation can be obtained in matrix form ($\mathbf{H_0}$) or vector form ($\mathbf{h}_{0,k}$) by replacing the initialization step of the CSA-MWF recursion equations with

$$\mathbf{H}_0 = \hat{\mathbf{S}}^+ \; ; \; \mathbf{d}_0 = \hat{\mathbf{S}}^{+H}\tilde{\mathbf{x}}(i) \tag{5.13}$$

or

$$\mathbf{h}_{0,k} = \hat{\mathbf{s}}_{\mathbf{k}}^+ \; ; \; d_{0,k} = \hat{\mathbf{s}}_{\mathbf{k}}^{+H}\tilde{\mathbf{x}}(i), \tag{5.14}$$

where in the case of Eq. (5.14) an additional subscript $k$ has been added to indicate that the recursions are now performed separately for each user $k$. That is, a bank of $K$ parallel Wiener filters, each operating in a reduced rank subspace, is employed. This structure is shown in Fig. 5.1. In this figure, the subscript $jk$ refers to stage $j$ in the correlation subtraction architecture (CSA) of the MWF for user $k$, respectively, where a total of $D$ stages and $K$ users are assumed. As with the single user Wiener filter, the bit estimates for each user are given by $b_k(i) = \epsilon_{0k}(i)$ for $k = 1, 2, ..., K$.

## 5.3 Comparison to Previous Multiuser Detectors

In this section, the full rank MMSE MUD solution obtained above is compared to existing solutions presented in the recent literature. The differences between the existing full rank solutions and the new reduced rank solution are described and discussed. This is important to ensure that the new solution does not contradict previous works. In [35], Eq. (9), the MUD solution is derived for synchronous users

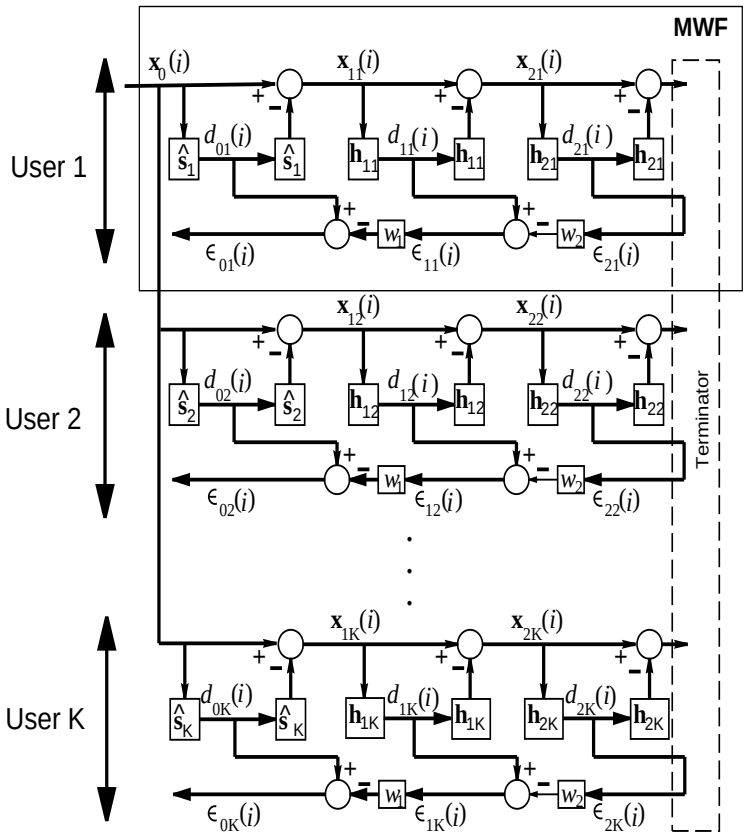


Figure 5.1: Parallel Multiuser Detector Using the Correlation Subtraction Architecture of the Multistage Wiener Filter (CSA-MWF), $D = 2$ stages; $\hat{\mathbf{s}}_k$=spreading code of user $k$ convolved with channel coefficients; $\epsilon_{0k}$=bit estimate of user $k$, $k = 1, 2, ..., K$

and, using the same notation as in this dissertation, is given by

$$\hat{\mathbf{C}}_{MMSE} = \hat{\mathbf{S}}(\hat{\mathbf{S}}^H\hat{\mathbf{S}} + \sigma^2\mathbf{I})^{-1}. \tag{5.15}$$

It can be shown via the Matrix Inversion Lemma (MIL), see e.g. [74], given below as

$$(A + BCD)^{-1} = A^{-1} - A^{-1}B(DA^{-1}B + C^{-1})^{-1}DA^{-1}, \tag{5.16}$$

that this solution can also be written as

$$\hat{\mathbf{C}}_{MMSE} = (\hat{\mathbf{S}}\hat{\mathbf{S}}^H + \sigma^2\mathbf{I})^{-1}\hat{\mathbf{S}}. \tag{5.17}$$

Comparing the new solution in Eq. (5.9) to Eq. (5.17), it can be seen that the former solution simplifies to the latter solution for the synchronous AWGN case. Indeed, by letting $\hat{\mathbf{S}}^{+} = \hat{\mathbf{S}}$ (and $\hat{\mathbf{S}}^{-} = \mathbf{0}$) as would be for synchronous users, the new solution is exactly that of Eq. (5.17). The amplitude matrix is absent because it is absorbed into the spreading code matrix in Eqs. (5.15) and (5.17). Note that the same result is also given in Eq. (15) of [33].

Another full rank MUD solution is presented in [95]. Converting this to the adopted notation, and applying the MIL, this solution can be reformulated as

$$\hat{\mathbf{C}}_{MMSE} = \mathbf{A}^{-1}[(\hat{\mathbf{S}}\hat{\mathbf{S}}^{H} + \sigma^{2}\mathbf{A}^{-2})^{-1}\hat{\mathbf{S}}]. \tag{5.18}$$

Since $\mathbf{A}$ is a diagonal matrix, the above equation can be written as

$$\hat{\mathbf{C}}_{MMSE} = (\hat{\mathbf{S}}\mathbf{A}^{2}\hat{\mathbf{S}}^{H} + \sigma^{2}\mathbf{I})^{-1}\hat{\mathbf{S}}\mathbf{A}. \tag{5.19}$$

This equation is also derived for the case of synchronous users in AWGN. Now, if the same conditions are again assumed for the new solution, namely that $\hat{\mathbf{S}}^{+} = \hat{\mathbf{S}}$ (and $\hat{\mathbf{S}}^{-} = \mathbf{0}$) as before and the value of $\hat{\mathbf{R}}$ given in Eq. (5.12) is substituted into Eq. (5.9), the solution of Eq. (5.19) is found to be identical. Thus, it is seen that under the same conditions, the new MUD solution agrees with the full rank solutions in the literature. However, the solution derived herein is more general in that it can be applied to asynchronous users in multipath environments. Furthermore, it is emphasized that computation of these full rank solutions is not feasible in practice due to the inability to obtain and/or invert the covariance matrix $\hat{\mathbf{R}}$. Thus, the reduced rank solution is highly useful.

Note that in practice, for the reverse link of a cellular communications system, either the parallel or the matrix multiuser detectors can be applied. In the parallel

case, only synchronization with the desired user is necessary for each SU detector, and all other users are suppressed. In the forward link, the handset is only interested in detecting one user, so in this case an SU detector performing IS is sufficient. However, performance will be the same as if each user performs MUD. Finally, note that the above derivation only suggests the use of a reduced rank scheme to implement the MUD solution in the form of a parallel bank of Wiener filters. It does not state that the rank of the parallel scheme will be equivalent to the rank of the joint MUD solution. In general, this will not be the case, as is analyzed in the next chapter.

## 5.4 Performance Analysis

In the previous section, it is shown that the optimum linear solution to the MUD problem can be implemented in reduced rank form using a bank of parallel CSA-MWF receivers, each performing IS. In this section, an analysis is performed to show how the bit error rate (BER) varies as a function of rank, the number of users and the synchronism among the users, and even the type of code employed (i.e. Hadamard or Gold code). First, note from Eqs. (5.4) and (5.10) that one can write the bit estimates for each user individually as

$$\tilde{\mathbf{b}}_k(i) = \hat{\mathbf{c}}_{k/MMSE}^H \hat{\mathbf{r}}(i). \tag{5.20}$$

Substituting for $\hat{\mathbf{c}}_{k/MMSE}$ using Eq. (5.11) and for the received signal using Eq. (4.1), the solution can be written explicitly as

$$\tilde{\mathbf{b}}_k(i) = \hat{\mathbf{R}}^{-1}\hat{\mathbf{s}}_k^{+H} A_k[\hat{\mathbf{S}}^{+}\mathbf{A}\mathbf{b}(i) + \hat{\mathbf{S}}^{-}\mathbf{A}\mathbf{b}(i-1) + \mathbf{n}(i)]. \tag{5.21}$$

It is seen from this equation that the quality of the bit estimates is largely determined by the ability of the receiver to suppress the cross-correlation of the desired user's

code with the codes of the interference; this implies that for good performance $\hat{\mathbf{s}}_k^{+H}\hat{\mathbf{S}}_i^{+}$ and $\hat{\mathbf{s}}_k^{+H}\hat{\mathbf{S}}_i^{-}$ should be as close to zero as possible for all $i \neq k$, in which $\hat{\mathbf{S}}_i^{+}$ and $\hat{\mathbf{S}}_i^{-}$ denote the $i^{th}$ columns of $\hat{\mathbf{S}}^{+}$ and $\hat{\mathbf{S}}^{-}$, respectively. Note that when $i = k$, $\hat{\mathbf{s}}_k^{+H}\hat{\mathbf{S}}_i^{+} = 1$ and $\hat{\mathbf{s}}_k^{+H}\hat{\mathbf{S}}_i^{-} = 0$ [82]. Thus, codes that have low cross-correlation properties are highly desirable. The codes currently in use on CDMA systems, and the ones being considered for the future generation systems are Hadamard and Gold codes. A brief description of each type of code is now provided to determine which ones have the most desirable properties.

**Hadamard Codes** : Hadamard codes are obtained from the columns of square Hadamard matrices. In a Hadamard matrix, the rows and columns form mutually orthogonal vectors containing elements only in $(+1, -1)$ [44]. The simplest $2 \times 2$ Hadamard matrix is given by

$$\mathbf{H}_2 = \begin{bmatrix} 1 & 1 \\ 1 & -1 \end{bmatrix}. \tag{5.22}$$

Hadamard codes of increasing powers of two can be found from the recursion

$$\mathbf{H}_{2N} = \begin{bmatrix} H_N & H_N \\ H_N & \bar{H}_N \end{bmatrix}, \tag{5.23}$$

where $N$ must be a power of two and $\bar{H}_N$ denotes the complement of $H_N$. Furthermore, if $H_a$ and $H_b$ are Hadamard matrices of order $a$ and $b$, respectively, then $H_{ab}$ is also a Hadamard matrix that is given by $H_a \times H_b$.

**Gold Codes** : While pseudo-random (PN) sequences have good auto-correlation properties, their cross-correlation properties can produce large peaks. Thus, while these sequences have desirable properties for CDMA applications, they are problematic in multiuser environments when each user transmits with a distinct PN code. As mentioned before, these codes limit the capacity of existing CDMA systems on the

reverse link. Gold codes are generated by the modulo-2 addition of two PN sequences that have been generated by two distinct polynomials. These codes were discovered [18] to overcome the cross-correlation problems of PN sequences. These codes are also easily generated, as two length $n$ shift registers can produce $2^n + 1$ Gold codes, compared to only $\Phi(2^n - 1)/n$ PN sequences. Here, $\Phi(x)$ denotes Euler's number, equal to the number of positive integers that are relatively prime to all the numbers less than $x$.

The cross-correlation functions of the length $N = 32$ Hadamard codes and length $N = 31$ Gold codes are illustrated in Fig. 5.2. The zeroth lag of the output correlation is in the middle of the grid, at element or row $N$. The corresponding plot showing the orthogonality properties is shown in Fig. 5.3. From these figures, note that Hadamard codes are orthogonal, but they have poor cross-correlation properties. Thus, when these codes are used as the spreading sequences in the case of asynchronous users and/or a multipath environment, performance is expected to degrade as the number of users increases. On the other hand, Gold codes have a limit in the maximum cross-correlation peak, and this limit is well-defined [65]. They also maintain good orthogonality. This is the reason why Gold codes should now be the preferred spreading codes of future CDMA systems, whereas Hadamard codes are used only to provide orthogonal modulation. This feature of Gold codes is especially important on the reverse link, where asynchronous transmission precludes the ability of the Hadamard codes to suppress large amounts of interference. Of course, in the absence of multipath, synchronous Hadamard codes would outperform Gold codes, given their ideal orthogonality properties [82]. Thus, for the forward link, which has synchronous transmission, if multipath is not severe, then the Hadamard code

is more suitable. This analysis clearly shows that future system designers should consider code selection carefully.

Now, the overall cross-correlation threshold of the Gold codes is lower. Thus, it is to be expected that these codes will perform at least as well as the Hadamard codes in the synchronous case, but better than the Hadamard codes in the asynchronous, multipath case. It is also expected that the performance will degrade as the number of users is increased for asynchronous Hadamard codes and synchronous or asynchronous Gold codes, as the properties are less than ideal. Synchronous Hadamard codes, however, will not cause degradation as the number of users increases, as their ability to suppress the perfectly orthogonal interference is maintained, although with multipath, slight losses are incurred. In addition, for both Hadamard and Gold codes, as the number of users increases, the optimum rank required to meet the full rank MMSE performance will increase. But, it is important to note that this is not a linear function, and performance is still optimum at a much reduced rank. This is an outstanding feature of the MWF that makes it a promising tool in a multitude of applications. Furthermore, it has been shown [32], that performance at low rank may exceed that of full rank. This can occur if the codes have good correlation properties that enable the MWF to suppress interference more reliably, as with Gold codes. These remarks are validated with simulation results using both Hadamard and Gold codes, presented in the next section.

## 5.5 Numerical Results

In this section, results obtained from Monte Carlo simulations to show the validity of the MUD solution derived above and its performance as a function of rank ($D$)

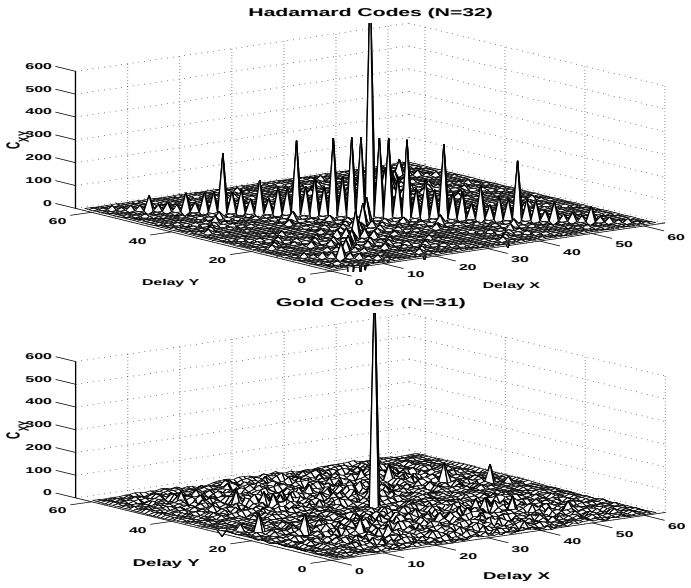


Figure 5.2: Cross-Correlation Functions (Hadamard and Gold Codes); spreading code length, $N$

and the number of users ($K$) are presented. Simulation results for synchronous and asynchronous users as a function of rank using Hadamard and Gold codes of length $N = 32$ and $N = 31$, respectively, are shown. The BER obtained is an average over all the users present in the system using the parallel MUD implementation shown in Fig. 5.1. The BER of the full rank MMSE receiver is averaged over all the runs for a better estimate, as its performance is independent of rank. The results are analyzed next.

Fig. 5.4 shows a plot of rank of the MWF versus the BER for synchronous, Hadamard codes. It is observed that performance meets, and even exceeds, full rank for 5, 10, and 15 users at extraordinary low ranks of about 1, 1, and 2, respectively. Furthermore, the BER converges to the same value in both cases. As mentioned

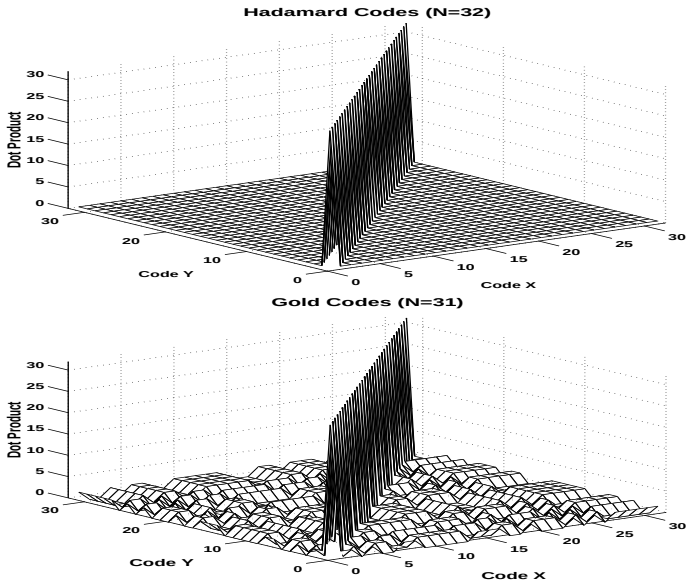


Figure 5.3: Orthogonality Functions (Hadamard and Gold Codes); spreading code length, $N$

above, this is due to the orthogonality property of the Hadamard codes and the ability of the MWF to suppress the orthogonal interference. The performance of the MWF does not significantly degrade except for the 15 user case at rank 1, i.e. a one stage filter. The MWF performance at these low ranks meets the full rank MMSE and maintains performance as rank increases.

The next curve in Fig. 5.6 shows rank versus BER for the case of 5, 10, and 15 asynchronous Hadamard codes. In this case, convergence of BER is seen at ranks of only 1, 1, and 5, respectively. But, note that unlike the synchronous case, the BER degrades slightly as more users are added to the system. As pointed out earlier, while Hadamard codes maintain orthogonality, they also have poor cross-correlation properties in general, and thus gradual degradation is expected with the asynchronous case as the number of users increases. Note also the overall performance degradation

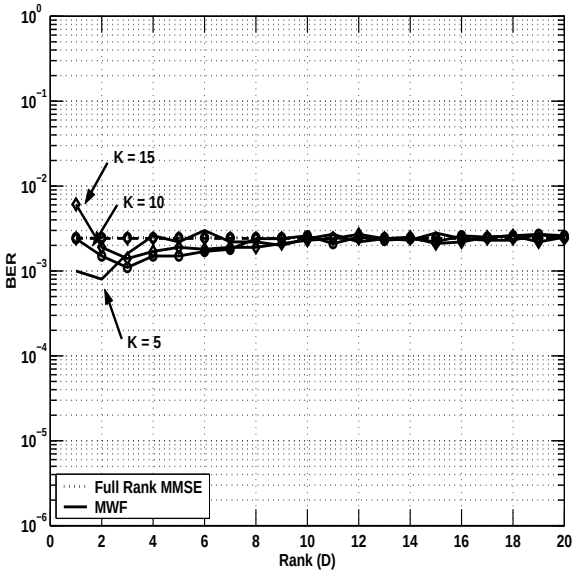


Figure 5.4: Multiuser Detector: Rank (D) vs. BER; synchronous CDMA; spreading code length, $N = 32$ (Hadamard Codes); $E_b/N_0 = 12$ dB; channel delay spread, $L = 5$; power of interfering users/power of desired user, $\Delta P = 0$ dB

versus the synchronous case, which again is attributed to the poor cross-correlation properties.

Recall for speech transmission, the BER should be about $10^{-3}$ or better to be considered operational. This translates to a minimum signal-to-noise ratio (S/N) requirement of about 30 dB. The simulations above show that in the synchronous case, the Hadamard codes fail to support the increasing capacity. For asynchronous users, Hadamard codes fail even with a capacity as low as 5 users. Thus, these codes are not suitable for future generation links, especially when users are asynchronous. To improve the performance on such a link, forward error control (FEC) would be needed. Convolutional codes are used in IS-95 to improve the BER, and it is seen that the Hadamard codes will not perform acceptably without them. A

convolutional encoder is used to add redundancy to the information bits prior to modulation [99]. The purpose of encoding is to reduce the required $E_b/N_0$ at the receiver at versus that of an uncoded system at the same BER. This difference in $E_b/N_0$ is known as coding gain. An example of a rate $\frac{1}{2}$ recursive convolutional encoder (RCC) of constraint length equal to 3 is shown in Fig. 5.5. This is an example of an encoder that employs recursive feedback so that for each information bit, denoted $x$ in the figure, the encoder transmits an additional parity bit, denoted $p$. The inherent limitations of Hadamard codes are overcome by Gold codes, as seen next.

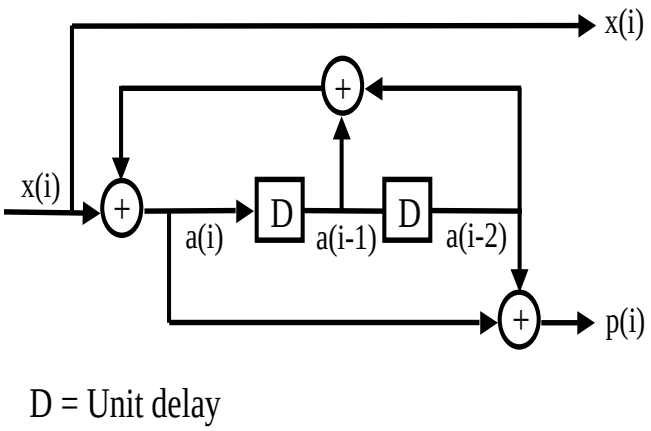


Figure 5.5: Rate $\frac{1}{2}$ Recursive Convolutional Encoder (RCC); $x(i)$=input bit, $p(i)$=parity bit at time i

Fig. 5.7 shows rank versus BER for the case of 5, 10, and 15 synchronous users with Gold sequences. In this case, convergence of BER is seen to occur quickly, at ranks of only 1 or 2. Note that the MWF performance *exceeds* full rank performance by up to two orders of magnitude at ranks from 2 to 9, but then eventually converges

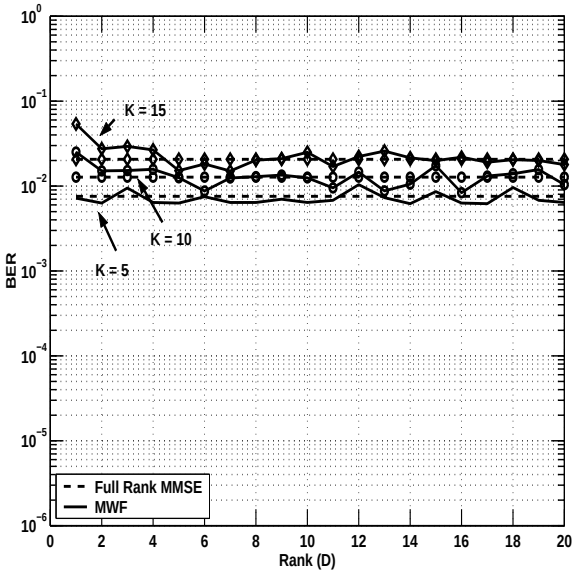


Figure 5.6: Multiuser Detector: Rank (D) vs. BER; asynchronous CDMA; spreading code length, $N = 32$ (Hadamard Codes); $E_b/N_0 = 12$ dB; channel delay spread, $L = 5$; power of interfering users/power of desired user, $\Delta P = 0$ dB

again. This effect is not observed for the case of Hadamard codes and can be explained by observing that the slight asynchronism produced by the multipath results in Hadamard codes separated by a very small amount. From Fig. 5.2, it is seen that this in turn results in high correlation peaks, which makes suppression difficult. In the case of the Gold codes, the high correlation peaks do not occur. This dramatic effect has also been shown in [32] and is a remarkable property of the MWF to simultaneously achieve a convergence substantially better than that achieved with full rank MMSE *and* a dramatically reduced computational burden as well. Intuitively speaking, the MWF achieves the best of both worlds - faster convergence and reduced computation - by applying the information inherently contained in both the covariance matrix and the cross-correlation vector in choosing the reduced-dimension

subspace in which the weight vector is constrained to lie. Finally, note that unlike the synchronous Hadamard codes, degradation in performance is observed with synchronous Gold codes. Again, this is due to the orthogonality properties, which are less than ideal.

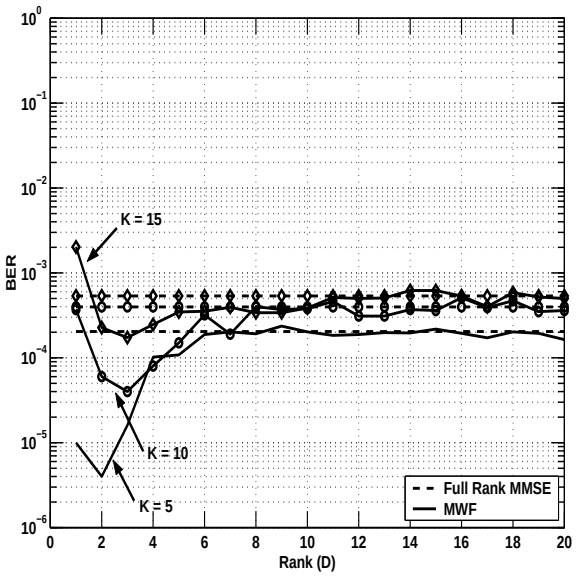


Figure 5.7: Multiuser Detector: Rank (D) vs. BER; synchronous CDMA; spreading code length, $N = 31$ (Gold Codes); $E_b/N_0 = 12$ dB; channel delay spread, $L = 5$; power of interfering users/power of desired user, $\Delta P = 0$ dB

Fig. 5.8 shows rank versus BER with 5, 10 and 15 asynchronous users using Gold codes. In this case, convergence of BER is seen at ranks of 1, 3, and 4. Note that unlike the synchronous case, the BER here also degrades as more users are added to the system. As seen in Fig. 5.2, while Gold codes have good cross-correlation properties, there still exists some correlation among them, and this effect is enhanced by the imperfect orthogonality, as seen also in Fig. 5.7. In the 15 user case, some form of coding would be needed to improve the BER. Nevertheless, the advantage of the

reduced rank MWF in terms of performance and rank reduction is clearly seen. Also, the benefit of employing codes with low correlation properties is clear.

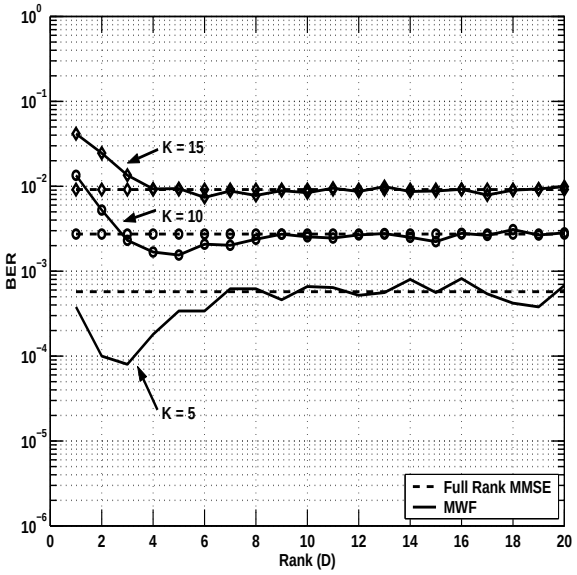


Figure 5.8: Multiuser Detector: Rank (D) vs. BER; asynchronous CDMA; spreading code length, $N = 31$ (Gold Codes); $E_b/N_0 = 12$ dB; channel delay spread, $L = 5$; power of interfering users/power of desired user, $\Delta P = 0$ dB

# Chapter 6

# Joint Reduced Rank Detection Techniques

In this chapter, the performance of the reduced rank adaptive filtering methods in the context of diversity processing schemes, including joint code-time processing (CTP), or multiuser detection (MUD), and joint space-time processing (STP) will be shown. Implementation is again described in terms of the correlation subtraction architecture of the multistage Wiener filter (CSA-MWF). For the joint multiuser detector, which uses a steering matrix whose columns are the spreading codes of all the users, convergence is shown to occur at a rank of only one. This effect occurs because the blocking matrix implicitly formed by the MWF constrains the weight vector for each user to lie in a subspace orthogonal to that of the other users from the first stage. This remarkable convergence property of the joint multiuser detector makes it a strong contender for use in future systems. The joint space-time processor is an natural extension in which the MWF is applied to a scheme employing multiple receive antennas for diversity. The complexity introduced by the multiple antenna structure is countered by the low complexity implementation of the MWF. The significant gains that can be obtained with such an architecture can therefore be applied

to future generation systems without concern for decoding complexity.

Both of these new architectures, of course, are suitable for the reverse CDMA links. The joint multiuser detector can be employed by the base station, which always has knowledge of the spreading codes of all the users. Since it is the base station which has to demodulate signals from multiple users, the low complexity decoding scheme introduced by the joint MUD scheme presented here is invaluable. Furthermore, multiple receive antennas can be deployed at the base station but not at the mobile, as the size of the handsets should always be made small. The extension to a three-dimensional joint space-time-code processing (STCP) scheme is straightforward and will be described briefly as well.

The parameters for simulations performed using the joint multiuser detector are summarized in Table 6.1. Here, it will be shown that the matrix MUD performs optimally at a rank of only one compared to the vector MUD, but both meet or exceed minimum mean square error (MMSE) performance at low ranks. Similarly, Table 6.2 summarizes the simulation parameters for the space-time processor. Here, it will be shown that with 5 receiver antennas, gains of 7 performance gains of 7 dB or more can be achieved at bit error rates of $10^{-3}$ or less.

Table 6.1: Joint Code-Time Processing (CTP) Simulation Parameters: $N$=length of spreading code, $E_b/N_0$=Bit energy divided by single-sided noise power spectral density (PSD), $M$=block size, $K$=number of users, $D$=rank of multistage Wiener filter (MWF), $L$=channel delay spread, $\Delta P$=power of interfering users/power of desired user

| | $N$ | $E_b/N_0$ [dB] | $M$ | $K$ | $D$ | $L$ | $\Delta P[dB]$ | Synchronism |
|---|---|---|---|---|---|---|---|---|
| Fig. 6.3 | 32 | N/A | 5000 | 12 | 7 | 5 | 6 | Synchronous |
| Fig. 6.4 | 32 | 12 | 5000 | 15 | N/A | 5 | Random | Synchronous |

Table 6.2: Joint Space-Time Processor Simulation Parameters: $N$=length of spreading code, $E_b/N_0$=Bit energy divided by single-sided noise power spectral density (PSD), $M$=block size, $K$=number of users, $D$=rank of multistage Wiener filter (MWF), $L$=channel delay spread, $\Delta P$=power of interfering users/power of desired user

| | $N$ | $E_b/N_0$ [dB] | $M$ | $K$ | $D$ | $L$ | $\Delta P[dB]$ | Synchronism |
|---|---|---|---|---|---|---|---|---|
| Fig. 6.6 | 32 | N/A | 5000 | 15 | 5 | 5 | 0 | Asynchronous |
| Fig. 6.7 | 32 | N/A | 5000 | 30 | 5 | 5 | 0 | Synchronous |
| Fig. 6.8 | 32 | N/A | 5000 | 30 | 5 | 5 | 6 | Synchronous |
| Fig. 6.9 | 31 | N/A | 5000 | 30 | 5 | 5 | 6 | Synchronous |

## 6.1 Joint Code-Time Processing (CTP)

### 6.1.1 Code-Time Processor Description

In this section, the solution which implements the matrix version of the MUD solution is analyzed further; this receiver is also called a joint code-time processor. This requires an $N \times K$ matrix of steering codes in place of the single user $N \times 1$ steering vector as is implemented in Chapters 4 and 5. The joint full rank MMSE matrix solution was derived in Chapter 5, and given in Eq. (5.9), which is repeated here for convenience as

$$\hat{\mathbf{C}}_{MMSE} = \hat{\mathbf{R}}^{-1}\hat{\mathbf{S}}^{+}\mathbf{A}. \tag{6.1}$$

Recall that $\hat{\mathbf{R}}$ is the covariance matrix of the data, $\hat{\mathbf{S}}^{+}$ is the matrix of spreading codes of the current bit in the asynchronous transmission, and $\mathbf{A}$ is the diagonal matrix of amplitudes. The implementation of this solution via the multistage Wiener filter (MWF) requires a matrix form of the correlation subtraction architecture (CSA) of the MWF to replace the original vector form.

To derive the exact matrix solution, first consider an alternate solution to the

multistage decomposition where the optimum matrix multistage Wiener filter can be obtained by minimizing the MSE of the MUD problem, given in Eq. (5.3) and rewritten here as

$$MSE_{MUD} = E[||\mathbf{b}(i) - \tilde{\mathbf{b}}(i)||^2] = E[||\mathbf{b}(i) - \hat{\mathbf{C}}^H \hat{\mathbf{r}}(i)||^2]. \tag{6.2}$$

For simplicity in the derivation, synchronous CDMA is assumed here. Substituting for the received signal $\hat{\mathbf{r}}(i)$ using Eq. (2.12),

$$MSE_{MUD} = E[||\mathbf{b}(i) - \hat{\mathbf{C}}^H \hat{\mathbf{S}}\mathbf{A}\mathbf{b}(i) - \hat{\mathbf{C}}^H \mathbf{n}(i))||^2] \tag{6.3}$$

which can be expanded as [19]

$$MSE_{MUD} = E[||\mathbf{b}(i) - \hat{\mathbf{C}}^H \hat{\mathbf{S}}\mathbf{A}\mathbf{b}(i)||^2] + trace(\hat{\mathbf{C}}^H \mathbf{R}_n \hat{\mathbf{C}}), \tag{6.4}$$

where $\mathbf{R}_n$ is the covariance matrix of the white noise samples. A further constraint is now imposed which requires that the minimum solution be independent of the bit estimates. In other words, the MSE should be independent of $\mathbf{b}(i)$, producing an unbiased solution. This condition in turn implies that the first term in Eq. (6.4) be zero, yielding the constraint

$$\hat{\mathbf{C}}^H \hat{\mathbf{S}}\mathbf{A} = \mathbf{I}_{K \times K}, \tag{6.5}$$

where $\mathbf{I}_{K \times K}$ is the $K \times K$ identity matrix. Note that the constraint results in the signature waveforms $\mathbf{S}$ being passed undistorted. Then, the MMSE solution can be written simply as

$$MMSE_{MUD} = min_{\mathbf{C}}\ trace(\hat{\mathbf{C}}^H \mathbf{R}_n \hat{\mathbf{C}}) \tag{6.6}$$

under the constraint given in Eq. (6.5). The solution to the above equation can be obtained by breaking up the multidimensional problem into $K$ single constraint

problems. That is, solve

$$MMSE_{MUD} = min_{\mathbf{c}_i}\ trace(\hat{\mathbf{c}}_\mathbf{i}^H \mathbf{R}_n \hat{\mathbf{c}}_\mathbf{i}) \tag{6.7}$$

subject to the constraint

$$\hat{\mathbf{c}}_\mathbf{i}^H \hat{\mathbf{s}}_\mathbf{i} \mathbf{A}_\mathbf{i} = \delta_{ij}, \tag{6.8}$$

where $\delta_{ij}$ is the Kronecker delta function, and $j = 1,\ 2,\ ...,\ K$. The solution is obtained using Lagrange multipliers [19] and is given by

$$\mathbf{c}_i = \mathbf{R}_n^{-1}\mathbf{S}(\mathbf{S}^H\mathbf{R}_n^{-1}\mathbf{S})^{-1}\mathbf{u}_i, \tag{6.9}$$

where $\mathbf{u}_i$ is the $K \times 1$ vector in which the $i^{th}$ element is one and the remaining $K-1$ elements are zero. The matrix form can then be written as

$$\mathbf{C} = \mathbf{R}_n^{-1}\mathbf{S}(\mathbf{S}^H\mathbf{R}_n^{-1}\mathbf{S})^{-1}. \tag{6.10}$$

While the above equation provides a joint solution to the MUD problem using the unbiased constraint assumption, it is seen that covariance matrix inversion is again required. This requirement will now be relaxed by performing a decomposition similar to that in Chapter 3.

To construct the decomposition, first formulate the matrix filter in the form of a generalized sidelobe canceller (GSC) as shown in Figure 6.1. Define

$$\Delta_0 = (\mathbf{S}^H\mathbf{S})^{1/2}. \tag{6.11}$$

As in the previous chapter, $\mathbf{H}_0$ is the normalized matrix of spreading codes, given by

$$\mathbf{H}_0 = \mathbf{S}\Delta_0^{-1}, \tag{6.12}$$

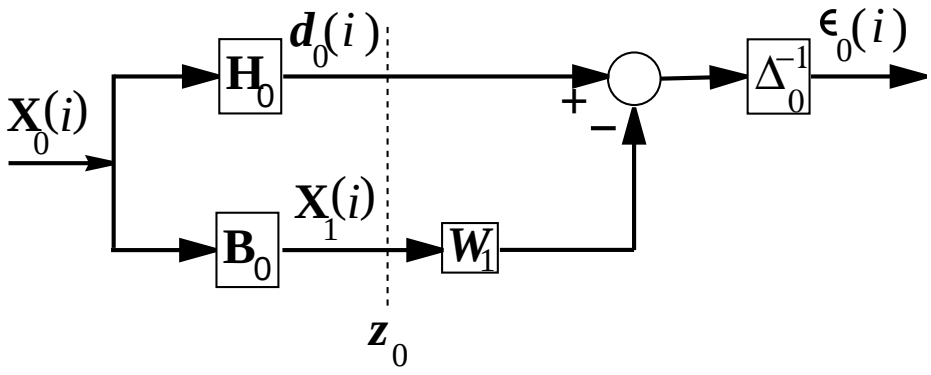


Figure 6.1: Matrix Form of Multistage Wiener Filter (MWF) as Generalized Sidelobe Canceller (GSC)

and $\mathbf{B}_0$ is the blocking matrix for $\mathbf{H}_0$. Define the transformation

$$\mathbf{T}_0 = \begin{bmatrix} \mathbf{H}_0^H \\ \mathbf{B}_0 \end{bmatrix}, \tag{6.13}$$

and define the output of the first stage of the decomposition, shown in Figure 6.1, by

$$\mathbf{z}_0 = \mathbf{T}_0 \mathbf{X}_0. \tag{6.14}$$

Note that $\mathbf{d}_0(i)$ is the matched filter output. The covariance matrix of the transformed process $\mathbf{z}_0$ is given by

$$\mathbf{R}_{z_0} = \mathbf{T}_0 \mathbf{R}_{X_0} \mathbf{T}_0^H, \tag{6.15}$$

where $\mathbf{R}_{X_0}$ is the covariance matrix of the input process $\mathbf{X}_0$. Solving the above equation for $\mathbf{R}_{X_0}$, one obtains

$$\mathbf{R}_{X_0} = \mathbf{T}_0^{-1} \mathbf{R}_{z_0} \mathbf{T}_0^{-H}, \tag{6.16}$$

or

$$\mathbf{R}_{X_0}^{-1} = \mathbf{T}_0^H \mathbf{R}_{z_0}^{-1} \mathbf{T}_0. \tag{6.17}$$

Continuing the decomposition, it can be shown that the covariance matrix of the process after $D$ stages can be written as

$$\mathbf{R}_{z_D} = \mathbf{T}_D \mathbf{R}_{X_0} \mathbf{T}_D^H, \tag{6.18}$$

where

$$\mathbf{T}_D = \begin{bmatrix} \mathbf{H}_0^H \\ \mathbf{H}_1^H \mathbf{B}_0 \\ \mathbf{H}_2^H \mathbf{B}_1 \mathbf{B}_0 \\ \vdots \end{bmatrix}, \tag{6.19}$$

and so

$$\mathbf{R}_{X_0}^{-1} = \mathbf{T}_D^H \mathbf{R}_{z_D}^{-1} \mathbf{T}_D. \tag{6.20}$$

Finally, the optimum Wiener solution is obtained by substituting Eq. (6.20) into the matrix Wiener filter solution in Eq. (6.1) to yield

$$\mathbf{C}_{MMSE} = \mathbf{T}_D^H \mathbf{R}_{z_0}^{-1} \mathbf{T}_D \hat{\mathbf{S}}^+ \mathbf{A}. \tag{6.21}$$

A full rank matrix inversion is still observed in this solution, but the matrix can be truncated to less than full rank. The rank one decomposition is performed by retaining only the first two rows of $\mathbf{T}_D$, equivalent to $\mathbf{T}_1$, or

$$\mathbf{T}_1 = \begin{bmatrix} \mathbf{H}_0^H \\ \mathbf{H}_1^H \mathbf{B}_0 \end{bmatrix}, \tag{6.22}$$

which gives the simple solution

$$\mathbf{C}_{MMSE} = \mathbf{T}_1^H \mathbf{R}_{z_0}^{-1} \mathbf{T}_1 \hat{\mathbf{S}}^+ \mathbf{A}. \tag{6.23}$$

For this solution, the claim of reduced rank processing can still be made even though a matrix inversion is required as long as $K < N/2$. This is true because the dimension

of the matrix to be inverted is now $2K \times 2K$ versus the original covariance matrix dimension of $N \times N$. Thus, while the computational reduction is not as pronounced as with the multistage Wiener filter, the reduction is still significant. As an example, if $K = 10$, and $N = 32$, the matrix MWF implemented this way requires on the order of $20^3 = 8,000$ flops, versus the full rank of $32^3 = 32,768$ flops, an improvement by a factor of approximately 4.

In [8] and [19], it is also shown that the optimum Wiener filter can be written as

$$\mathbf{C}_{MMSE} = \mathbf{T}_0^H \begin{bmatrix} \mathbf{I} \\ -\mathbf{R}_{X_1}^{-1}\mathbf{R}_{X_1 d_1} \end{bmatrix} \Delta_0^{-1} = (\mathbf{H}_0 - \mathbf{B}_0^H \mathbf{W}_1)\Delta_0^{-1}, \tag{6.24}$$

as shown in Figure 6.1. The decomposition outlined above would thus also yield the optimum Wiener filter. The multistage decomposition of this solution (given in detail in [19]) yields the filter of Figure 6.2, which is directly analogous to the single user MWF. Note that this solution provides the best reduced rank implementation, matrix inversions have been eliminated. Furthermore, this matrix MWF can often be truncated after only one or two stages because of its use of all the users' spreading codes as a multiple constraint. In fact, construction of the blocking matrix as $\mathbf{B}_0 = (\mathbf{I} - \mathbf{H}_0\mathbf{H}_0^H)$ forces the weight vectors for each user to be orthogonal to those of the other users, so typically only one stage is required. The quantities $\mathbf{H}_0$ and $\mathbf{d}_0$ are defined in Eq. (5.13). Note that now $\epsilon_0(i)$ is a $1 \times K$ vector containing the bit estimates of all the users instead of a scalar for a given user, i.e. $\epsilon_0(i) = [\epsilon_{01}(i)\ \epsilon_{02}(i),\ ...,\ \epsilon_{0K}(i)]$, where $\epsilon_{0k}(i)$ refers to the bit estimate for the $k^{th}$ user at time $i$.

The rank one solution can be obtained using the standard MWF with the steering vector replaced by the steering matrix. The multistage decomposition using this solution assumes (as for the vector MWF), that the covariance matrix is tri-diagonalized

at each stage. This assumption is not valid for the matrix MWF, because the covariance matrix is now full rank and banded, and further research must be done to determine the recursion equations in the multistage decomposition. This is beyond the scope of this dissertation, but simulation results and the alternate solution given above indicate that truncating the decomposition after one stage is sufficient, so violation of this assumption is not important. Significant rank reduction is thus attained.

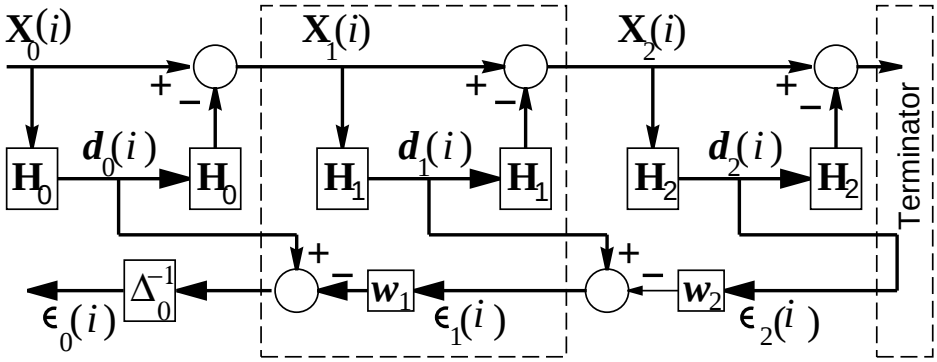


Figure 6.2: Joint Code-Time (Matrix) Form of Correlation Subtraction Architecture of the Multistage Wiener Filter (CSA-MWF) Processor, $D = 2$ stages

The matrix MWF operates on all of the spreading codes and thus maximizes the mutual information between the received data and the spreading codes jointly. Thus, the only interference that it requires to suppress is the additional noise and multipath. Using the MMSE/rake concept, the multipath can be handled. Regardless of this, it is expected that the joint (matrix) CSA-MWF will converge much quicker in terms of rank than its single user counterpart. This claim is validated with simulation results next. Note that for this matrix CSA-MWF to jointly process all the users, they must be synchronous. This means that the incoming data from many asynchronous

users must be synchronized first before applying the matrix CSA-MWF.

### 6.1.2 Numerical Results

In this section, the matrix MUD is compared to the vector MUD derived in Chapter 5 using Monte Carlo simulations. The parallel form of the CSA-MWF is denoted 'Vector MUD' and the joint CTP form of the CSA-MWF is called 'Matrix MUD'. The matrix MWF of Figure 6.2 is used to implement the joint CTP.

Figure 6.3 shows a plot of $E_b/N_0$ vs. bit error rate (BER) for synchronous users, $N = 32$ Hadamard codes and $K = 12$ users. Note the remarkable ability of the joint CTP implemented by the CSA-MWF to suppress interference rapidly. In fact, while the vector CSA-MWF requires only a rank of seven to achieve the full rank solution, the matrix solution requires only an astounding rank of one (i.e. one stage) to achieve the full rank solution, as explained in the preceding section. While this may not always be the case, e.g. when inter-cell interference or other external sources of interference are present, simulations for fully loaded systems have repeatedly shown that a rank of one or at most two is sufficient. Note that if there is inter-cell interference from another cell using the same frequency and another user employing the same spreading code, other interference mitigation techniques are required. Since this type of signal will be correlated with that of the user of interest in the desired cell, the interference it creates will leak through the CSA-MWF.

Fig. 6.4 shows a plot of rank of the multistage Wiener filter versus the BER for synchronous users. The powers of some of the users are randomly set up to 4 dB above the others to simulate a near-far scenario. The slight variation in BER for the MMSE and rake methods is due to the nature of the Monte Carlo simulation, since their performance is independent of rank. Note that the matrix multiuser detector achieves

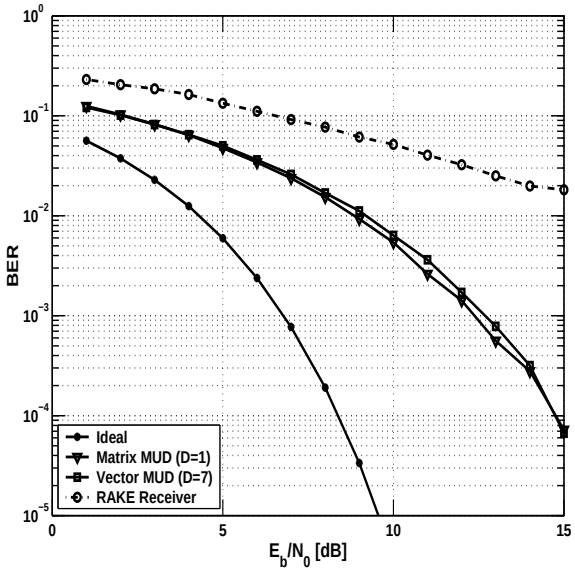


Figure 6.3: Joint Code-Time CSA-MWF Processor: $E_b/N_0$ vs. BER; Synchronous CDMA, $N = 32$ (Hadamard Codes), $K = 12$, $D = 7$, $L = 5$, $\Delta P = 6$ dB

better than full rank performance at a rank of only one, by employing knowledge of all the users' spreading codes. For a rank as low as 3, the vector MWF converges to the matrix MUD solution and maintains this performance as rank increases. The matrix multiuser detector is held at rank one, and thus the performance curve across rank is flat. On the other hand, the rank of the vector MWF increases, and it eventually converges to match the full rank MMSE solution. The performance of the vector MUD does not substantially degrade even at a rank as low as 2, which is significantly less than the processing gain of $N = 32$. Again, the rake receiver fails in the presence of interference. Note that even here, because synchronous Hadamard codes are used, MWF performance is seen to do better than MMSE at low rank.

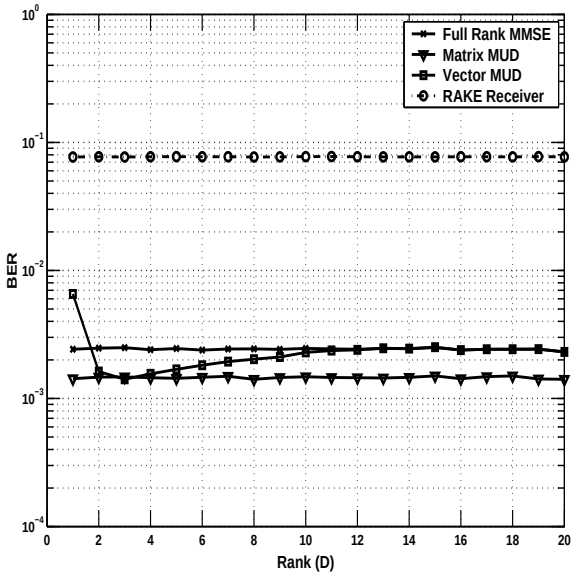


Figure 6.4: Joint Code-Time Form of Correlation Subtraction Architecture of the Multistage Wiener Filter (CSA-MWF) Processor: Rank (D) vs. BER; synchronous CDMA; spreading code length, $N = 32$ (Hadamard Codes); $E_b/N_0 = 12$ dB; number of users, $K = 15$; channel delay spread, $L = 5$

## 6.2 Joint Space-Time Processing (STP)

### 6.2.1 Space-Time Processor Description

In this section, the performance gains using a joint space-time adaptive pre-processor at the receiver in conjunction with multiple receiver antennas is determined. In [67], a two-dimensional matched filter is shown to provide spatial and temporal diversity gain for DS-CDMA. Figure 6.5 shows the structure of the pre-processor assuming the number of receiver antenna elements is $L_r$. This structure is similar to that cited in [45], [52], and [53]. The receiver coefficients to be computed by the adaptive process are represented in matrix form by $\mathbf{C} = [\mathbf{c}_1, \mathbf{c}_2, ..., \mathbf{c}_{L_r}]$, where each $\mathbf{c}_l$ represents the $N \times 1$ vector of coefficients at receiver antenna element $l$. It is assumed that a linear

antenna array is used, with equally spaced elements. Note that with a single array element, we simply set

$$\mathbf{C} = \mathbf{c}_1 = \hat{\mathbf{s}}_1. \tag{6.25}$$

With multiple array elements, the received signal is computed by taking the Kronecker product of the incoming vector and the receiver array manifold [45]. This represents the phase shift produced on an incoming waveform impinging upon multiple, equally spaced elements from a random direction. The phase shift $\theta_k$ is related to the separation between the elements. The array manifold can be written as

$$\mathbf{a}(\theta_k) = \begin{bmatrix} 1 \\ e^{-j\theta_k} \\ e^{-j2\theta_k} \\ \vdots \\ e^{-j(L_r-1)\theta_k} \end{bmatrix}. \tag{6.26}$$

The matched filter at the receiver following the pre-processor is also given by a Kronecker product, resulting in a space-time spreading code denoted by

$$\mathbf{s}_k^{\kappa} = \mathbf{a}(\theta_k) \otimes \mathbf{s}_k, \tag{6.27}$$

where the superscript $\kappa$ denotes Kronecker. The MMSE/rake concept can also be exploited to include multipath compensation. This yields

$$\hat{\mathbf{s}}_k^{\kappa} = \mathbf{a}(\theta_k) \otimes \hat{\mathbf{s}}_k, \tag{6.28}$$

The receiver can now process the data as usual, using an MMSE or MWF based detector. The effect of taking a Kronecker product is that now all dimension $N$ signals now become dimension $NL_r$. That is, $\mathbf{x}_0(i)$ and $\mathbf{d}_0(i)$ are now $NL_r \times 1$ vectors. This in turn means that the covariance matrix $\hat{\mathbf{R}}$ also increases in each dimension by a

factor $L_r$. Even for a three or four antenna system, the computational complexity associated with inverting such a matrix can be tremendous. Since this type of matrix inversion is usually not practical for a real-time system, it is desirable to determine an implementation of the solution with the reduced rank CSA-MWF.

Noting the analogy between the data dimensions and covariance matrices from the original MWF structure, it is observed that the CSA-MWF can be employed by initializing with the pre-processor matched filter. In other words, set $\mathbf{h}_0(i)$ in the original structure (Figure 3.4) equal to the spreading code given in Eq. (6.28), which is the new matched filter.

Note that the joint code-time processor of the preceding section and the space-time processor can be combined to form a joint space-time-code processor (STCP). This would involve forming a Kronecker product on the spreading code matrix, namely,

$$\hat{\mathbf{S}}^{\kappa} = [\hat{\mathbf{s}}_1^{\kappa}\ \hat{\mathbf{s}}_2^{\kappa},\ ...,\ \hat{\mathbf{s}}_K^{\kappa}] = [\mathbf{a}(\theta_1) \otimes \hat{\mathbf{s}}_1,\ \mathbf{a}(\theta_2) \otimes \hat{\mathbf{s}}_2,\ ...,\ \mathbf{a}(\theta_K) \otimes \hat{\mathbf{s}}_K]. \tag{6.29}$$

As with the single receiver antenna structure, this could be implemented in either joint (matrix) or parallel (vector) form.

### 6.2.2 Numerical Results

A plot showing the $BER$ versus $E_b/N_0$ for $L_r = 1$ (no space-time gain) and $L_r = 5$ antenna elements in a Monte Carlo simulation is shown in Figure 6.6. For the simulation, length $N = 32$ asynchronous Hadamard codes are used for spreading, the number of users is $K = 15$, the rank of the CSA-MWF is $D = 5$, and the number of bits per block is $M = 1000$. All the users have normalized equal power. Note that the analytic gain can be computed by taking

$$\mathbf{G}_{STP} = 10 \cdot log_{10} L_r, \tag{6.30}$$

which for $L_r = 5$ yields about 7 dB gain. From the plot, it is seen that this is the gain achieved over low bit error rates. Even with two or three receiver antennas, significant gains of about 3 or 4.75 dB can be achieved, respectively. This would be a suitable technique for the reverse link of a CDMA system, where multiple antennas can be deployed at the base station without significant cost. To improve transmission on the forward link, transmit antennas could be employed with similar processing gains expected. Alternatively, space-time codes exploiting multiple transmit antennas could be used, so that again the burden is placed on the base station. These are described in Chapter 8. A similar plot showing the curves for a highly loaded system supporting $K = 30$ synchronous users is presented in Figure 6.7. Here the performance as $E_b/N_0$ increases does not fall off as steeply as with the previous plot. This, of course, is due to the large number of interfering users present in the system. But, gains of $5 - 7$ dB over the non-diversity case are still achieved. The last plot shown in Figure 6.8 repeats the results of the previous plot except that the desired user is 6 dB below all of the interferers. Significant gain with the multiple antennas is still observed. Note, as seen in Chapter 5 with MUD performance using Hadamard and Gold codes in multipath, that all of the above results would improve if Gold codes are used. Figure 6.9 shows a sample result with Gold codes of length 31 using the same simulation parameters as in Figure 6.8.

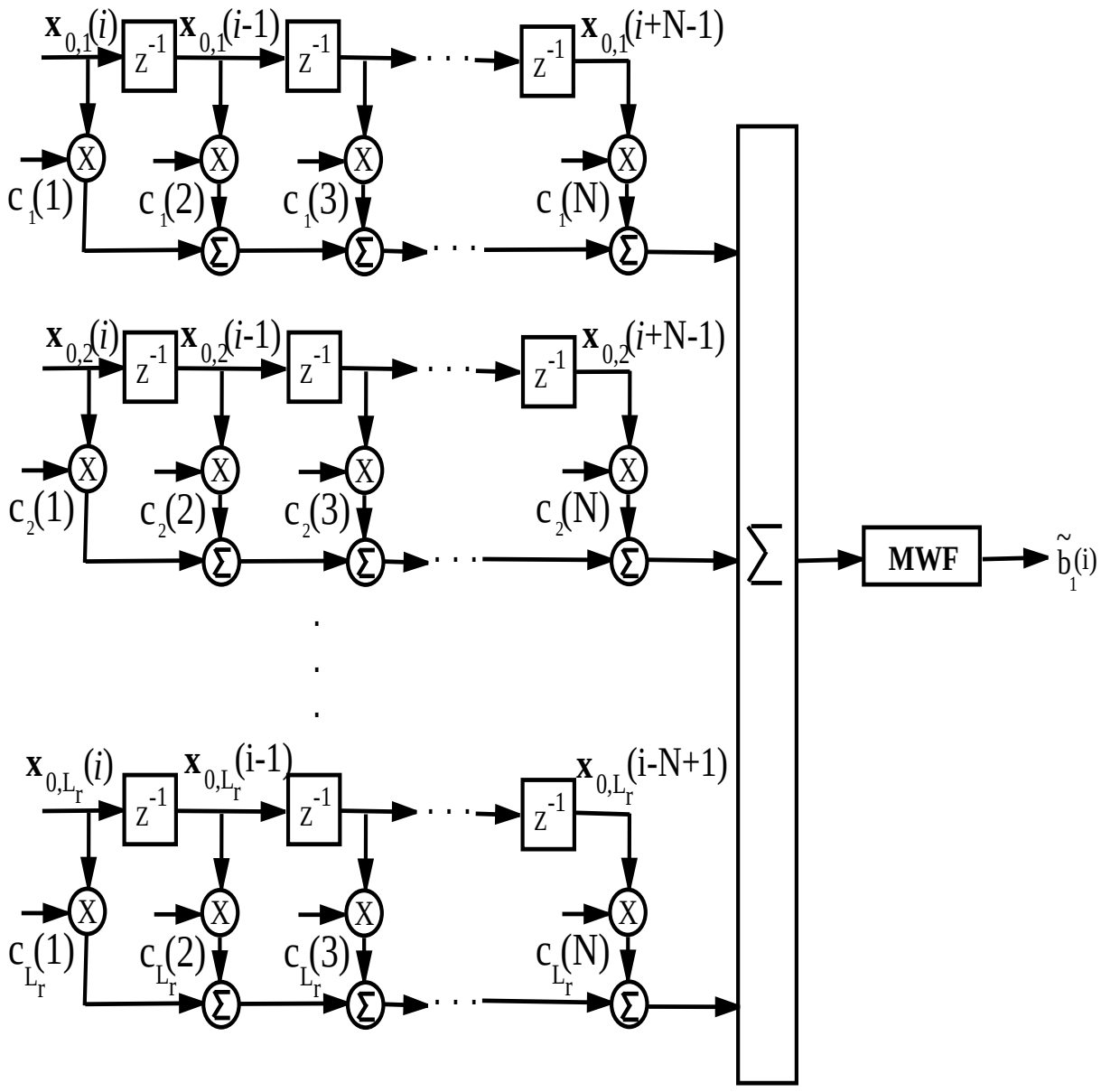


Figure 6.5: Multistage Wiener Filter (MWF) Using Joint Space-Time Pre-Processor; $L_r$=number of receiver antennas; $\mathbf{x}_{0,l}$=observed signal at receiver antenna element $l$; $\mathbf{c}_l$=the $N \times 1$ vector of coefficients at receiver antenna element $l$; $\tilde{b}_1(i)$=bit estimate for user one

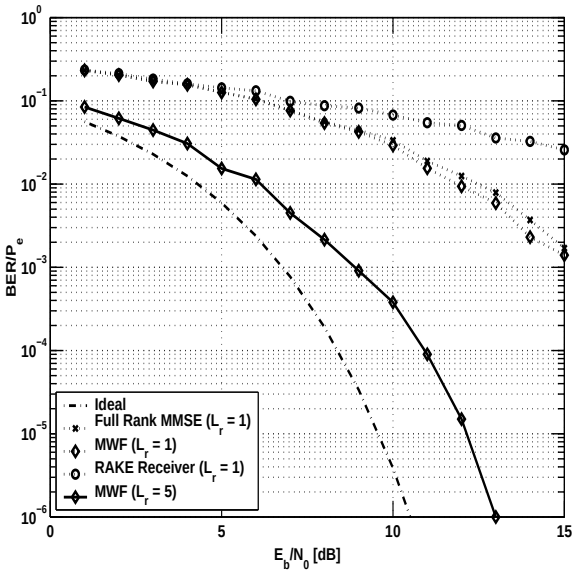


Figure 6.6: Multistage Wiener Filter (MWF) with Joint Space-Time Pre-Processor: $E_b/N_0$ vs. BER; asynchronous CDMA; spreading code length, $N = 32$ (Hadamard Codes); number of users, $K = 15$; rank of MWF, $D = 5$; channel delay spread, $L = 5$; power of interfering users/power of desired user, $\Delta P = 0$ dB

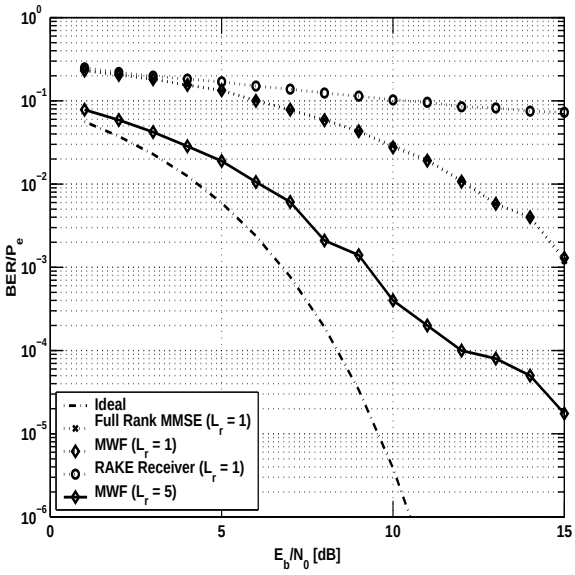


Figure 6.7: Multistage Wiener Filter (MWF) with Joint Space-Time Pre-Processor: $E_b/N_0$ vs. BER; synchronous CDMA; spreading code length, $N = 32$ (Hadamard Codes); number of users, $K = 30$; rank of MWF, $D = 5$; channel delay spread, $L = 5$; power of interfering users/power of desired user, $\Delta P = 0$ dB

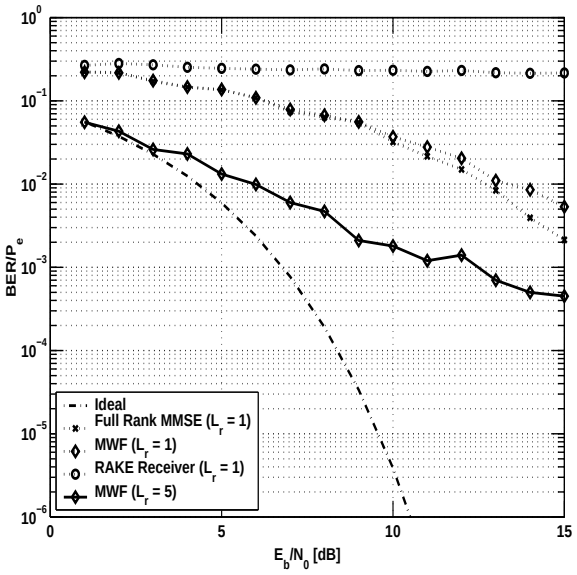


Figure 6.8: Multistage Wiener Filter (MWF) with Joint Space-Time Pre-Processor: $E_b/N_0$ vs. BER; synchronous CDMA; spreading code length, $N = 32$ (Hadamard Codes); number of users, $K = 30$; rank of MWF, $D = 5$; channel delay spread, $L = 5$; power of interfering users/power of desired user, $\Delta P = 6$ dB.

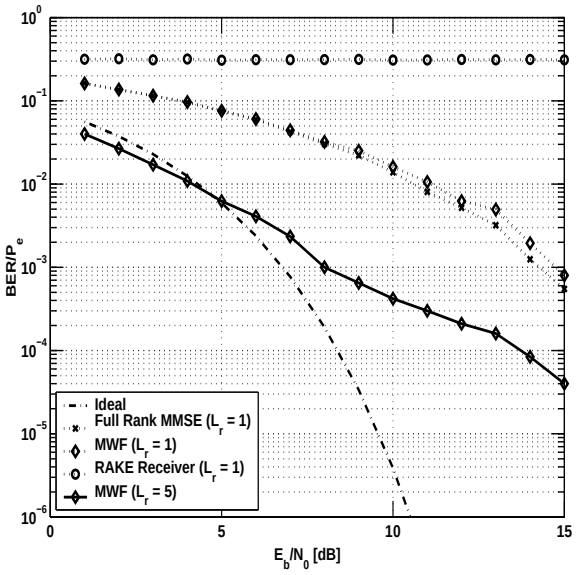


Figure 6.9: Multistage Wiener Filter (MWF) with Joint Space-Time Pre-Processor: $E_b/N_0$ vs. BER; synchronous CDMA; spreading code length, $N = 31$ (Gold Codes); number of users, $K = 30$; rank of MWF, $D = 5$; channel delay spread, $L = 5$; power of interfering users/power of desired user, $\Delta P = 6$ dB.

# Chapter 7

# Non-linear Reduced Rank Multiuser Detection (MUD) and Interference Suppression (IS)

In this chapter, conventional non-linear interference cancellation (IC) techniques are implemented using the efficient correlation subtraction architecture of the multistage Wiener filter (CSA-MWF). Thus, interference suppression (IS) is done at each successive stage in place of the matched filter (MF). Serial interference cancellation (SIC) and parallel interference cancellation (PIC) schemes are considered. The non-linearity occurs because hard decisions are performed to obtain bit estimates for cancellation and a feedback loop is employed to cancel successive users. The analytical model (AM) is expanded to determine the probability of error associated with these interference cancellation schemes, and these models are compared to the results obtained with Monte Carlo (MC) methods for a simple case of one interferer to validate the Monte Carlo method. Simulations of the SIC and PIC are then performed via Monte Carlo methods when multiple interferers are introduced as analytical evaluation becomes difficult. Performance of these non-linear MWF/SIC and MWF/PIC are compared to conventional cancellation schemes involving the matched filter (MF/SIC and

MF/PIC) as well as the standard full rank MMSE and rake receiver. Performance is expected to improve greatly over the conventional cancellation schemes as the number of users increases, as the matched filter fails when multiple users are present. It is shown that these new techniques perform better than full rank MMSE, with the additional benefit of lower complexity. It is also shown that the new non-linear SIC and PIC receivers continue to perform well even where conventional SIC and PIC fail.

Table 7.1 summarizes the simulation parameters for the serial interference canceller. It will be shown that as the number of users increases, the MWF performs consistently better than MMSE by about 2 dB, and continues to maintain its performance even at low error rates. The conventional SIC, however, fails quickly as the number of users is increased. Table 7.2 summarizes the simulation parameters for the parallel interference canceller. In this case, it will be shown that significant performance gains, about $1-4$ dB over conventional MMSE and about $2-6$ dB over conventional PIC, can be achieved at bit error rates from $10^{-3}$ to $10^{-6}$. In both of the new schemes, it is shown that a large number of users can be easily supported, thereby enabling larger capacities for future systems. The conventional SIC and PIC schemes are not suitable for the high capacity CDMA systems of the future.

Table 7.1: Serial Interference Cancellation (SIC) Simulation Parameters: $N$=length of spreading code, $E_b/N_0$=Bit energy divided by single-sided noise power spectral density (PSD), $M$=block size, $K$=number of users, $D$=rank of multistage Wiener filter (MWF), $L$=channel delay spread, $\Delta P_{step}$=power step size

| | $N$ | $E_b/N_0$ [dB] | $M$ | $K$ | $D$ | $L$ | $\Delta P_{step}[dB]$ | Synchronous |
|---|---|---|---|---|---|---|---|---|
| Fig. 7.3 | 31 | N/A | 5000 | 10 | 5 | 5 | 1 | Synchronous |
| Fig. 7.4 | 31 | N/A | 5000 | 15 | 5 | 5 | 1 | Synchronous |
| Fig. 7.5 | 31 | N/A | 5000 | 20 | 5 | 5 | 1 | Synchronous |
| Fig. 7.6 | 31 | N/A | 5000 | 25 | 5 | 5 | 1 | Synchronous |

Table 7.2: Parallel Interference Cancellation (PIC) Simulation Parameters: $N$=length of spreading code, $E_b/N_0$=Bit energy divided by single-sided noise power spectral density (PSD), $M$=block size, $K$=number of users, $D$=rank of multistage Wiener filter (MWF), $L$=channel delay spread, $\Delta P$ =power of interfering users/power of desired user

| | $N$ | $E_b/N_0$ [dB] | $M$ | $K$ | $D$ | $L$ | $\Delta P[dB]$ | Synchronous |
|---|---|---|---|---|---|---|---|---|
| Fig. 7.9 | 31 | N/A | 1000 | 20 | 8 | 5 | 0 | Synchronous |
| Fig. 7.10 | 31 | N/A | 1000 | 25 | 12 | 5 | 0 | Synchronous |
| Fig. 7.11 | 31 | N/A | 1000 | 20 (3 Cells) | 12 | 5 | 0 | Synchronous |

## 7.1 Serial Interference Cancellation (SIC)

The conventional serial interference canceller (SIC) provides cancellation of strong users first by either prior knowledge of each user's transmitted power or by estimation of the user's power via a correlation of its spreading code with the received signal. The correlation is obtained using a filter matched to the spreading code of the desired user. A hard decision on the correlator output is used to regenerate the decoded signal and subtract it out of the received signal for the next stage in the cancellation. Thus, each user is decoded successively ([62] and [40]). In this new scheme, it is proposed to replace the conventional correlator at each stage with the MMSE receiver, implemented using the CSA-MWF. The bit estimates used to regenerate the signal will be more accurate as the MMSE receiver will provide interference suppression whereas the MF cannot. A block diagram of this MWF/SIC scheme is shown in Figure 7.1.

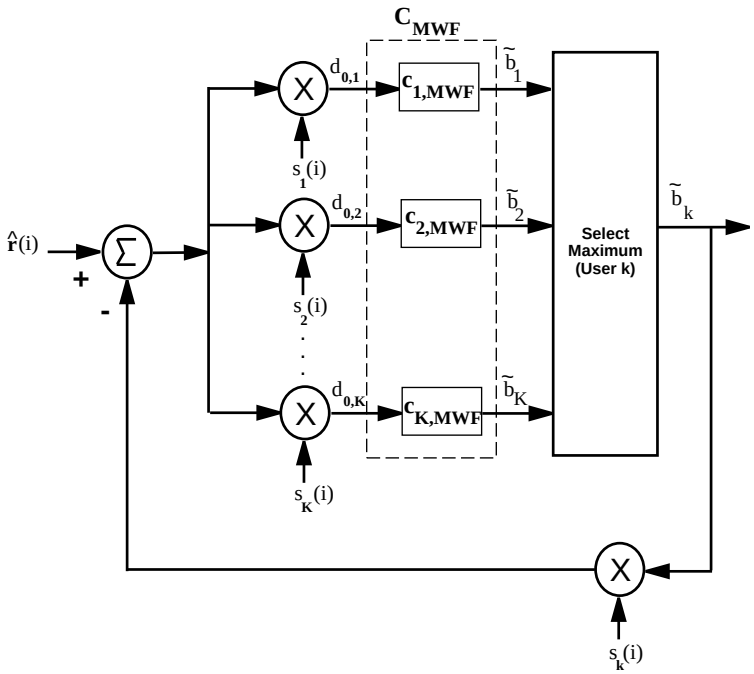


Figure 7.1: Serial Interference Cancellation (SIC) via Correlations Subtraction Architecture of the Multistage Wiener Filter (CSA-MWF)

### 7.1.1 Probability of Error ($P_e$) Derivation

The $P_e$ for a simple SIC is derived in [62] by treating the interference due to both the uncancelled users and the imperfectly cancelled users as Gaussian noise. In [12] and [13] the an accurate probability of error for a decorrelating multiuser decision feedback (DF) detector is derived for synchronous CDMA systems by utilizing decisions of the high energy users to decode the weaker ones. Those structures can be modified by replacing the forward filter by the MMSE filter, implemented by the MWF. This is the approach taken here. Since the SIC is a form of multiuser detector, one should begin by writing the received CDMA signal in the presence of multipath in matrix

form. Recall from Eq. (2.11) that this expression is given by

$$\hat{\mathbf{r}}(i) = \hat{\mathbf{S}}^{+}\mathbf{A}\mathbf{b}(i) + \hat{\mathbf{S}}^{-}\mathbf{A}\mathbf{b}(i-1) + \mathbf{n}(i), \tag{7.1}$$

where $\mathbf{S}^{+} = (\mathbf{s}_1^{+}\ \mathbf{s}_2^{+}\ ...\ \mathbf{s}_K^{+})$ and $\mathbf{S}^{-} = (\mathbf{s}_1^{-}\ \mathbf{s}_2^{-}\ ...\ \mathbf{s}_K^{-})$ are the $N \times K$ matrices containing the spreading codes of the users associated with asynchronous transmission. Also, $\mathbf{A} = diag(A_1,\ A_2,\ ...,\ A_K)$ is a $K \times K$ matrix in which the signal amplitudes are the diagonal components, $\mathbf{b}(i) = (b_1(i),\ b_2(i),\ ...,\ b_K(i))^T$ is a $K \times 1$ vector containing the bits for each user $k$ for $k = 1,\ 2,\ ...,\ K$, and $\mathbf{n}(i)$ are additive white Gaussian noise (AWGN) samples. As in preceding chapters, $\hat{(\cdot)}$ denotes convolution of the quantity with the channel. Referring to Figure 7.1 [80], the first operation performed in the SIC is a matched filter for each of the $K$ users. For the next block, the feedforward filter of the DF detector described in [12], is replaced by the equivalent matrix form of the MWF. It is shown in Chapter 5 that the MUD filter is equivalent to the concatenation of a bank of IS filters, and thus the matrix of coefficients can be written as $\mathbf{C}_{MWF} = [\mathbf{c}_{1,MWF}\ \mathbf{c}_{2,MWF},\ ...,\ \mathbf{c}_{K,MWF}]$ where $\mathbf{c}_{k,MWF}$ denotes the vector of coefficients for user $k$. With this substitution, the structure of Figure 7.1 is identical to that in [12] with $\mathbf{C}_{MWF}$ taking on the role of $(F^T)^{-1}$. An outline of the derivation of the $P_e$, following the notation in [12] is presented below.

First assume that correct decisions are fed back to the SIC, so that the output signal-to-noise ratio (SNR) for user $k$ can be written as

$$SNR_{k,SIC} = F_{k,k}^2 A_k^2/\sigma^2. \tag{7.2}$$

Recall that $A_k$ is the amplitude of the $k^{th}$ user's signal, and $\sigma$ is the standard deviation of the AWGN. Then, the $P_e$ can be written by applying Eq. (2.27) to obtain

$$P_{e_{k,SIC}} = Q(F_{k,k}A_k/\sigma) \tag{7.3}$$

Now, assuming that some errors occur, a more accurate probability of error can be calculated by first computing the conditional error probability assuming a particular error and then averaging over all the possible errors for all of the previously cancelled $k-1$ users. This expression can be written as

$$P_{e_{k,SIC}} = E[\Delta b_1, ..., \Delta b_{k-1}]Q(\frac{F_{k,k}A_k + \sum_{i=1}^{k-1} F_{k,i}A_i\Delta b_i}{\sigma}) \tag{7.4}$$

where the error for the $i^{th}$ user is $\Delta b_i = (b_i - \tilde{b}_i)$. For the binary system under consideration, $\Delta b_i$ can only take on the values 2 or $-2$. Substituting $\mathbf{C}_{MWF}$ for $\mathbf{F}$, the expression for $P_e$ is written as

$$P_{e_{k,SIC}} = E[\Delta b_1, ..., \Delta b_{k-1}]Q(\frac{c_{k,MWF}A_k + \sum_{i=1}^{k-1} c_{i,MWF}A_i\Delta b_i}{\sigma}) \tag{7.5}$$

The final expression of the probability of error given in Eq. (7.5) is complicated to evaluate even for the binary problem because of the presence of multiple users and will therefore be evaluated using a simple example to validate the corresponding MC simulations.

**Example** : In this example, a two-user system is considered to simplify the expression for $P_e$ above. The $E_b/N_0$ vs. $P_e$ curve obtained with this expression is then compared to the MC simulation generating bit error rate (BER) with the same system parameters. This result is thus used to validate the MC simulation used in the next section to provide numerical results with multiple interferers. Assume that the first user has higher power than the second user and is thus cancelled first. First, note that the probability of error for the stronger user is given by the output of the first stage of the SIC, i.e. the MF followed by the MWF. This is denoted $P_1$ and is given by

$$P_1 = Q(c_{1,MWF}A_1/\sigma). \tag{7.6}$$

Then, the input to the decision device for the second user is $A_2 b_2 + c_{1,MWF} A_1 (b_1 - \tilde{b}_1) + n_2$. By averaging over the two possible values that can be taken on by $b_1 - \tilde{b}_1$, the error probability for the second user, denoted $P_2$, can be written as

$$P_2 = (1 - P_1) Q(A_2/\sigma) + \frac{P_1}{2} [Q(\frac{A_2 - 2c_{1,MWF} A_1}{\sigma}) + Q(\frac{A_2 + 2c_{1,MWF} A_1}{\sigma})]. \quad (7.7)$$

To test the result via simulation, a synchronous CDMA system with Gold codes of length $N = 31$ is used. The number of users again is $K = 2$, the rank of the MWF is $D = 5$, the multipath channel has $L = 5$ taps, and the power difference between the two users is $\Delta P = 1$ dB. The BER and $P_e$ are plotted as a function of the $E_b/N_0$ and are shown in Figure 7.2 below. Note the excellent agreement between the simulation models. Having validated the Monte Carlo model, the model is now used to provide results with multiple users in the next section.

### 7.1.2 Numerical Results

In this section, results from Monte Carlo simulations are provided to determine the performance gain of the MWF/SIC over the standard MMSE and conventional SIC receivers. Synchronous users are shown, although performance with asynchronous users can be assessed by treating each asynchronous user as two synchronous users. Performance of the standard rake receiver is also shown for comparison. Using Gold codes of length $N = 31$, plots of $E_b/N_0$ versus BER are shown in Figures 7.3, 7.4, 7.5, and 7.6 for 10, 15, 20, and 25 users, respectively, assuming that the power difference among the users, from one user to the next, is 1 dB. This means that the strongest user can be as much as 19 dB above the weakest for the 20 user case. The strongest user is detected first, and the BER is computed for the *weakest* user. Note that in the range of $10^{-3}$ to $10^{-5}$ BER, the MWF IS/SIC gives a performance gains of about

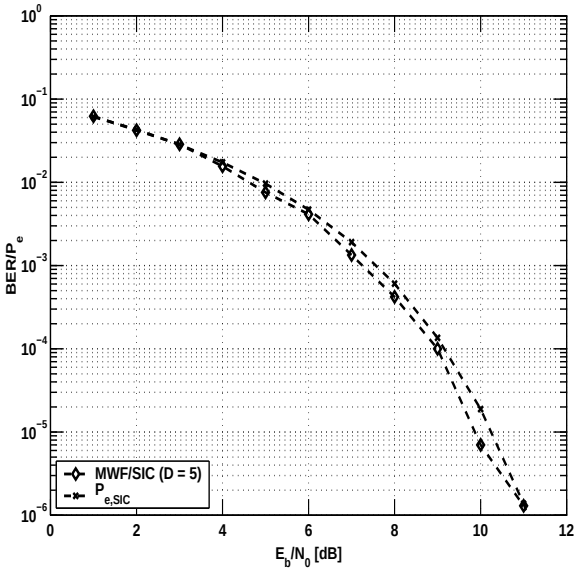


Figure 7.2: Comparison of Monte Carlo and Analytical Serial Interference Cancellation (SIC) Models: $E_b/N_0$ [dB] vs. Probability of Error ($P_e$) and BER; synchronous CDMA; spreading code length, $N = 31$ (Gold Codes); number of users, $K = 2$; rank of MWF, $D = 5$; channel delay spread, $L = 5$; power of interfering user/power of desired user, $\Delta P = 1$ dB

2 dB over full rank MMSE and at least 6 dB over conventional SIC, which fails if the number of users is too high. Furthermore, the relative performance gain over the conventional SIC as the number of users increases is significant. The conventional SIC degrades rapidly as the number of users increases due to the fact that the matched filter is interference limited. Thus, bit error rates in the desired range for speech ($10^{-3}$) cannot be achieved. On the other hand, the MWF based schemes can support bit error rates lower than $10^{-6}$, which makes this detection scheme suitable even for digital data.

A few noteworthy observations are now made. First, it was observed in simulations that if the power difference among the codes is too great, the SIC does not offer

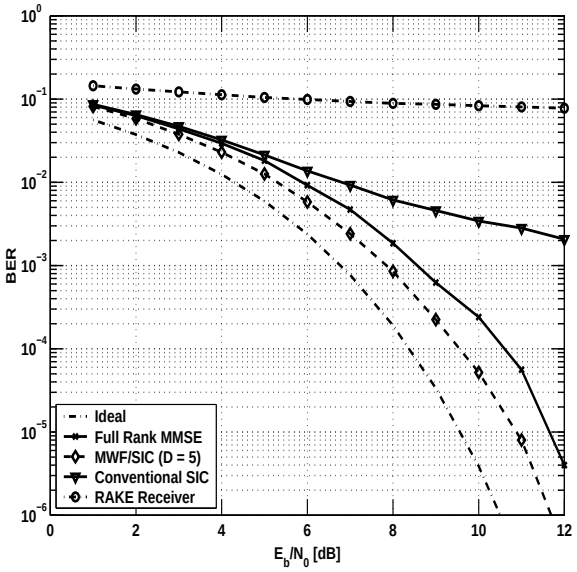


Figure 7.3: Comparison of Serial Interference Cancellation (SIC) Schemes: $E_b/N_0$ [dB] vs. BER; synchronous CDMA; spreading code length, $N = 31$ (Gold Codes); number of users, $K = 10$; rank of MWF, $D = 5$; channel delay spread, $L = 5$; power step size, $\Delta P_{step} = 1$ dB

improvement over the MMSE receiver. This is explained by noting first that a power difference of $\Delta P = 3$ dB with, say, $K = 15$ users results in a 45 dB difference between the strongest and weakest user. In this case, the difference is so high that the MMSE receiver suffices to produce valid bit estimates. Furthermore, the BER shown is only for the weakest user. If the BER is averaged over all the users, the result would be much better than what is shown in the plots. Next, it is noted that performance of the SIC with Hadamard codes did not do as well as with Gold codes. This is explained by again by pointing out the poor cross-correlation properties of the Hadamard codes, so that when multipath is present, correct detection and estimation for the signal-to-noise ratios under consideration is less accurate, and so

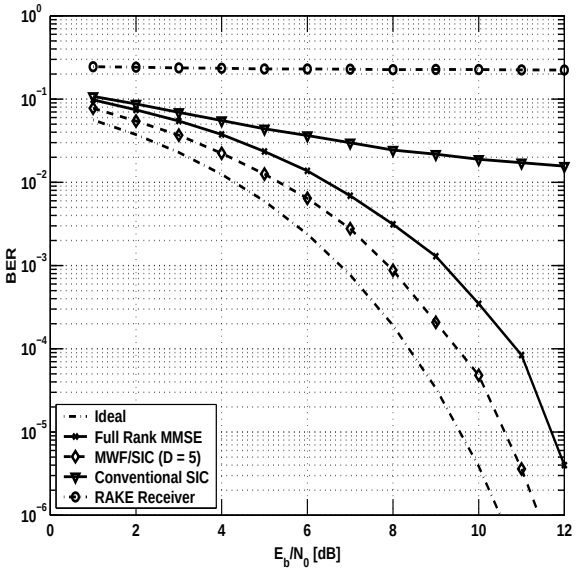


Figure 7.4: Comparison of Serial Interference Cancellation (SIC) Schemes: $E_b/N_0$ [dB] vs. BER; synchronous CDMA; spreading code length, $N = 31$ (Gold Codes); number of users, $K = 15$; rank of MWF, $D = 5$; channel delay spread, $L = 5$; power step size, $\Delta P_{step} = 1$ dB

error propagation occurs. Recall, though, that Hadamard codes are typically not used for spreading. It is also noted that performance of the MWF/SIC at a rank of $D = 12$ improved by about 1 dB over $D = 5$.

## 7.2 Parallel Interference Cancellation (PIC)

The standard parallel interference canceller (PIC) provides cancellation of all of the equal (or nearly equal) power interferers from the received signal at successive stages before decoding the bits transmitted by the desired user. Again the decoding of the interfering users is done by correlation with a matched filter. A hard decision on each correlator output is used to regenerate the decoded interfering signals and

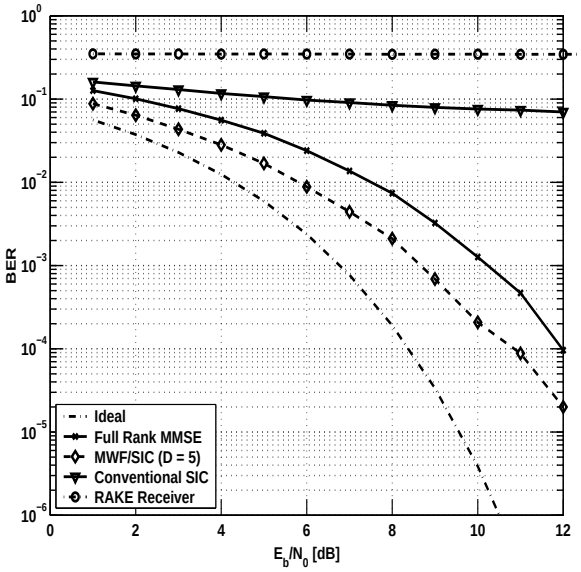


Figure 7.5: Comparison of Serial Interference Cancellation (SIC) Schemes: $E_b/N_0$ [dB] vs. BER; synchronous CDMA; spreading code length, $N = 31$ (Gold Codes); number of users, $K = 20$; rank of MWF, $D = 5$; channel delay spread, $L = 5$; power step size, $\Delta P_{step} = 1$ dB

subtract them out of the received signal. Following the last stage of the PIC, the desired user's bits are then decoded. An improved Gaussian approximation to the conventional PIC is developed in [6]. In [93], a multistage detector that is moderately complex but sub-optimal is derived. In [11], a PIC scheme that includes tentative decision devices at each stage is developed. The complexity of this implementation is linear in the number of users. The idea of combining linear detectors with non-linear interference cancellation has also been explored in many papers. An MMSE/PIC detector is presented in [36]. A decorrelating linear detector in combination with a PIC is considered in [94]. In this paper, an exact expression for $P_e$ is derived. In [9], a combined MMSE/PIC is derived, and the $P_e$ is computed using the Gaussian

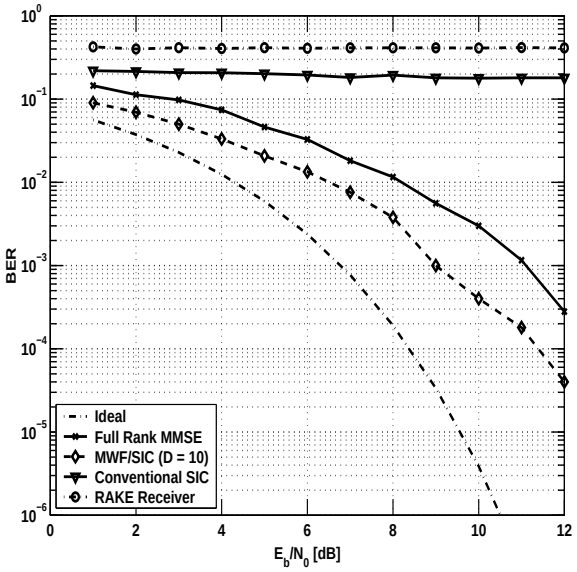


Figure 7.6: Comparison of Serial Interference Cancellation (SIC) Schemes: $E_b/N_0$ [dB] vs. BER; synchronous CDMA; spreading code length, $N = 31$ (Gold Codes); number of users, $K = 25$; rank of MWF, $D = 5$; channel delay spread, $L = 5$; power step size, $\Delta P_{step} = 1$ dB

assumption. Finally, a mathematical approach to the analysis of linear PIC schemes is presented in [27].

In this new scheme, it is again proposed to replace the conventional correlator at each stage in the PIC with the CSA-MWF. The IS performed at each stage is again expected to improve performance. A partial block diagram of a two-stage PIC structure similar to that shown in [36] is shown in Figure 7.7 [80]. Further stages can be concatenated by subtracting the re-spread bit estimates at each stage from the input to the MWF of that stage, which has the estimates of the previous stages already removed.

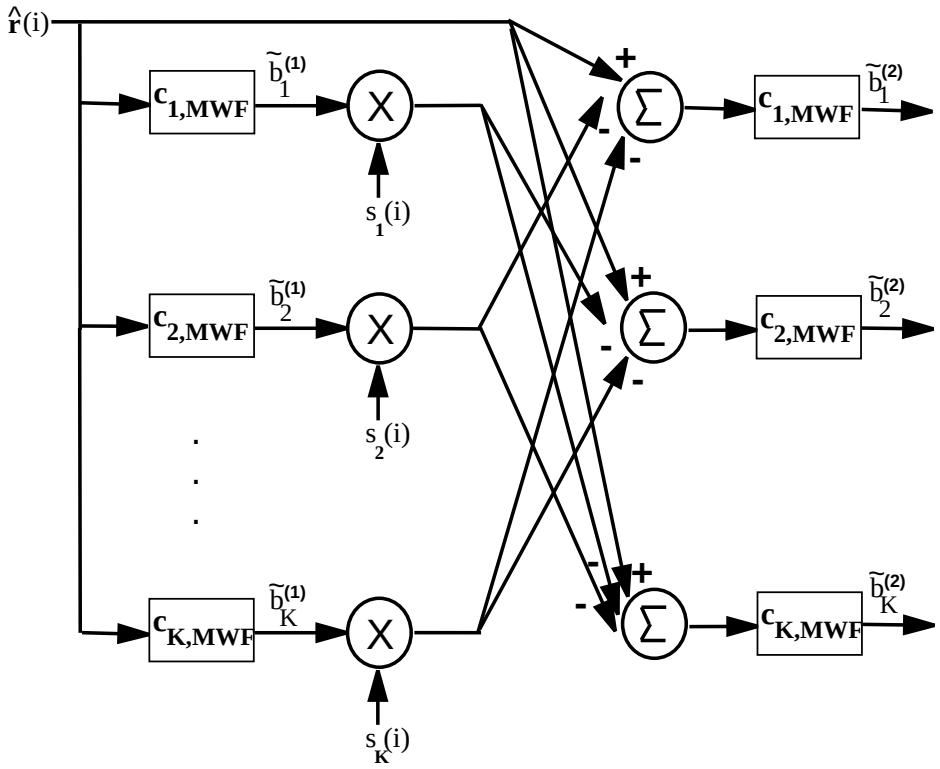


Figure 7.7: Parallel Interference Cancellation (PIC) via Correlations Subtraction Architecture of the Multistage Wiener Filter (CSA-MWF) (Two-Stage)

### 7.2.1 Probability of Error ($P_e$) Derivation

The $P_e$ derivation in this section can be obtained easily from that presented in [36], in which an approximate formula for $P_e$ using an MMSE/PIC is derived and bounded. By replacing the MMSE detector with the equivalent MWF, the MWF/PIC solution is obtained. The expression for $P_e$ is complicated and is bounded in [36], Eq. (31). Note the similarity between this equation and Eq. (7.5), derived for the SIC. In fact, it can be shown that these equations are identical. Alternatively, note the similarity between the structures in Figures 7.1 and 7.7. This is because

the single stage SIC structure is identical to that of the two-stage PIC, with the only exception being the way the users are cancelled. In the PIC, the users are assumed equal power, and therefore all cancelled simultaneously whereas in the SIC, users of higher power are cancelled first. For a multistage PIC, the derivation is difficult, and Monte Carlo simulations are a more reasonable alternative. Performance of the PIC is again evaluated using a simple example. A two user system is again considered, and the parameters are identical to that of the SIC example. However, now the powers of the two users are set equal, to 0 dB. In Figure 7.8, the $P_e$ and BER are plotted vs. $E_b/N_0$. Note again the good agreement between the two models.

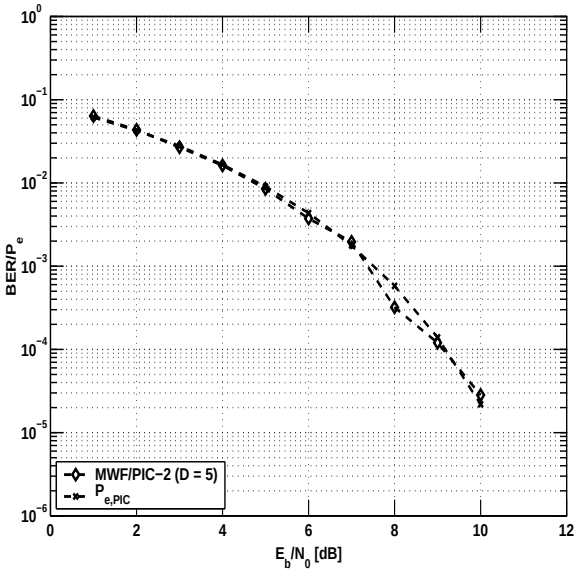


Figure 7.8: Comparison of Monte Carlo and Analytical Parallel Interference Cancellation (PIC) Models: $E_b/N_0$ [dB] vs. Probability of Error ($P_e$) and BER; synchronous CDMA; spreading code length, $N = 31$ (Gold Codes); number of users, $K = 2$; rank of MWF, $D = 5$; channel delay spread, $L = 5$; power of interfering user/power of desired user, $\Delta P = 0$ dB

### 7.2.2 Numerical Results

Results from Monte Carlo simulations are now provided to determine the performance gain of the MWF/PIC over the standard MMSE and conventional PIC receivers. Synchronous users are again used and performance is demonstrated for a three stage PIC. Performance of the standard rake receiver is also shown for comparison. Plots of $E_b/N_0$ versus BER are shown in Figures 7.9 and 7.10 for highly loaded systems containing 20, and 25 users. For optimal PIC performance, users of equal powers are considered. The last plot in Figure 7.11 shows the same results as in 7.9 for $K = 20$ users except the effect of inter-cell interference from two cells is also included. Blocks of size $M = 1000$ are used to keep the Monte Carlo simulation run times reasonable, as block sizes of $M = 5000$ would cause the BER to reduce further by an order of magnitude. Note that performance suffers at low $E_b/N_0$. This occurs because high noise levels cause errors in the first stages to propagate to later stages, thereby causing a performance loss. Typically, PICs are only used in high signal-to-noise environments where error propagation is not a concern. A similar effect is not observed in the SIC, because the highest power users are cancelled first, increasing detection reliability and reducing the number of errors. Performance gains of $2 - 4$ dB are observed. The loss due to the inter-cell interference is about 1 dB.

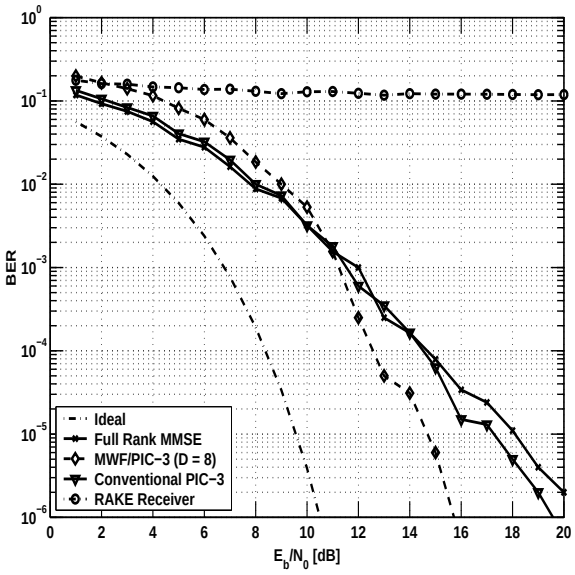


Figure 7.9: Three Stage Parallel Interference Cancellation (PIC): $E_b/N_0$ [dB] vs. BER; synchronous CDMA; spreading code length, $N = 31$ (Gold Codes); number of users, $K = 20$; rank of MWF, $D = 8$; channel delay spread, $L = 5$; power of interfering users/power of desired user, $\Delta P = 0$ dB

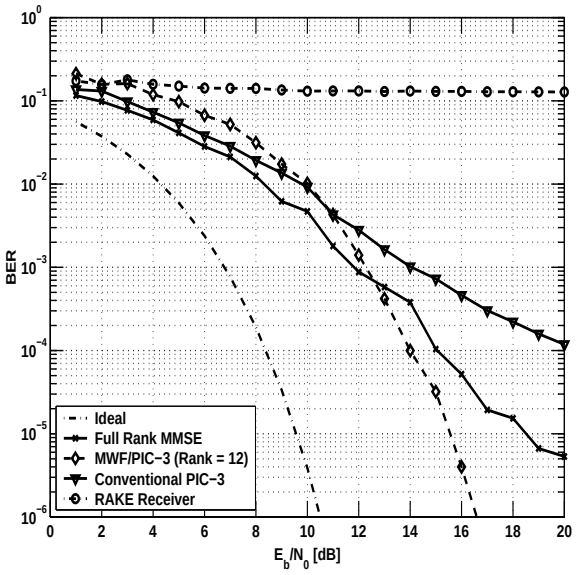


Figure 7.10: Three Stage Parallel Interference Cancellation (PIC): $E_b/N_0$ [dB] vs. BER; synchronous CDMA; spreading code length, $N = 31$ (Gold Codes); number of users, $K = 25$; rank of MWF, $D = 12$; channel delay spread, $L = 5$; power of interfering users/power of desired user, $\Delta P = 0$ dB

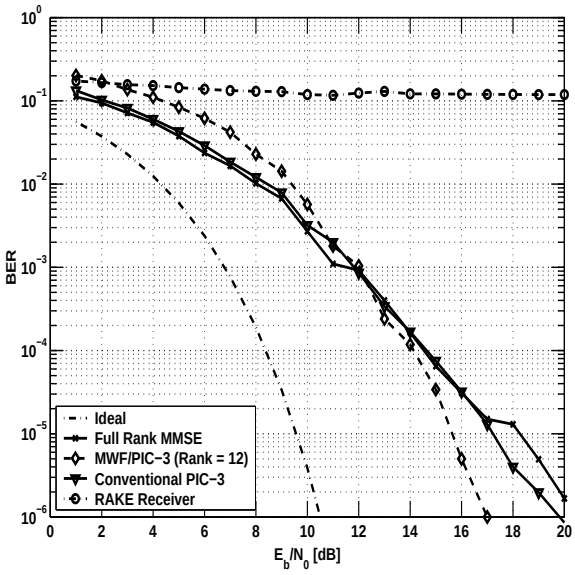


Figure 7.11: Three Stage Parallel Interference Cancellation (PIC): $E_b/N_0$ [dB] vs. BER; synchronous CDMA; 3 Cells; spreading code length, $N = 31$ (Gold Codes); number of users, $K = 20$; rank of MWF, $D = 12$; channel delay spread, $L = 5$; power of interfering users/power of desired user, $\Delta P = 0$ dB

# Chapter 8

# Reduced Rank Space-Time Coding (STC)

In this chapter, the joint detection techniques from Chapter 6 are extended to space-time codes. With space-time codes, the data bit of a particular user is mapped into a set of symbols and the symbols are transmitted over separate antennas. In a CDMA system, the symbols are also multiplied by the appropriate spreading codes. The received codeword is decoded at the receiver using a maximum likelihood (ML) or minimum mean square error (MMSE) approach, and a bit estimate is determined. The impact of antenna spatial diversity on wireless communications systems is shown in [100]. In [103], space-time codes are combined with Turbo codes and processed via combined MMSE and parallel interference cancellation (PIC) detection. A quasi-orthogonal space-time block code is designed in [41]. In this chapter, a reduced rank interference suppression (IS) algorithm using the correlation subtraction architecture of the multistage Wiener filter (CSA-MWF) is presented. The goal is again to show the reduction in complexity while achieving or often *exceeding* the performance of the original ML solution. For ease in implementation, attention is restricted to flat fading channels. That is, the spread due to the multipath is neglected. However,

the techniques developed in Chapter 5 to optimize performance in multipath could be applied.

Performance will be analyzed for specific $2 \times 2$ and $4 \times 4$ space-time codes. The theory to be described is valid for any type of space-time code, but the specific receiver structure must be modified for different codes. Performance improvements, in terms of coding gain, over non-encoded systems are studied using Gold codes for spreading. These codes have already been shown to exhibit properties better than any other (e.g. Hadamard or PN) codes, especially when the users are transmitted asynchronously. Performance gains over the full rank MMSE implementation for detecting the bits using the space-time codes is also studied. It is shown that performance benefits over unencoded systems are huge, up to 18 dB. Performance benefits versus the MMSE receiver are also significant, up to 4 dB. These benefits are attributed once again to the excellent ability of the MWF to suppress interference induced by non-orthogonal multiplexing of Gold codes, which have good cross-correlation properties. The benefits will be most pronounced in the asynchronous environment. In the synchronous case, since flat fading is assumed, ideal orthogonal (Hadamard) codes would be best, but to limit the number of simulations, only Gold codes are used. The simulation parameters are summarized in Table 8.1.

The construction of such codes will first be provided. Since the design of such codes is not the focus here, only code examples will be cited. For detailed theory on code design, see [41], [86], and [88]. The optimum estimation of the bits from the received codewords is obtained by the ML solution, which can be implemented using the MMSE receiver structure. The implementation of the solution in reduced rank is shown. Numerical results are provided and analyzed. Numerical results obtained

Table 8.1: Space-Time Code Simulation Parameters: $N$=length of spreading code, $E_b/N_0$=Bit energy divided by single-sided noise power spectral density (PSD), $M$=block size, $K$=number of users, $D$=rank of multistage Wiener filter (MWF), $L$=channel delay spread, $\Delta P$ =power of interfering users/power of desired user

| | $N$ | $E_b/N_0$ [dB] | $M$ | $K$ | $D$ | $L$ | $\Delta P[dB]$ | Synchronism |
|---|---|---|---|---|---|---|---|---|
| Fig. 8.3 | 31 | N/A | 5000 | 2 | 1 | 1 | 0 | Asynchronous |
| Fig. 8.4 | 31 | N/A | 5000 | 15 | 5 | 1 | 0 | Asynchronous |
| Fig. 8.5 | 31 | N/A | 5000 | 15 | 5 | 1 | 0 | Synchronous |
| Fig. 8.6 | 31 | N/A | 5000 | 4 | 1 | 1 | 0 | Asynchronous |
| Fig. 8.7 | 31 | N/A | 5000 | 15 | 5 | 1 | 0 | Asynchronous |
| Fig. 8.8 | 31 | N/A | 5000 | 15 | 5 | 1 | 0 | Synchronous |

using the MWF will be compared to the full rank MMSE to determine the coding gain associated with the space-time codes.

## 8.1 Space-Time Code Construction

The simplest and most cited space-time code for transmission with two transmit antennas is developed in [1]. This scheme was generalized later in [86] and [88] to an arbitrary number of antennas and is able to achieve the full diversity capacity of the transmit and receive antenna system. For the purposes of this discussion, attention is restricted to simple cases of 2 and 4 transmit antenna systems, with the same number of receive antennas, hereafter referred to as the $2 \times 2$ and $4 \times 4$ systems, respectively.

In the $2 \times 2$ case, at a given time period $t$, symbol $c_1$ is transmitted from antenna one, and symbol $c_2$ is transmitted from antenna two. During the next time period, $t+T$, symbol $-c_2$ is transmitted from antenna one, and symbol $c_1$ is transmitted from antenna two. This simple code, also termed the Alamouti code after its inventor, can

be written as

$$\mathbf{C}_{2x2} = \begin{bmatrix} c_1 & c_2 \\ -c_2 & c_1 \end{bmatrix}. \tag{8.1}$$

The sequence is also shown in Table 8.2. In this notation, the column $i$ of the code matrix denotes the signals transmitted from antenna $i$, and the row $t$ denotes transmission at time $t$. In the CDMA system under consideration, referring back to Figure 2.1, these symbols could represent bits for any given user multiplied by that user's spreading codes.

Table 8.2: $2 \times 2$ Space-Time Coding (STC) Scheme

| | Antenna 1 | Antenna 2 |
|---|---|---|
| Time t | $c_1$ | $c_2$ |
| Time t+T | $-c_2$ | $c_1$ |

An example of a $4 \times 4$ space-time code constructed from orthogonal designs is presented in [86] and is given by

$$\mathbf{C}_{4x4} = \begin{bmatrix} c_1 & c_2 & c_3 & c_4 \\ -c_2 & c_1 & -c_4 & c_3 \\ -c_3 & c_4 & c_1 & -c_2 \\ -c_4 & -c_3 & c_2 & c_1 \end{bmatrix}. \tag{8.2}$$

This code is also summarized in Table 8.3 below. The complex conjugation operations found in the original development are neglected here because all data is assumed to be real. The design of this code is based on the mathematical theory of orthogonal designs, in which an $n \times n$ code can be produced but only for certain sporadic values of $n$. Codes for arbitrary $n$ can also be designed using a generalization of the orthogonal code design [86]. From this development, it can be seen that the transmission rates achieved with these code designs are the maximum possible with transmit

diversity. This will be true in general for real codes based on orthogonal designs.

Table 8.3: $4 \times 4$ Space-Time Coding (STC) Scheme

| | Antenna 1 | Antenna 2 | Antenna 3 | Antenna 4 |
|---|---|---|---|---|
| Time t | $c_1$ | $c_2$ | $c_3$ | $c_4$ |
| Time t+T | $-c_2$ | $c_1$ | $-c_4$ | $c_3$ |
| Time t+2T | $-c_3$ | $c_4$ | $c_1$ | $-c_2$ |
| Time t+3T | $-c_4$ | $-c_3$ | $c_2$ | $c_1$ |

Other work in the construction of space-time codes is as follows: In [55], an overview of block and trellis space-time coding schemes as well as their corresponding decoding schemes are analyzed. Generalized design theory, performance criteria, and performance results in multipath channels is presented in [87], [88], and [89]. A space-time code for a four transmit antenna system is presented in [60]. Performance gain of space-time coding schemes coupled with optimum antenna selection is given in [26]. Finally, high rate space-time codes that can be constructed for any configuration of transmit and receive antennas is given in [29].

## 8.2 Derivation of Minimum Mean Square Error (MMSE) Solution

The MMSE solution will first be derived for the $2 \times 2$ code and then for the $4 \times 4$ codes described above [79]. The MMSE solution for the $2 \times 2$ code has been previously shown in [55] and shown specifically for CDMA systems in [47]. The solution will be briefly described here to determine the implementation of the solution via the MWF. The development follows that shown in [47]. The $4 \times 4$ solution is derived in a similar way. Extension to more complicated codes is straightforward. To

make mathematical analysis easier, the model is developed assuming synchronous users. But, the solution can be applied to asynchronous users as well assuming that the receiver is synchronized with the desired user.

### 8.2.1 $2 \times 2$ Space-Time Code

Recall for the $2 \times 2$ code, $c_1$ is transmitted from antenna one and $c_2$ is transmitted from antenna two at time $T$. In the next time period, $-c_2$ and $c_1$ are transmitted from antennas one and two, respectively. Define $h_{ij}$ as the channel coefficient from the $i^{th}$ transmit antenna to the $j^{th}$ receive antenna. These coefficients are modelled as Rayleigh distributed random variables. Denote the received signals over the two consecutive symbol periods as $\mathbf{r}_j(i)$ and $\mathbf{r}_j(i-1)$. Assuming, as mentioned earlier, that each $h_{ij}$ is approximately constant over two consecutive symbol periods, one can write the received signal at antenna $j = 1$ or $j = 2$ as

- $\mathbf{r}_j(i) = \sum_{k=1}^{K} A_k(h_{1j}\mathbf{s}_k b_k(i) + h_{2j}\mathbf{s}_k b_k(i-1)) + \mathbf{n}_j(i)$
- $\mathbf{r}_j(i-1) = \sum_{k=1}^{K} A_k(-h_{2j}\mathbf{s}_k b_k(i) + h_{1j}\mathbf{s}_k b_k(i-1)) + \mathbf{n}_j(i-1)$,

where $\mathbf{n}_j(i)$ and $\mathbf{n}_j(i-1)$ are $N \times 1$ AWGN vectors. To ease the development, define the received signal vector by $\mathbf{r}(i) = [\mathbf{r}_j(i)\ \mathbf{r}_j(i-1)]^T$ and the noise vector by $\mathbf{n} = [\mathbf{n}_j(i)\ \mathbf{n}_j(i-1)]^T$. Define code symbol vectors by

$$\mathbf{c}_{jk,1} = [h_{1j}\mathbf{s}_k^T\ h_{2j}\mathbf{s}_k^T]^T \tag{8.3}$$

$$\mathbf{c}_{jk,2} = [-h_{2j}\mathbf{s}_k^T\ h_{1j}\mathbf{s}_k^T]^T. \tag{8.4}$$

This can also be written as

$$\mathbf{c}_{jk,1} = \zeta_{k,1}\mathbf{h}_j \tag{8.5}$$

$$\mathbf{c}_{jk,2} = \zeta_{k,2}\mathbf{h}_j, \tag{8.6}$$

where

$$\zeta_{k,1} = \begin{bmatrix} \mathbf{s}_k & \mathbf{0} \\ \mathbf{0} & \mathbf{s}_k \end{bmatrix} \tag{8.7}$$

$$\zeta_{k,2} = \begin{bmatrix} \mathbf{0} & -\mathbf{s}_k \\ \mathbf{s}_k & \mathbf{0} \end{bmatrix}, \tag{8.8}$$

and $\mathbf{h}_j = [h_{1j}\ h_{2j}]^T$. One can further define

$$\mathbf{h} = [\mathbf{h}_1^T\ \mathbf{h}_2^T]^T, \tag{8.9}$$

and

$$\mathbf{c}_{k,1} = [\mathbf{c}_{1k,1}^T\ \mathbf{c}_{2k,1}^T]^T = (\mathbf{I}_2 \otimes \zeta_{k,1})\mathbf{h} \tag{8.10}$$

$$\mathbf{c}_{k,2} = [\mathbf{c}_{1k,2}^T\ \mathbf{c}_{2k,2}^T]^T = (\mathbf{I}_2 \otimes \zeta_{k,2})\mathbf{h}, \tag{8.11}$$

where $\mathbf{I}_2$ denotes a $2 \times 2$ identity matrix and $\otimes$ denotes the Kronecker product as before. Writing the received signal as the sum of the outputs of both receiver antennas, the output becomes

$$\mathbf{r}(i) = \sum_{k=1}^{K} A_k(\mathbf{c}_{k,1}b_k(i) + \mathbf{c}_{k,2}b_k(i-1)) + \mathbf{n}(i), \tag{8.12}$$

where $\mathbf{n} = [\mathbf{n}_1^T\ \mathbf{n}_2^T]^T$.

The MMSE receiver must detect the vector of received bits $\mathbf{b}(i) = [b_1(i)\ b_2(i)\ ...b_K(i)]^T$ from the received signal vector $\mathbf{r}(i)$. To compute the MMSE solution, minimize the MSE, given by

$$MSE_{STC} = arg_{\Im} min E[\|\mathbf{b}(i) - \Im^H \mathbf{r}(i)\|^2]. \tag{8.13}$$

The MMSE solution can be written directly as

$$\Im = \mathbf{R}_{rr}^{-1}\mathbf{R}_{rb}, \tag{8.14}$$

where $\mathbf{R}_{rr}$ is the data covariance matrix and $\mathbf{R}_{rb}$ is the cross-correlation vector. From Eq. (8.12), the cross-correlation vector can be written as

$$\mathbf{R}_{yb} = E[\mathbf{r}(i)\mathbf{b}(i)] = \mathbf{CA}, \tag{8.15}$$

where $\mathbf{C} = [\mathbf{C}_1\ \mathbf{C}_2\ ...\ \mathbf{C}_K]$, $\mathbf{C}_k = [\mathbf{c}_{k,1}\ \mathbf{c}_{k,2}]$, and $\mathbf{A}$ is the diagonal matrix of signal amplitudes defined previously. Assuming without loss of generality that user one is the desired user, the MMSE simplifies to

$$\Im_{SU} = A_1\mathbf{R}_{rr}^{-1}\mathbf{C}_1. \tag{8.16}$$

### 8.2.2 $4 \times 4$ Space-Time Code

The derivation of the MMSE solution for the $4 \times 4$ STC can be obtained analogously to that for the $2 \times 2$ code. The parameters $h_{ij}$ are as defined for the $2 \times 2$ code. The received signals over four consecutive symbol periods at antenna $j$, $j = 1, 2, 3, 4$, are defined, respectively, as

- $\mathbf{r}_j(i) = \sum_{k=1}^{K} A_k(h_{1j}\mathbf{s}_k b_k(i) + h_{2j}\mathbf{s}_k\ b_k(i-1) + h_{3j}\mathbf{s}_k b_k(i-2) + h_{4j}\mathbf{s}_k b_k(i-3)) + \mathbf{n}_j(i)$
- $\mathbf{r}_j(i-1) = \sum_{k=1}^{K} A_k(-h_{2j}\mathbf{s}_k b_k(i) + h_{1j}\mathbf{s}_k b_k(i-1) - h_{4j}\mathbf{s}_k b_k(i-3) + h_{3j}\mathbf{s}_k b_k(i-4)) + \mathbf{n}_j(i-1)$,
- $\mathbf{r}_j(i-2) = \sum_{k=1}^{K} A_k(-h_{3j}\mathbf{s}_k b_k(i) + h_{4j}\mathbf{s}_k b_k(i-1) + h_{1j}\mathbf{s}_k b_k(i-3) + h_{2j}\mathbf{s}_k b_k(i-4)) + \mathbf{n}_j(i-2)$,
- $\mathbf{r}_j(i-3) = \sum_{k=1}^{K} A_k(-h_{4j}\mathbf{s}_k b_k(i) - h_{3j}\mathbf{s}_k b_k(i-1) + h_{2j}\mathbf{s}_k b_k(i-3) + h_{1j}\mathbf{s}_k b_k(i-4)) + \mathbf{n}_j(i-3)$,

where $\mathbf{n}_j(i)$, $\mathbf{n}_j(i-1)$, $\mathbf{n}_j(i-2)$, and $\mathbf{n}_j(i-3)$ are $N \times 1$ AWGN vectors. Write the received vector as $\mathbf{r}(i) = [\mathbf{r}_j(i)\ \mathbf{r}_j(i-1)\ \mathbf{r}_j(i-2)\ \mathbf{r}_j(i-3)]^T$ and the noise vector by

$\mathbf{n} = [\mathbf{n}_j(i)\ \mathbf{n}_j(i-1)\ \mathbf{n}_j(i-2)\ \mathbf{n}_j(i-3)]^T$. Define the code symbol vectors by

$$\mathbf{c}_{jk,1} = [h_{1j}\mathbf{s}_k^T\ h_{2j}\mathbf{s}_k^T\ h_{3j}\mathbf{s}_k^T\ h_{4j}\mathbf{s}_k^T]^T \tag{8.17}$$

$$\mathbf{c}_{jk,2} = [-h_{2j}\mathbf{s}_k^T\ h_{1j}\mathbf{s}_k^T\ -h_{4j}\mathbf{s}_k^T\ h_{3j}\mathbf{s}_k^T]^T \tag{8.18}$$

$$\mathbf{c}_{jk,3} = [-h_{3j}\mathbf{s}_k^T\ h_{4j}\mathbf{s}_k^T\ h_{1j}\mathbf{s}_k^T\ -h_{2j}\mathbf{s}_k^T]^T \tag{8.19}$$

$$\mathbf{c}_{jk,4} = [-h_{4j}\mathbf{s}_k^T\ -h_{3j}\mathbf{s}_k^T\ h_{2j}\mathbf{s}_k^T\ h_{1j}\mathbf{s}_k^T]^T. \tag{8.20}$$

Each of the above equations can also be written as

$$\mathbf{c}_{jk,i} = \zeta_{k,i}\mathbf{h}_j, \tag{8.21}$$

where

$$\zeta_{k,1} = \begin{bmatrix} \mathbf{s}_k & \mathbf{0} & \mathbf{0} & \mathbf{0} \\ \mathbf{0} & \mathbf{s}_k & \mathbf{0} & \mathbf{0} \\ \mathbf{0} & \mathbf{0} & \mathbf{s}_k & \mathbf{0} \\ \mathbf{0} & \mathbf{0} & \mathbf{0} & \mathbf{s}_k \end{bmatrix}, \tag{8.22}$$

$$\zeta_{k,2} = \begin{bmatrix} \mathbf{0} & -\mathbf{s}_k & \mathbf{0} & \mathbf{0} \\ \mathbf{s}_k & \mathbf{0} & \mathbf{0} & \mathbf{0} \\ \mathbf{0} & \mathbf{0} & \mathbf{0} & -\mathbf{s}_k \\ \mathbf{0} & \mathbf{0} & \mathbf{s}_k & \mathbf{0} \end{bmatrix}, \tag{8.23}$$

$$\zeta_{k,3} = \begin{bmatrix} \mathbf{0} & \mathbf{0} & -\mathbf{s}_k & \mathbf{0} \\ \mathbf{0} & \mathbf{0} & \mathbf{0} & \mathbf{s}_k \\ \mathbf{s}_k & \mathbf{0} & \mathbf{0} & \mathbf{0} \\ \mathbf{0} & -\mathbf{s}_k & \mathbf{0} & \mathbf{0} \end{bmatrix}, \tag{8.24}$$

$$\zeta_{k,4} = \begin{bmatrix} \mathbf{0} & \mathbf{0} & \mathbf{0} & -\mathbf{s}_k \\ \mathbf{0} & \mathbf{0} & -\mathbf{s}_k & \mathbf{0} \\ \mathbf{0} & \mathbf{s}_k & \mathbf{0} & \mathbf{0} \\ \mathbf{s}_k & \mathbf{0} & \mathbf{0} & \mathbf{0} \end{bmatrix}, \tag{8.25}$$

and $\mathbf{h}_j = [h_{1j}\ h_{2j}\ h_{3j}\ h_{4j}]^T$. One can further define

$$\mathbf{h} = [\mathbf{h}_1^T\ \mathbf{h}_2^T\ \mathbf{h}_3^T\ \mathbf{h}_4^T]^T, \tag{8.26}$$

and

$$\mathbf{c}_{k,1} = [\mathbf{c}_{1k,1}^T\ \mathbf{c}_{2k,1}^T\ \mathbf{c}_{3k,1}^T\ \mathbf{c}_{4k,1}^T]^T = (\mathbf{I}_4 \otimes \zeta_{k,1})\mathbf{h} \tag{8.27}$$

$$\mathbf{c}_{k,2} = [\mathbf{c}_{1k,2}^T\ \mathbf{c}_{2k,2}^T\ \mathbf{c}_{3k,2}^T\ \mathbf{c}_{4k,2}^T]^T = (\mathbf{I}_4 \otimes \zeta_{k,2})\mathbf{h} \tag{8.28}$$

$$\mathbf{c}_{k,3} = [\mathbf{c}_{1k,3}^T\ \mathbf{c}_{2k,3}^T\ \mathbf{c}_{3k,3}^T\ \mathbf{c}_{4k,3}^T]^T = (\mathbf{I}_4 \otimes \zeta_{k,3})\mathbf{h} \tag{8.29}$$

$$\mathbf{c}_{k,4} = [\mathbf{c}_{1k,4}^T\ \mathbf{c}_{2k,4}^T\ \mathbf{c}_{3k,4}^T\ \mathbf{c}_{4k,4}^T]^T = (\mathbf{I}_4 \otimes \zeta_{k,4})\mathbf{h} \tag{8.30}$$

The received signal can now be written as

$$\mathbf{r}(i) = \sum_{k=1}^{K} A_k(\mathbf{c}_{k,1}b_k(i) + \mathbf{c}_{k,2}b_k(i-1) + \mathbf{c}_{k,3}b_k(i-2) + \mathbf{c}_{k,4}b_k(i-3)) + \mathbf{n}(i), \tag{8.31}$$

where $\mathbf{n} = [\mathbf{n}_1^T\ \mathbf{n}_2^T\ \mathbf{n}_3^T\ \mathbf{n}_4^T]^T$.

With the first user as the user of interest, the MMSE solution is

$$\Im_{SU} = A_1\mathbf{R}_{rr}^{-1}\mathbf{C}_1, \tag{8.32}$$

where $\mathbf{R}_{rr}$ is the data covariance matrix defined previously, $\mathbf{C} = [\mathbf{C}_1\ \mathbf{C}_2\ ...\ \mathbf{C}_K]$ as before, and $\mathbf{C}_k = [\mathbf{c}_{k,1}\ \mathbf{c}_{k,2}\ \mathbf{c}_{k,3}\ \mathbf{c}_{k,4}]$.

## 8.3 Implementation using the Correlation Subtraction Architecture (CSA) of the Multistage Wiener Filter (MWF)

To implement the MMSE solution for space-time codes via the MWF, note the analogy between the original MMSE solution in Eq. (2.23) and that of the STC in Eq. (8.16). In the original solution, $\mathbf{R}$ is the covariance matrix, computed using an expectation of

the received signal times its Hermitian. In the MMSE solution above, a similar result is obtained. Here, the desired covariance matrix is computed exactly the same way, using the joint received vector $\mathbf{r}$, defined in Eq. (8.12) or Eq. (8.31). Similarly, the spreading code $\mathbf{s}_1$ employed in the original solution is now replaced by $\mathbf{C}_1$, defined as $\mathbf{C}_1 = [\mathbf{c}_{k,1}\ \mathbf{c}_{k,2}]$ for the $2 \times 2$ code and $\mathbf{C}_1 = [\mathbf{c}_{k,1}\ \mathbf{c}_{k,2}\ \mathbf{c}_{k,3}\ \mathbf{c}_{k,4}]$ for the $4 \times 4$ code. This substitution causes $\mathbf{d}_0(i)$ to become a vector instead of a scalar. A matrix MWF or a parallel implementation must therefore be used. The outputs, $[\hat{b}_1(i)\ \hat{b}_1(i-1)]$ for the $2 \times 2$ code, and $[\hat{b}_1(i)\ \hat{b}_1(i-1)\ \hat{b}_1(i-2)\ \hat{b}_1(i-3)]^T$ for the $4 \times 4$ code, are delayed appropriately and summed together to determine the final bit estimate. Thus, the MWF algorithm is initialized by setting $\mathbf{d}_0(i) = \mathbf{C}_1^H \mathbf{r}(i)$ and $\mathbf{x}_0(i) = \mathbf{B}_{\mathbf{C}_1}\mathbf{r}(i)$ for the $2 \times 2$ code, and similarly for the $4 \times 4$ code. The blocking matrix $\mathbf{B}_{\mathbf{C}_1}$ is defined to be orthogonal to $\mathbf{C}_1$ as always. The parallel MWF structures are shown for the $2 \times 2$ code and the $4 \times 4$ code in Figures 8.1 and 8.2, respectively. These are the structures used to obtain the simulation results presented in the next section.

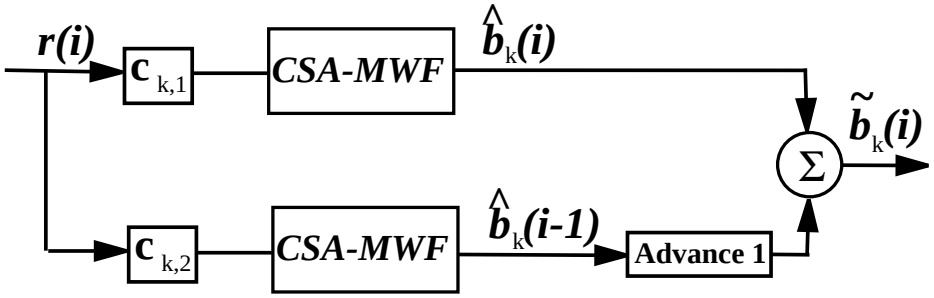


Figure 8.1: $2 \times 2$ Space Time Code (STC) Decoding Scheme Using the Correlation Subtraction Architecture of the Multistage Wiener Filter (CSA-MWF); $\mathbf{r}(i)$=received signal at time $i$; $\mathbf{c}_{k,i}$=code symbol vector for user $k$ at transmit antenna $i$; $\tilde{b}_k(i)$=bit estimate for user $k$ at time $i$

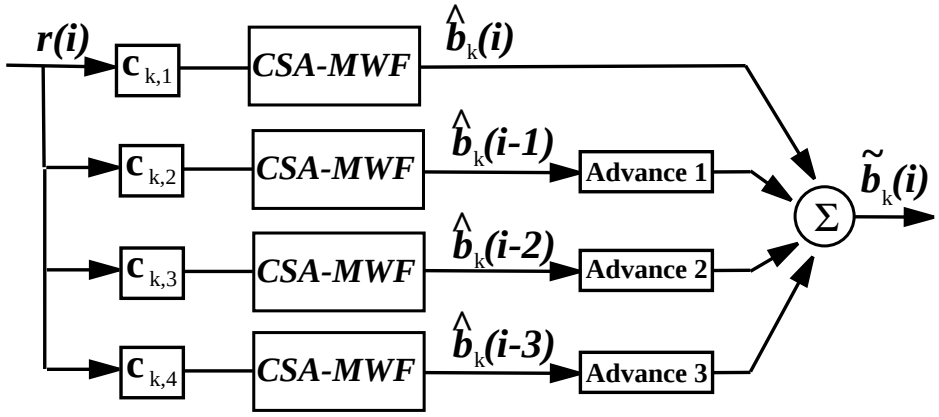


Figure 8.2: $4 \times 4$ Space Time Code (STC) Decoding Scheme Using the Correlation Subtraction Architecture of the Multistage Wiener Filter (CSA-MWF); $\mathbf{r}(i)$=received signal at time $i$; $\mathbf{c}_{k,i}$=code symbol vector for user $k$ at transmit antenna $i$; $\tilde{b}_k(i)$=bit estimate for user $k$ at time $i$

## 8.4 Numerical Results

In this section, numerical results comparing $E_b/N_0$ vs. BER for the MMSE solution and the MWF solution are compared. Performance gains over a conventional system without space-time coding are also determined. Sample results for the $2 \times 2$ and $4 \times 4$ codes are evaluated. For ease in implementation, only one receiver antenna is assumed. Significant additional gains can be attained by exploiting multiple receiver antennas as shown in Chapter 6.

### 8.4.1 $2 \times 2$ Space-Time Code

Figure 8.3 is a plot of $E_b/N_0$ vs. BER for a $2 \times 2$ STC assuming the values of the code symbols are $\epsilon$ $(-1, +1)$. The channel taps are chosen randomly from a Rayleigh distribution and equal power, asynchronous, users are assumed. The full

rank MMSE without the use of coding is shown for comparison. The performance is close to ideal even in this case because the number of users is only $K = 2$. As desired, the STC/MWF algorithm converges to the full rank solution at a rank of only one, due to the presence of only one interferer and the diversity. Significant performance gains of up to about 12 dB are observed, due to the transmit code diversity and time diversity. Note also that the MWF outperforms the MMSE by about 1 dB at the low rank of one. Figure 8.4 shows the same case but with $K = 15$ users and a rank of $D = 5$. Performance gains of up to 17 dB are observed here. Figure 8.5 is a plot of $E_b/N_0$ vs. BER for a $2 \times 2$ STC assuming $K = 15$ synchronous users. Performance gains of up to 11 dB are observed here due to the transmit code diversity, time diversity, and receiver antenna diversity. Note also that the MWF performance meets that of full rank at a rank of 5.

### 8.4.2 $4 \times 4$ Space-Time Code

Figure 8.6 is a plot of $E_b/N_0$ vs. BER for the $4 \times 4$ STC. The channel taps are again chosen randomly, and all users have equal power. The number of users in the system is $K = 4$, and the users are asynchronous and transmit equal power. Again, the STC/MWF algorithm performs with 2 to 4 dB less $E_b/N_0$ than the full rank solution at a rank of only one. This occurs because the MWF is able to compress the received signal subspace to a smaller dimension containing the desired signal, thereby eliminating more noise. Performance gains of 17 dB are observed over the unencoded system. The complexity of the MMSE solution is also greatly reduced by employing the MWF as the dimension of the covariance matrix now increases from $N$ to $NL_t$ (or $NL_r$). So now, the number of required flops for the MWF and the MMSE implementations is $O(2DNL_t)$ and $O((NL_t)^3)$, respectively. With $L_t = 4$,

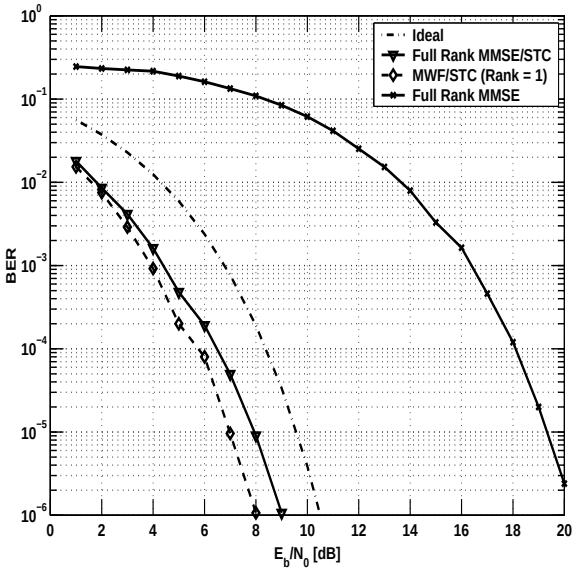


Figure 8.3: 2×2 Space Time Code (STC): $E_b/N_0$ [dB] vs. BER; asynchronous CDMA; spreading code length, $N = 31$ (Gold Codes); number of users, $K = 2$; rank of MWF, $D = 1$; channel delay spread, $L = 1$; power of interfering users/power of desired user, $\Delta P = 0$ dB

this number can become impractically large, even for small $N$, and reduced rank implementation is clearly desirable. The need for reduced rank implementation is greater still when the code length increases beyond $N = 31$, and even more so if multiuser detection (MUD) is required and $K$ is large, as with the next example.

Figure 8.7 shows the result for the same $4 \times 4$ case but with $K = 15$ users. The benefit of using the reduced rank MWF in conjunction with space-time coding is most apparent here. For a highly loaded system in flat fading, the MMSE solution requires high values of $E_b/N_0$. Low bit error rates are attainable at very low $E_b/N_0$ only by employing the reduced rank MWF with space-time coding. Here, the MWF/STC performance exceeds that of full rank MMSE/STC by 2 dB and improves over the standalone MMSE by an astonishing 21 dB. Of course, the drawback is the cost and

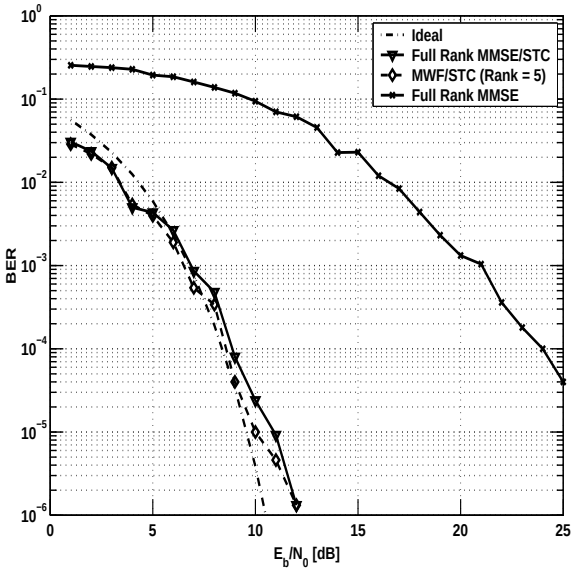


Figure 8.4: $2 \times 2$ Space Time Code (STC): $E_b/N_0$ [dB] vs. BER; asynchronous CDMA; spreading code length, $N = 31$ (Gold Codes); number of users, $K = 15$; rank of MWF, $D = 5$; channel delay spread, $L = 1$; power of interfering users/power of desired user, $\Delta P = 0$ dB

complexity of deploying multiple receive antennas. However, the use of the MWF for decoding greatly reduces complexity, and the coding gain justifies the additional cost.

Finally, Figure 8.8 is a plot of $E_b/N_0$ vs. BER for the $4 \times 4$ STC with $K = 15$ synchronous users. For this highly loaded system in flat fading, the MMSE solution requires high values of $E_b/N_0$. Low BERs are attainable at very low $E_b/N_0$ by employing the reduced rank MWF with space-time coding, with the added benefit of low complexity implementation as described above. Here, the MWF/STC performance improves over full rank MMSE by nearly 15 dB, again at a rank of 5.

The solutions derived for the $2 \times 2$ and $4 \times 4$ codes and the MMSE solution via

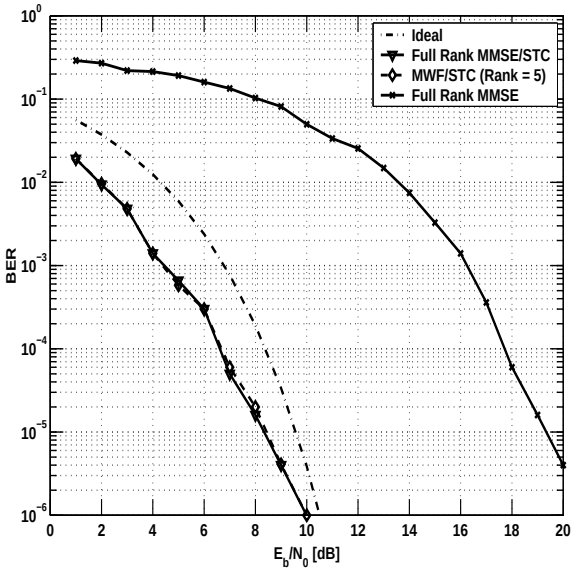


Figure 8.5: $2 \times 2$ Space Time Code (STC): $E_b/N_0$ [dB] vs. BER; synchronous CDMA; spreading code length, $N = 31$ (Gold Codes); number of users, $K = 15$; rank of MWF, $D = 5$; channel delay spread, $L = 1$; power of interfering users/power of desired user, $\Delta P = 0$ dB

the MWF can be extended to more complicated codes. However, as the number of users and code complexity increases, MWFs running in parallel to detect each code symbol are required. To reduce this computational burden further, one can simply design the system to process only the user of interest and treat the other users as AWGN, as the conventional rake receiver does. Due to the significant coding gains from the STC, desired BERs can be attained.

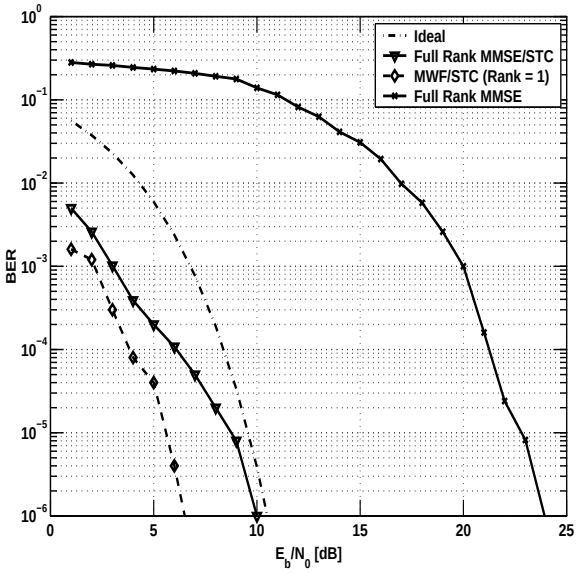


Figure 8.6: $4\times4$ Space Time Code (STC): $E_b/N_0$ [dB] vs. BER; asynchronous CDMA; spreading code length, $N = 31$ (Gold Codes); number of users, $K = 4$; rank of MWF, $D = 1$; channel delay spread, $L = 1$; power of interfering users/power of desired user, $\Delta P = 0$ dB

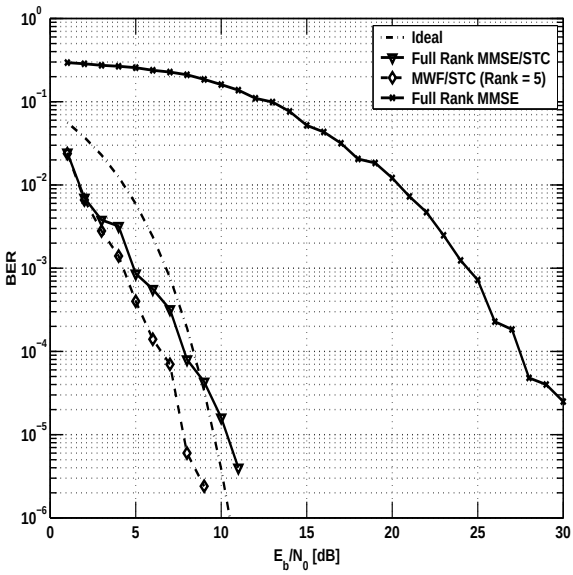


Figure 8.7: $4 \times 4$ Space Time Code (STC): $E_b/N_0$ [dB] vs. BER; asynchronous CDMA; spreading code length, $N = 31$ (Gold Codes); number of users, $K = 15$; rank of MWF, $D = 5$; channel delay spread, $L = 1$; power of interfering users/power of desired user, $\Delta P = 0$ dB

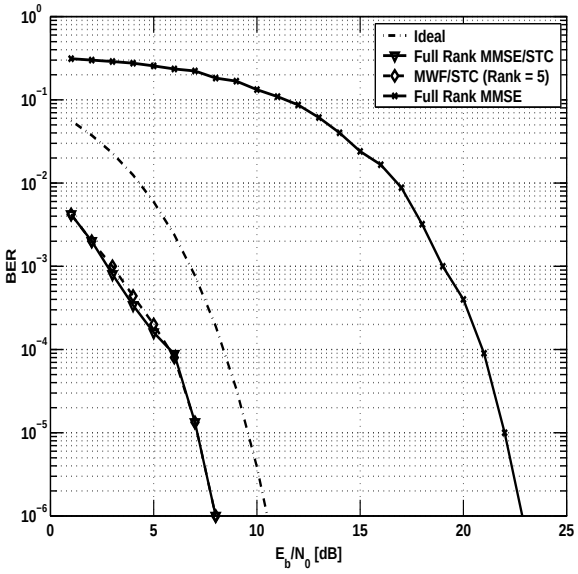


Figure 8.8: $4 \times 4$ Space Time Code (STC): $E_b/N_0$ [dB] vs. BER; synchronous CDMA; spreading code length, $N = 31$ (Gold Codes); number of users, $K = 15$; rank of MWF, $D = 5$; channel delay spread, $L = 1$; power of interfering users/power of desired user, $\Delta P = 0$ dB

# Chapter 9

# Conclusions

In this dissertation, novel interference mitigation methods for future generation wideband cellular code division multiple access (CDMA) systems are presented. The techniques developed all apply a new method for performing reduced rank statistical signal processing, i.e. the multistage Wiener filter (MWF). Reduced rank signal processing in CDMA systems is motivated by the requirement for increased data rates, multimedia access, and increased capacity. These requirements in turn fuel the need for low complexity detection algorithms. The MWF has been shown in previous work to provide several advantages to prior reduced rank algorithms such as principal components (PC) and the cross-spectral (CS) metric, as well as existing full rank algorithms, because it enables significant signal subspace compression, thereby greatly reducing computational complexity. In CDMA, this translates to higher data rates and faster convergence of the algorithm in terms of the required sample support. The MWF also does not rely on eigen-based decomposition, which is computationally complex, and does not require calculation or inversion of the traditional data covariance matrix, as does the full rank minimum mean square error (MMSE). Furthermore, rank reduction with the MWF is nearly independent of the

number of signals, which is of crucial importance to CDMA systems because the number of users in a CDMA system is typically unknown (especially at the mobile handset) and is continuously changing in time. The reduction in required sample support further implies fast adaptation in stationary environments, and the ability to adapt optimally to real, non-stationary environments in which the channel is changing too rapidly to allow enough samples to be obtained to form a reliable solution via alternate methods. The MWF is implemented efficiently via the correlation subtraction architecture (CSA) [72].

The MWF is applied here to the CDMA problem, and the significant performance benefits that are achievable along with the added benefit of reduction in complexity are determined. Operation of the MWF in this dissertation is blind, that is, no training data (pilot channel) is assumed. Naturally, if a pilot is available, additional performance benefits will be achieved. The optimum receiver is derived first in additive white Gaussian noise (AWGN) and then extended to the frequency selective multipath channel. It is shown that the MWF, with its initial stage being a filter matched to the spreading code and channel of the desired user, is the optimal solution. Thus, the MWF is shown to be a colored noise matched filter (CNMF). An alternate derivation shows how to improve upon the performance of the conventional rake receiver by applying an MMSE correlator implemented by the MWF at each rake 'finger' of the receiver. Though sub-optimum to the previous receiver, significant gains are achieved, and this receiver can be used as a plug-n-play fix to the rake for existing systems. It is demonstrated that the MWF is robust in colored noise environments, where conventional reduced rank processing techniques fail, while greatly reducing the computational complexity of full rank techniques. Thus, it is shown

that, in general, the benefit is two-fold - one can achieve an order of magnitude complexity reduction in terms of rank and sample support in addition to an order or more of magnitude performance improvement in terms of bit error rate (BER) - with no negative consequences. As a result, future CDMA systems can enjoy higher capacities (number of users that can be supported), faster data rates and throughput, as well as improved decoding performance at low complexity. Hence, it is expected that these techniques will revolutionize future CDMA system standards and capabilities.

These results are extended to the multiuser detection (MUD) problem, in which a bank of MWFs or a joint MWF are both shown to provide the optimal solution. In terms of rank, the joint MWF is shown to converge at an *astounding* low rank of one, by optimally combining the spreading codes of all the users to form the initial stage matched filter. Perhaps more importantly, it is shown that the MUD implemented by the MWF can *exceed* MMSE performance. The amount of performance gain is largely determined by minimization of the cross-correlation properties between the codes used to transmit the data. Gold codes, which have good correlation properties, are shown to provide one or even two orders of magnitude improvement in BER with extremely low complexity (rank). This is due to the aforementioned cross-correlation properties and the ability of the MWF to suppress the uncorrelated interference. The results demonstrate the remarkable property of the MWF to simultaneously achieve a convergence substantially better than that achieved with full rank MMSE *and* a dramatically reduced computational burden as well. Intuitively speaking, the MWF achieves the best of both worlds - faster convergence and reduced computation - by applying the information inherently contained in both the covariance matrix and the cross-correlation vector in choosing the best reduced-dimension subspace in which the

weight vector is constrained to lie. Performance of the parallel MUD solution requires slightly higher ranks than the joint MUD because all of the information contained in the spreading codes is not used, but is still shown to converge at much less than full rank, while suffering no loss in performance.

The significance of these results for CDMA is that the joint and parallel MUD receivers implemented by the MWF can be applied to the CDMA reverse and forward links, respectively, with tremendous savings in computational complexity. In the forward link, only a single spreading code is known so the parallel (single user) receiver should be applied. However, in the reverse link, since the base station has knowledge of every user's spreading code, the joint implementation will provide significant computational savings over any prior technique since it requires only one stage of the MWF and no matrix inversions. The MWF matched filter input can also be applied to the problem in which multiple receiver antennas provide temporal processing diversity. The new (matched filter) initial stage of the MWF is derived and results again show significant performance gains can be attained with great reduction in computational complexity over MMSE. With future systems heading towards multiple antenna structures, low complexity implementation is a must.

Non-linear interference cancellation (IC) schemes employing the MWF to do interference suppression at each stage in place of the conventional matched filter correlator are also studied. These receivers prove robust and provide huge gains over the conventional IC schemes, which fail even in modest capacity situations. An expression for the probability of error is derived and Monte Carlo simulation results show that the MWF easily provides desired bit error rates even in highly loaded systems where the conventional IC schemes fail. This suggests significant capacity increases for future

systems are feasible.

Finally, application of the MWF to systems employing space-time codes at the transmitter and multiple transmit antennas is also studied. The MWF solution is described for the $2\times2$ code and also for the $4\times4$ code. Extension of the decoding methods to more complicated codes is straightforward and is expected to yield significant coding gains. Utilization of the MWF greatly reduces the decoding complexity, which increases non-linearly as a function of the code dimension. Substantial performance gains over the full rank MMSE are also shown to occur, especially when asynchronous Gold codes are transmitted, since this maximizes the ability of the MWF to suppress the non-correlated interference. This improves the feasibility of employing a multiple transmit and receive antenna system for superior decoding capability far beyond any existing system.

A future research topic related to the work presented here is rank optimization for the MWF; i.e. an algorithm that uses some criteria to automatically determine the rank that provides the best solution (in terms of the desired optimization parameter). The application of the MWF to interference mitigation for other types of systems such as the Advanced Mobile Phone System (AMPS) and the Global System for Mobile Communication (GSM) is another broad research area for the future (see [4] or [68] for a detailed description of such systems). Application of the MWF to these problems is not obvious because the matched filter is not well-defined, as with CDMA, and because there does not exist a repeating sequence that can be used to form a data matrix to apply to the MWF algorithm.

Yet another challenging problem facing system designers is the synchronization of signals or detection in the absence of timing information. The application of the

MWF to this problem is introduced in [70], in which shifted versions of the MWF are applied to a signal and that which produces the maximum correlated output with the desired data is selected. Other references relating to this problem are [51], [102], and [106]. Accurate blind synchronization techniques are important for the design of future cellular systems, especially in the absence of a pilot channel. One final application is that of channel estimation. One idea is to apply the MWF in training mode to train the weights to the combined effects of the unknown channel and interference and then to apply the weights to the data. This could be done efficiently if a pilot signal were used; however, in the absence of continuous training data, other methods would need to be developed. A dual MWF system in which the MWF is applied first to account for interference and then to correct for channel effects is one possible solution to this problem.

Derivations for an exact expression for the probability of error for multiple stage interference cancellers are also left for future research. In general, these expressions are mathematically very difficult to evaluate. Extension of all the techniques discussed to more complicated modulation schemes such as quadrature amplitude modulation (QAM), and continuous phase modulation (CPM) is another topic needing further investigation. These modulation schemes may also be of interest as they are used in other types of systems in which reduced rank processing may be beneficial. However, none of the aforementioned techniques is limited to binary phase shift keying (BPSK). Extension to quadrature phase shift keying (QPSK) is straightforward, as each of the quadrature channels may be treated independently at the receiver and by the MWF prior to combining.

# Appendix: Cited Papers

## REDUCED RANK MATRIX MULTISTAGE WIENER FILTER WITH APPLICATIONS IN MMSE JOINT MULTIUSER DETECTION FOR DS-CDMA

*Paula Cifuentes, Wilbur L. Myrick, Seema Sud, J. Scott Goldstein*
*Science Applications International Corporation*
*4001 Fairfax Dr., Suite 675*
*Arlington, VA 22203-1303, USA*

*Michael D. Zoltowski*
*Department of Electrical and Computer Engineering*
*Purdue University*
*West Lafayette, IN 47907-1285, USA*

### ABSTRACT

*A generalized statistical signal processing framework developed in [2] is utilized for interference suppression for Joint Multiuser Detection (MUD). Previous work on the efficient correlations subtractive architecture form of the reduced rank multistage Wiener filter (CSA-MWF) is extended by considering the multiple signal constraint case. The reduced rank algorithm is not based on an eigen-decomposition, which requires the signal subspace rank to be greater than or equal to the number of signals present in the system. The solution meets or exceeds full rank MMSE at a significantly reduced rank. System performance is characterized for a highly loaded synchronous DS-CDMA system in the presence of multipath. The bit error rate (BER) performance of the Joint CSA-MWF (JCSA-MWF) is compared to MMSE and RAKE receivers.*

### 1. INTRODUCTION

We present an algorithm which gives the minimum mean-square error (MMSE) for multiple signal detection in the presence of noise. We show this algorithm can be implemented as a joint filter using the correlations subtractive architecture of the multistage Wiener filter (MWF)( [1], [3], [4], [7]). Performance is shown to meet or *exceed* MMSE performance at a significantly low rank.

One application of the JCSA-MWF for the general case of a synchronous DS-CDMA system in frequency selective multipath is presented. We show via simulation results the new reduced rank JCSA-MWF performs as well as the full rank MUD for synchronous users in multipath and for all levels of signal-to-noise ($E_b/N_0$) and system loads. We compare JCSA-MWF to banks of parallel single user MMSE receivers and RAKE receivers. We begin by describing the signal model.

### 2. CDMA SIGNAL MODEL

We assume a DS-CDMA system, in which we have $K$ users and develop a model for synchronous transmission. As in [5] and [6], user $k$ transmits a baseband signal given by

$$x_k(t) = \sum_i A_k b_k(i) s_k(t - iT), \tag{1}$$

where $b_k(i)$ is the symbol transmitted by user $k$ at time $i$, $s_k(t)$ is the spreading code associated with user $k$, and $A_k$ is the amplitude, assumed real. We assume the symbols $b_k(i)$ $\in$ (-1,+1) are independent and identically distributed. The spreading sequence can be written as

$$s_k(t) = \sum_{i=1}^{N-1} a_k[i] \Psi(t - iT_c), \tag{2}$$

where $a_k[i] \in (\frac{+1}{\sqrt{N}}, \frac{-1}{\sqrt{N}})$ is a normalization factor for the spreading code. The processing gain of the CDMA system, or equivalently the bandwidth spreading factor, is given by $N = \frac{T}{T_c}$. Here, $T_c$ is the chip period, and $T$ is the symbol period. We assume DS-CDMA so that $\Psi(t)$ is a constant.

Define the sampled transmitted signal $\mathbf{y}(i)$ as the N-vector composed of synchronous combinations of the data for each user multiplied with its respective spreading sequence, which is written as

$$\mathbf{y}(i) = \sum_{k=1}^{K} A_k b_k(i) \mathbf{s_k}. \tag{3}$$

Here, $\mathbf{s_k}$ is the $N \times 1$ spreading code associated with user $k$, where $k = 1, 2, ..., K$. To simplify the notation and to make the mathematical analysis easier, we rewrite Eq. (3) in matrix form as

$$\mathbf{y}(i) = \mathbf{S}\mathbf{A}\mathbf{b}(i), \tag{4}$$

where $\mathbf{S} = [\mathbf{s_1}\ \mathbf{s_2} ... \mathbf{s_K}]$, $\mathbf{A} = diag(A_1, A_2, ..., A_K)$, and $\mathbf{b}(i) = [b_1(i), b_2(i), ..., b_K(i)]^T$.

## 3. REDUCED RANK MUD BASED ON JCSA-MWF

We present the MUD solution for synchronous users in multipath and show it can be implemented using the JCSA-MWF. Consider the case of a multipath channel, modeled in discrete time by an L-tap tapped-delay line whose coefficients are represented by $\mathbf{h} = [h_1, h_2, ..., h_L]$. The received vector can be written as

$$\hat{\mathbf{r}}(i) = \hat{\mathbf{y}}(i) + \mathbf{n}(i), \tag{5}$$

where $\hat{\mathbf{y}}(i) = \mathbf{y}(i) * \mathbf{h}$, $*$ denotes convolution, and $\mathbf{n}(i)$ are samples of an additive white Gaussian noise (AWGN) process.

The MMSE solution [8] is given by

$$\hat{\mathbf{C}}_{\text{MMSE}} = \hat{\mathbf{R}}^{-1}\hat{\mathbf{S}}\mathbf{A}. \tag{6}$$

where $\hat{(\cdot)}$ denotes convolution of the operand with the channel $\mathbf{h}$ and $\hat{\mathbf{R}} = E\{\hat{\mathbf{r}}(i)\hat{\mathbf{r}}^H(i)\}$.

From Eq. (6), we see the computation of the MMSE MUD solution requires inversion of the $(N+L-1)\times(N+L-1)$ covariance matrix $\hat{\mathbf{R}}$, which can be quite computationally intense. Also, if the channel or signals are changing in time, then the sample covariance matrix estimated from the data does not depict the true non-stationary signal environment. Thus, it is desirable to find alternate solutions that approach, or exceed, the performance of the MMSE receiver but require much fewer computations and can adapt rapidly. The matrix inversion requirement can be eliminated by performing a multistage decomposition similar to that provided by the single user MWF. The joint (matrix) MWF filtering diagram is shown in Fig. 1.

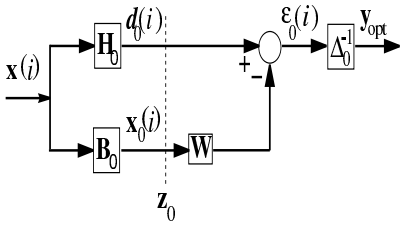


**Fig. 1.** The J-MWF Filtering Diagram

Define

$$\mathbf{\Delta}_0 = (\hat{\mathbf{S}}^H\hat{\mathbf{S}})^{1/2} \tag{7}$$

and $\mathbf{H}_0$ to be the normalized matrix of spreading codes, given by

$$\mathbf{H}_0 = \hat{\mathbf{S}}\mathbf{\Delta}_0^{-1}, \tag{8}$$

and $\mathbf{B}_0$ is the blocking matrix for $\mathbf{H}_0$. Define

$$\mathbf{T}_0 = \begin{bmatrix}\mathbf{H}_0^H \\ \mathbf{B}_0\end{bmatrix}, \quad \mathbf{z}_0 = \mathbf{T}_0\mathbf{x}. \tag{9}$$

The covariance matrix of the transformed process $\mathbf{z}_0$ is given by

$$\mathbf{R}_{\mathbf{z}_0} = \mathbf{T}_0\mathbf{R}_{\mathbf{x}}\mathbf{T}_0^H = \begin{bmatrix}\mathbf{R}_{\mathbf{d}_0} & \mathbf{R}_{\mathbf{x}_0\mathbf{d}_0}^H \\ \mathbf{R}_{\mathbf{x}_0\mathbf{d}_0} & \mathbf{R}_{\mathbf{x}_0}\end{bmatrix}, \tag{10}$$

where $\mathbf{d}_0 = \mathbf{H}_0^H\mathbf{x}$ and $\mathbf{x}_0 = \mathbf{B}_0\mathbf{x}$. Solving (10) for $\mathbf{R}_{\mathbf{x}}$, one obtains

$$\mathbf{R}_{\mathbf{x}} = \mathbf{T}_0^{-1}\mathbf{R}_{\mathbf{z}_0}\mathbf{T}_0^{-H}, \tag{11}$$

or

$$\mathbf{R}_{\mathbf{x}}^{-1} = \mathbf{T}_0^H\mathbf{R}_{\mathbf{z}_0}^{-1}\mathbf{T}_0. \tag{12}$$

Continuing the decomposition, it can be shown that the covariance matrix after $D$ stages can be written as

$$\mathbf{R}_{\mathbf{z}_D} = \mathbf{T}_D\mathbf{R}_{\mathbf{x}}\mathbf{T}_D^H, \tag{13}$$

where

$$\mathbf{T}_D = \begin{bmatrix}\mathbf{H}_0^H \\ \mathbf{H}_1^H\mathbf{B}_0 \\ \mathbf{H}_2^H\mathbf{B}_1\mathbf{B}_0 \\ \vdots \\ \mathbf{H}_D^H\mathbf{B}_{D-1}\ldots\mathbf{B}_0\end{bmatrix}. \tag{14}$$

and so

$$\mathbf{R}_{\mathbf{x}}^{-1} = \mathbf{T}_D^H\mathbf{R}_{\mathbf{z}_0}^{-1}\mathbf{T}_D. \tag{15}$$

Finally, the optimum Wiener solution is obtained by substituting Eq. (15) into Eq. (6) to yield

$$\hat{\mathbf{C}}_{MMSE} = \mathbf{T}_D^H\mathbf{R}_{\mathbf{z}_0}^{-1}\mathbf{T}_D\hat{\mathbf{S}}\mathbf{A}. \tag{16}$$

Note the matrix can be truncated to less than full rank. The rank one decomposition is performed by retaining only the first two rows of $\mathbf{T}_D$, equivalent to $\mathbf{T}_1$, which gives

$$\hat{\mathbf{C}}_{MMSE} = \mathbf{T}_1^H\mathbf{R}_{\mathbf{z}_0}^{-1}\mathbf{T}_1\hat{\mathbf{S}}\mathbf{A}. \tag{17}$$

For this solution, the claim of reduced rank processing is valid even though a matrix inversion is required as long as $K < N/2$. This is true because the dimension of the matrix to be inverted is now $2K \times 2K$ versus the original covariance matrix dimension of $(N+L-1)\times(N+L-1)$. As an example, if $K = 10$, and $N = 32$, the matrix MWF requires $20^3 = 8{,}000$ flops, versus the full rank of $32^3 = 32{,}768$ flops, an improvement by a factor of approximately 4.

Another way of calculating the optimal Wiener filter can be found in [2], where

$$\hat{\mathbf{C}}_{MMSE} = \mathbf{T}_0^H\begin{bmatrix}\mathbf{I} \\ -\mathbf{R}_{\mathbf{x}_0}^{-1}\mathbf{R}_{\mathbf{x}_0\mathbf{d}_0}\end{bmatrix}\mathbf{\Delta}_0^{-1} = (\mathbf{H}_0 - \mathbf{B}_0^H\mathbf{W})\mathbf{\Delta}_0^{-1} \tag{18}$$

and $\mathbf{W} = \mathbf{R}_{\mathbf{x}_0}^{-1}\mathbf{R}_{\mathbf{x}_0\mathbf{d}_0}$. The filtered output data vector is given by

$$\mathbf{y}_{opt} = \hat{\mathbf{C}}_{MMSE}^H\mathbf{x} = \mathbf{\Delta}_0^{-1}(\mathbf{H}_0^H - \mathbf{W}^H\mathbf{B}_0)\mathbf{x} = \mathbf{\Delta}_0^{-1}\epsilon_0, \tag{19}$$

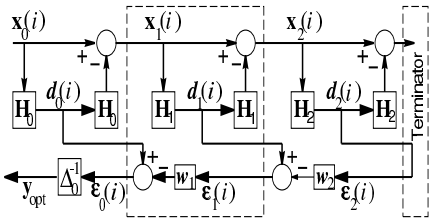


**Fig. 2.** JCSA-MWF (D=2 stages)

where the $K \times 1$ error-vector is

$$\epsilon_0 = (\mathbf{H}_0^H - \mathbf{W}^H \mathbf{B}_0)\mathbf{x}. \quad (20)$$

If $D$ stages are used in the matrix MWF, where $D > 1$, $\mathbf{T}_D$ would become a $(D+1)K \times N$ matrix. If $(N+L-1)/2 < K$, then the system would become overdetermined. In the simulations provided in Section 4, we assume prior knowledge of all the spreading codes of all the users, so only one stage of the decomposition is needed since the projection onto all the signals' subspace is performed simultaneously. This eliminates the need for blocking matrices in the decomposition. An orthogonal multistage decomposition for eqs. (18)-(20) analogous to the single constraint case is given below.

The multiuser multistage decomposition of the MWF for $D = 2$ stages is shown in Fig. 2. The single user structure is first described by Ricks, et. al., in [7]. The multiuser structure is not dependent on prior knowledge of all user in the system, but more stages would be required to achieve optimal performance. For the multipath channel, we set $\mathbf{H_0}$ and $\mathbf{d}_0(i)$as described above, where $\mathbf{x}(i)$ is the input signal, equal to $\hat{\mathbf{r}}(i)$. The forward recursion equations, presented below, are similar to those used to implement the block residual correlation algorithm ([4] and [5]) but instead are extended for multiple constraints and without computation of the blocking matrices.

- *Initialization:* $\mathbf{d}_0$, $\mathbf{H}_0$ and $\mathbf{x}$
- *Forward Recursion:* For $j = 1, 2, ..., D$:

$$\begin{aligned} \mathbf{\Delta}_j &= (\mathbf{R}^H_{x_{j-1}d_{j-1}} \mathbf{R}_{x_{j-1}d_{j-1}})^{1/2} \\ \mathbf{H}_j &= \mathbf{R}^H_{x_{j-1}d_{j-1}} \mathbf{\Delta}_j^{-1} \\ \mathbf{d}_j &= \mathbf{H}_j^H \mathbf{x}_{j-1} \\ \mathbf{x}_j &= \mathbf{x}_{j-1} - \mathbf{H}_j \mathbf{d}_j \end{aligned}$$

- *Backward Recursion:* For $j = D, D-1, ..., 1$, with $\epsilon_D = \mathbf{d}_D$ and $\mathbf{\Pi}_D = \mathbf{R}_{\epsilon_D}$ :

$$\begin{aligned} \mathbf{W}_j &= \mathbf{\Pi}_j^{-1} \mathbf{\Delta}_j \\ \epsilon_{j-1} &= \mathbf{d}_{j-1} - \mathbf{W}_j^H \epsilon_j \\ \mathbf{\Pi}_{j-1} &= \mathbf{R}_{d_{j-1}} - \mathbf{\Delta}_j^H \mathbf{\Pi}_j^{-1} \mathbf{\Delta}_j \end{aligned}$$

where $D$ denotes the number of stages, i.e. the rank, of the filter. Finally, $\mathbf{y}_{opt}$ can be computed where it is the $K \times 1$ vector representing the bit estimates for all $K$ users. Performance results of the single user MWF for synchronous CDMA in AWGN are in [5].

## 4. NUMERICAL RESULTS

We present results obtained from Monte Carlo simulations to show the validity of the MUD solution derived above. Hadamard codes with a processing gain of $N = 64$ are employed in spreading, and an $L$=5 tap channel is used to simulate the multipath, using one tap per chip.

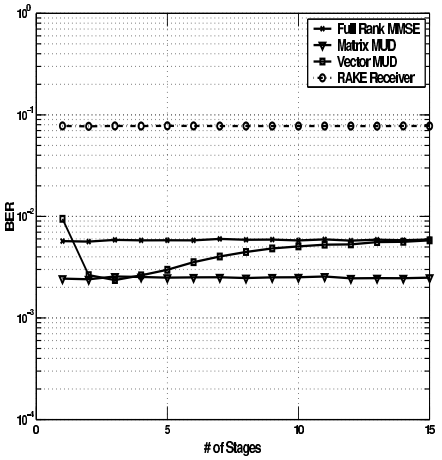


**Fig. 3.** Joint Multiuser Detector (MUD): Rank (D) vs. BER; Synchronous Blind CDMA, $N = 64$ (Hadamard Codes), $E_b/N_0 = 12$ dB, $K = 33$, $L = 5$

In both plots, the joint (matrix) MUD and the parallel (vector) MUD are compared. The full rank MMSE solution employing the covariance matrix inversion is labeled accordingly. Fig. 3 shows a plot of rank for the MWF versus BER for synchronous users. The small fluctuations in BER for the MMSE and RAKE methods are due to the Monte Carlo simulation, since their performance is independent of rank. Note that the matrix MUD obtains full rank performance at a rank of only one, by employing knowledge of all the users' spreading codes. This is an astounding result that shows for MMSE performance, all that is required is a matched filter and a matrix-vector multiplication. This is a significant advantage when the base station typically has prior knowledge of all the users. For a rank as low as three, the vector MWF achieves the matrix MUD solution and converges to full rank MMSE performance as rank increases. The performance of the joint MUD *exceeds* that of the MMSE receiver, and does not degrade even at a rank as

low as one, which is significantly less than the processing gain of $N = 64$.

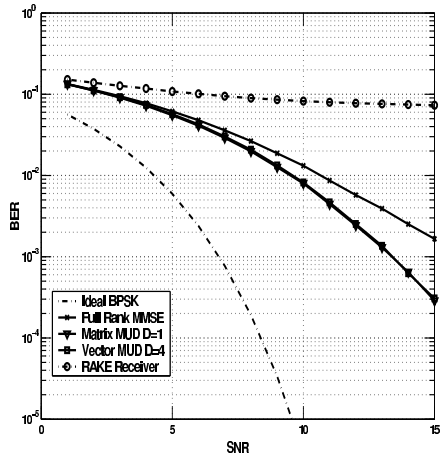


**Fig. 4.** Joint Multiuser Detector (MUD): $E_b/N_0$ vs. BER; Synchronous Blind CDMA, $N = 64$ (Hadamard Codes), $K = 33$, $L = 5$, $\Delta P = 0$ dB

Fig. 4 shows a plot of $E_b/N_0$ of the MWF versus the BER for synchronous users. The matrix MUD has converged at a rank ($D$) of only one, due to the fact that it has knowledge of all the users' spreading codes and can thus determine the signal subspace instantly. In general, the rank at which the matrix MUD converges is a function of the number of users' spreading codes that it has knowledge of (termed the constraint length of the matrix MUD), although it is not a linear relationship. The vector MWF performs as well as the matrix version at a rank of four. Thus, while performance as a function of rank differs between these two methods, they both perform well at remarkably low ranks. In both plots, both the vector and matrix MWF dramatically outperform the RAKE receiver (which cannot combat large numbers of interfering users) and the MMSE receiver.

## 5. CONCLUSION

We showed how to implement the MUD solution using the reduced rank MWF in joint matrix form. The matrix implementation is shown to be equivalent at one stage to the optimal vector form MUD solution in terms of performance. The reduced rank solution is compared to existing full rank solutions to assess its performance. BER performance is evaluated as a function of rank and $E_b/N_0$ for a highly loaded DS-CDMA system distorted by multipath. It is demonstrated that the reduced rank MUD performs as well as the single user, full rank MUD MMSE solutions at a much lower rank, both in matrix and in vector form.

## 6. ACKNOWLEDGMENTS

We thank Professors Michael Honig of Northwestern University and Irving Reed of the University of Southern California.

## 7. REFERENCES

[1] Goldstein, J.S., and Reed, I.S., "Multidimensional Wiener Filtering Using a Nested Chain of Orthogonal Scalar Wiener Filters", University of Southern California, Dec. 1996, CSI-96-12-04.

[2] Goldstein, J.S., and Reed, I.S., "Adaptive Target Detection and Identification", SAIC-ASE Technical Report no. 99-10-001, October, 1999.

[3] Goldstein, J.S., and Reed, I.S., "A New Method of Wiener Filtering and its Application to Interference Mitigation for Communications", *Proceedings of IEEE MILCOM*, Vol. 3, pp. 1087-1091, Monterey, CA, Nov. 1997.

[4] Goldstein, J.S., Reed, I.S., and Scharf, L.L., "A Multistage Representation of the Wiener Filter Based on Orthogonal Projections", in *IEEE Transactions on Information Theory*, Vol. 44, No. 7, Nov. 1998.

[5] Honig, M.L., and Goldstein, J.S., "Adaptive Reduced-Rank Residual Correlation Algorithms for DS-CDMA Interference Suppression", in *Proceedings of Asilomar*, Jul. 1998.

[6] Honig, M.L., and Poor, H.V., Adaptive Interference Suppression. In Poor, H.V., and Wornell, G.W., editors, "Wireless Communications: Signal Processing Perspectives", Prentice Hall: Englewood Cliffs, New Jersey, pgs. 64-102, 1998.

[7] Ricks, D.C., and Goldstein, J.S. "Efficient Architectures for Implementing Adaptive Algorithms", *Proceedings of the 2000 Antenna Applications Symposium*, pgs. 29-41, Allerton Park, Monticello, Illinois, Sep. 20-22, 2000.

[8] Sud, S., Myrick, W.L., Cifuentes, P.G., and Goldstein, J.S. "A Reduced Rank MMSE Multiuser Detector for DS-CDMA", *To appear in Proceedings of the 35th Annual Asilomar Conference on Signals, Systems, and Computers*, Nov. 4 - 7, 2001.

# MMSE CORRELATOR BASED RAKE RECEIVER FOR DS-CDMA

*Wilbur L. Myrick, Seema Sud, J. Scott Goldstein*

SAIC
4001 N. Fairfax Drive
Arlington, VA 22203
myrickw@saic.com, suds@saic.com
sgoldstein@trg1.saic.com

*Michael D. Zoltowski*

School of Electrical Engineering
Purdue University
West Lafayette, IN 47907-1285
mikedz@ecn.purdue.edu

**ABSTRACT**

This paper investigates the performance of a reduced rank MMSE correlator for a RAKE receiver in the context of CDMA in frequency selective multipath. The MMSE correlator based on the Correlations Subtractive Architecture (CSA) is derived for frequency selective multipath. It is demonstrated that the standard multiuser limited RAKE receiver can achieve BER performance close to the MMSE receiver spanning multiple symbols by replacing its conventional correlator with an MMSE correlator. The CSA generates an MMSE correlator without requiring matrix inversion (thereby reducing computational complexity) and facilitates direct replacement of the standard RAKE correlator.

## 1. INTRODUCTION

The RAKE receiver is designed to operate in a multipath environment, but is limited in performance due to Multiuser Access Interference (MAI). The MAI contribution causes the RAKE receiver to degrade rapidly as the number of users are increased in a CDMA system. To mitigate the MAI effects and automatically combine the multipath, one can utilize the (coherent) MMSE receiver that spans more than one symbol to account for the multipath delay spread. The purpose of this paper is to modify the conventional RAKE receiver in such a way that it has performance comparable to the MMSE receiver that spans more than one symbol.

## 2. CDMA SIGNAL MODEL

We assume a DS-CDMA system, in which we have $K$ synchronous users in a frequency selective multipath channel. The notation used here is similar to that used by Honig, et. al., in [1] and [2]. User $k$ transmits a baseband signal given by

$$x_k(t) = \sum_n A_k b_k(n) s_k(t - nT - \tau_k), \qquad (1)$$

where $b_k(n)$ is the symbol transmitted by user $k$ at time $n$, $s_k(t)$ is the spreading code associated with user $k$, and $A_k$ and $\tau_k$ are the real valued amplitude and delay, respectively. We assume binary signaling, so that the symbols $b_k(n) \in$ (-1,+1). We also assume that the bits are independent, identically distributed. The spreading sequence can be written as

$$s_k(t) = \sum_{n=1}^{N-1} a_k[n] \Psi(t - nT_c), \qquad (2)$$

where $a_k[n] \in (\frac{+1}{\sqrt{N}}, \frac{-1}{\sqrt{N}})$ is a normalization factor for the spreading code. The processing gain of the CDMA system, or equivalently the bandwidth spreading factor, is given by $N = \frac{T}{T_c}$. Here, $T_c$ is the chip period, and $T$ is the symbol period. We assume that the spreading code is a square wave sequence with no pulse shaping, so that the chip sequence $\Psi(t)$ is a constant.

The chip rate sampled received signal based on this model in a frequency selective channel over $m$ symbols is defined in [6] to be

$$\mathbf{r}_m = \tilde{b}_0(n)\mathbf{u}_0 + \sum_{i=1}^{I} \tilde{b}_i(n)\mathbf{u}_i + \mathbf{w}_m(n) \qquad (3)$$

based on the equivalent synchronous model from [3]. Assuming user 1 is the desired user, without loss of generality, the desired symbol is $\tilde{b}_0(n) = b_1(n)$, the vector $\mathbf{w}_m(n)$ contains samples from an AWGN process, and the interfering symbols are $\tilde{b}_i(n)$, where $i = 1, ..., I$, consist of $(L_b + m - 1)(K - 1)$ Multiuser Access Interference (MAI) and $L_b + m - 2$ ISI symbols for a total of $I = (L_b + m - 1)K - 1$ [6]. $L_b$ is the channel length in bit duration defined as $\lceil \frac{L+N-1}{N} \rceil$, where $\lceil x \rceil$ is the smallest integer greater than or equal to $x$, and $L$ is the number of multipaths. The

transmitted code matrix for the desired user is defined to be

$$\mathbf{C}_1 = \begin{bmatrix} s(0) & & 0 \\ \vdots & \ddots & s(0) \\ s(N-1) & & \vdots \\ 0 & \ddots & s(N-1) \\ & \mathbf{0} & \end{bmatrix}_{mN \times L} \quad (4)$$

The desired signal vector $\mathbf{u}_0$ can now be defined as

$$\mathbf{u}_0 = \mathbf{C}_1 \mathbf{h}_1 \quad (5)$$

where $\mathbf{h}_1$ consists of the channel tap coefficients.

The desired signal $\mathbf{u}_0$ can be interpreted as a zero padded coherent RAKE receiver. The significance of this interpretation when considering equation (3) is that the RAKE receiver is unable to suppress the MAI due to the other interfering vectors $\mathbf{u}_i$. The inability of the RAKE receiver to suppress MAI leads to the development of finding a RAKE receiver with such capabilities. The next section develops the formulation of (5) as a RAKE receiver.

## 3. COHERENT RAKE RECEIVER

It is necessary to understand the different interpretations of the RAKE receiver to provide insight into how it is possible to improve upon its performance to account for MAI. Let us assume that $\mathbf{y} = \mathbf{r}_{L_b}(m = L_b)$. The decision variable at the output of the RAKE receiver can be written as

$$z = \sum_{n=0}^{L-1} \int_0^T r\,(t - T_c n)\, c_n^*(t) s^*(t) dt \quad (6)$$

where $L$ denotes the number of paths, $T$ is the symbol period, $s$ is the coefficient of the spreading code of length $N$, $T_c$ is the chip delay, $y$ is the received signal, and $c_n$ are the channel tap coefficients. If one assumes the channel is slowly fading, the channel tap weights can be regarded as constant over a few chip periods; therefore, equation (6) can be written as

$$\begin{aligned} z &= \sum_{n=0}^{L-1} c_n^* \int_0^T y\,(t - T_c n)\, s^*(t) dt \\ &= \sum_{n=0}^{L-1} c_n^* \int_0^T s^*\,(t - T_c n)\, y(t) dt. \end{aligned} \quad (7)$$

The last equality holds due to the linearity of the convolution operation. Equation (7) can be written in discrete vector form by exploiting the inner product equivalences between discrete vectors and continuous time functions, i.e.

$$\int_0^T s^*\,(t - T_c n)\, y(t) dt = \langle \mathbf{s}_n, \mathbf{y} \rangle = \mathbf{s}_n^H \mathbf{y} \quad (8)$$

where $\mathbf{s}_n$ are shifted versions of the spreading code within a time interval spanning multiple symbols that form the columns of a convolution matrix. Equation (7) can be rewritten as

$$z = \sum_{n=0}^{L-1} c_n^* \mathbf{s}_n^H \mathbf{y} = \mathbf{c}^H \beta \quad (9)$$

where $\mathbf{c} = [c_0, c_1, ..., c_{L-1}]^T$ and $\beta = [\mathbf{s}_0^H \mathbf{y}, \mathbf{s}_1^H \mathbf{y}, ...\mathbf{s}_{L-1}^H \mathbf{y}]^T$ (the output at each "finger" of the RAKE receiver). One can then rewrite equation (9) as

$$z = \mathbf{c}^H \mathbf{C}_s^H \mathbf{y} = \mathbf{s}^H \mathbf{C}_c^H \mathbf{y} = (\mathbf{C}_c \mathbf{s})^H \mathbf{y} \quad (10)$$

where $\mathbf{C_s}$ and $\mathbf{C_c}$ are convolution matrices relative to $\mathbf{s}$ and $\mathbf{c}$ respectively. In particular $\mathbf{C_s}$ is defined as

$$\begin{aligned} \mathbf{C_s} &= [\mathbf{s}_0, \mathbf{s}_1, ..., \mathbf{s}_{L-1}] \\ &= \begin{bmatrix} s(0) & & 0 \\ \vdots & \ddots & s(0) \\ s(N-1) & & \vdots \\ 0 & \ddots & s(N-1) \end{bmatrix}. \end{aligned} \quad (11)$$

This establishes the equivalent zero padded matrix interpretation of the RAKE receiver from equation (5) as

$$\mathbf{u}_0 = \mathbf{C}_1 \mathbf{h}_1 = \begin{bmatrix} \mathbf{C}_s \mathbf{c} \\ \mathbf{0} \end{bmatrix}. \quad (12)$$

Rewriting equation (10) with the last equality establishes the framework for deriving the MMSE correlator using the fact that the RAKE receiver is just a linear filter that can be defined as

$$\mathbf{w}_{RAKE} = \mathbf{C}_c \mathbf{s}. \quad (13)$$

## 4. MMSE CORRELATOR FOR THE RAKE RECEIVER

It was shown in Section 3 that the standard RAKE receiver can be interpreted as just being a linear filter defined as $\mathbf{w}_{RAKE} = \mathbf{C}_c \mathbf{s}$. It is desirable to find a correlator other than $\mathbf{s}$ that will suppress MAI for each RAKE "finger". The idea is to reduce MAI at each RAKE "finger" mathematically defined in $\beta$ utilizing an MMSE correlator. It is first necessary to understand how one can find such a correlator based on the MMSE solution. The MMSE solution over multiple chips that will automatically combine multipath while mitigating interference can be defined as

$$\mathbf{w}_{mmse} = \mathbf{R}^{-1} \mathbf{C_c} \mathbf{s} \quad (14)$$

where $\mathbf{R} = E\{\mathbf{y}\mathbf{y}^H\}$. It should be emphasized again that vector $\mathbf{y}$ spans multiple symbols accounting for the delay spread of the channel. In deriving the MMSE correlator, it

is desired to find a correlator $\mathbf{s}_{mmse}$ based on the spreading code that will yield improved MAI suppression compared to the standard RAKE receiver. The MMSE correlator is suboptimal compared to $\mathbf{w}_{mmse}$ because the data window for suppressing MAI at the correlator is much smaller than the convolution channel window. The MMSE correlator can be derived by first rewriting $\beta$ as

$$\beta = [\mathbf{y}_0^H\mathbf{s}, \mathbf{y}_1^H\mathbf{s}, ...\mathbf{y}_{L-1}^H\mathbf{s}]^H \quad (15)$$

where now instead of shifting the spreading code across the data, the data is delayed by the time associated with the $l^{th}$ diversity path. Instead of trying to suppress MAI over the span of multiple symbols, one can suppress MAI per delayed symbol along each diversity path of the RAKE receiver. One can utilize MMSE MAI suppression by rewriting equation (15) as

$$\begin{aligned}\beta_{mmse}^{corr} &= [\{\mathbf{R}_0^{-1}\mathbf{y}_0\}^H\mathbf{s}, ..., \{\mathbf{R}_{L-1}^{-1}\mathbf{y}_{L-1}\}^H\mathbf{s}]^H \\ &= [\mathbf{y}_0^H\mathbf{R}_0^{-1}\mathbf{s}, ..., \mathbf{y}_{L-1}^H\mathbf{R}_{L-1}^{-1}\mathbf{s}]^H \\ &= [\mathbf{y}_0^H s_{mmse_1}, ..., \mathbf{y}_{L-1}^H s_{mmse_{L-1}}]^H \end{aligned} \quad (16)$$

where $\mathbf{R}_l = E\{\mathbf{y}_l\mathbf{y}_l^H\}$ denotes the $N \times N$ covariance matrix windowed to the data symbol corresponding to the $l^{th}$ diversity path. The MMSE correlator for each diversity path given in equation (16) is defined as being $s_{mmse_l} = \mathbf{R}_l^{-1}\mathbf{s}$. It can be shown that the $\beta_{mmse}$ output that utilizes the solution of equation (14) can be written as

$$\beta_{mmse} = [\mathbf{s}_0^H\mathbf{R}^{-1}\mathbf{y}, \mathbf{s}_1^H\mathbf{R}^{-1}\mathbf{y}, ..., \mathbf{s}_{L-1}^H\mathbf{R}^{-1}\mathbf{y}]^T. \quad (17)$$

One can interpret $\mathbf{s}_{mmse}$ as a correlator that can mitigate multiple access inteference over a limited data window. Now that it is known that the MMSE correlator exists and has been defined, it is necessary to derive an efficient implementation of this filter. The CSA facilitates such an implementation.

## 5. DERIVING THE MMSE CORRELATOR FOR THE RAKE RECEIVER BASED ON MWF

The MWF is an efficient innovative reduced rank algorithm for finding the MMSE solution not requiring any type of matrix inversions [4]. The MWF is based on multiple orthogonal projections and backward recursions to find the MMSE solution. To derive the MMSE correlator it is necessary to only consider the first orthogonal decomposition initially. The MWF MMSE solution can be written as

$$\mathbf{w}_{MWF} = \mathbf{s} - \mathbf{B}\mathbf{w}_r = \mathbf{R}_l^{-1}\mathbf{s} = \mathbf{s}_{mmse_l} \quad (18)$$

where $\mathbf{B}$ is chosen such that $\mathbf{B}^H\mathbf{s} = \mathbf{0}$. The important contributions of the CSA deal with how one picks $\mathbf{B}$ and solve for $\mathbf{w}_r$ in an efficient implementation. This implementation yields the desired MMSE correlator. The MMSE correlator for the RAKE receiver has an interesting interpretation. With no interference suppression (assuming $\mathbf{w}_r = \mathbf{0}$), the solution yields the standard correlator of the RAKE receiver, but with interference suppression it is now possible for the correlator to mitigate MAI before the RAKE receiver does any type of optimal combining based on the channel coefficients. Since the channel coefficients are already utilized for the standard RAKE receiver, no additional information is needed to get MMSE performance besides generating $\mathbf{B}$ and $\mathbf{w}_r$. The CSA structure is utilized to indirectly generate $\mathbf{B}$ and $\mathbf{w}_r$ to construct the MMSE correlator.

## 6. MMSE CORRELATOR BASED ON CSA

In the MWF, there is no computation of eigenvectors. It has been shown that the MWF implicitly constrains the desired weight vector to lie in the Krylov subspace spanned by $\{\mathbf{s}_N, \mathbf{R}\mathbf{s}_N, ..., \mathbf{R}^{D-1}\mathbf{s}_N\}$[5]. The word "implicit" is used since there are implementations of the MWF that do not require the formation of the correlation matrix such as the CSA. A benefit of the MWF is that this algorithm can work in the critical low-sample support operational environment where other adaptive algorithms fail. In other words, the ability for rapid adaptation is matched by a lower requirement for training data to estimate the statistics. Thus while many least-squares algorithms or orthogonal filter structures may offer faster convergence than stochastic gradient algorithms, the MWF is the only algorithm which actually reduces the sample support requirements without degrading performance. This facilitates tracking in a nonstationary signal environment.

The MWF based on the CSA algorithm is summarized below. The algorithm is initialized with a "desired" signal $d_0(n) = \mathbf{s}^H\mathbf{y}(n)$ and $\mathbf{y}_0(n) = \mathbf{y}(n) - \mathbf{s}d_0(n)$. Note that $\mathbf{y}(n)$ corresponds to $\mathbf{y}_l$ of each diversity branch of the RAKE receiver. This implies that the CSA structure would replace each correlator at the $l^{th}$ path in the RAKE receiver.

- *Initialization:* $d_0(n)$ and $\mathbf{y}_0(n)$
- *Forward Recursion:* For $k = 1, 2, ..., D$:

$$\begin{aligned}\mathbf{p}_k &= E\{d_{k-1}^*(n)\mathbf{y}_{k-1}(n)\} \\ \mathbf{h}_k &= \mathbf{p}_k/||\mathbf{p}_k|| \\ d_k(n) &= \mathbf{h}_k^H\mathbf{y}_{k-1}(n) \\ \mathbf{y}_k(n) &= \mathbf{y}_{k-1}(n) - \mathbf{h}_k d_k(n)\end{aligned}$$

- *Backward Recursion:* For $k = D, D-1, ..., 1$, with

$\epsilon_D(n) = d_D(n)$:

$$\begin{aligned} w_k &= E\{d^*_{k-1}(n)\epsilon_k(n)\}/E\{|\epsilon_k(n)|^2\} \\ \epsilon_{k-1}(n) &= d_{k-1}(n) - w^*_k\epsilon_k(n) \end{aligned}$$

A low complexity implementation of the MMSE correlator is depicted in Figure 1 known as the CSA. This figure clearly displays the multiple stages and modular structure highlighted by the dashed box. Operating in a D-dimensional space is tantamount to "terminating" all stages beyond the $D$-th stage. It is important to notice that all operations of the CSA after the first stage involve complex vector-vector products, not complex matrix-vector products, thereby implying $O(ND)$ per snapshot. This particular implementation of the MWF was first discovered by Ricks and Goldstein[8]. To reduce implementation complexity, they exploited the structure of the full dimension orthogonal projection matrix. Compared to other MMSE based algorithms having operations of $O(N^3)$, the CSA is by far more computationally efficient.

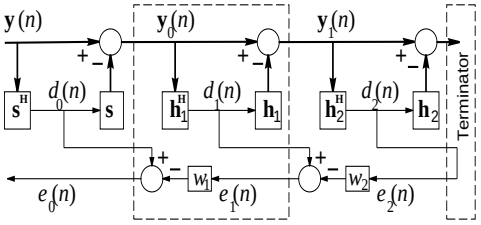


**Fig. 1**. Efficient implementation of the MMSE correlator based on the CSA modular filter structure.

## 7. SIMULATIONS

A simulation was generated to show the decreased BER (bit error rate) performance of the RAKE receiver by using the MMSE correlator. A 4 tap channel model was used to simulate multi-path effects where $\mathbf{c} = [1, .63, .32, .13]^T$. The system consisted of $K = 15$ synchronous equal power users utilizing spreading codes $\mathbf{s}$ of length $N = 16$ generated from Hadamard sequences. Analytical BER curves were derived based on equation (3). Further details about generating (3) can be found in [6]. Figure 2 illustrates how the MMSE correlator improves the RAKE receiver to performances close to the full rank MMSE solution that spans multiple symbols. It will not reach full rank MMSE performance due to interference suppression in a reduced data window. Figure 3 illustrates the interference suppression capabilities of the MWF correlator based RAKE receiver for different stages. Notice that even at stage 1 out of $N$ stages, a significant improvement in BER compared to the standard RAKE receiver is achieved. Figure 4 illustrates the importance of having an adequate data window size (based on processing gain) for the RAKE MWF correlator to suppress interference. For each processing gain $N$, $N-1$ equal power users were simulated using the same channel model **c**. The full rank MMSE and RAKE curves in Figure 4 were generated with $N = 16$ and $K = 15$ for comparison purposes. A processing gain of at least 8 for the specified channel model allows significant MAI suppression.

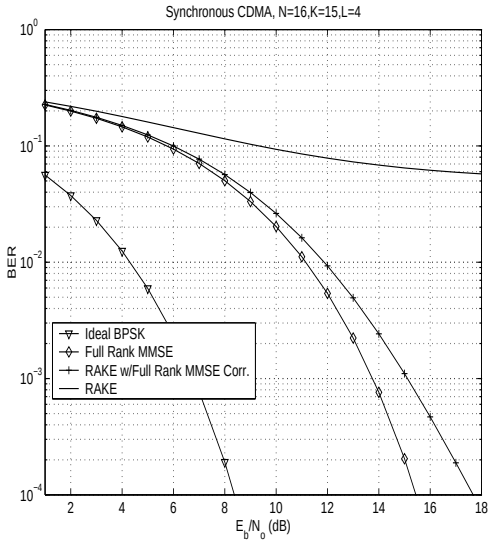


**Fig. 2**. Performance of the RAKE MMSE correlator, MMSE RAKE, and RAKE Receiver.

## 8. CONCLUSION

A reduced-rank MMSE correlator for the standard RAKE receiver is described based on the low complexity correlations subtractive architecture. It is shown that the MMSE correlator can dramatically improve the performance of the RAKE receiver just by replacing the standard correlator with an MMSE correlator that reduces MAI from other users. The structure of the MMSE correlator facilitates rapid implementation into the RAKE receiver, thereby minimizing receiver modifications.

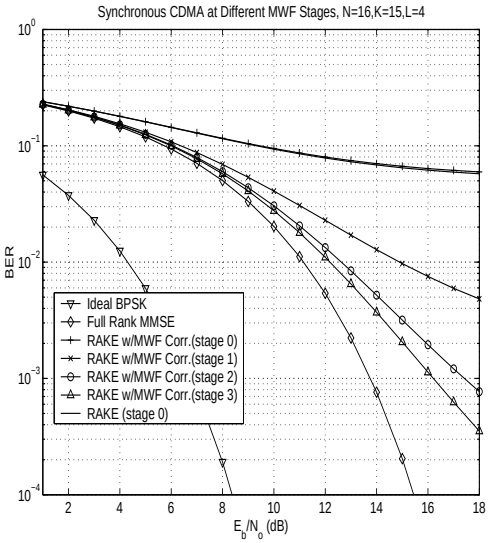


**Fig. 3**. Performance of the RAKE MWF correlator, MMSE RAKE, and RAKE Receiver.

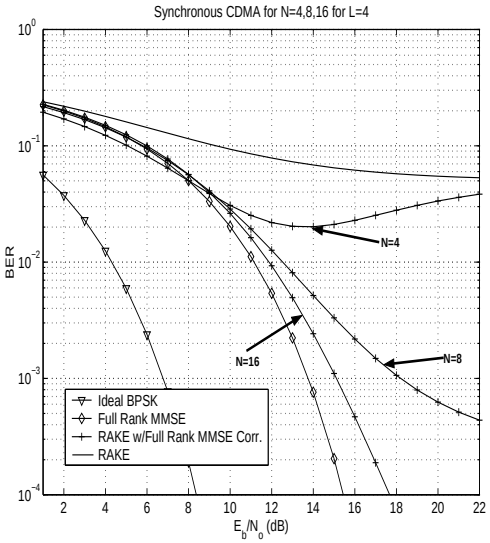


**Fig. 4**. Performance of the MWF RAKE correlators at Different Processing Gains.

## 9. REFERENCES


[1] Honig, M.L., and Goldstein, J.S., "Adaptive Reduced-Rank Residual Correlation Algorithms for DS-CDMA Interference Suppression", in *Proceedings of Asilomar*, Jul. 1998.

[2] Honig, M.L., and Poor, H.V., Adaptive Interference Suppression. In Poor, H.V., and Wornell, G.W., editors, "Wireless Communications: Signal Processing Perspectives", Prentice Hall: Englewood Cliffs, New Jersey, pgs. 64-102, 1998.

[3] U. Madhow, "Blind adaptive interference suppression for direct-sequence CDMA," *Proc. IEEE*, vol. 86, pp. 2049-2069, Oct. 1998.

[4] J. Scott Goldstein, I. S. Reed, and L. L. Scharf, "A multistage representation of the wiener filter based on orthogonal Projections," *IEEE Trans. on Information Theory*, vol. 44, pp. 2943-2959, Nov. 1998.

[5] M. L. Honig and W. Xiao, "Large System Analysis of Reduced-Rank Linear Interference Suppression," *Proceedings 37th Annual Allerton Conference on Communications, Systems, and Computing*, 23-24 Sept. 1999.

[6] Y. Song and S. Roy, "Blind adaptive reduced-rank detection for DS-CDMA signals in multipath channels," *IEEE Journal on Selected Areas in Communications*, vol. 17, no. 11, pp. 1960-1970, Nov. 1999.

[7] W.L. Myrick, M.D. Zoltowski and J.Scott Goldstein, "Exploiting conjugate symmetry in power minimization based pre-processing for GPS: reduced complexity and smoothness," *Proc. of 2000 IEEE Int'l Conf. on Acoustics, Speech, and Signal Processing*, Istanbul, Turkey, 5-9 June 2000.

[8] D. C. Ricks and J. S. Goldstein, "Efficient architectures for implementing adaptive algorithms," *Proceedings of the 2000 Antenna Applications Symposium*,pp. 29-41, Allerton Park, Monticello, Illinois, September 20-22,2000.

# A LOW COMPLEXITY RECEIVER FOR SPACE-TIME CODED CDMA SYSTEMS

*Seema Sud and J. Scott Goldstein*

Science Applications International Corporation
4001 Fairfax Dr., Suite 675 Arlington, VA 22203-1303, USA

## ABSTRACT

A novel receiver for space-time coded systems based on the reduced rank multistage Wiener filter (MWF) is presented. It is shown that this receiver has a complexity that is only a linear function of the processing gain ($N$), the number of transmit antennas ($L_t$), and the rank ($D$) of the MWF. The complexity of the equivalent MMSE solution is a function of $(NL_t)^3$. It is also demonstrated by numerical simulation that this receiver meets MMSE performance at a significantly low rank. The MMSE implementation is derived and performance is evaluated for highly loaded synchronous CDMA systems in flat fading.

## 1. INTRODUCTION

Systems employing code division multiple access (CDMA) are typically interference limited. The interference is due to the non-orthogonal multiplexing of signals that results from multipath induced by the channel, causing intersymbol interference (ISI). Interference can also arise from multiple users sharing a common bandwidth for different services, such as voice and data transmission. This interference severely limits system capacity and increasing demand for access has brought forth the requirements for better interference suppression techniques for future systems. Recently, diversity schemes employing space-time codes have been studied to combat interference and channel fading using diversity processing. In this paper, a low complexity receiver based on the multistage Wiener filter (MWF) ([2]) for space-time coded systems is presented and evaluated.

## 2. CDMA SIGNAL MODEL

We assume a CDMA system with $K$ synchronous users, as is typical of the forward link where space-time codes would by typically used. User $k$ transmits a baseband signal given by

$$x_k(t) = \sum_i A_k b_k(i) s_k(t - iT - \tau_k), \tag{1}$$

where $b_k(i)$ is the symbol transmitted by user $k$ at time $i$, $s_k(t)$ is the spreading code associated with user $k$, and $A_k$ and $\tau_k$ are the real valued amplitude and delay, respectively. We assume binary signaling, so that the symbols $b_k(i) \in$ (-1,+1). The spreading sequence can be written as

$$s_k(t) = \sum_{i=1}^{N-1} a_k[i] \Psi(t - iT_c), \tag{2}$$

where $a_k[i] \in (\frac{+1}{\sqrt{N}}, \frac{-1}{\sqrt{N}})$ is a normalization factor for the spreading code. The processing gain of the CDMA system is given by $N = \frac{T}{T_c}$, where $T_c$ is the chip period, and $T$ is the symbol period. We assume direct sequence (DS) CDMA, so that the chip sequence $\Psi(t)$ is a constant.

## 3. DERIVATION OF MMSE SOLUTION FOR SPACE-TIME CODES

With space-time codes, the data bit of a particular user is transmitted over multiple antennas. In a CDMA system, the symbols are also multiplied by the appropriate spreading codes. The received codeword is decoded using an ML or MMSE approach, and a bit estimate is determined. In this section, a reduced rank IS algorithm using the MWF is presented. Attention is restricted to Rayleigh distributed, flat fading channels. For the $2 \times 2$ space-time code in [1], at a given time period $t$, symbol $c_1$ is transmitted from antenna one, and symbol $c_2$ is transmitted from antenna two. During the next time period, $t+T$, symbol $-c_2$ is transmitted from antenna one, and symbol $c_1$ is transmitted from antenna two. The code can be written as

$$\mathbf{C}_{2x2} = \begin{bmatrix} c_1 & c_2 \\ -c_2 & c_1 \end{bmatrix}. \tag{3}$$

An example of a $4 \times 4$ space-time code ([5]) is

$$\mathbf{C}_{4x4} = \begin{bmatrix} c_1 & c_2 & c_3 & c_4 \\ -c_2 & c_1 & -c_4 & c_3 \\ -c_3 & c_4 & c_1 & -c_2 \\ -c_4 & -c_3 & c_2 & c_1 \end{bmatrix}. \tag{4}$$

The MMSE solution will be derived for the $2\times2$ and $4\times4$ codes described above but can be easily extended to other codes. Synchronous users are assumed, but the solution can be applied to asynchronous users assuming the receiver is synchronized to the desired user.

### 3.1. $2 \times 2$ Space-Time Code

Define $h_{ij}$ as the channel coefficient from the $i^{th}$ transmit antenna to the $j^{th}$ receive antenna. Denote the received signals over the two consecutive symbol periods as $\mathbf{r}_j(i)$ and $\mathbf{r}_j(i-1)$. Assuming, as mentioned earlier, that each $h_{ij}$ is approximately constant over two consecutive symbol periods, we can write the received signal at antenna $j = 1$ or $j = 2$ as ([4])

- $\mathbf{r}_j(i) = \sum_{k=1}^{K} A_k(h_{1j}\mathbf{s}_k b_k(i) + h_{2j}\mathbf{s}_k b_k(i-1)) + \mathbf{n}_j(i)$

- $\mathbf{r}_j(i-1) = \sum_{k=1}^{K} A_k(-h_{2j}\mathbf{s}_k b_k(i) + h_{1j}\mathbf{s}_k b_k(i-1)) + \mathbf{n}_j(i-1)$,

where $\mathbf{n}_j(i)$ and $\mathbf{n}_j(i-1)$ are $N \times 1$ AWGN vectors. Define the received signal vector by $\mathbf{r}(i) = [\mathbf{r}_j(i)\ \mathbf{r}_j(i-1)]^T$ and the noise vector by $\mathbf{n} = [\mathbf{n}_j(i)\ \mathbf{n}_j(i-1)]^T$. Define code symbol vectors by

$$\mathbf{c}_{jk,1} = [h_{1j}\mathbf{s}_k^T\ h_{2j}\mathbf{s}_k^T]^T \tag{5}$$
$$\mathbf{c}_{jk,2} = [-h_{2j}\mathbf{s}_k^T\ h_{1j}\mathbf{s}_k^T]^T. \tag{6}$$

This can also be written as

$$\mathbf{c}_{jk,1} = \zeta_{k,1}\mathbf{h}_j \tag{7}$$
$$\mathbf{c}_{jk,2} = \zeta_{k,2}\mathbf{h}_j, \tag{8}$$

where

$$\zeta_{k,1} = \begin{bmatrix} \mathbf{s}_k & \mathbf{0} \\ \mathbf{0} & \mathbf{s}_k \end{bmatrix} \tag{9}$$

$$\zeta_{k,2} = \begin{bmatrix} \mathbf{0} & -\mathbf{s}_k \\ \mathbf{s}_k & \mathbf{0} \end{bmatrix}, \tag{10}$$

and $\mathbf{h}_j = [h_{1j}\ h_{2j}]^T$. We further define

$$\mathbf{h} = [\mathbf{h}_1^T\ \mathbf{h}_2^T]^T, \tag{11}$$

and

$$\mathbf{c}_{k,1} = [\mathbf{c}_{1k,1}^T\ \mathbf{c}_{2k,1}^T]^T = (\mathbf{I}_2 \otimes \zeta_{k,1})\mathbf{h} \tag{12}$$
$$\mathbf{c}_{k,2} = [\mathbf{c}_{1k,2}^T\ \mathbf{c}_{2k,2}^T]^T = (\mathbf{I}_2 \otimes \zeta_{k,2})\mathbf{h}, \tag{13}$$

where $\mathbf{I}_2$ denotes a $2 \times 2$ identity matrix and $\otimes$ denotes the Kronecker product. The received signal is now given by

$$\mathbf{r}(i) = \sum_{k=1}^{K} A_k(\mathbf{c}_{k,1}b_k(i) + \mathbf{c}_{k,2}b_k(i-1)) + \mathbf{n}(i), \tag{14}$$

where $\mathbf{n} = [\mathbf{n}_1^T\ \mathbf{n}_2^T]^T$.

The MMSE receiver must estimate the vector of bits $\mathbf{b}(i) = [b_1(i),\ b_2(i),\ ...,\ b_K(i)]$ from the received signal vector $\mathbf{r}(i)$. To compute the MMSE solution, minimize the MSE, given by

$$MSE_{STC} = arg_{\Im} min E[\|\mathbf{b}(i) - \Im^H \mathbf{r}(i)\|^2]. \tag{15}$$

The MMSE solution can then be written directly as

$$\Im = \mathbf{R}_{rr}^{-1}\mathbf{R}_{rb}, \tag{16}$$

where $\mathbf{R}_{rr}$ is the data covariance matrix and $\mathbf{R}_{rb}$ is the cross-correlation vector. From Eq. (14), the cross-correlation vector can be written as

$$\mathbf{R}_{yb} = E[\mathbf{r}(i)\mathbf{b}(i)] = \mathbf{CA}, \tag{17}$$

where $\mathbf{C} = [\mathbf{C}_1\ \mathbf{C}_2\ ...\ \mathbf{C}_K]$, $\mathbf{C}_k = [\mathbf{c}_{k,1}\ \mathbf{c}_{k,2}]$, and $\mathbf{A}$ is the diagonal matrix of signal amplitudes defined previously. If we assume that user one is the desired user, the MMSE simplifies to

$$\Im_{SU} = A_1\mathbf{R}_{rr}^{-1}\mathbf{C}_1. \tag{18}$$

### 3.2. $4 \times 4$ Space-Time Code

The parameters $h_{ij}$ are as defined for the $2 \times 2$ code. The received signals over four consecutive symbol periods at antenna $j$, $j = 1, 2, 3, 4$, are defined, respectively, as

- $\mathbf{r}_j(i) = \sum_{k=1}^{K} A_k(h_{1j}\mathbf{s}_k b_k(i) + h_{2j}\mathbf{s}_k\, b_k(i-1) + h_{3j}\mathbf{s}_k b_k(i-2) + h_{4j}\mathbf{s}_k b_k(i-3)) + \mathbf{n}_j(i)$
- $\mathbf{r}_j(i-1) = \sum_{k=1}^{K} A_k(-h_{2j}\mathbf{s}_k b_k(i) + h_{1j}\mathbf{s}_k b_k(i-1) - h_{4j}\mathbf{s}_k b_k(i-3) + h_{3j}\mathbf{s}_k b_k(i-4)) + \mathbf{n}_j(i-1)$,
- $\mathbf{r}_j(i-2) = \sum_{k=1}^{K} A_k(-h_{3j}\mathbf{s}_k b_k(i) + h_{4j}\mathbf{s}_k b_k(i-1) + h_{1j}\mathbf{s}_k b_k(i-3) + h_{2j}\mathbf{s}_k b_k(i-4)) + \mathbf{n}_j(i-2)$,
- $\mathbf{r}_j(i-3) = \sum_{k=1}^{K} A_k(-h_{4j}\mathbf{s}_k b_k(i) - h_{3j}\mathbf{s}_k b_k(i-1) + h_{2j}\mathbf{s}_k b_k(i-3) + h_{1j}\mathbf{s}_k b_k(i-4)) + \mathbf{n}_j(i-3)$,

where $\mathbf{n}_j(i)$, $\mathbf{n}_j(i-1)$, $\mathbf{n}_j(i-2)$, and $\mathbf{n}_j(i-3)$ are $N \times 1$ AWGN vectors. Write the received vector as $\mathbf{r}(i) = [\mathbf{r}_j(i)\ \mathbf{r}_j(i-1)\ \mathbf{r}_j(i-2)\ \mathbf{r}_j(i-3)]^T$ and the noise vector by $\mathbf{n} = [\mathbf{n}_j(i)\ \mathbf{n}_j(i-1)\ \mathbf{n}_j(i-2)\ \mathbf{n}_j(i-3)]^T$. Define the code symbol vectors by

$$\mathbf{c}_{jk,1} = [h_{1j}\mathbf{s}_k^T\ h_{2j}\mathbf{s}_k^T\ h_{3j}\mathbf{s}_k^T\ h_{4j}\mathbf{s}_k^T]^T \tag{19}$$
$$\mathbf{c}_{jk,2} = [-h_{2j}\mathbf{s}_k^T\ h_{1j}\mathbf{s}_k^T\ -h_{4j}\mathbf{s}_k^T\ h_{3j}\mathbf{s}_k^T]^T. \tag{20}$$
$$\mathbf{c}_{jk,3} = [-h_{3j}\mathbf{s}_k^T\ h_{4j}\mathbf{s}_k^T\ h_{1j}\mathbf{s}_k^T\ -h_{2j}\mathbf{s}_k^T]^T. \tag{21}$$
$$\mathbf{c}_{jk,4} = [-h_{4j}\mathbf{s}_k^T\ -h_{3j}\mathbf{s}_k^T\ h_{2j}\mathbf{s}_k^T\ h_{1j}\mathbf{s}_k^T]^T. \tag{22}$$

Each of the above equations can also be written as

$$\mathbf{c}_{jk,i} = \zeta_{k,i}\mathbf{h}_j, \tag{23}$$

where

$$\zeta_{k,1} = \begin{bmatrix} \mathbf{s}_k & \mathbf{0} & \mathbf{0} & \mathbf{0} \\ \mathbf{0} & \mathbf{s}_k & \mathbf{0} & \mathbf{0} \\ \mathbf{0} & \mathbf{0} & \mathbf{s}_k & \mathbf{0} \\ \mathbf{0} & \mathbf{0} & \mathbf{0} & \mathbf{s}_k \end{bmatrix}, \tag{24}$$

$$\zeta_{k,2} = \begin{bmatrix} \mathbf{0} & -\mathbf{s}_k & \mathbf{0} & \mathbf{0} \\ \mathbf{s}_k & \mathbf{0} & \mathbf{0} & \mathbf{0} \\ \mathbf{0} & \mathbf{0} & \mathbf{0} & -\mathbf{s}_k \\ \mathbf{0} & \mathbf{0} & \mathbf{s}_k & \mathbf{0} \end{bmatrix}, \tag{25}$$

$$\zeta_{k,3} = \begin{bmatrix} \mathbf{0} & \mathbf{0} & -\mathbf{s}_k & \mathbf{0} \\ \mathbf{0} & \mathbf{0} & \mathbf{0} & \mathbf{s}_k \\ \mathbf{s}_k & \mathbf{0} & \mathbf{0} & \mathbf{0} \\ \mathbf{0} & -\mathbf{s}_k & \mathbf{0} & \mathbf{0} \end{bmatrix}, \tag{26}$$

$$\zeta_{k,4} = \begin{bmatrix} \mathbf{0} & \mathbf{0} & \mathbf{0} & -\mathbf{s}_k \\ \mathbf{0} & \mathbf{0} & -\mathbf{s}_k & \mathbf{0} \\ \mathbf{0} & \mathbf{s}_k & \mathbf{0} & \mathbf{0} \\ \mathbf{s}_k & \mathbf{0} & \mathbf{0} & \mathbf{0} \end{bmatrix}, \tag{27}$$

and $\mathbf{h}_j = [h_{1j}\ h_{2j}\ h_{3j}\ h_{4j}]^T$. We also define

$$\mathbf{h} = [\mathbf{h}_1^T\ \mathbf{h}_2^T\ \mathbf{h}_3^T\ \mathbf{h}_4^T]^T, \tag{28}$$

and

$$\mathbf{c}_{k,1} = [\mathbf{c}_{1k,1}^T \ \mathbf{c}_{2k,1}^T \ \mathbf{c}_{3k,1}^T \ \mathbf{c}_{4k,1}^T]^T = (\mathbf{I}_4 \otimes \zeta_{k,1})\mathbf{h} \quad (29)$$

$$\mathbf{c}_{k,2} = [\mathbf{c}_{1k,2}^T \ \mathbf{c}_{2k,2}^T \ \mathbf{c}_{3k,2}^T \ \mathbf{c}_{4k,2}^T]^T = (\mathbf{I}_4 \otimes \zeta_{k,2})\mathbf{h} \quad (30)$$

$$\mathbf{c}_{k,3} = [\mathbf{c}_{1k,3}^T \ \mathbf{c}_{2k,3}^T \ \mathbf{c}_{3k,3}^T \ \mathbf{c}_{4k,3}^T]^T = (\mathbf{I}_4 \otimes \zeta_{k,3})\mathbf{h} \quad (31)$$

$$\mathbf{c}_{k,4} = [\mathbf{c}_{1k,4}^T \ \mathbf{c}_{2k,4}^T \ \mathbf{c}_{3k,4}^T \ \mathbf{c}_{4k,4}^T]^T = (\mathbf{I}_4 \otimes \zeta_{k,4})\mathbf{h} \quad (32)$$

The received signal can now be written as

$$\mathbf{r}(i) = \sum_{k=1}^{K} A_k \sum_{t=1}^{4} (\mathbf{c}_{k,t} b_k(i-t+1)) + \mathbf{n}(i) \quad (33)$$

where $\mathbf{n} = [\mathbf{n}_1^T \ \mathbf{n}_2^T \ \mathbf{n}_3^T \ \mathbf{n}_4^T]^T$.

With the first user as the user of interest, the MMSE solution is

$$\Im_{SU} = A_1 \mathbf{R}_{rr}^{-1} \mathbf{C}_1, \quad (34)$$

where $\mathbf{R}_{rr}$ is the data covariance matrix defined previously, $\mathbf{C} = [\mathbf{C}_1 \ \mathbf{C}_2 \ ... \ \mathbf{C}_K]$ as before, and $\mathbf{C}_k = [\mathbf{c}_{k,1} \ \mathbf{c}_{k,2} \ \mathbf{c}_{k,3} \ \mathbf{c}_{k,4}]$.

## 4. MMSE IMPLEMENTATION VIA THE MWF

To implement the MMSE solution for space-time codes via the MWF, note the analogy between the standard MMSE solution ([3]),

$$\mathbf{c}_{MMSE} = \mathbf{R}^{-1}\mathbf{s}_1, \quad (35)$$

and that of the STC in Eq. (18) or Eq. (34). The desired covariance matrix is computed using the joint received vector $\mathbf{r}$, defined in Eq. (14) or Eq. (33). Similarly, the spreading code $\mathbf{s}_1$ is replaced by $\mathbf{C}_1$, defined as $\mathbf{C}_1 = [\mathbf{c}_{k,1} \ \mathbf{c}_{k,2}]$ for the $2 \times 2$ code and $\mathbf{C}_1 = [\mathbf{c}_{k,1} \ \mathbf{c}_{k,2} \ \mathbf{c}_{k,3} \ \mathbf{c}_{k,4}]$ for the $4 \times 4$ code. Note that $\mathbf{d}_0(i)$ is now a vector instead of a scalar; a parallel implementation must therefore be used. The outputs, $[\hat{b}_1(i) \ \hat{b}_1(i-1)]$ for the $2 \times 2$ code, and $[\hat{b}_1(i) \ \hat{b}_1(i-1) \ \hat{b}_1(i-2) \ \hat{b}_1(i-3)]^T$ for the $4 \times 4$ code, are delayed appropriately and added to determine the final bit estimate. Thus, the MWF algorithm (see [2] and Figure 1) is initialized by setting $\mathbf{d}_0(i) = \mathbf{C}_1^H \mathbf{r}(i)$ and $\mathbf{x}_0(i) = \mathbf{B}_{\mathbf{C}_1}\mathbf{r}(i)$ for the $2 \times 2$ code, and similarly for the $4 \times 4$ code, where the blocking matrix $\mathbf{B}_{\mathbf{C}_1}$ is defined to be orthogonal to $\mathbf{C}_1$. The recursion equations for the MWF (see Table 1), are described in detail in [2] and [3]. The receivers are shown for the $2 \times 2$ code and the $4 \times 4$ code in Figures 2 and 3, respectively.

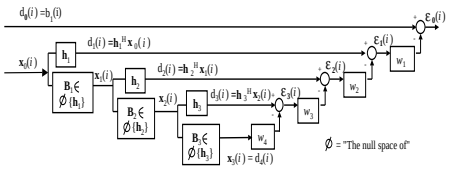


Figure 1: Multistage Wiener Filter (MWF), D=4 stages

*Computational Savings of the MWF:* The zeroth stage of the standard MWF is the matched filter, requiring $N$ operations per block. Next, the output is re-spread with the spreading code and subtracted from the received signal, requiring another $N$ flops. This is the dominant term in the computations, and for $D$ stages, the result is a requirement of $O(2DN)$ flops. For the MMSE, the dominant term is the $N \times N$ matrix inversion, which requires $O(N^3)$ operations per block. With space-time coding, the complexity of the MMSE solution is greatly reduced by employing the MWF as the dimension of the covariance matrix now increases from $N$ to $NL_t$ (or $NL_r$), where $L_t$ and $L_r$ are the number of transmit and receive antennas, respectively. So now, the number of required flops for the MWF and the MMSE implementations is $O(2DNL_t)$ and $O(N^3 L_t^3)$, respectively. This number can become impractically large even for $L_t = 2$ or $L_t = 4$.

Table 1: Recursion Equations for the MWF

Initialization: $d_0(i)$ and $\mathbf{x}_0(i)$
Forward Recursion: For $j = 1, 2, ..., D$:

$$\mathbf{h}_j = \frac{\sum_\Omega \{d_{j-1}^*(i)\mathbf{x}_{j-1}(i)\}}{||\sum_\Omega \{d_{j-1}^*(i)\mathbf{x}_{j-1}(i)\}||}$$

$$d_j(i) = \mathbf{h}_j^H \mathbf{x}_{j-1}(i)$$

$$\mathbf{x}_j(i) = \mathbf{B}_j \mathbf{x}_{j-1}(i)$$

Backward Recursion: For $j = D, D-1, ..., 1$

$$e_D(i) = d_D(i)$$

$$w_j = \frac{\sum_\Omega \{d_{j-1}^*(i) e_j(i)\}}{\sum_\Omega \{|e_j(i)|^2\}}$$

$$e_{j-1}(i) = d_{j-1}(i) - w_j^* e_j(i)$$

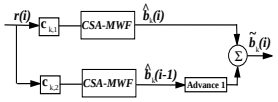


Figure 2: $2 \times 2$ STC Decoding Scheme Using the MWF

## 5. NUMERICAL RESULTS

We use length $N = 31$ Gold codes in spreading. Figure 4 is a plot of $E_b/N_0$ vs. BER for a $2 \times 2$ STC assuming $K = 15$ users. Performance gains of up to 8 dB are observed here due to the transmit code diversity, time diversity, and receiver antenna diversity. Note also that the MWF performance meets that of full rank at a rank of 5. Figure 5 is a plot of $E_b/N_0$ vs. BER for the $4 \times 4$ STC with $K = 15$ users. For this highly loaded system in flat fading, the MMSE solution requires high SNR. Low BERs are attainable at very low SNRs by employing the reduced rank MWF with the STC, with the added benefit of low complexity implementation as described above. Here, the MWF/STC performance improves over full rank MMSE by nearly 9 dB, again at rank 5.

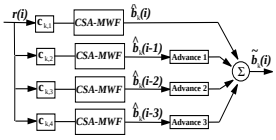


Figure 3: $4 \times 4$ STC Decoding Scheme Using the MWF

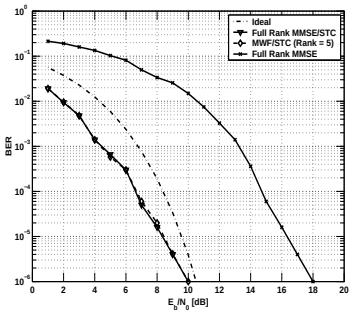


Figure 4: $2 \times 2$ Space-Time Code Example

## 6. CONCLUSION

A new receiver for space-time coded systems based on the multistage Wiener filter is introduced. The MMSE solution is derived for a $2 \times 2$ and a $4 \times 4$ coding scheme. Implementation of the solution using the reduced rank MWF is then shown. The implementation complexity of the reduced rank MWF versus the MMSE is $O(2DNL_t)$ and $O(N^3L_t^3)$, respectively, with $D \ll N$. Numerical results show that the MWF meets full rank performance at a rank as low as 5 for processing gains of 32. Performance gains up to 9 dB versus the uncoded system are demonstrated.

## REFERENCES

[1] Alamouti, S.M., "A Simple Transmit Diversity Technique for Wireless Communications", *IEEE Journal on Selected Areas in Communications*, Vol. 16, No. 8, pgs. 1451-1458, Oct. 1998.

[2] Goldstein, J.S., Reed, I.S., and Scharf, L.L., "A Multistage Representation of the Wiener Filter Based on Orthogonal Projections", *IEEE Transactions on Information Theory*, Vol. 44, No. 7, Nov. 1998.

[3] Honig, M.L., and Goldstein, J.S., "Adaptive Reduced-Rank Residual Correlation Algorithms for DS-CDMA Interference Suppression", *Proceedings of Asilomar*, Jul. 1998.

[4] Lu, X., and Li, H., "Blind Multiuser Detection for Space Time Coded Systems", *Proceedings of ICASSP*, Salt Lake City, UT, May 2001.

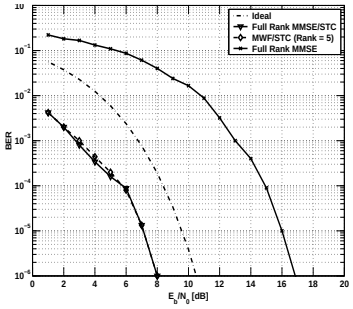


Figure 5: $4 \times 4$ Space-Time Code Example

[5] Tarokh, V., Jafarkhani, H., and Calderbank, A.R., "Space-Time Block Codes from Orthogonal Designs", *IEEE Transactions on Information Theory*, Vol. 45, No. 5, pgs. 1456-1467, Jul. 1999.

# EFFICIENT INTERFERENCE CANCELLATION ALGORITHMS FOR CDMA UTILIZING INTERFERENCE SUPPRESSION AND MULTIPATH COMBINING

*Seema Sud and J. Scott Goldstein*

Science Applications International Corporation
4001 Fairfax Dr., Suite 675
Arlington, VA 22203-1303, USA

*Timothy Pratt*

Bradley Department of Electrical and Computer Engineering
Virginia Tech
Blacksburg, VA 24061, USA

## ABSTRACT

*A new, low rank adaptive algorithm that performs serial and parallel interference cancellation for a DS-CDMA in frequency selective multipath is presented. The algorithm provides interference suppression (IS) in place of matched filtering at each stage of the cancellation for better interference mitigation. It employs a computationally efficient, correlation-subtraction architecture (CSA) based on the multistage Wiener filter (MWF) to do the IS at each successive stage. This CSA-MWF structure meets MMSE performance but requires substantially fewer computations than the MMSE receiver, and eliminates the need for matrix inversion, eigen-decomposition, or the construction of blocking matrices. Embedded within the new structure is also a RAKE receiver that combines the multipath components for added performance gain. It is shown that this technique performs significantly better than the conventional matched filter (MF) SIC. The performance gains of the joint MWF/SIC and MWF/PIC structures over the conventional SIC and PIC, MMSE, and RAKE receivers are determined for a highly loaded synchronous DS-CDMA system in frequency selective multipath, and the computational costs and performance benefits are presented.*

## 1. INTRODUCTION

Code Division Multiple Access (CDMA) has been proposed for future generation wireless communications systems due to its' potential for providing high system capacity over other multiple access schemes. However, systems employing CDMA are typically interference limited. The interference is often exacerbated by what is commonly called the near-far effect, in which a user near the base station causes a large amount of interference to a user far away. Many commercial systems employ stringent power control to mitigate this problem. Others employ multiuser detection (MUD) to suppress multi-access interference (MAI) ([7]). However, optimal multiuser detection schemes, i.e. maximum likelihood (ML) are often computationally complex. In serial interference cancellation (SIC) schemes, the output of a bank of correlators is used to determine the highest power user to then subtract that user's signal out of the received signal. This process is repeated for the next highest power user, and so on. When users have equal power, parallel interference cancellation (PIC) schemes can be used. Prior work in the development of SIC and PIC receivers is found in e.g. [7], [5], and [11].

In this paper, we present SIC and PIC schemes that perform IS along with multipath combining. The matched filter (MF) correlators in the SIC are replaced by the efficient CSA structure of the MWF ([2], [3], and [8]) to do IS at each stage. It has been shown that the MWF meets full rank MMSE performance at a low rank, thereby giving a significant improvement in performance over the conventional MF, but without the covariance matrix inversion required by the full rank MMSE receiver. It has also been shown that this implementation of the MWF can be used to perform multiuser detection (MUD) with no performance loss over matrix version (full rank) MUD schemes. Multipath combining is obtained by allowing the zeroth stage correlator of the MWF to span more than one bit.

We begin by describing the MMSE solution to the CDMA detection problem, which includes a RAKE type processor, and show how this solution is efficiently implemented with the CSA-MWF. The computational cost and performance benefit of the MWF are also analyzed. We then describe the SIC and PIC structures using the CSA-MWF and formulate an expression for probability of error ($P_e$). The $P_e$ expression is compared to the bit error rate (BER) output of a Monte Carlo simulation using a simple two user example. Then, we show the performance benefits of the MWF/SIC and PIC via Monte Carlo simulation and compare the new structures with that of the standard SIC and PIC, as well as the MMSE and the conventional RAKE receiver.

## 2. CDMA SIGNAL MODEL

We assume a synchronous CDMA system with $K$ users. Performance with asynchronous users can be assessed by treating each asynchronous user as two synchronous users. User $k$ transmits a baseband signal given by

$$x_k(t) = \sum_i A_k b_k(i) s_k(t - iT - \tau_k), \qquad (1)$$

where $b_k(i)$ is the symbol transmitted by user $k$ at time $i$, $s_k(t)$ is the spreading code associated with user $k$, and $A_k$ and $\tau_k$ are the amplitude and delay, respectively. We assume binary signaling, so that the symbols $b_k(i) \in$ (-1,+1). The

spreading sequence can be written as

$$s_k(t) = \sum_{i=1}^{N-1} a_k[i]\Psi(t - iT_c), \tag{2}$$

where $a_k[i] \in (\frac{+1}{\sqrt{N}}, \frac{-1}{\sqrt{N}})$. The processing gain is given by $N = \frac{T}{T_c}$, where $T_c$ is the chip period, and $T$ is the symbol period. We assume that the chip sequence $\Psi(t)$ is a constant, i.e. direct sequence (DS) CDMA.

Assume, without loss of generality, that we are interested in detecting user 1 and write the transmitted signal as

$$\mathbf{y}(i) = b_1(i)\mathbf{s_1} + \sum_{k=2}^{K} A_k b_k(i)\mathbf{s_k}. \tag{3}$$

Here, $\mathbf{s_1}$ is the spreading sequence of user 1, and $\mathbf{s_k}$ is the $N \times 1$ vector containing the spreading code associated with the $k^{th}$ interfering user. To simplify the notation, we rewrite Eq. (3) in matrix form as

$$\mathbf{y}(i) = \mathbf{SAb}(i), \tag{4}$$

where $\mathbf{S} = (\mathbf{s}_1\ \mathbf{s}_2\ ...\ \mathbf{s}_K)$, $\mathbf{A} = diag(A_1, A_2, ..., A_K)$, and $\mathbf{b}(i) = (b_1(i), b_2(i), ..., b_K(i))^T$. $\mathbf{S}$ is an $N \times K$ matrix, $\mathbf{A}$ is a $K \times K$ matrix, and $\mathbf{b}(i)$ is a $K \times 1$ vector. Our goal is to extract the desired information, i.e., the bits transmitted by user 1 ($b_1$) while suppressing the interference represented by the term in the summation of Eq. (3).

## 3. THE REDUCED RANK CSA-MWF

In this section, we present the MMSE solution for a synchronous, DS-CDMA system in a channel distorted by frequency selective multipath and its implementation via the reduced rank MWF.

Consider a multipath channel, modeled by an L-tap chip-spaced tapped-delay line with coefficients $\mathbf{h} = [h_1, h_2, ..., h_L]$. The parameter L is known as the delay spread of the channel. The received signal can now be written as

$$\hat{\mathbf{r}}(i) = \hat{\mathbf{y}}(i) + \mathbf{n}(i), \tag{5}$$

where $\hat{\mathbf{y}} = \mathbf{y} * \mathbf{h}$ and $*$ denotes convolution. Substituting for $\mathbf{y}$ from Eq. (3), we can write the received signal explicitly as

$$\hat{\mathbf{r}}(i) = b_1(i)\hat{\mathbf{s}}_\mathbf{1} + \sum_{k=2}^{K} A_k b_k(i)\hat{\mathbf{s}}_\mathbf{k} + \mathbf{n}(i), \tag{6}$$

where $\hat{(\cdot)}$ denotes convolution of the operand with the channel vector $\mathbf{h}$. In this paper, it is assumed that the channel vector is known. The goal of the MMSE receiver is to minimize the mean square error between the transmitted bit and its' estimate, defined by

$$MSE = E[|b_1(i) - \hat{\mathbf{c}}^H\hat{\mathbf{r}}(i)|^2], \tag{7}$$

where $E[\cdot]$ denotes the expected value operator and $(\cdot)^H$ denotes Hermitian transpose. The MMSE solution in the presence of multipath is ([9])

$$\hat{\mathbf{c}}_{MMSE} = \hat{\mathbf{R}}^{-1}\hat{\mathbf{s}}_\mathbf{1} = E[\hat{\mathbf{r}}\hat{\mathbf{r}}^H]^{-1}\hat{\mathbf{s}}_\mathbf{1}. \tag{8}$$

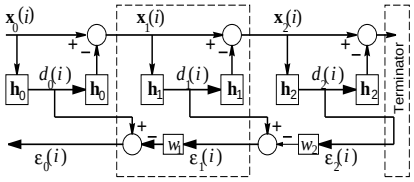


Figure 1: CSA-MWF (D=2 stages)

Note that computation of the MMSE solution requires inversion of the $(N+L-1) \times (N+L-1)$ covariance matrix $\hat{\mathbf{R}}$, which can be quite computationally intensive and may not even be possible in real-time for a high data rate system. Also, if the channel or signals are changing in time, then the sample covariance matrix estimated from the data does not depict the true non-stationary signal environment. Thus, it is desirable to find alternative solutions that approach, or exceed, the performance of the MMSE receiver but require much fewer computations and can adapt rapidly. The MWF has demonstrated the ability to do this (e.g., see [2]). The multistage decomposition of the Wiener filter, based on the correlation-subtraction architecture (CSA) for $D = 2$ stages is shown in Fig. 1 ([8]).

The MWF solution for the multipath channel is obtained by setting $\mathbf{h_0} = \hat{\mathbf{s}}_\mathbf{1}$, the spreading code of the desired user convolved with the channel impulse response. Then, $\mathbf{d_0}(n) = \hat{\mathbf{s}}_1^H\mathbf{x}_0(n)$, where the input signal $\mathbf{x}_0(n)$ is a vector composed of a block of M bits of the received sampled signal: $[\hat{\mathbf{r}}(n-M+1)\ \hat{\mathbf{r}}(n-M+2)\ ...\ \hat{\mathbf{r}}(n)]$. The filter in Fig. 1 demonstrates the low complexity of this implementation of the MWF and the fact that the computation of signal blocking matrices are no longer necessary for subspace partitioning. The recursion equations are shown below ([3] and [4]).

- *Initialization:* $d_0(n)$ and $\mathbf{x}_0(n)$
- *Forward Recursion:* For $k = 1, 2, ..., D$:

$$\begin{aligned} \mathbf{h}_k &= \frac{\sum_\Omega\{d^*_{k-1}(n)\mathbf{x}_{k-1}(n)\}}{||\sum_\Omega\{d^*_{k-1}(n)\mathbf{x}_{k-1}(n)\}||} \\ d_k(n) &= \mathbf{h}_k^H\mathbf{x}_{k-1}(n) \\ \mathbf{x}_k(n) &= \mathbf{x}_{k-1}(n) - \mathbf{h}_k d_k(n) \end{aligned}$$

- *Backward Recursion:* For $k = D, D-1, ..., 1$, with $\epsilon_D(n) = d_D(n)$:

$$\begin{aligned} w_k &= \frac{\sum_\Omega\{d^*_{k-1}(n)\epsilon_k(n)\}}{\sum_\Omega\{|\epsilon_k(n)|^2\}} \\ \epsilon_{k-1}(n) &= d_{k-1}(n) - w_k^*\epsilon_k(n) \end{aligned}$$

where $\Omega$ denotes the region of sample support used to compute the statistics. Note that the RAKE solution, which only incorporates the effects of multipath and neglects interference, can be written simply as ([6]) $\mathbf{c}_{RAKE} = \hat{\mathbf{s}}_\mathbf{1}$ and in the presence of only AWGN, this further reduces to the matched filter (MF) solution, $\mathbf{c}_{MF} = \mathbf{s_1}$.

*Computational Cost/Benefit of the MWF:* In the matched filter, $N$ multiplications and $N-1$ additions are required for each bit of data, equivalently approximately $N$ floating point operations (or flops) are required. For a block of data, $O(NM)$ flops are needed, where $O$ denotes 'on the order of'. The zeroth stage of the MWF is the matched filter, requiring $N$ operations per block. Next, the output is re-spread with the spreading code and subtracted from the received signal, requiring another $N$ flops. This is the dominant term in the computations, and for $D$ stages and $M$ blocks, the result is a requirement of $O(2DNM)$ flops. Finally, for the MMSE, the dominant term is the $N \times N$ matrix inversion, which requires $O(N^3)$ operations per block or a total of $O(N^3M)$ operations. As an example, let $N = 32$, $D = 5$, and $M = 100$. Then, the computational cost associated with the MF, MWF, and MMSE are $3,200$, $32,000$, and $3,276,800$ flops, respectively. The minimal complexity increase of the MWF over the MF is outweighed by the performance benefits, as the MF fails in a highly loaded system.

## 4. JOINT IS/SIC VIA THE CSA-MWF

The conventional SIC provides cancellation of strong users first by correlating with a filter matched to the spreading code of the desired user. A hard decision on the correlator output is used to regenerate the decoded signal and subtract it out of the received signal for the next stage in the cancellation ([7]). In the new scheme, it is proposed to replace the conventional correlator at each stage with an MMSE receiver, implemented using the CSA-MWF. The bit estimates used to regenerate the signal will improve as the MWF does IS whereas the MF cannot. A block diagram of the new scheme is shown in Figure 2.

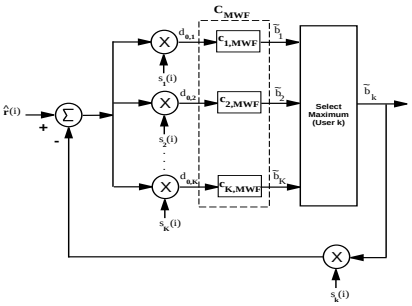


Figure 2: SIC via CSA-MWF

The $P_e$ for a simple SIC is derived in [7] by treating the interference due to both the uncancelled users and the imperfectly cancelled users as Gaussian noise. In [1] an accurate $P_e$ for a decorrelating multiuser decision feedback (DF) detector is derived for synchronous CDMA systems by utilizing decisions of the high energy users to decode the weaker ones. Those structures can be modified to replace the forward filter by the MWF. Since the SIC is a form of multiuser detector, one should begin by writing the received signal in matrix form. Using matrix notation of Eq. (4), we can write the received signal in Eq. (6) as

$$\hat{\mathbf{r}}(i) = \hat{\mathbf{S}}\mathbf{A}\mathbf{b}(i) + \mathbf{n}(i). \tag{9}$$

Referring to Figure 2, the first operation performed in the SIC is a matched filter for each of the spreading codes. For the next block, the feedforward filter of the DF detector described in [1], is replaced here by the equivalent matrix form of the MWF. It can be shown that the MUD filter is equivalent to the concatenation of a bank of IS filters ([10]), and thus the matrix of coefficients can be written as $\mathbf{C}_{MWF} = [\mathbf{c}_{MWF,1}\ \mathbf{c}_{MWF,2},\ ...,\ \mathbf{c}_{MWF,K}]$ where $\mathbf{c}_{MWF,k}$ denotes the vector of coefficients for user $k$. Writing the MWF as a vector of filter coefficients (from Figure 1), it can be shown that the solution for user 1 is given by $\epsilon_0(n) = \mathbf{c}_{MWF,1}^H \mathbf{x}_0(n)$ where

$$\mathbf{c}_{MWF,1} = \hat{\mathbf{s}}_1 - w_1\mathbf{h}_1 + w_1w_2\mathbf{h}_2 - w_1w_2w_3\mathbf{h}_3 + \cdots. \tag{10}$$

The solution for the other users is obtained similarly. With this substitution, the structure of Figure 2 is identical to that in [1] with $\mathbf{C}_{MWF}$ replacing $(F^T)^{-1}$ and $\mathbf{c}_{MWF,k}$ replacing $\mathbf{F}_{i,k}$. An outline of the derivation of the $P_e$, following that in [1], is presented below:

First assume that correct decisions are fed back to the SIC, so that the output SNR for user $k$ can be written as

$$SNR_k = \mathbf{c}_{MWF,k}^2 A_k^2/\sigma^2. \tag{11}$$

Recall that $A_k$ is the amplitude of the $k^{th}$ user and $\sigma$ is the standard deviation of the white noise. Then, the $P_e$ is

$$P_{e_k} = Q(\mathbf{c}_{MWF,k}A_k/\sigma), \tag{12}$$

where $Q()$ denotes the Q function. Now, assuming that errors occur, a more accurate probability of error can be calculated by first computing the conditional error probability assuming a particular error and then averaging over all the possible errors for all of the previously cancelled $k-1$ users. This expression is given by

$$P_{e_k} = E[\Delta b_1, ..., \Delta b_{k-1}]Q(\frac{A_k(\mathbf{c}_{MWF,k} + \sum_{i=1}^{k-1}\mathbf{c}_{MWF,i}\Delta b_i)}{\sigma}) \tag{13}$$

where the error for the $i^{th}$ user is $\Delta b_i = (b_i - \tilde{b}_i)$. For the binary system under consideration, $\Delta b_i$ only takes on the values 2 or $-2$.

## 5. JOINT IS/PIC VIA THE CSA-MWF

The standard PIC provides cancellation of all of the equal (or nearly equal) power interferers from the received signal at successive stages before decoding the bits transmitted by the desired user. Again the decoding of the interfering users is done by correlation with a matched filter followed by a hard decision and subtraction. Following the last stage of the PIC, the desired user's bits are then decoded. Again, we replace the conventional correlator at each stage in the PIC with the CSA-MWF to improve performance. A partial

block diagram of a two-stage PIC structure similar to that in [5] is shown in Figure 3. Further stages can be concatenated by subtracting the re-spread bit estimates at each stage from the input to the MWF of that stage, which has the estimates of the previous stages already removed.

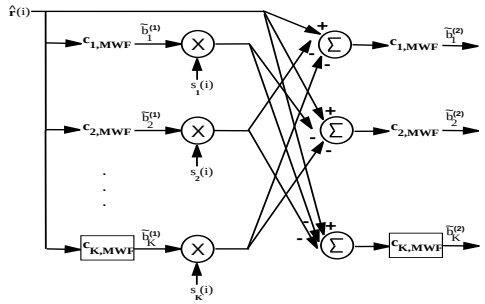


Figure 3: PIC via CSA-MWF (Two-Stage)

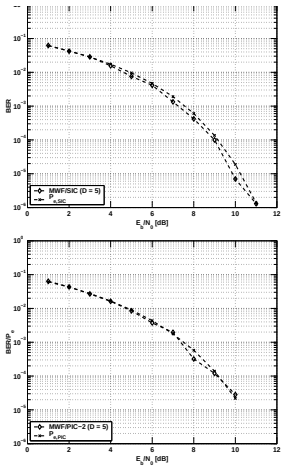


Figure 4: Monte Carlo vs. Analytical SIC and PIC ($K = 2$)

The $P_e$ derivation in this section can be obtained easily from that presented in [5], in which an approximate formula for $P_e$ using an MMSE/PIC is derived and bounded. By replacing the MMSE detector with the equivalent MWF, the MWF/PIC solution is obtained. The expression for $P_e$ is complicated and is bounded in [5], Eq. (31). Note the similarity between this equation and Eq. (13), derived for the SIC. In fact, it can be shown that these equations are identical. Alternatively, note the similarity between the structures in Figures 2 and 3. This is because the single stage SIC structure is identical to that of the two-stage PIC, with the only exception being the way the users are cancelled. In the PIC, the users are assumed equal power, and therefore all cancelled simultaneously whereas in the SIC, users of higher power are cancelled first.

## 6. A TWO-USER EXAMPLE

The final expression for $P_e$ given in Eq. (13) is complicated to evaluate even for the binary problem because of the presence of multiple users. It will therefore be evaluated using a simple, two user example to validate the Monte Carlo simulation to provide numerical results in the next section. For the SIC, assume that the first user has higher power than the second user and is thus cancelled first (for the PIC equal power users are assumed and either one can be cancelled first). First, note that the $P_e$ for the stronger user is given by the output of the first stage of the SIC, i.e. the MF followed by the MWF, or

$$P_{e,1} = Q(\mathbf{c}_{MWF,1} A_1/\sigma). \tag{14}$$

Then, the input to the decision device for the second user is $A_2 b_2 + \mathbf{c}_{MWF,1} A_1 (b_1 - \tilde{b}_1) + n_2$. By averaging over the two possible values that can be taken on by $b_1 - \tilde{b}_1$, the $P_e$ can be written as

$$P_{e,2} = (1 - P_1) Q(A_2/\sigma) + \frac{P_1}{2}[Q(\frac{\epsilon_1}{\sigma}) + Q(\frac{\epsilon_2}{\sigma})]. \tag{15}$$

where $\epsilon_1 = A_2 - 2\mathbf{c}_{MWF,1} A_1$ and $\epsilon_2 = A_2 + 2\mathbf{c}_{MWF,1} A_1$. To test the validity of this expression, a synchronous CDMA system with Gold codes of length $N = 31$ is assumed. The number of users again is $K = 2$, the rank of the MWF is $D = 5$, the multipath channel has $L = 5$ taps, and the power difference between the two users is $\Delta P = 1$ dB. The BER and $P_e$ are plotted as a function of the SNR in Figure 4 below. Performance of the PIC is evaluated using a similar two-user system; however, now the powers of the two users are set to 0 dB. This result is also shown in Figure 4. Note, in both cases, there is excellent agreement between the two models.

## 7. NUMERICAL RESULTS

We compare performance gains of the joint MWF SIC/PIC over conventional SIC/PIC, MMSE, and RAKE. Gold codes of length 31 are assumed with a multipath delay spread of $L = 5$, $K = 20$ users, and rank $D = 5$. A plot of $E_b/N_0$ versus BER for the SIC is shown in Figure 5. We assume that the power difference among the users, from one user to the next, is 1 dB. This means that the strongest user can be as much as 19 dB above the weakest (since $K = 20$). The BER is computed for the *weakest* user, so that the average BER over all users would be significantly better. Note that in the range of $10^{-3}$ to $10^{-5}$ BER, the MWF IS/SIC gives a performance gain of 2-4 dB over the conventional SIC and MMSE. Note also that the conventional SIC performs poorly due to the fact that the conventional matched filter is interference limited. Thus, low bit error rates cannot be achieved. Performance of the MWF/SIC at $D = 12$ can improve by about 1 dB over $D = 5$. A plot of $E_b/N_0$ versus BER is shown for the PIC in Figure 6 for the same system as above, but now with equal power users and $D = 8$. Performance gains of $2-4$ dB are observed at high $E_b/N_0$. Performance suffers at low $E_b/N_0$ because high noise levels cause

errors in the first stages to propagate to later stages. Typically, PICs are only used in high SNR environments where error propagation is not a concern. A similar effect is not observed in the SIC, because the highest power users are cancelled first, increasing detection reliability and reducing the number of errors.

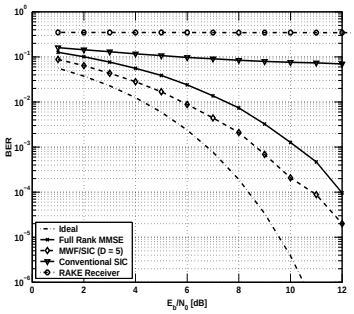


Figure 5: SIC ($K = 20$; $D = 5$)

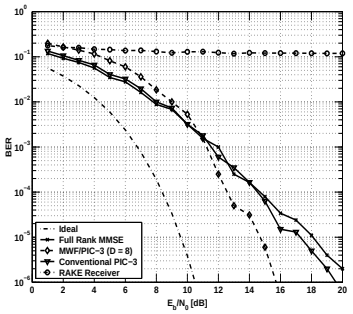


Figure 6: Three-Stage PIC ($K = 20$; $D = 8$)

## 8. CONCLUSION

In this paper, joint reduced rank IS and SIC/PIC schemes are described. These novel IC schemes are implemented by replacing the conventional matched filter at each stage with a reduced rank MMSE receiver, implemented using an efficient CSA structure of the MWF. It is shown via Monte Carlo simulation that for a highly loaded DS-CDMA system, this IS/SIC performs significantly better than the MMSE receiver and the conventional SIC. Performance gains of 2-4 dB are observed at low ranks of only 5 versus full rank of 31.

## 9. ACKNOWLEDGMENTS

We thank Dr. Wilbur Myrick at SAIC and Dr. Michael Zoltowski of Purdue University for valuable suggestions.

## REFERENCES

[1] Duel-Hallen, A., "Decorrelating Decision-Feedback Multiuser Detector for Synchronous Code-Division Multiple Access Channel", *IEEE Transactions on Communications*, Vol. 41, No. 2, pgs. 285-290, Feb. 1993.

[2] Goldstein, J.S., and Reed, I.S., "A New Method of Wiener Filtering and its Application to Interference Mitigation for Communications", *Proceedings of IEEE MILCOM*, Vol. 3, pp. 1087-1091, Monterey, CA, Nov. 1997.

[3] Goldstein, J.S., Reed, I.S., and Scharf, L.L., "A Multistage Representation of the Wiener Filter Based on Orthogonal Projections", in *IEEE Transactions on Information Theory*, Vol. 44, No. 7, Nov. 1998.

[4] Honig, M.L., and Goldstein, J.S., "Adaptive Reduced-Rank Residual Correlation Algorithms for DS-CDMA Interference Suppression", in *Proceedings of Asilomar*, Jul. 1998.

[5] Høst-Madsen, A., and Cho, K., "MMSE/PIC Multiuser Detection for DS/CDMA Systems with Inter- and Intra-Cell Interference", *IEEE Transactions on Communications*, Vol. 47, No. 2, pgs. 291-299, Feb. 1999.

[6] Myrick, W.L., Sud, S., Goldstein, J.S., and Zoltowski, M.D., "MMSE Correlator Based RAKE Receiver for DS-CDMA", To appear in *Proceedings of IEEE MILCOM*, McLean, VA, Oct. 28-31, 2001.

[7] Patel, P., and Holtzman, J., "Analysis of a Simple Successive Interference Cancellation Scheme in a DS/CDMA System", IEEE Journal on Selected Areas in Communications, Vol. 12, No. 5, pgs. 796-807, Jun. 1994.

[8] Ricks, D.C., and Goldstein, J.S. "Efficient Architectures for Implementing Adaptive Algorithms", *Proceedings of the 2000 Antenna Applications Symposium*, pgs. 29-41, Allerton Park, Monticello, Illinois, Sep. 20-22, 2000.

[9] Sud, S., Myrick, W., Goldstein, J.S., and Zoltowski, M.D., "A Reduced Rank MMSE Receiver for a DS-CDMA System in Frequency Selective Multipath", To appear in *Proceedings of IEEE MILCOM*, McLean, VA, Oct. 28-31, 2001.

[10] Sud, S., Myrick, W., Goldstein, J.S., and Zoltowski, M.D., "Performance Analysis of a Reduced Rank MMSE MUD for DS-CDMA", To appear in *Proceedings of IEEE Globecom*, San Antonio, TX, Nov. 25-29, 2001.

[11] Varanasi, M.K., and Aazhang, B., "Multistage Detection in Asynchronous Code-Division Multiple-Access Communications", *IEEE Transactions on Communications*, Vol. 38, No. 4, pgs. 509-519, Apr. 1990.

# A LOW COMPLEXITY MMSE MULTIUSER DETECTOR FOR DS-CDMA

*Seema Sud, Wilbur Myrick, Paula Cifuentes, J. Scott Goldstein*

Science Applications International Corporation
4001 Fairfax Dr., Suite 675
Arlington, VA 22203-1303, USA

*Michael D. Zoltowski*

Dept. of Electrical and Computer Engineering
Purdue University
West Lafayette, IN 47907-1285, USA

## ABSTRACT

*A novel, low complexity, reduced rank multiuser detector (MUD) for DS-CDMA is presented. The solution is derived for the general case of an asynchronous DS-CDMA system in frequency selective multipath. The joint MUD solution is shown to be equivalent to a bank of parallel, single user detectors, previously shown only for synchronous users. The algorithm is implemented in low complexity form using the efficient correlations subtractive architecture of the reduced rank multistage Wiener filter (CSA-MWF). The reduced rank algorithm is not based on an eigen-decomposition, which requires the signal subspace rank to be greater than or equal to the number of signals present in the system, and is shown to be nearly independent on the number of signals. It is shown that the joint and parallel CSA-MWF implementations perform identically to the full rank MMSE MUD and approaches single user, full rank performance at significantly reduced ranks. Bit error rate (BER) performance as a function of rank, signal-to-noise ratio, number of users, code type, and synchronism among the codes is analyzed.*

## 1. INTRODUCTION

Systems employing code division multiple access (CDMA) are typically interference limited. The interference arises from the very nature of the systems, which must often accommodate multiple users transmitting simultaneously via a common physical channel. This is due to the non-orthogonal multiplexing of signals that results from multipath induced by the channel, causing intersymbol interference (ISI). Interference can also arise from multiple users sharing a common bandwidth for different services, such as voice and data transmission. On the forward link, the goal of the handset is to suppress the interference introduced by the other users and extract only the information intended for that user. For the reverse link, however, the base station must demodulate and detect the signals transmitted by all the users. This falls under the topic of multiuser detection (MUD). For the high speed voice and data applications proposed for the third generation (3G) systems, adaptive, low complexity, reduced rank MUD is highly desirable.

In this paper, we present the minimum mean-square error (MMSE) MUD solution for signal detection in the presence of multipath. We show that implementation of this solution using the correlations subtractive architecture of the multistage Wiener filter (MWF) ( [1], [2], [3], [11]) can be implemented as a joint structure or as a bank of parallel filters. Performance is shown to meet or *exceed* MMSE performance at a low rank. We also compare the full rank MUD to other MUD receivers presented in the recent literature. We show via simulation results that the new reduced rank MUD performs as well as the full rank MUD for both synchronous and asynchronous users in multipath and for all levels of signal-to-noise ($E_b/N_0$) and system loads. We begin by describing the general asynchronous DS-CDMA system model.

## 2. CDMA SIGNAL MODEL

We assume a DS-CDMA system, in which we have $K$ users and develop a model for asynchronous transmission. The notation used here is similar to that used by Honig, et. al., in [5] and [7]. User $k$ transmits a baseband signal given by

$$x_k(t) = \sum_i A_k b_k(i) s_k(t - iT - \tau_k), \tag{1}$$

where $b_k(i)$ is the symbol transmitted by user $k$ at time $i$, $s_k(t)$ is the spreading code associated with user $k$, and $A_k$ and $\tau_k$ are the amplitude and delay, assumed to be real valued, respectively. We assume binary signaling, so that the symbols $b_k(i) \in$ (-1,+1). We also assume that the bits are independent and identically distributed. The spreading sequence can be written as

$$s_k(t) = \sum_{i=1}^{N-1} a_k[i] \Psi(t - iT_c), \tag{2}$$

where $a_k[i] \in (\frac{+1}{\sqrt{N}}, \frac{-1}{\sqrt{N}})$ is a normalization factor for the spreading code. The processing gain of the CDMA system, or equivalently the bandwidth spreading factor, is given by $N = \frac{T}{T_c}$. Here, $T_c$ is the chip period, and $T$ is the symbol period. We assume that the spreading code is a square wave sequence with no pulse shaping, so that the chip sequence $\Psi(t)$ is a constant.

Define the sampled transmitted signal $\mathbf{y}(i)$ as the N-vector composed of asynchronous combinations of the data for each user multiplied with its respective spreading sequence. Assume also, without loss of generality, that the receiver has timing information to synchronize to the spreading code of any user. The transmitted signal may then be written in the form

$$\mathbf{y}(i) = \sum_{k=1}^{K} A_k [b_k(i) \mathbf{s}_\mathbf{k}^+ + b_k(i-1) \mathbf{s}_\mathbf{k}^-]. \tag{3}$$

Here, $\mathbf{s_k}^+$ and $\mathbf{s_k}^-$ are the $N \times 1$ vectors of spreading codes associated with user $k$, where $k = 1, 2, ..., K$. In the case of asynchronous transmission, as is inherent to the reverse link of a cellular system, both the current bit of user $k$, denoted $b_k(i)$, and the previous bit of user $k$, denoted $b_k(i-1)$, multiplied with their respective portions of the spreading code, are interfering with the current bit of user 1. For synchronous users, $\mathbf{s_k}^+$ is equal to $\mathbf{s_k}$ and $\mathbf{s_k}^-$ is zero. To simplify the notation and to make the mathematical analysis easier, we rewrite Eq. (3) in matrix form as

$$\mathbf{y}(i) = \mathbf{S}^+\mathbf{A}\mathbf{b}(i) + \mathbf{S}^-\mathbf{A}\mathbf{b}(i-1), \tag{4}$$

where $\mathbf{S}^+ = (\mathbf{s_1}^+ \ \mathbf{s_2}^+ \ ... \ \mathbf{s_K}^+)$, $\mathbf{A} = diag(A_1, A_2, ..., A_K)$, and $\mathbf{b}(i) = (b_1(i), b_2(i), ..., b_K(i))^T$. We would like to extract the desired information, i.e., the bits transmitted by all the users, $\mathbf{b}(i)$, while suppressing the interference due to the asynchronous transmission and multipath. Thus, we turn our attention to the linear multiuser detection technique presented next.

## 3. REDUCED RANK MUD BASED ON CSA-MWF

In this section, we present the derivation of the MUD solution for asynchronous users in multipath and show how it can be implemented using the CSA-MWF.

### 3.1. MUD Derivation

Consider the case of a multipath channel, modeled in discrete time by an L-tap tapped-delay line whose coefficients are represented by $\mathbf{h} = [h_1, h_2, ..., h_L]$. The parameter L, when viewed in units of time, is known as the delay spread of the channel and is typically on the order of 5 to 10 microseconds for a cellular system. The received vector can be written as

$$\hat{\mathbf{r}}(i) = \hat{\mathbf{y}}(i) + \mathbf{n}(i), \tag{5}$$

where $\hat{\mathbf{y}}(i) = \mathbf{y}(i) * \mathbf{h}$, $*$ denotes convolution, and $\mathbf{n}(i)$ are samples of an additive white Gaussian noise (AWGN) process. Note that in an AWGN channel, this reduces to $\mathbf{r}(i) = \mathbf{y}(i) + \mathbf{n}(i)$. Substituting for $\mathbf{y}$ using Eq. (4), we can write the received signal explicitly as

$$\hat{\mathbf{r}}(i) = \hat{\mathbf{S}}^+\mathbf{A}\mathbf{b}(i) + \hat{\mathbf{S}}^-\mathbf{A}\mathbf{b}(i-1) + \mathbf{n}(i), \tag{6}$$

where $\hat{(\cdot)}$ denotes convolution of the operand with the channel vector $\mathbf{h}$. In this paper, we assume the channel vector is known, or that it can be estimated by some means. For the single user (SU) MMSE receiver, we choose the receiver filter coefficients, denoted in vector form by $\hat{\mathbf{c}}$, to minimize the mean-square error (MSE) between the transmitted bit of the desired user and its estimate. Assuming without loss of generality that user one is the user of interest, this is given by

$$MSE_{SU} = E[|b_1(i) - \hat{\mathbf{c}}^H\hat{\mathbf{r}}(i)|^2], \tag{7}$$

where $E[\cdot]$ denotes the expected value operator and $(\cdot)^H$ represents the Hermitian transpose operator. The MMSE solution in the presence of multipath is given by

$$\hat{\mathbf{c}}_{MMSE} = \hat{\mathbf{R}}^{-1}\hat{\mathbf{s}}_\mathbf{1} = E[\hat{\mathbf{r}}\hat{\mathbf{r}}^H]^{-1}\hat{\mathbf{s}}_\mathbf{1}, \tag{8}$$

where $\hat{\mathbf{R}}$ is the well-known covariance matrix and is given by $E[\hat{\mathbf{r}}(i)\hat{\mathbf{r}}(i)^H]$. Note that the RAKE solution, which only incorporates the effects of the multipath and neglects the interference induced by the other users, can be written simply as

$$\mathbf{c}_{RAKE} = \hat{\mathbf{s}}_\mathbf{1}. \tag{9}$$

In the presence of only AWGN, this reduces further to the matched filter (MF) solution, $\mathbf{c}_{MF} = \mathbf{s_1}$.

Now, for the MUD problem, we must choose the receiver filter coefficients, denoted in matrix form by $\hat{\mathbf{C}}$, to minimize the MSE between the vector of transmitted bits, $\mathbf{b}(i) = (b_1(i)\ b_2(i)\ ...\ b_K(i))$ and their estimates. This can be written as

$$MSE_{MUD} = E[||\mathbf{b}(i) - \hat{\mathbf{C}}^H\hat{\mathbf{r}}(i)||^2]. \tag{10}$$

To obtain the MMSE solution, we minimize the above quantity. First, using the identity $||\mathbf{x}||^2 = trace(\mathbf{x}, \mathbf{x}^H)$ we write

$$\min_{\hat{\mathbf{C}}} E[trace((\mathbf{b}(i) - \hat{\mathbf{C}}^H\hat{\mathbf{r}}(i))(\mathbf{b}(i) - \hat{\mathbf{C}}^H\hat{\mathbf{r}}(i))^H)]. \tag{11}$$

Since the trace of the covariance of a vector quantity is always non-negative, we can ignore the trace operation. Expanding the quantity in brackets, we obtain

$$\min_{\hat{\mathbf{C}}} E[\mathbf{b}(i)\mathbf{b}(i)^H - \mathbf{b}(i)\hat{\mathbf{r}}(i)^H\hat{\mathbf{C}} - \hat{\mathbf{C}}^H\hat{\mathbf{r}}(i)\mathbf{b}(i)^H - \hat{\mathbf{C}}^H\hat{\mathbf{r}}\hat{\mathbf{r}}^H\hat{\mathbf{C}}]. \tag{12}$$

Next, from the linearity property of the $E[\cdot]$ operation, consider separately each of the terms in the brackets:

- $E[\mathbf{b}(i)\mathbf{b}(i)^H] = \mathbf{I}$
- $E[\mathbf{b}(i)\hat{\mathbf{r}}(i)^H\hat{\mathbf{C}}]$
  $= E[\mathbf{b}(i)(\mathbf{b}(i)^H\mathbf{A}\hat{\mathbf{S}}^{+H} + \mathbf{b}(i-1)^H\mathbf{A}\hat{\mathbf{S}}^{-H} + \mathbf{n}(i))]\hat{\mathbf{C}}$
  $= \mathbf{A}\hat{\mathbf{S}}^{+H}\hat{\mathbf{C}}$
- $E[\hat{\mathbf{C}}^H\hat{\mathbf{r}}(i)\mathbf{b}(i)^H]$
  $= \hat{\mathbf{C}}^H E[(\hat{\mathbf{S}}^+\mathbf{A}\mathbf{b}(i) + \hat{\mathbf{S}}^-\mathbf{A}\mathbf{b}(i-1) + \mathbf{n}(i))\mathbf{b}(i)^H]$
  $= \hat{\mathbf{C}}^H\hat{\mathbf{S}}^+\mathbf{A}$
- $E[\hat{\mathbf{C}}^H\hat{\mathbf{r}}\hat{\mathbf{r}}^H\hat{\mathbf{C}}] = \hat{\mathbf{C}}^H E[\hat{\mathbf{r}}\hat{\mathbf{r}}^H]\hat{\mathbf{C}} = \hat{\mathbf{C}}^H\hat{\mathbf{R}}\hat{\mathbf{C}}$.

In the second and third expressions above, we have used the fact that $\mathbf{b}(i)$ and $\mathbf{b}(i-1)$ are independent, identically distributed random variables so that their expected value is zero. We have also used the fact that $\mathbf{A}$ is a real, diagonal matrix so that $\mathbf{A}^H = \mathbf{A}$. Furthermore, since the noise $\mathbf{n}(i)$ is AWGN, its samples are uncorrelated with the data, so the expected value of their product is zero. Finally, we used the definition of the covariance matrix $\hat{\mathbf{R}}$ from Eq. (8) in the last term. Substituting these expressions into Eq. (12), we can write the MSE as

$$\min_{\hat{\mathbf{C}}}[\mathbf{I} - \mathbf{A}\hat{\mathbf{S}}^{+H}\hat{\mathbf{C}} - \hat{\mathbf{C}}^H\hat{\mathbf{S}}^+\mathbf{A} + \hat{\mathbf{C}}^H\hat{\mathbf{R}}\hat{\mathbf{C}}]. \tag{13}$$

To solve Eq. (13), we take its gradient with respect to the minimization parameter $\hat{\mathbf{C}}$ and set the result equal to zero. This yields

$$-\mathbf{A}\hat{\mathbf{S}}^{+H} - \mathbf{A}\hat{\mathbf{S}}^{+H} + \hat{\mathbf{C}}^H\hat{\mathbf{R}}^H + \hat{\mathbf{C}}^H\hat{\mathbf{R}} = \mathbf{0}. \tag{14}$$

Now, using the property that the covariance matrix of a stationary discrete time random process is Hermitian, or $\hat{\mathbf{R}}^H$=$\hat{\mathbf{R}}$ (see e.g. [4], p. 101), the final solution is easily obtained, and is given by

$$\hat{\mathbf{C}}_{\mathbf{MMSE}} = \hat{\mathbf{R}}^{-1}\hat{\mathbf{S}}^{+}\mathbf{A}. \quad (15)$$

Before proceeding to the implementation of this solution, we pause to make a few observations. First, note that we can write the solution for the $k^{th}$ user individually by simply extracting the $k^{th}$ columns of $\hat{\mathbf{S}}^{+}$ and of $\mathbf{A}$. That is, we can write the MUD solution as

$$\hat{\mathbf{C}}_{\mathbf{MMSE}} = [\hat{\mathbf{c}}_{\mathbf{1/MMSE}},\ \hat{\mathbf{c}}_{\mathbf{2/MMSE}},\ ...,\ \hat{\mathbf{c}}_{\mathbf{K/MMSE}}], \quad (16)$$

where

$$\hat{\mathbf{c}}_{\mathbf{k/MMSE}} = \hat{\mathbf{R}}^{-1}\hat{\mathbf{s}}^{+}_{\mathbf{k}}A_k \quad (17)$$

for the $k^{th}$ user. Thus, the matrix form of the MUD solution can be implemented in joint matrix or vector form using parallel single user detectors. This agrees with the analysis presented in [8] for synchronous users. Note the similarity between the MUD solution in Eqs. (15) and (17) and the single user solution given in Eq. (8). Second, note that the synchronous solution is obtained by setting $\hat{\mathbf{S}}^{+} = \hat{\mathbf{S}}$ or setting $\hat{\mathbf{s}}^{+}_{\mathbf{k}} = \hat{\mathbf{s}}_{\mathbf{k}}$ in Eqs. (15)and (17), respectively. Furthermore, observe that the covariance matrix, if expanded in terms of the received signal $\hat{\mathbf{r}}(i)$ in Eq. (6), is given as

$$\hat{\mathbf{R}} = \hat{\mathbf{S}}^{+}\mathbf{A}^2\hat{\mathbf{S}}^{+H} + \hat{\mathbf{S}}^{-}\mathbf{A}^2\hat{\mathbf{S}}^{-H} + \sigma^2\mathbf{I}. \quad (18)$$

Even though in the presence of multipath, $\hat{\mathbf{S}}^{+}$ and $\hat{\mathbf{S}}^{-}$ are not orthogonal, the independence of the data bits $\mathbf{b}(i)$ and $\mathbf{b}(i-1)$ forces the expectation of the cross-terms to zero. This equation is similar to Eq. (10) of [5], which is shown for the AWGN case.

### 3.2. Implementation of MUD Using the CSA-MWF

From Eqs. (15) or (17), we see that computation of the MMSE solution requires inversion of the $N \times N$ covariance matrix $\hat{\mathbf{R}}$, which can be quite computationally intense and may not even be possible in real-time for a high data rate system. Also, if the channel or signals are changing in time, then the sample covariance matrix estimated from the data does not depict the true non-stationary signal environment. Thus, it is desirable to find alternate solutions that approach, or exceed, the performance of the MMSE receiver but require much fewer computations and can adapt rapidly. The multistage Wiener filter ([1], [2], and [3]) is a pioneering breakthrough in reduced rank algorithms in that it meets or exceeds MMSE performance but does not require any matrix inversions nor computationally complex eigen-decompositions. By contrast, in an eigen-decomposition, if the subspace rank is less than the number of signals (users) present, i.e. $D < K$, then performance can degrade quite rapidly as the number of users increases. This is a common occurrence is cellular CDMA systems, because the number of users may be continuously changing. Intuitively speaking, the MWF achieves faster convergence *and* reduced computation by applying the information inherently contained in both the covariance matrix and the cross-correlation vector in choosing the reduced-dimension subspace that the weight vector is constrained to lie within. Another benefit of the MWF is that it can operate in critical low-sample support operational environments where other adaptive algorithms fail. In other words, the ability for rapid adaptation is matched by a lower requirement for training data to estimate the statistics.

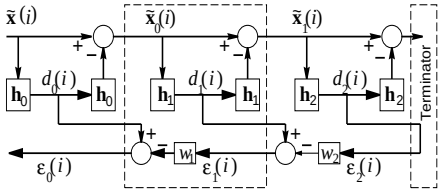


Figure 1: CSA-MWF (D=2 stages)

The MWF structure is obtained by performing successive decompositions based on maximizing the cross-correlation between the desired signal and the observed signal. This results in two subspaces, one in the direction of the cross-correlation and one orthogonal to it. Note that this approach naturally creates signal subspaces at successive stages that are orthogonal to those of the previous stage. The multistage structure is obtained by repeated correlations of the signal that lies in the orthogonal subspace at the previous stage and thus is often termed the residual correlation algorithm ([5]).

The single user multistage decomposition of the Wiener filter for $D = 2$ stages is shown in Fig. 1. This is a new structure of the multistage Wiener filter, based on a correlation-subtraction architecture (or CSA-MWF) as first described by Ricks, et. al., in [11]. For the multipath channel, we simply set $\mathbf{h_0} = \hat{\mathbf{s}}_{\mathbf{1}}$, the spreading code of the desired user convolved with the channel. Then, $d_0(i) = \hat{\mathbf{s}}_1^H\tilde{\mathbf{x}}(i)$, where $\tilde{\mathbf{x}}(i)$ is the input signal, equal to $\hat{\mathbf{r}}(i)$. Note that $d_0(i)$ is simply the matched filter solution matched to the code and the channel. The filter in Fig. 1 demonstrates the low complexity of this implementation of the MWF and the fact that the computation of signal blocking matrices are no longer necessary for any subspace partitioning such as that required for constrained adaptation. The forward recursion equations, presented below, are identical to those used to implement the block residual correlation algorithm ([3] and [5]) but without computation of the blocking matrices.

- *Initialization:* $d_0(i)$ and $\tilde{\mathbf{x}}(i)$
- *Forward Recursion:* For $j = 1, 2, ..., D$:

$$\begin{aligned} \mathbf{h}_j &= \frac{\sum_\Omega\{d^*_{j-1}(i)\mathbf{x}_{j-1}(i)\}}{||\sum_\Omega\{d^*_{j-1}(i)\mathbf{x}_{j-1}(i)\}||} \\ d_j(i) &= \mathbf{h}_j^H\mathbf{x}_{j-1}(i) \\ \mathbf{x}_j(i) &= \mathbf{x}_{j-1}(i) - \mathbf{h}_j d_j(i) \end{aligned}$$

- *Backward Recursion:* For $j = D, D-1, ..., 1$, with $e_D(i) = d_D(i)$:

$$\begin{aligned} w_j &= \frac{\sum_\Omega \{d^*_{j-1}(i) e_j(i)\}}{\sum_\Omega \{|e_j(i)|^2\}} \\ e_{j-1}(i) &= d_{j-1}(i) - w^*_j e_j(i) \end{aligned}$$

where $\Omega$ denotes the region of sample support used to compute the sample statistics and $D$ is the number of stages, i.e. the rank, of the filter. Performance results of the multistage Wiener filter for asynchronous CDMA in AWGN can be found in [5].

For the MUD problem, the solution of Eqs. (15) or (17) show that the MUD implementation can be obtained in matrix form ($\mathbf{H_0}$) or vector form ($\mathbf{h}_{0,k}$) by replacing the initialization step of the recursion equations with

$$\mathbf{H}_0 = \hat{\mathbf{S}}^+ \; ; \; \mathbf{d}_0 = \hat{\mathbf{S}}^{+H} \tilde{\mathbf{x}}(i) \tag{19}$$

and

$$\mathbf{h}_{0,k} = \hat{\mathbf{s}}^+_{\mathbf{k}} \; ; \; d_{0,k} = \hat{\mathbf{s}}^{+H}_{\mathbf{k}} \tilde{\mathbf{x}}(i), \tag{20}$$

where in Eq. (20) an additional subscript $k$ has been added to indicate that the recursions are now performed separately for each user $k$. That is, we employ a bank of parallel Wiener filters operating in a reduced rank subspace. Note that the above derivation only suggests the use of a reduced rank scheme to implement the MUD solution in the form of a parallel bank of Wiener filters. It does not state that the rank of the parallel scheme will be equivalent to the rank of the MUD solution. In general, as shown in Section 5, this will not be the case.

## 4. COMPARISON OF REDUCED RANK AND FULL RANK MUD SOLUTIONS

In this section, we compare the new reduced rank MUD solution obtained above to full rank MMSE MUD solutions in the recent literature and discuss and explain the differences between them. In Eq. (9) of [8], the MUD solution is derived for synchronous users and, using the same notation as in the present paper, is given by

$$\hat{\mathbf{C}}_{MMSE} = \hat{\mathbf{S}} (\hat{\mathbf{S}}^H \hat{\mathbf{S}} + \sigma^2 \mathbf{I})^{-1}. \tag{21}$$

It can be shown via the matrix inversion lemma that this solution can also be written as

$$\hat{\mathbf{C}}_{MMSE} = (\hat{\mathbf{S}} \hat{\mathbf{S}}^H + \sigma^2 \mathbf{I})^{-1} \hat{\mathbf{S}}. \tag{22}$$

Comparing our solution in Eq. (15) to Eq. (22), we see that our solution simplifies to this solution for the synchronous AWGN case. Indeed, if we let $\hat{\mathbf{S}}^+ = \hat{\mathbf{S}}$ (and $\hat{\mathbf{S}}^- = \mathbf{0}$) as would be for synchronous users, then the two solutions exactly agree. The amplitude matrix is absent because it is absorbed into the spreading code matrix in Eqs. (21) and (22). The same result is also given in Eq. (15) of [6].

Another full rank MUD solution is presented in [12] (p. 295). Using our notation, and applying the matrix inversion lemma as we did before, we can write this solution as

$$\hat{\mathbf{C}}_{MMSE} = \mathbf{A}^{-1} [(\hat{\mathbf{S}} \hat{\mathbf{S}}^H + \sigma^2 \mathbf{A}^{-2})^{-1} \hat{\mathbf{S}}]. \tag{23}$$

Since $\mathbf{A}$ is a diagonal matrix, we can rewrite the above equation as

$$\hat{\mathbf{C}}_{MMSE} = (\hat{\mathbf{S}} \mathbf{A}^2 \hat{\mathbf{S}}^H + \sigma^2 \mathbf{I})^{-1} \hat{\mathbf{S}} \mathbf{A}. \tag{24}$$

This equation is also derived for synchronous users in AWGN. Now, if we again assume the same conditions for our solution, namely that $\hat{\mathbf{S}}^+ = \hat{\mathbf{S}}$ (and $\hat{\mathbf{S}}^- = \mathbf{0}$) and substitute the value of $\mathbf{R}$ given in Eq. (18) into Eq. (15), we obtain exactly the solution of Eq. (24). Thus, we see that under the same conditions, our MUD solution agrees with the full rank solutions in the literature. However, our solution is more general in that it includes the asynchronous/multipath situation. Furthermore, we emphasize that computation of these full rank solutions is not feasible in practice due to the inability to obtain and/or invert the covariance matrix $\hat{\mathbf{R}}$. Thus, the reduced rank implementation is highly useful.

## 5. NUMERICAL RESULTS

We present results obtained from Monte Carlo simulations to show the validity of the MUD solutions derived above. Hadamard codes or Gold codes with processing gains of $N = 32$ and $N = 31$, respectively, are employed in spreading, and an $L$=5 tap channel is used to simulate the multipath, using one tap per chip. For the Monte Carlo simulations, the data in the CSA-MWF is processed in blocks of $M$ bits, so that the $N \times 1$ vector $\tilde{\mathbf{x}}(i)$ becomes an $N \times M$ matrix $\tilde{\mathbf{X}}(i) = [\tilde{\mathbf{x}}(i) \; \tilde{\mathbf{x}}(i+1) \; ... \; \tilde{\mathbf{x}}(i+M-1)]$ Similarly, the scalar $d_0(i)$ is replaced by an $1 \times M$ vector of bits given by $\mathbf{d_{0,k}}(i) = [b_k(i) \; b_k(i+1) \; ... \; b_k(i+M-1)]$. Typically $M \geq 2N$ data bits are required for reliable processing according to the RMB rule (named for Reed, Mallett, and Brennan who first proved it in [9]). Then, estimates are also produced one block at a time and are given by $\hat{\mathbf{b}}_{\mathbf{k}}(i) = \epsilon_{\mathbf{0,k}}(i)$ for user $k$ in blind mode. The number of bits per block is $M = 1000$, and the number of blocks is at least 25 (chosen to produce enough errors to obtain a valid statistical bit error rate estimate).

In the first two plots, the joint (matrix) MUD and the parallel (vector) MUD are compared. The full rank MMSE solution employing the covariance matrix inversion is labeled accordingly. Fig. 2 shows a plot of rank of the multistage Wiener filter versus the bit error rate (BER) for synchronous users. The powers of some of the users are randomly set up to 4 dB above the others to simulate a near-far scenario. The variation in BER for the MMSE and RAKE methods is due to the nature of the Monte Carlo simulation, since their performance is independent of rank. Note that the matrix MUD obtains full rank performance at a rank of only one, by employing knowledge of all the users' spreading codes. This is an astounding result that shows for MMSE performance, all that is required is a matched filter and a matrix-vector multiplication. For a rank as low as three, the vector MWF converges to the matrix MUD solution and maintains this

performance as rank increases. The performance of the vector MUD does not substantially degrade even at a rank as low as two, which is significantly less than the processing gain of $N = 32$. Both reduced rank MUD solutions consistently perform better than the RAKE receiver, which cannot combat large numbers of interfering users.

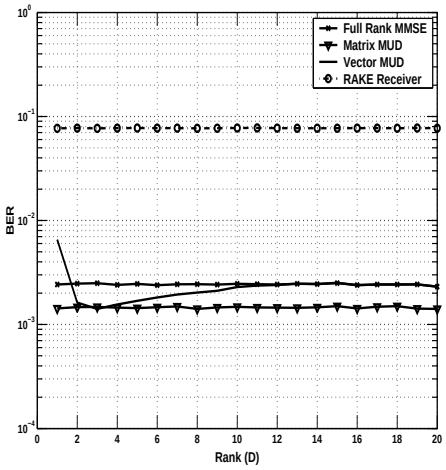


Figure 2: Multiuser Detector (MUD): Rank (D) vs. BER; Synchronous Blind CDMA, $N = 32$ (Hadamard Codes), $E_b/N_0 = 12$ dB, $K = 15$, $L = 5$

Fig. 3 shows a plot of $E_b/N_0$ of the multistage Wiener filter versus the bit error rate (BER) for synchronous users. The matrix MUD has converged at a rank ($D$) of only one, due to the fact that it has knowledge of all the users' spreading codes and can thus determine the signal subspace instantly. In general, the rank at which the matrix MUD converges is a function of the number of users' spreading codes that it has knowledge of (termed the constraint length of the matrix MUD), although it is not a linear relationship. The vector MWF performs as well as the matrix version at a rank of seven. Thus, while performance as a function of rank differs between these two methods, they both perform well at remarkably low ranks. Again, both the vector and matrix MWF dramatically outperform the RAKE receiver.

The next two plots show performance as a function of rank ($D$), number of users ($K$), and the synchronism among the users for the vector MUD implementation. Fig. 4 has rank of the MWF versus the bit error rate (BER) for synchronous, Hadamard codes. We observe that performance exceeds full rank for 5, 10 and 15 users at ranks of about 1, 1, and 2, respectively. Furthermore, the BER converges to the same value in all cases. This is due to the orthogonality property of the Hadamard codes and the ability of the MWF to suppress the orthogonal interference quickly. The performance of the MWF does not degrade except for the 15 user case at rank one, i.e. a one stage filter. The MWF performance meets the full rank MMSE performance as rank increases.

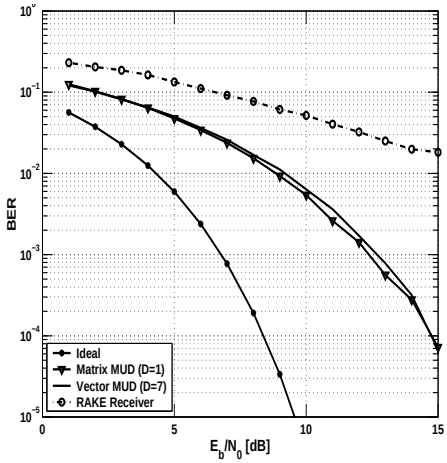


Figure 3: Vector Multiuser Detector (MUD): $E_b/N_0$ vs. BER; Synchronous Blind CDMA, $N = 32$ (Hadamard Codes), $K = 12$, $L = 5$, $\Delta P = 0$ dB

Fig. 5 shows a plot of rank (D) versus BER with 5, 10 and 15 asynchronous users employing Gold codes for spreading. In this case, convergence of BER is seen at ranks of only 1, 3, and 4. This is a tremendous improvement over other reduced rank techniques such as the eigenvector based principal components, which would require a rank greater than or equal to the number of users present. Note that the BER degrades as more users are added to the system. While Gold codes have good cross-correlation properties, there still exists some maximum level of correlation among them, and this effect is enhanced by the imperfect orthogonality. Nevertheless, the advantage of the reduced rank MWF in terms of performance and rank reduction is evident.

## 6. CONCLUSION

In this paper, we present a formulation for the MMSE MUD receiver for a general asynchronous DS-CDMA in a frequency selective multipath channel. We show how to implement the MUD solution using the reduced rank multistage Wiener filter both in vector form as a bank of single user detectors and joint matrix form. The parallel implementation is shown to be equivalent to the joint MUD solution in terms of performance. The reduced rank solution is compared to existing full rank solutions to assess its validity. BER performance is evaluated as a function of rank and $E_b/N_0$ via Monte Carlo simulations for a highly loaded DS-CDMA system distorted by multipath. The performance of the reduced rank vector and matrix MUD solutions are compared to the standard, full rank MMSE receiver. It is demonstrated that the reduced rank MUD performs as well as the single user, full rank MUD MMSE solutions at a much lower rank, both in vector and in matrix form. This allows the design in low complexity, high speed receivers.

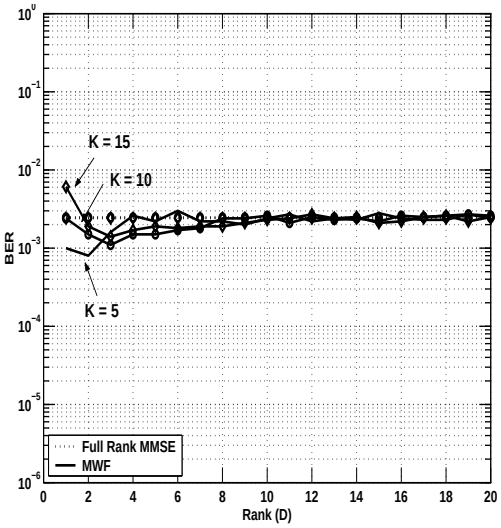


Figure 4: Vector Multiuser Detector (MUD): Rank (D) vs. BER; Synchronous Blind CDMA, $N = 32$ (Hadamard Codes), $E_b/N_0 = 12$ dB, $L = 5$, $\Delta P = 0$ dB

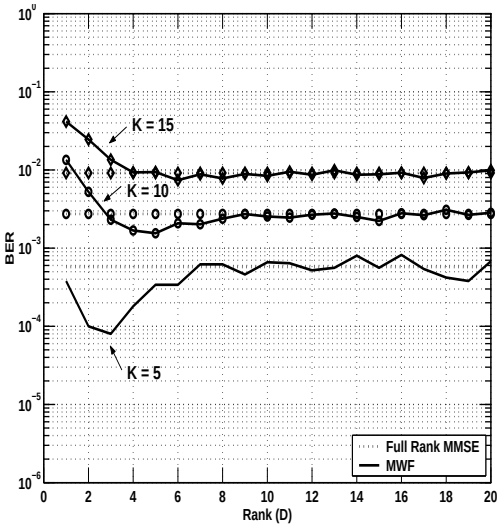


Figure 5: Multiuser Detector (MUD): Rank (D) vs. BER; Asynchronous Blind CDMA, $N = 31$ (Gold Codes), $E_b/N_0 = 12$ dB, $L = 5$, $\Delta P = 0$ dB

## 7. ACKNOWLEDGMENTS

We gratefully thank Professors Michael Honig of Northwestern University and Irving Reed of the University of Southern California for many fruitful conversations during this effort. We also thank Steven Huang for his expertise.

## REFERENCES

[1] Goldstein, J.S., and Reed, I.S., "Multidimensional Wiener Filtering Using a Nested Chain of Orthogonal Scalar Wiener Filters", University of Southern California, Dec. 1996, CSI-96-12-04.

[2] Goldstein, J.S., and Reed, I.S., "A New Method of Wiener Filtering and its Application to Interference Mitigation for Communications", *Proceedings of IEEE MILCOM*, Vol. 3, pp. 1087-1091, Monterey, CA, Nov. 1997.

[3] Goldstein, J.S., Reed, I.S., and Scharf, L.L., "A Multistage Representation of the Wiener Filter Based on Orthogonal Projections", in *IEEE Transactions on Information Theory*, Vol. 44, No. 7, Nov. 1998.

[4] Haykin, S., "Adaptive Filter Theory", Third Edition, Prentice Hall, New Jersey, 1996.

[5] Honig, M.L., and Goldstein, J.S., "Adaptive Reduced-Rank Residual Correlation Algorithms for DS-CDMA Interference Suppression", in *Proceedings of Asilomar*, Jul. 1998.

[6] Honig, M.L., Madhow, U., and Verdu, S., "Blind Adaptive Multiuser Detection", in *IEEE Transactions on Information Theory*, Vol. 41, No. 4, Jul. 1995.

[7] Honig, M.L., and Poor, H.V., Adaptive Interference Suppression. In Poor, H.V., and Wornell, G.W., editors, "Wireless Communications: Signal Processing Perspectives", Prentice Hall: Englewood Cliffs, New Jersey, pgs. 64-102, 1998.

[8] Honig, M.L., and Tsatsanis, M.K., "Adaptive Techniques for Multiuser CDMA Receivers", in *IEEE Transactions on Signal Processing*, Vol. 17, No. 3, pgs. 49-61, May 2000.

[9] Reed, I.S., Mallett, J.D., and Brennan, L.E., "Rapid Convergence Rate in Adaptive Arrays", *IEEE Transactions on Aerospace and Electronic Systems*, Vol. 10, pgs. 853-863, Nov. 1974.

[10] Rice, G.W., Garcia-Alis, D., Stirling, I.G., Weiss, S., Stewart, R.W., "An Adaptive MMSE RAKE Receiver", in *Proceedings of Asilomar*, 2000.

[11] Ricks, D.C., and Goldstein, J.S. "Efficient Architectures for Implementing Adaptive Algorithms", *Proceedings of the 2000 Antenna Applications Symposium*, pgs. 29-41, Allerton Park, Monticello, Illinois, Sep. 20-22, 2000.

[12] Verdu, S., "Multiuser Detection", Cambridge University Press, 1998.

# Performance Analysis of a Reduced Rank MMSE MUD for DS-CDMA

Seema Sud, Wilbur L. Myrick, J. Scott Goldstein
Science Applications International Corporation
4001 Fairfax Dr., Suite 675
Arlington, VA 22203-1303, USA

Michael D. Zoltowski
Department of Electrical and Computer Engineering
Purdue University
West Lafayette, IN 47907-1285, USA

*Abstract*— **A new reduced rank multiuser detector (MUD) for DS-CDMA is presented. The algorithm is derived for the general case of an asynchronous DS-CDMA system in frequency selective multipath. The MUD solution is shown to be equivalent to a bank of parallel, single user detectors. The algorithm is implemented in reduced rank form using the correlations subtractive algorithm of the multistage Wiener filter (CSA-MWF). It is shown that the CSA-MWF implementation performs identically to the full rank solutions of MMSE MUD and meets single user, full rank performance at a substantially reduced rank for all levels of system load.**

## I. Introduction

Systems employing code division multiple access (CDMA) are typically interference limited. The interference arises from the very nature of the systems, which must often accommodate multiple users transmitting simultaneously via a common physical channel. This is due to the non-orthogonal multiplexing of signals that results from multipath induced by the channel, causing intersymbol interference (ISI). Interference can also arise from multiple users sharing a common bandwidth for different services, such as voice and data transmission. On the forward link, the goal of the handset is to suppress the interference introduced by the other users and extract only the information intended for that user. For the reverse link, however, the base station must demodulate and detect the signals transmitted by all the users. This falls under the topic of multiuser detection (MUD). For the high speed voice and data applications proposed for the third generation (3G) systems, adaptive, reduced rank MUD is highly desirable.

In this paper, we present the minimum mean-square error (MMSE) MUD solution for signal detection in the presence of multipath. We show that implementation of this solution using the CSA structure of the multistage Wiener filter (MWF) ([1], [2], [3], and [10]) meets MMSE performance at a low rank. We show via simulation results that the new reduced rank MUD performs as well as the full rank MUD in both the synchronous and asynchronous multipath case. We begin by describing the general asynchronous DS-CDMA system model.

## II. CDMA Signal Model

We assume a DS-CDMA system, in which we have $K$ users and develop a model for asynchronous users. The notation used here is similar to that used by Honig, et. al., in [5] and [6]. User $k$ transmits a baseband signal given by

$$x_k(t) = \sum_i A_k b_k(i) s_k(t - iT - \tau_k), \tag{1}$$

where $b_k(i)$ is the symbol transmitted by user $k$ at time $i$, $s_k(t)$ is the spreading code associated with user $k$, and $A_k$ and $\tau_k$ are the real valued amplitude and delay, respectively. We assume binary data, so that the symbols $b_k(i) \in$ (-1,+1) and that the bits are independent, identically distributed. We further assume that the spreading code is a square wave sequence with no pulse shaping and write

$$s_k(t) = \sum_{i=1}^{N-1} a_k[i]\Psi(t - iT_c), \tag{2}$$

where $a_k[i] \in (\frac{+1}{\sqrt{N}}, \frac{-1}{\sqrt{N}})$ is a normalization factor and $\Psi(t)$ is a constant. The processing gain of the CDMA system, or equivalently the bandwidth spreading factor, is given by $N = \frac{T}{T_c}$. Here, $T_c$ is the chip period, and $T$ is the symbol period.

Define the sampled transmitted signal $\mathbf{y(i)}$ as the $N \times 1$ vector composed of asynchronous combinations of the data for each user multiplied with its respective spreading sequence. Assume also, without loss of generality, that the receiver has timing information to synchronize to the spreading code of any user. The transmitted signal may then be written in the form

$$\mathbf{y(i)} = \sum_{\mathbf{k=1}}^{\mathbf{K}} \mathbf{A_k}[\mathbf{b_k(i)s_k^+ + b_k(i-1)s_k^-}]. \tag{3}$$

Here, $\mathbf{s_k^+}$ and $\mathbf{s_k^-}$ are the $N \times K$ matrices of spreading codes associated with the $K$ users. In the case of asynchronous transmission, as is inherent to the reverse link of a cellular system, both the current bit of user $k$, denoted $b_k(i)$, and the previous bit of user $k$, denoted $b_k(i-1)$, multiplied with their respective portions of the spreading code, interfere with the current bit of all other users $b_j(i)$, $j \neq k$. For synchronous users, $\mathbf{s_k^+}$ is equal to $\mathbf{s_k}$ and $\mathbf{s_k^-}$ is zero. To simplify the notation and to make the mathematical analysis easier, we rewrite Eq. (3) in matrix form as

$$\mathbf{y(i)} = \mathbf{S^+Ab(i)} + \mathbf{S^-Ab(i-1)}, \tag{4}$$

where $\mathbf{S^+} = [\mathbf{s_1^+}, \mathbf{s_2^+}, ..., \mathbf{s_K^+}]$, $\mathbf{S^-} = [\mathbf{s_1^-}, \mathbf{s_2^-}, ..., \mathbf{s_K^-}]$, $\mathbf{A} = \mathbf{diag}[\mathbf{A_1}, \mathbf{A_2}, ..., \mathbf{A_K}]$, and $\mathbf{b(i)} = [\mathbf{b_1(i)}, \mathbf{b_2(i)}, ..., \mathbf{b_K(i)}]^\mathbf{T}$. We would like to extract the desired information, i.e., the bits transmitted by all the users, $\mathbf{b(i)}$, while suppressing the interference due to the asynchronous transmission. Thus, we turn our attention to the linear multiuser detection technique presented next.

## III. CSA-MWF Based Reduced Rank MUD

In this section, we present the derivation of the MUD solution for asynchronous users in multipath and show how it can be implemented using the CSA-MWF.

### A. MUD Solution

Consider a multipath channel, modeled in discrete time by an L-tap tapped-delay line whose coefficients are represented by $\mathbf{h} = [\mathbf{h_1}, \mathbf{h_2}, ..., \mathbf{h_L}]$. The parameter L, when viewed in units of time, is known as the delay spread of the channel and is typically on the order of 5 to 10 microseconds for a cellular system. The received vector can be written as

$$\hat{\mathbf{r}}(\mathbf{i}) = \hat{\mathbf{y}}(\mathbf{i}) + \mathbf{n}(\mathbf{i}), \tag{5}$$

where $\hat{\mathbf{y}}(\mathbf{i}) = \mathbf{y}(\mathbf{i}) * \mathbf{h}$, $*$ denotes convolution, and $\mathbf{n}(\mathbf{i})$ are samples of an additive white Gaussian noise (AWGN) process. Note that in an AWGN channel, this reduces to $\mathbf{r}(\mathbf{i}) = \mathbf{y}(\mathbf{i}) + \mathbf{n}(\mathbf{i})$. Substituting for $\mathbf{y}$ using Eq. (4), we can write the received signal explicitly as

$$\hat{\mathbf{r}}(\mathbf{i}) = \hat{\mathbf{S}}^{+}\mathbf{A}\mathbf{b}(\mathbf{i}) + \hat{\mathbf{S}}^{-}\mathbf{A}\mathbf{b}(\mathbf{i-1}) + \mathbf{n}(\mathbf{i}), \tag{6}$$

In this paper, we assume that the channel vector is known, or can be estimated by some means. For the single user (SU) MMSE receiver, we choose the receiver filter coefficients, denoted in vector form by $\hat{\mathbf{c}}$, to minimize the mean-square error (MSE) between the transmitted bit and its estimate. Assuming user one is the desired user, this is given by

$$MSE_{SU} = E[|b_1(i) - \hat{\mathbf{c}}^{\mathbf{H}}\hat{\mathbf{r}}(\mathbf{i})|^{\mathbf{2}}], \tag{7}$$

where $E[\cdot]$ denotes the expected value operator and $(\cdot)^H$ represents the Hermitian transpose operator. The MMSE solution in the presence of multipath is given by

$$\hat{\mathbf{c}}_{\mathbf{MMSE}} = \hat{\mathbf{R}}^{-\mathbf{1}}\hat{\mathbf{s}}_{\mathbf{1}}\mathbf{A_1} = \mathbf{E}[\hat{\mathbf{r}}\hat{\mathbf{r}}^{\mathbf{H}}]^{-\mathbf{1}}\hat{\mathbf{s}}_{\mathbf{1}}\mathbf{A_1}, \tag{8}$$

where $\hat{\mathbf{R}}$ is the well-known covariance matrix and is given by $E[\hat{\mathbf{r}}(\mathbf{i})\hat{\mathbf{r}}(\mathbf{i})^{\mathbf{H}}]$. Note that the RAKE solution, which only incorporates the effects of the multipath and neglects the interference induced by the other users, can be written as

$$\mathbf{c_{RAKE}} = \hat{\mathbf{s}}_{\mathbf{1}}. \tag{9}$$

In the presence of only AWGN, this reduces further to the matched filter (MF) solution, $\mathbf{c_{MF}} = \mathbf{s_1}$.

For the MUD problem, we choose the receiver filter coefficients, denoted in matrix form by $\hat{\mathbf{C}}$, to minimize the MSE between the $K \times 1$ vector of transmitted bits, $\mathbf{b}(\mathbf{i}) = [\mathbf{b_1}(\mathbf{i}),\ \mathbf{b_2}(\mathbf{i}),\ ...,\ \mathbf{b_K}(\mathbf{i})]$ and the corresponding bit estimates $\tilde{\mathbf{b}}(\mathbf{i}) = [\tilde{\mathbf{b}}_{\mathbf{1}}(\mathbf{i}),\ \tilde{\mathbf{b}}_{\mathbf{2}}(\mathbf{i}),\ ...,\ \tilde{\mathbf{b}}_{\mathbf{K}}(\mathbf{i})]$. This can be written as

$$MSE_{MUD} = E[||\mathbf{b}(\mathbf{i}) - \tilde{\mathbf{b}}(\mathbf{i})||^{\mathbf{2}}], \tag{10}$$

where

$$\tilde{\mathbf{b}}(\mathbf{i}) = \hat{\mathbf{C}}^{\mathbf{H}}\hat{\mathbf{r}}(\mathbf{i}). \tag{11}$$

It can be shown that the MMSE solution is

$$\hat{\mathbf{C}}_{\mathbf{MMSE}} = \hat{\mathbf{R}}^{-\mathbf{1}}\hat{\mathbf{S}}^{+}\mathbf{A}. \tag{12}$$

Before proceeding with the implementation of this solution, we pause to make a few observations. First, note that we can write the solution for the $k^{th}$ user individually by simply extracting the $k^{th}$ columns of $\hat{\mathbf{S}}^{+}$ and of $\mathbf{A}$. That is, we can write the MUD solution as

$$\hat{\mathbf{C}}_{\mathbf{MMSE}} = [\hat{\mathbf{c}}_{\mathbf{1/MMSE}},\ \hat{\mathbf{c}}_{\mathbf{2/MMSE}},\ ...,\ \hat{\mathbf{c}}_{\mathbf{K/MMSE}}], \tag{13}$$

where

$$\hat{\mathbf{c}}_{\mathbf{k/MMSE}} = \hat{\mathbf{R}}^{-\mathbf{1}}\hat{\mathbf{s}}_{\mathbf{k}}^{+}\mathbf{A_k} \tag{14}$$

for the $k^{th}$ user. Thus, the matrix form of the MUD solution can be implemented in vector form using parallel single user detectors. This agrees with the results stated in [7]. Note the similarity between the MUD solution in Eqs. (12) and (14) and the single user solution given in Eq. (8). Second, note that the synchronous solution is obtained by setting $\hat{\mathbf{S}}^{+} = \hat{\mathbf{S}}$ or setting $\hat{\mathbf{s}}_{\mathbf{k}}^{+} = \hat{\mathbf{s}}_{\mathbf{k}}$ in Eqs. (12)and (14), respectively (with $\hat{\mathbf{S}}^{-} = \mathbf{0}$ and $\hat{\mathbf{s}}_{\mathbf{k}}^{-} = \mathbf{0}$). Furthermore, the covariance matrix, if expanded in terms of the received signal $\hat{\mathbf{r}}(\mathbf{i})$ in Eq. (6), is given as

$$\hat{\mathbf{R}} = \hat{\mathbf{S}}^{+}\mathbf{A^2}\hat{\mathbf{S}}^{+\mathbf{H}} + \hat{\mathbf{S}}^{-}\mathbf{A^2}\hat{\mathbf{S}}^{-\mathbf{H}} + \sigma^{\mathbf{2}}\mathbf{I}. \tag{15}$$

Even though in the presence of multipath, $\hat{\mathbf{S}}^{+}$ and $\hat{\mathbf{S}}^{-}$ are not orthogonal, the independence of the current bits $\mathbf{b}(\mathbf{i})$ and previous bits $\mathbf{b}(\mathbf{i-1})$ forces the expectation of the cross-terms to zero. This equation is similar to Eq. (10) of [5], which is shown for the AWGN case.

### B. Implementation of MUD Using the CSA-MWF

From Eqs. (12) or (14), we see that computation of the MMSE MUD solution requires inversion of the $N \times N$ covariance matrix $\hat{\mathbf{R}}$, which can be quite computationally intense and possibly un-invertible in a real-time, high data rate system. Also, if the channel or signals are changing in time, then the sample covariance matrix estimated from the data does not depict the true non-stationary signal environment. Thus, it is desirable to find alternative solutions that approach, or exceed, the performance of the MMSE receiver but require much fewer computations and can adapt rapidly. The multistage Wiener filter has demonstrated the ability to do this (e.g., see [2] and [5]). The single user multistage decomposition of the Wiener filter for rank D=2 is shown in Fig. 1. This is a new structure of the multistage Wiener filter, based on a correlation-subtraction structure (or MWF-CSA) as first described by Ricks, et. al., in [10]. Assume, without loss of generality, that user one, with spreading code $\mathbf{s_1}$, is the desired user. For the multipath channel, we simply let $\mathbf{h_0} = \hat{\mathbf{s}}_{\mathbf{1}}$, the spreading code of the desired user convolved with the channel. Then, $d_0(i) = \hat{\mathbf{s}}_{\mathbf{1}}^{\mathbf{H}}\tilde{\mathbf{x}}(\mathbf{i})$, where $\tilde{\mathbf{x}}(i)$ is the input signal, equal to $\hat{\mathbf{r}}(\mathbf{i})$. The bit estimate is given by $b_1(i) = \epsilon_0(i)$. The filter in Fig. 1 demonstrates the low complexity of this implementation of the MWF and the fact that the computation of signal blocking matrices are no longer necessary for any subspace partitioning such as that required for constrained adaptation.

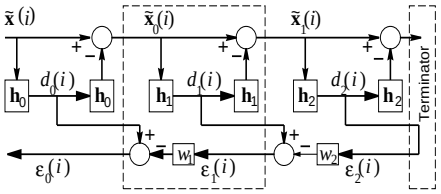


Fig. 1. CSA-MWF (D=2 stages)

The recursion equations, presented below, are similar to those used to implement the block residual correlation algorithm ([3] and [5]). Performance results of the multistage Wiener filter for asynchronous CDMA in AWGN can be found in [5].

- *Initialization:* $d_0(i)$ and $\tilde{\mathbf{x}}(i)$
- *Forward Recursion:* For $j = 1, 2, ..., D$:

$$\begin{aligned} \mathbf{h}_j &= \frac{\sum_\Omega \{d^*_{j-1}(i)\mathbf{x}_{j-1}(i)\}}{||\sum_\Omega \{d^*_{j-1}(i)\mathbf{x}_{j-1}(i)\}||} \\ d_j(i) &= \mathbf{h}_j^H \mathbf{x}_{j-1}(i) \\ \mathbf{x}_j(i) &= \mathbf{x}_{j-1}(i) - \mathbf{h}_j d_j(i) \end{aligned}$$

- *Backward Recursion:* For $j = D, D-1, ..., 1$, with $e_D(i) = d_D(i)$:

$$\begin{aligned} w_j &= \frac{\sum_\Omega \{d^*_{j-1}(i)e_j(i)\}}{\sum_\Omega \{|e_j(i)|^2\}} \\ e_{j-1}(i) &= d_{j-1}(i) - w_j^* e_j(i) \end{aligned}$$

where $\Omega$ denotes the region of sample support used to compute the sample statistics.

For the MUD problem, the solution of Eqs. (12) or (14) show that the MUD implementation can be obtained in matrix form ($\mathbf{H_0}$) or vector form ($\mathbf{h_{0,k}}$) by replacing the initialization step of the recursion equations with

$$\mathbf{H_0} = \hat{\mathbf{S}}^+ \ ; \ \mathbf{d_0} = \hat{\mathbf{S}}^{+\mathbf{H}} \tilde{\mathbf{x}}(\mathbf{i}) \tag{16}$$

or

$$\mathbf{h_{0,k}} = \hat{\mathbf{s}}_\mathbf{k}^+ \ ; \ \mathbf{d_{0,k}} = \hat{\mathbf{s}}_\mathbf{k}^{+\mathbf{H}} \tilde{\mathbf{x}}(\mathbf{i}), \tag{17}$$

where in the case of Eq. (17) an additional subscript $k$ has been added to indicate that the recursions are now performed separately for each user $k$. That is, we employ a bank of $K$ parallel Wiener filters, each operating in a reduced rank subspace. This structure is shown in Fig. 2. In this figure, the subscript $jk$ refers to stage $j$ in the MWF-CSA and user $k$, respectively, where a total of $D$ stages and $K$ users are assumed. As with the single Wiener filter, the bit estimates for each user are given by $b_k(i) = \epsilon_{0k}(i)$ for $k = 1, 2, ..., K$.

## IV. Performance Analysis

In the previous section, we show that the optimum linear solution to the MUD problem can be implemented in reduced rank form using the CSA-MWF. In this section, we

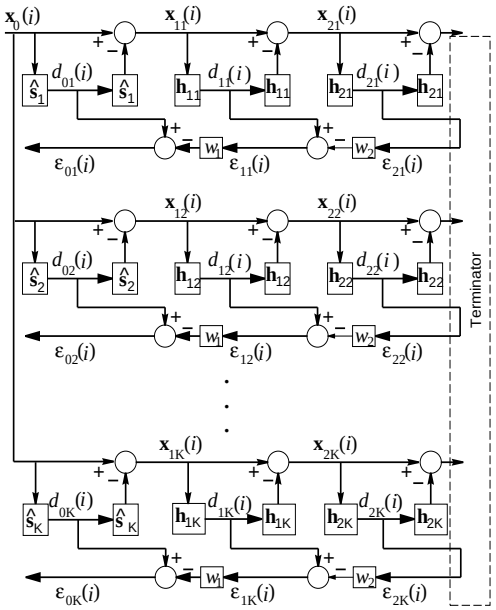


Fig. 2. Parallel MUD Using CSA-MWF (D=2 stages)

do an analysis to show how performance varies as a function of rank, the number of users, and the synchronism among the users . Gold codes are used for the analysis. First, note from Eqs. (11) and (13) that we can write the bit estimates for each user individually as

$$\tilde{\mathbf{b}}_\mathbf{k}(\mathbf{i}) = \hat{\mathbf{c}}^\mathbf{H}_{\mathbf{k/MMSE}} \hat{\mathbf{r}}(\mathbf{i}). \tag{18}$$

Substituting for $\hat{\mathbf{c}}_{\mathbf{k/MMSE}}$ using Eq. (14) and for the received signal using Eq. (6), we obtain

$$\tilde{\mathbf{b}}_\mathbf{k}(\mathbf{i}) = \hat{\mathbf{R}}^{-\mathbf{1}} \hat{\mathbf{s}}_\mathbf{k}^{+\mathbf{H}} \mathbf{A_k} [\hat{\mathbf{S}}^+ \mathbf{A} \mathbf{b}(\mathbf{i}) + \hat{\mathbf{S}}^- \mathbf{A} \mathbf{b}(\mathbf{i-1}) + \mathbf{n}(\mathbf{i})]. \tag{19}$$

We see from this equation that the quality of the bit estimates is largely determined by the ability of the receiver to suppress the cross-correlation of the desired user's code with the codes of the interference; this implies that for good performance we should have $\hat{\mathbf{s}}_\mathbf{k}^{+\mathbf{H}} \hat{\mathbf{s}}_\mathbf{i}^+$ and $\hat{\mathbf{s}}_\mathbf{k}^{+\mathbf{H}} \hat{\mathbf{s}}_\mathbf{i}^-$ as close to zero as possible for all $i \neq k$, in which $\hat{\mathbf{s}}_\mathbf{i}^+$ and $\hat{\mathbf{s}}_\mathbf{i}^-$ denote the $i^{th}$ columns of $\hat{\mathbf{S}}^+$ and $\hat{\mathbf{S}}^-$, respectively.

From the cross-correlation function of the length $N = 31$ Gold codes, the zeroth lag of the output correlation is in the middle of the grid, at element or row $N$. From the corresponding plot showing the orthogonality properties we see that properly chosen Gold codes, which are created using modulo two addition of two PN codes ([8] and [9]), have a limit in the maximum cross-correlation peak and maintain good orthogonality. This is the reason why Gold codes are the preferred spreading codes of CDMA systems, whereas Hadamard codes, which have poor cross-correlation properties but perfect orthogonality, are used only to provide

orthogonal modulation. This feature of Gold codes is especially important on the reverse link, where asynchronous transmission precludes the ability of the Hadamard codes to suppress interference. Of course, in the absence of multipath, Hadamard codes would outperform Gold codes, given their ideal orthogonality properties.

Now, because the cross-correlation of Gold codes is not perfect, we expect their performance to degrade as the number of users increases. In addition, the optimum rank required to meet the full rank MMSE performance will increase. But, it is important to note that this is not a linear function, and performance is still optimum at a much reduced rank. This is an outstanding feature of the MWF that makes it a promising tool in a multitude of applications. Furthermore, as we will see, performance at low rank may exceed that of full rank, when the codes have good correlation properties that enable the MWF to suppress interference more reliably. These remarks are validated with simulation results, presented in the next section.

## V. Numerical Results

In this section, we present results obtained from Monte Carlo simulations to show the validity of the MUD solution derived above and its performance as a function of rank (D) and the number of users (K). An $L = 5$ tap channel is used to simulate the multipath, using one tap per chip at a fixed $E_b/N_0$ of 12 dB. We process binary (BPSK) baseband data in blocks, where the number of bits per block is 1000 and the number of blocks is at least 5 (chosen to produce enough errors to obtain a valid statistical bit error rate estimate). The powers of all the users are equal. We perform simulations for synchronous and asynchronous users as a function of rank using Gold codes of length $N = 31$. The BER obtained is an average over all the users present in the system using the parallel MUD implementation shown in Fig. 2. The BER of the full rank MMSE receiver is averaged over all the runs for a better estimate, as its' performance is independent of rank. The results are analyzed next.

Fig. 3 shows rank versus BER for the case of 5, 10, and 15 synchronous users using Gold sequences. In this case, convergence of BER is seen to occur quickly, at ranks of only 1 or 2. Note that the MWF performance *exceeds* full rank performance at ranks from about 3 to 9, but then eventually converges again. This is due to the aforementioned cross-correlation properties and the ability of the MWF to suppress the uncorrelated interference. This is an effect that has also been shown in [5] and is a remarkable property of the MWF to simultaneously achieve a convergence substantially better than that achieved with full rank MMSE *and* a dramatically reduced computational burden as well. Intuitively speaking, the MWF achieves the best of both worlds - faster convergence and reduced computation - by applying the information inherently contained in both the covariance matrix and the cross-correlation vector in choosing the reduced-dimension subspace in which the weight vector is constrained to lie. Finally, note that degradation in performance as a function of the number of users is present, even with synchronous users, as expected.

Fig. 4 shows rank versus BER with 5, 10 and 15 asynchronous users. In this case, convergence of BER is seen at ranks of 1, 3, and 4. Note that unlike the synchronous case, the BER here also degrades as more users are added to the system. As pointed out earlier, while Gold codes have good cross-correlation properties, there still exists some correlation among them, and this effect is enhanced by the asynchronism and imperfect orthogonality, as seen also in Fig. 3. Nevertheless, the advantage of the reduced rank MWF in terms of performance and rank reduction is clearly seen.

## VI. Conclusion

In this paper, we show how to implement the solution for the MMSE MUD using the reduced rank multistage Wiener filter both in parallel and joint form. It is demonstrated via Monte Carlo simulations that the performance of the reduced rank MMSE MUD meets or exceeds the full rank MMSE MUD solutions at a much lower rank. The benefit of the MWF in conjunction with codes with good cross-correlation properties, such as Gold codes, when multipath and/or asynchronism is present is also shown. In this case, the MWF is shown to exceed full rank performance, also at a much reduced rank.

## VII. Acknowledgments

We gratefully acknowledge Dr. Michael Honig of Northwestern University and Dr. Irving Reed of the University of Southern California.

## References

[1] Goldstein, J.S., and Reed, I.S., "Multidimensional Wiener Filtering Using a Nested Chain of Orthogonal Scalar Wiener Filters", University of Southern California, Dec. 1996, CSI-96-12-04.

[2] Goldstein, J.S., and Reed, I.S., "A New Method of Wiener Filtering and its Application to Interference Mitigation for Communications", *Proceedings of IEEE MILCOM*, Vol. 3, pp. 1087-1091, Monterey, CA, Nov. 1997.

[3] Goldstein, J.S., Reed, I.S., and Scharf, L.L., "A Multistage Representation of the Wiener Filter Based on Orthogonal Projections", in *IEEE Transactions on Information Theory*, Vol. 44, No. 7, Nov. 1998.

[4] Haykin, S., "Adaptive Filter Theory", Third Edition, Prentice Hall, New Jersey, 1996.

[5] Honig, M.L., and Goldstein, J.S., "Adaptive Reduced-Rank Residual Correlation Algorithms for DS-CDMA Interference Suppression", in *Proceedings of Asilomar*, Jul. 1998.

[6] Honig, M.L., and Poor, H.V., Adaptive Interference Suppression. In Poor, H.V., and Wornell, G.W., editors, "Wireless Communications: Signal Processing Perspectives", Prentice Hall: Englewood Cliffs, New Jersey, pgs. 64-102, 1998.

[7] Honig, M.L., and Tsatsanis, M.K., "Adaptive Techniques for Multiuser CDMA Receivers", in *IEEE Transactions on Signal Processing*, Vol. 17, No. 3, pgs. 49-61, May 2000.

[8] Lee, J.S., and Miller, L.E., "CDMA Systems Engineering Handbook", Boston: Artech House, 1998.

[9] Proakis, J.G., and Salehi, M., "Contemporary Communication Systems Using MATLAB", Brooks/Cole Publishing Co., Nov. 1999.

[10] Ricks, D.C., and Goldstein, J.S. "Efficient Architectures for Implementing Adaptive Algorithms", *Proceedings of the 2000 Antenna Applications Symposium*, pgs. 29-41, Allerton Park, Monticello, Illinois, Sep. 20-22, 2000.

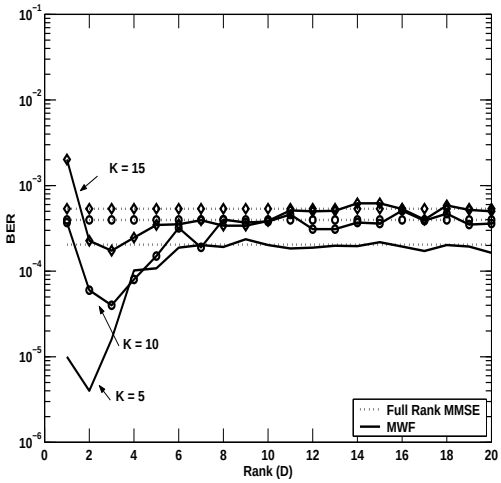


Fig. 3. Synchronous Gold Codes; N=31

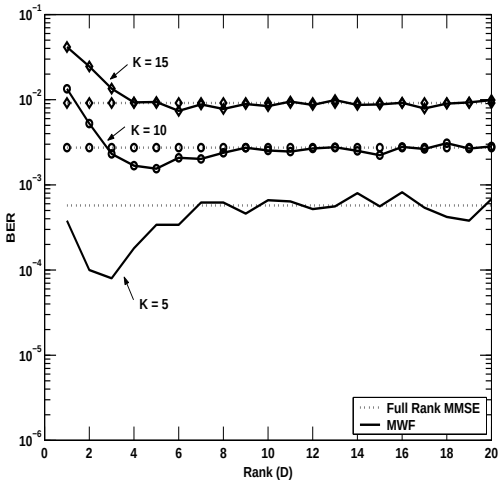


Fig. 4. Asynchronous Gold Codes; N=31

# A REDUCED RANK MMSE RECEIVER FOR A DS-CDMA SYSTEM IN FREQUENCY SELECTIVE MULTIPATH

*Seema Sud, Wilbur L. Myrick, J. Scott Goldstein*

Science Applications International Corporation
4001 Fairfax Dr., Suite 675
Arlington, VA 22203-1303, USA

*Michael D. Zoltowski*

Department of Electrical and Computer Engineering
Purdue University
West Lafayette, IN 47907-1285, USA

## ABSTRACT

*A new reduced rank adaptive algorithm for asynchronous, DS-CDMA interference suppression in the presence of frequency selective multipath is presented. The algorithm employs a computationally efficient, correlation-subtraction architecture based on the multistage Wiener filter. It is shown that this reduced rank technique performs nearly as well as the full rank MMSE solution without requiring matrix inversion, eigen-decomposition, or the construction of blocking matrices. System performance is characterized for a highly loaded asynchronous DS-CDMA system in the presence of multipath and the performance of the multistage Wiener filter is compared to the MMSE and RAKE receivers.*

## 1. INTRODUCTION

Code Division Multiple Access (CDMA) has been proposed as the technique of choice for the next generation of wireless communications systems. This method of multiple access allows for an increase in system capacity over other approaches to provide multiple access such as Time Division Multiple Access (TDMA) or Frequency Division Multiple Access (FDMA). However, systems employing CDMA are typically interference limited. The interference arises from the very nature of the systems, which must often accommodate multiple users transmitting simultaneously through a common physical channel. This is due to the non-orthogonal multiplexing of signals that results from multipath induced by the channel and occurs in cellular environments due to the reflections of signals off local surroundings, such as buildings, cars, terrain, trees, etc. When multipath is present in the signal, intersymbol interference (ISI) causes additional degradation. Interference can also arise from multiple users sharing a common bandwidth for different services, such as voice and data transmission. Thus, interference suppression techniques for CDMA have received much attention in the recent research. For the high speed voice and data applications proposed for the third generation (3G) systems, adaptive, reduced rank interference suppression is highly desirable.

In this paper, we present the minimum mean-square error (MMSE) solution for interference suppression and signal detection in the presence of multipath. We show that implementation of this solution using the multistage Wiener filter (MWF) [2-4] meets MMSE performance at a low rank. We also show performance results of the RAKE receiver for comparison.

The most recent research in interference suppression has focused on data aided or blind MMSE receivers, which are suboptimal in multipath channels. The results presented in this paper differ from those in [8], which considers an MMSE/RAKE solution that incorporates multipath but operates in a full rank environment. In [4], a reduced rank asynchronous CDMA system is considered, but without the presence of multipath. Finally, [6] discusses the reduced rank multistage Wiener filter for suppressing interference induced in asynchronous, DS-CDMA systems but does not include any additional processing to combat multipath.

## 2. CDMA SIGNAL MODEL

We assume a DS-CDMA system, in which we have $K$ users. The notation used here is similar to that used by Honig, et. al., in [4] and [5]. User $k$ transmits a baseband signal given by

$$x_k(t) = \sum_i A_k b_k(i) s_k(t - iT - \tau_k), \tag{1}$$

where $b_k(i)$ is the symbol transmitted by user $k$ at time $i$, $s_k(t)$ is the spreading code associated with user $k$, and $A_k$ and $\tau_k$ are the amplitude and delay, respectively. We assume binary signaling, so that the symbols $b_k(i) \in$ (-1,+1). The spreading sequence can be written as

$$s_k(t) = \sum_{i=1}^{N-1} a_k[i] \Psi(t - iT_c), \tag{2}$$

where $a_k[i] \in (\frac{+1}{\sqrt{N}}, \frac{-1}{\sqrt{N}})$ is a normalization factor for the spreading code. The processing gain of the CDMA system, or equivalently the bandwidth spreading factor, is given by $N = \frac{T}{T_c}$. Here, $T_c$ is the chip period, and $T$ is the symbol period. We assume that the spreading code is a square wave sequence with no pulse shaping, so that the chip sequence $\Psi(t)$ is a constant.

Define the sampled transmitted signal $\mathbf{y}(i)$ as the N-vector composed of asynchronous combinations of the data for each user multiplied with its respective spreading sequence. Assume also, without loss of generality, that we are interested in detecting user 1, and that the receiver has timing information to synchronize to the spreading code of

the desired user. The transmitted signal may then be written in the form

$$\mathbf{y}(i) = b_1(i)\mathbf{s_1} + \sum_{k=2}^{K} A_k[b_k(i)\mathbf{s_k^+} + b_k(i-1)\mathbf{s_k^-}]. \quad (3)$$

Here, $\mathbf{s_1}$ is the spreading sequence of user 1, and $\mathbf{s_k^+}$ and $\mathbf{s_k^-}$ are the $N \times (K-1)$ matrices of spreading codes associated with the $K$-1 interfering users. Due to the asynchronous transmission, as is inherent to the reverse link of a cellular system, both the current bit of user $k$, denoted $b_k(i)$, and the previous bit of user $k$, denoted $b_k(i-1)$, multiplied with their respective portions of the spreading code, are interfering with the current bit of user 1. We would like to extract the desired information, i.e., the bits transmitted by user 1 ($b_1$) while suppressing the interference represented by the term in the summation of Eq. (3). Ideally, we would like to subtract out the interference term and then multiply by the spreading code of user 1, $\mathbf{s_1}$, to extract $b_1$ from the received signal. This is not possible in practice because the interference is unknown and embedded in the received signal, and the channel will further distort the transmitted signal. Thus, we turn our attention to the linear detection techniques presented next.

## 3. LINEAR REDUCED RANK MMSE DETECTION

In this section, we first provide the MMSE solution for the asynchronous, DS-CDMA system, following the notation used in [10], assuming an additive, white, Gaussian noise (AWGN) channel. We then describe the MMSE solution for a channel distorted by frequency selective multipath. In both cases, we show how to implement the MMSE solution using the reduced rank multistage Wiener filter.

### 3.1. AWGN Channel

First, consider the case where the channel is simply an AWGN channel, so that the sampled received signal is an N-vector containing samples at the output of a chip-matched filter at each symbol $i$, represented by

$$\mathbf{r}(i) = \mathbf{y}(i) + \mathbf{n}(i). \quad (4)$$

Substituting Eq. (3) for $\mathbf{y}(i)$, we can write

$$\mathbf{r}(i) = b_1(i)\mathbf{s_1} + \sum_{k=2}^{K} A_k[b_k(i)\mathbf{s_k^+} + b_k(i-1)\mathbf{s_k^-}] + \mathbf{n}(i). \quad (5)$$

For the MMSE receiver, we choose the receive filter coefficients, denoted in vector form by $\mathbf{c}$, to minimize the mean-square error (MSE) between the transmitted bit and its estimate, given by

$$MSE = E[|b_1(i) - \mathbf{c}^H\mathbf{r}(i)|^2], \quad (6)$$

where $E[\cdot]$ denotes the expected value operator and $(\cdot)^H$ represents the Hermitian transpose operator. Solving Eq. (6) yields

$$\mathbf{c}_{MMSE} = \mathbf{R}^{-1}\mathbf{s_1}, \quad (7)$$

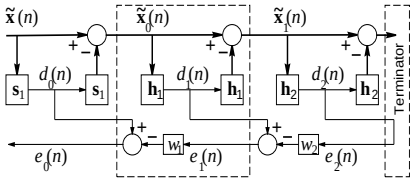


Figure 1: Multistage Wiener Filter (D=2 stages)

where $\mathbf{R}$ is the well-known covariance matrix and is given by $E[\mathbf{r}(i)\mathbf{r}(i)^H]$.

Note that computation of the MMSE solution requires inversion of the $N \times N$ covariance matrix $\mathbf{R}$, which can be quite computationally intense and may not even be possible in real-time for a high data rate system. Also, if the channel or signals are changing in time, then the sample covariance matrix estimated from the data does not depict the true non-stationary signal environment. Thus, it is desirable to find alternate solutions that approach, or exceed, the performance of the MMSE receiver but require much fewer computations and can adapt rapidly. The multistage Wiener filter has demonstrated the ability to do this (e.g., see [2] and [4]). The multistage decomposition of the Wiener filter for D=2 stages is shown in Fig. 1. This is a new structure of the multistage Wiener filter, based on a correlation-subtraction architecture (or MWF-CSA) as first described by Ricks, et. al., in [9]. For the AWGN channel, we simply set $\mathbf{h_0} = \mathbf{s_1}$, the spreading code of the desired user. Then, $\mathbf{d_0}(n) = \mathbf{s}_1^H\tilde{\mathbf{x}}(n)$, where the input signal $\tilde{\mathbf{x}}(n)$ is a vector composed of a block of M bits of the received sampled signal: $[\mathbf{r}(n-M+1)\ \mathbf{r}(n-M+2)\ ...\ \mathbf{r}(n)]$. The filter in Fig. 1 demonstrates the low complexity of this implementation of the MWF and the fact that the computation of signal blocking matrices are no longer necessary for any subspace partitioning such as that required for constrained adaptation.

The forward recursion equations, presented below, are identical to those used to implement the block residual correlation algorithm ([3] and [4]). Performance results of the multistage Wiener filter for asynchronous CDMA in AWGN can be found in [4].

- *Initialization:* $d_0(n)$ and $\tilde{\mathbf{x}}(n)$
- *Forward Recursion:* For $k = 1, 2, ..., D$:

$$\begin{aligned} \mathbf{h}_k &= \frac{\sum_\Omega\{d_{k-1}^*(n)\mathbf{x}_{k-1}(n)\}}{||\sum_\Omega\{d_{k-1}^*(n)\mathbf{x}_{k-1}(n)\}||} \\ d_k(n) &= \mathbf{h}_k^H\mathbf{x}_{k-1}(n) \\ \mathbf{x}_k(n) &= \mathbf{x}_{k-1}(n) - \mathbf{h}_k d_k(n) \end{aligned}$$

- *Backward Recursion:* For $k = D, D-1, ..., 1$, with $e_D(n) = d_D(n)$:

$$w_k = \frac{\sum_\Omega\{d_{k-1}^*(n)e_k(n)\}}{\sum_\Omega\{|e_k(n)|^2\}}$$

$$e_{k-1}(n) \quad = \quad d_{k-1}(n) - w_k^{\sim} e_k(n)$$

where $\Omega$ denotes the region of sample support used to compute the sample statistics.

### 3.2. Multipath Channel

Now consider the case of a multipath channel, modeled in discrete time by an L-tap tapped-delay line whose coefficients are represented by $\mathbf{h} = [h_1, h_2, ..., h_L]$. The parameter L, when viewed in units of time, is known as the delay spread of the channel and is typically on the order of 5 to 10 microseconds. The received signal can now be written as

$$\hat{\mathbf{r}}(i) = \hat{\mathbf{y}}(i) + \mathbf{n}(i), \tag{8}$$

where $\hat{\mathbf{y}} = \mathbf{y} * \mathbf{h}$ and $*$ denotes convolution. Substituting for $\mathbf{y}$ using Eq. (3), we can write the received signal explicitly as

$$\hat{\mathbf{r}}(i) = b_1(i)\hat{\mathbf{s}}_\mathbf{1} + \sum_{k=2}^{K} A_k[b_k(i)\hat{\mathbf{s}}_\mathbf{k}^+ + b_k(i-1)\hat{\mathbf{s}}_\mathbf{k}^-] + \mathbf{n}(i), \tag{9}$$

where $\hat{(\cdot)}$ denotes convolution of the operand with the channel vector $\mathbf{h}$. In this paper, we assume that the channel vector is known, or can be estimated by some means. Using the analogy between Eq. (5) for the AWGN channel and Eq. (9) for the multipath channel, the MMSE solution in the presence of multipath can now be written directly from the AWGN solution in Eq. (7), or

$$\hat{\mathbf{c}}_{MMSE} = \hat{\mathbf{R}}^{-1}\hat{\mathbf{s}}_\mathbf{1} = E[\hat{\mathbf{r}}\hat{\mathbf{r}}^H]^{-1}\hat{\mathbf{s}}_\mathbf{1}. \tag{10}$$

The multistage Wiener filter solution can be obtained similarly, by setting $\mathbf{h_0} = \hat{\mathbf{s}}_\mathbf{1}$. Note that the RAKE solution, which only incorporates the effects of the multipath and neglects the interference, can be written simply as

$$\mathbf{c}_{RAKE} = \hat{\mathbf{s}}_\mathbf{1}. \tag{11}$$

In the presence of only AWGN, this reduces to the matched filter (MF) solution, $\mathbf{c}_{MF} = \mathbf{s}_\mathbf{1}$. The equations above provide us with a simple and elegant way of representing the RAKE, multistage Wiener filter, and MMSE filter coefficients when multipath is present. We present results obtained from Monte Carlo simulations using these equations in the next section.

## 4. NUMERICAL RESULTS

In this section, we present results from Monte Carlo simulations of the linear, reduced rank MMSE receiver using the multistage Wiener filter and compare the results with the full rank MMSE receiver and the RAKE receiver. The bit estimates can be obtained by multiplying the received signal by the receiver filter coefficients and forming a hard decision. Thus, in the case of MMSE and RAKE we compute

$$\hat{b}_1(i) = \mathbf{c}_{\mathbf{MMSE/RAKE}}^{\mathbf{H}}\mathbf{r(i)}. \tag{12}$$

In the case of the MWF, the bit estimate is produced at the last stage of the filter and can be written simply as

$$\hat{b}_1(i) = \epsilon_\mathbf{0}(i). \tag{13}$$

For the Monte Carlo simulation results, unless otherwise indicated, the processing gain is $N$=32, and the number of users is fixed at $K$=15. An $L$=5 tap channel is used to simulate the multipath, using one tap per chip. The number of bits per block is 5000, and the number of blocks is at least 10 (chosen to produce enough errors to obtain a valid statistical bit error rate estimate). The power of the interfering users is set to 6 dB greater than that of the desired user to determine performance in a near-far situation.

Fig. 2 shows a plot of rank of the multistage Wiener filter versus the bit error rate (BER). The variation in BER for the MMSE and RAKE methods is due to the nature of the Monte Carlo simulation, since their performance is independent of rank. Note that for a rank as low as seven, the MWF performs as well as the full rank MMSE and maintains this performance as rank increases. The performance of the MWF does not significantly degrade until the rank is reduced below five. The MWF performance at full rank exactly matches the full rank MMSE, as expected. Both the MWF and MMSE consistently perform better than the RAKE receiver, which cannot combat the large number of interfering users.

Fig. 3 shows a plot of $E_b/N_0$ versus BER. In this case, the rank of the MWF is seven. We see here that the MWF performs as well as the MMSE receiver and significantly better than the RAKE receiver. Note that there is about a 6 dB degradation in performance from the ideal BPSK curve. This degradation is directly related to the desired user having 6 dB less power relative to the interferers. To a lesser extent, it is also caused by the system being asynchronous and the environment, including the effects of multipath. The performance here could be improved using decision feedback.

Next, Fig. 4 shows a plot of the number of users ($K$) versus BER. Here, the $E_b/N_0$ is 15 dB, and the rank of the multistage Wiener filter is again seven. The number of users varies from 1 to 25. We see here that for a lightly loaded system, the RAKE receiver performs reasonably well, but its error rate degrades rapidly as the load is increased. As before, the MWF meets MMSE performance over the entire range of loading. Note also that when the number of users increases beyond half the processing gain, the performance degrades substantially. This occurs because we have asynchronous CDMA signals but the $N$+$L$-1 taps of the receiver in each case span only one bit interval (see [7]). To correct this problem, a receiver with taps that span two symbols would be required. Another possible way to mitigate this problem would be to increase the sampling rate, which is equivalent to increasing the number of taps per bit. Then, the effect of the asynchronism would have less of an impact.

Finally, Fig. 5 is a curve showing the number of bits per block versus BER. For this result, the $E_b/N_0$ is 15 dB, $K$=12, and the rank of the MWF is again seven. Note that the MMSE curve requires about 1500 samples to converge to a bit error rate of about $2 \cdot 10^{-3}$. However, the MWF

requires only about 1000 samples per block to converge to the same error rate. Thus, the MWF is less sensitive to sample support than the full rank MMSE. This in turn implies that the MWF can track changes in signals that are varying in time faster than MMSE, which is an important advantage of the reduced rank processing provided by the MWF. In addition, the MMSE solution requires inversion of an $N \times N$ covariance matrix, but the MWF does not. This illustrates the computational savings that can be obtained by employing the reduced rank MWF, which yields the same performance as full rank MMSE. As before, the RAKE receiver does significantly worse, achieving an error rate of only $10^{-1}$.

## 5. CONCLUSION

In this paper, we present a formulation for the MMSE receiver in a frequency selective multipath channel. We then show how to implement this solution using the reduced rank multistage Wiener filter. Monte Carlo simulation results of the MMSE receiver and multistage Wiener filter are compared to those of the RAKE receiver. A highly loaded, asynchronous DS-CDMA system distorted by a five tap multipath channel is used for the simulation, and bit error rate performance is evaluated as a function of rank, $E_b/N_0$, number of users, and block size. It is demonstrated that the multistage Wiener filter performs as well as the full rank MMSE and significantly outperforms the RAKE receiver at a considerably reduced rank.

## 6. ACKNOWLEDGMENTS

The authors would like to thank Professors Michael Honig of Northwestern University and Irving Reed of the University of Southern California for many fruitful conversations during this effort.

## REFERENCES

[1] Goldstein, J.S., and Reed, I.S., "Multidimensional Wiener Filtering Using a Nested Chain of Orthogonal Scalar Wiener Filters", University of Southern California, Dec. 1996, CSI-96-12-04.

[2] Goldstein, J.S., and Reed, I.S., "A New Method of Wiener Filtering and its Application to Interference Mitigation for Communications", in *IEEE Transactions on Information Theory*, Jun. 1997.

[3] Goldstein, J.S., Reed, I.S., and Scharf, L.L., "A Multistage Representation of the Wiener Filter Based on Orthogonal Projections", in *IEEE Transactions on Information Theory*, Vol. 44, No. 7, Nov. 1998.

[4] Honig, M.L., and Goldstein, J.S., "Adaptive Reduced-Rank Residual Correlation Algorithms for DS-CDMA Interference Suppression", in *Proceedings of Asilomar*, Jul. 1998.

[5] Honig, M.L., and Poor, H.V., Adaptive Interference Suppression. In Poor, H.V., and Wornell, G.W., editors, "Wireless Communications: Signal Processing Perspectives", Prentice Hall: Englewood Cliffs, New Jersey, pgs. 64-102, 1998.

[6] Honig, M.L., and Tsatsanis, M.K., "Adaptive Techniques for Multiuser CDMA Receivers", in *IEEE Transactions on Signal Processing*, Vol. 17, No. 3, pgs. 49-61, May 2000.

[7] Madhow, U., "Blind Adaptive Interference Suppression for Direct-Sequence CDMA", in *Proceedings of the IEEE, Special Issue on Blind Identification and Equalization*, pgs. 2049-2069, Oct. 1998.

[8] Rice, G.W., Garcia-Alis, D., Stirling, I.G., Weiss, S., Stewart, R.W., "An Adaptive MMSE RAKE Receiver", in *Proceedings of Asilomar*, 2000.

[9] Ricks, D.C., and Goldstein, J.S. "Efficient Architectures for Implementing Adaptive Algorithms", *Proceedings of the 2000 Antenna Applications Symposium*, pgs. 29-41, Allerton Park, Monticello, Illinois, Sep. 20-22, 2000.

[10] Verdu, S., "Multiuser Detection", Cambridge University Press, 1998.

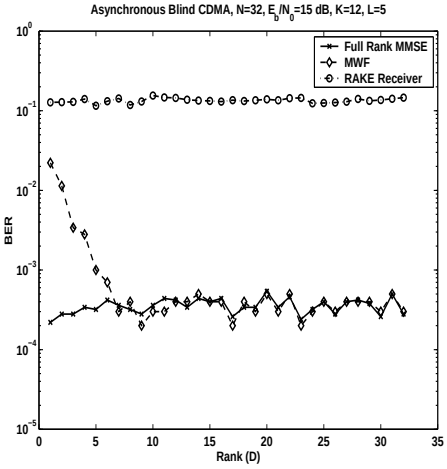


Figure 2: Rank (D) vs. BER

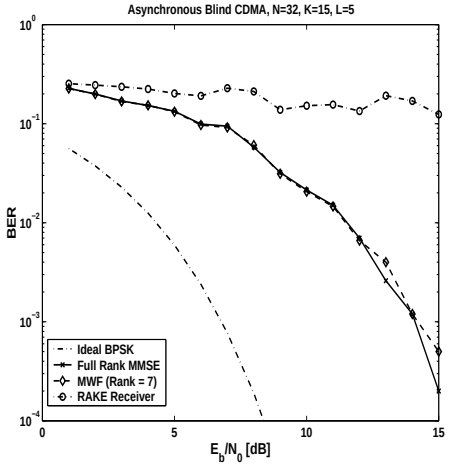


Figure 3: $E_b/N_0$ [dB] vs. BER

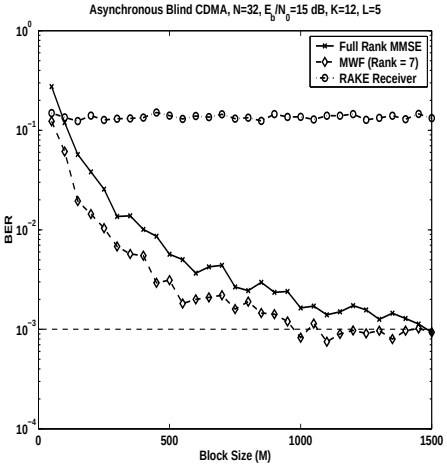


Figure 5: Block Size (M) vs. BER

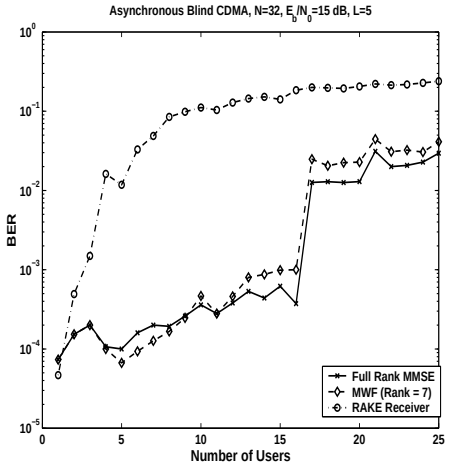


Figure 4: Number of Users vs. BER

# Bibliography


[1] Alamouti, S.M., "A Simple Transmit Diversity Technique for Wireless Communications", *IEEE Journal on Selected Areas in Communications*, Vol. 16, No. 8, pgs. 1451-1458, Oct. 1998.

[2] Benedetto, S., and Montorsi, G., "Unveiling Turbo Codes: Some Results on Parallel Concatenated Coding Schemes", *IEEE Transactions. on Information Theory*, Vol. 42, No. 2, pgs. 409-429, Mar. 1996.

[3] Berrou, C., Glavieux, A., and Thitimasjshima, P., "Near Shannon Limit Error-Correcting Coding and Decoding: Turbo-Codes", *Proceedings of the IEEE International Conference on Communications*, Geneva, Switzerland, pgs. 1064-1070, May, 1993.

[4] Black, U., "Second Generation Mobile and Wireless Networks", Prentice Hall: Upper Saddle River, New Jersey, 1999.

[5] Brooks, L.W., and Reed, I.S., "Equivalence of the Likelihood Ratio Processor, and Maximum Signal-to-Noise Ratio Filter, and the Wiener Filter", *IEEE Transactions on Aerospace and Electronic Systems*, Vol. 8, pgs. 690-692, Sep. 1972.

[6] Buehrer, R.M., and Woerner, B.D., "Analysis of Adaptive Multistage Interference Cancellation for CDMA Using an Improved Gaussian Approximation", *IEEE Transactions on Communications*, Vol. 44, Oct. 1996.

[7] Chowdhury, S., Zoltowski, M.D., and Goldstein, J.S., "Application of Reduced-rank Chip-level MMSE Equalization to the Forward Link DS-CDMA with Frequency Selective Multipath", *Proc. Allerton*, 2000.

[8] Cifuentes, P.G., Myrick, W.L., Sud, S., Goldstein, J.S., and Zoltowski, M.D., "Reduced Rank Matrix Multistage Wiener Filter with Applications in MMSE Joint Multiuser Detection for DS-CDMA", *Proceedings of IEEE ICASSP*, Orlando, FL, May 13-17, 2002.

[9] Cruickshank, D.G.M., "Suppression of Multiple Acess Interference in a DS-CDMA System Using Wiener Filtering and Parallel Cancellation", *Proc. Inst. Elect. Eng. Commun.*, Vol. 143, No. 4, pgs. 226-230, Aug. 1996.

[10] Cui, S., and Luo, Z. "Robust Blind Multiuser Detection Against CDMA Signature Mismatch", *Proceedings of ICASSP*, Salt Lake City, UT, May 2001.

[11] Divsalar, D., Simon, M.K., Raphaeli, D., "Improved Parallel Interference Cancellation for CDMA", *IEEE Transactions on Communications*, Vol. 46, No. 2, pgs. 258-268, Feb. 1998.

[12] Duel-Hallen, A., "Decorrelating Decision-Feedback Multiuser Detector for Synchronous Code-Division Multiple Access Channel", *IEEE Transactions on Communications*, Vol. 41, No. 2, pgs. 285-290, Feb. 1993.

[13] Duel-Hallen, A., "A Family of Multiuser Decision-Feedback Detectors for Asynchronous Code-Division Multiple Access Channels", *IEEE Transactions on Communications*, Vol. 43, No. 2/3/4, pgs. 421-434, Feb./Mar./Apr. 1995.

[14] Eckart, C., and Young, G., "The Approximation of One Matrix by Another of Lower Rank", *Psychometrica*, Vol. 1, pgs. 211-218, 1936.

[15] Freeman, R.L., "Radio System Design for Telecommunications", New York: Wiley and Sons, 1997.

[16] Garg, V.K., "IS-95 CDMA and CDMA 2000: Cellular/PCS Systems Implementation", Prentice Hall, Nov. 1999.

[17] Garg, V.K., Rappaport T. (Editor), "Wireless Network Evolution: 2G to 3G", Prentice Hall, Apr. 2001.

[18] Gold, R., "Optimal Binary Sequences for Spread Spectrum Muliplexing", *IEEE Transactions on Information Theory*, Vol. 13, No. 4, pgs. 619-621, Oct. 1967.

[19] Goldstein, J.S., and Reed, I.S., "Adaptive Target Detection and Identification", SAIC/ASE Technical Report Number 99-10-001, Oct. 1999.

[20] Goldstein, J.S., and Reed, I.S., "Multidimensional Wiener Filtering Using a Nested Chain of Orthogonal Scalar Wiener Filters", University of Southern California, CSI-96-12-04, Dec. 1996.

[21] Goldstein, J.S., Reed, I.S., and Scharf, L.L., "A Multistage Representation of the Wiener Filter Based on Orthogonal Projections", *IEEE Transactions on Information Theory*, Vol. 44, No. 7, Nov. 1998.

[22] Goldstein, J.S., and Reed, I.S., "A New Method of Wiener Filtering and its Application to Interference Mitigation for Communications", *Proceedings of IEEE MILCOM*, Vol. 3, pp. 1087-1091, Monterey, CA, Nov. 1997.

[23] Goldstein, J.S., Reed, I.S., and Scharf, L.L, "A New Method of Wiener Filtering", *Proceedings of the 1st AFOSR/DSTO Workshop on Defense Applications of Signal Processing*, Victor Harbor, Australia, Jun. 1997.

[24] Goldstein, J.S., *Optimal Reduced Rank Statistical Signal Processing, Detection, and Estimation Theory*, Ph.D. Thesis, Dept. of Electrical Engineering, University of Southern California, Los Angeles, CA, Dec. 1997.

[25] Goldstein, J.S., and Reed, I.S., "Reduced Rank Adaptive Filtering", *IEEE Transactions on Signal Processing*, Vol. 45, No. 2, pgs. 492-496, Feb. 1997.

[26] Gore, D., and Paulraj, A., "Space-Time Block Coding with Optimal Antenna Selection", *Proceedings of ICASSP*, Salt Lake City, UT, May 2001.

[27] Guo, D., Rasmussen, L.K., Sun, S., and Lim, T.J., "A Matrix-Algebraic Approach to Linear Parallel Interference Cancellation in CDMA", *IEEE Transactions on Communications*, Vol. 48, No. 1, pgs. 152-161, Jan. 2000.

[28] Haardt, M., and Nossek, J., "3-D Unitary ESPRIT for Joint 2-D Angle and Carrier Estimation", *Proceedings of IEEE*, 1997.

[29] Hassibi, B., and Hochwald, B., "High-Rate Linear Space-Time Codes", *Proceedings of ICASSP*, Salt Lake City, UT, May 2001.

[30] Haykin, S., "Adaptive Filter Theory", Prentice Hall: Upper Saddle River, New Jersey, 1994.

[31] Honig, M.L., "A Comparison of Subspace Adaptive Filtering Techniques for DS-CDMA Interference Suppression", *Proceedings of IEEE MILCOM*, Vol. 2, pgs. 836-840, Monterey, CA, Nov. 1997.

[32] Honig, M.L., and Goldstein, J.S., "Adaptive Reduced-Rank Residual Correlation Algorithms for DS-CDMA Interference Suppression", *Proceedings of Asilomar*, Jul. 1998.

[33] Honig, M.L., Madhow, U., and Verdú, S., "Blind Adaptive Multiuser Detection", *IEEE Transactions on Information Theory*, Vol. 41, No. 4, Jul. 1995.

[34] Honig, M.L., and Poor, H.V., Adaptive Interference Suppression. In Poor, H.V., and Wornell, G.W., editors, "Wireless Communications: Signal Processing Perspectives", Prentice Hall: Englewood Cliffs, New Jersey, pgs. 64-102, 1998.

[35] Honig, M.L., and Tsatsanis, M.K., "Adaptive Techniques for Multiuser CDMA Receivers", *IEEE Transactions on Signal Processing*, Vol. 17, No. 3, pgs. 49-61, May 2000.

[36] Høst-Madsen, A., and Cho, K., "MMSE/PIC Multiuser Detection for DS/CDMA Systems with Inter- and Intra-Cell Interference", *IEEE Transactions on Communications*, Vol. 47, No. 2, pgs. 291-299, Feb. 1999.

[37] Hotelling, H., "Analysis of a Complex Set of Statistical Variables into Principal Components", *Journal of Educational Psychology*, Vol. 24, pgs. 417-441 and 498-520, 1933.

[38] Householder, A.S., "The Approximate Solution of Matrix Problems", *J. Assoc. Comput. Mach.*, Vol. 5, pgs. 204-243, 1958.

[39] Householder, A.S., "Unitary Triangularization of a Nonsymmetric Matrix", *J. Assoc. Comput. Mach.*, Vol. 5, pgs. 339-342, 1958.

[40] Hui, A., and Letaief, K.B., "Successive Interference Cancellation for Multiuser Asynchronous DS/CDMA Detectors in Multipath Fading Links", *IEEE Transactions on Communications*, Vol. 46, No. 3, pgs. 384-391, Mar. 1998.

[41] Jafarkhani, H., "A Quasi-Orthogonal Space-Time Block Code", *IEEE Transactions on Communications*, Vol. 6, Jun. 2000.

[42] Krauss, T.P., and Zoltowski, M.D., "Chip-level MMSE Equalization at the Edge of the Cell", *Proceedings of the IEEE Wireless Communications and Networking Conference*, Chicago, IL, Sep. 22-28, 2000.

[43] Lee, D., *Adaptive Detection of DS/CDMA Signals Using Reduced-Rank Multistage Wiener Filter*, Ph.D. Thesis, Dept. of Electrical Engineering, University of Southern California, Los Angeles, CA, Mar. 2000.

[44] Lee, J.S., and Miller, L.E., "CDMA Systems Engineering Handbook", Boston: Artech House, 1998.

[45] Liberti, J.C., and Rappaport, T.S., "Smart Antennas for Wireless Communications: IS-95 and Third Generation CDMA Applications", Prentice Hall: Upper Saddle River, New Jersey, 1999.

[46] Liu, H., "Signal Processing Applications in CDMA Communications", Boston: Artech House, 2000.

[47] Lu, X., and Li, H., "Blind Multiuser Detection for Space Time Coded Systems", *Proceedings of ICASSP*, Salt Lake City, UT, May 2001.

[48] Madhow, U., "Blind Adaptive Interference Suppression for Direct-Sequence CDMA", *Proceedings of the IEEE, Special Issue on Blind Identification and Equalization*, pgs. 2049-2069, Oct. 1998.

[49] Madhow, U., and Honig, M.L., "MMSE Interference Suppression for Direct-Sequence Spread-Spectrum CDMA", *IEEE Transactions on Communications*, Vol. 42, No. 12, pgs. 3178-3188, Dec. 1994.

[50] Mathworks, Inc., "Signal Processing Toolbox For Use with MATLAB", Jan. 1998.

[51] Moon, T.K., Xie, Z., Rushforth, C.K., and Short, R.T., "Parameter Estimation in a Multi-User Communication System", *IEEE Transactions on Communications*, Vol. 42, No. 8, pgs. 2553-2559, Aug. 1994.

[52] Myrick, W.L., Zoltowski, M.D., and Goldstein, J.S., "Anti-Jam Space-Time Preprocessor for GPS Based On Multistage Nested Wiener Filter", *IEEE Transactions on Communications*, Vol. 5, pgs. 675-681, May 1999.

[53] Myrick, W.L., *Anti-Jam Space-Time Preprocessor for GPS Based On Multistage Nested Wiener Filter*, Ph.D. Thesis, School of Electrical Engineering, Purdue University, West Lafayette, IN, Dec. 2000.

[54] Myrick, W.L., Sud, S., Goldstein, J.S., and Zoltowski, M.D., "MMSE Correlator Based RAKE Receiver for DS-CDMA", *Proceedings of IEEE MILCOM*, McLean, VA, Oct. 28-31, 2001.

[55] Naguib, A.F., Seshadhri, N., and Calderbank, A.R., "Space-Time Coding and Signal Processing for High Data Rate Wireless Communications", *IEEE Signal Processing Magazine*, pgs. 77-92, May 2000.

[56] Naguib, A.F., and Seshadhri, N., "Combined Interference Cancellation and ML Decoding of Space-Time Block Codes", *IEEE Journal on Selected Areas in Communications*, 2000, submitted.

[57] Ojanperä, T., and Prasad, R., "An Overview of Air Interface Multiple Access for IMT-2000/UMTS", *IEEE Communications Magazine*, Vol. 36, pgs. 82-95, Sep. 1998.

[58] Oppenheim, A.V., Willsky, A.S., and Young, I.T., "Signals and Systems", Prentice Hall: Englewood Cliffs, New Jersey, 1983.

[59] Pados, D.A., and Batalama, S.N., "Joint Space-Time Auxiliary-Vector Filtering for DS/CDMA Systems with Antenna Arrays", *IEEE Transactions on Communications*, Vol. 47, pgs. 1406-1415, Sep. 1999.

[60] Papadias, C.B., and Foschini, G.J., "A Space-Time Coding Approach for Systems Employing Four Transmit Antennas", *Proceedings of ICASSP*, Salt Lake City, UT, May 2001.

[61] Papoulis, A., "Probability, Random Variables, and Stochastic Processes", New York: McGraw-Hill, 1991.

[62] Patel, P., and Holtzman, J., "Analysis of a Simple Successive Interference Cancellation Scheme in a DS/CDMA System", IEEE Journal on Selected Areas in Communications, Vol. 12, No. 5, pgs. 796-807, Jun. 1994.

[63] Pratt, T., and Bostian, C., "Satellite Communications", John Wiley and Sons, Sep. 1999.

[64] Price, R., and Green, J.P.E., "A Communication Technique for Multipath Channels", *Proceedings of IRE*, Vol. 46, pgs. 555-570, Mar. 1958.

[65] Proakis, J.G., "Digital Communications", New York: McGraw-Hill, 1995.

[66] Proakis, J.G., and Salehi, M., "Contemporary Communication Systems Using MATLAB", Brooks/Cole Publishing Co., Nov. 1999.

[67] Ramos, J., Zoltowski, M.D., and Liu, H., "Low-Complexity Space-Time Processor for DS-CDMA Communications", *IEEE Transactions on Signal Processing*, Vol. 48, No. 1, pgs. 39-52, Jan. 2000.

[68] Rappaport, T., "Wireless Communications: Principles and Practices", Prentice Hall, Sep. 1995.

[69] Reed, I.S., Mallett, J.D., and Brennan, L.E., "Rapid Convergence Rate in Adaptive Arrays", *IEEE Transactions on Aerospace and Electronic Systems*, Vol. 10, pgs. 853-863, Nov. 1974.

[70] Reed, I.S., Thanyasrisung, P., Goldstein, J.S., Truong, T.K., and Hu, C., "A Self-Synchronizing Adaptive Multistage Receiver for CDMA Systems", *Submitted to IEEE Transactions on Signal Processing*, SP EDICS 3-WIRL, 2001.

[71] Rice, G.W., Garcia-Alis, D., Stirling, I.G., Weiss, S., Stewart, R.W., "An Adaptive MMSE RAKE Receiver", *Proceedings of Asilomar*, 2000.

[72] Ricks, D.C., and Goldstein, J.S., "Efficient Architectures for Implementing Adaptive Algorithms", *Proceedings of the 2000 Antenna Applications Symposium*, pgs. 29-41, Allerton Park, Monticello, Illinois, Sep. 20-22, 2000.

[73] Sandhu, S., and Paulraj, A., "Union Bound on Error Probability of Linear Space-Time Block Codes", *Proceedings of ICASSP*, Salt Lake City, UT, May 2001.

[74] Scharf, L.L., and Demeure, C., "Statistical Signal Processing: Detection, Estimation, and Time Series Analysis", Addison Wesley Longman: Reading, Massachusetts, 1991.

[75] Sklar, B., "Digital Communications: Fundamentals and Applications", Prentice Hall, 2001.

[76] Song, Y., and Roy, S., "A Blind Reduced Rank CDMA Detector for Multipath Channels", *Proceedings of the* $8^{th}$ *CTMC*, ICC '99, pgs. 62-66, 1999.

[77] Strang, G., "Linear Algebra and Its Applications", Harcourt Brace Jovanovich, San Diego, CA, 1988.

[78] Stüber, G.L., "Principles of Mobile Communication", Boston: Kluwer Academic Publishers, 1996.

[79] Sud, S., and Goldstein, J.S., "A Low Complexity Receiver for Space-Time Coded Systems", *To appear in Proceedings of IEEE ICASSP*, Orlando, FL, May 13-17, 2002.

[80] Sud, S., Goldstein, J.S., and Pratt, T., "Efficient Interference Cancellation Algorithms for CDMA Utilizing Interference Suppression and Multipath Combining", newblock *To appear in Proceedings of the 6th World Multiconference on Systemics, Cybernetics and Informatics*, Orlando, FL, Jul. 14-18, 2002.

[81] Sud, S., Myrick, W., Cifuentes, P., Goldstein, J.S., and Zoltowski, M.D., "A Low Complexity MMSE Multiuser Detector for DS-CDMA", *Proceedings of the 35th Annual Asilomar Conference on Signals, Systems, and Computers*, Pacific Grove, CA, Nov. 4-7, 2001.

[82] Sud, S., Myrick, W., Goldstein, J.S., and Zoltowski, M.D., "Performance Analysis of a Reduced Rank MMSE MUD for DS-CDMA", *Proceedings of IEEE Globecom*, San Antonio, TX, Nov. 25-29, 2001.

[83] Sud, S., Myrick, W.L., Goldstein, J.S., and Zoltowski, M.D., "A Reduced Rank MMSE Receiver for a DS-CDMA System in Frequency Selective Multipath", *Proceedings of IEEE MILCOM*, McLean, VA, Oct. 28-31, 2001.

[84] Sud, S., and Paris, B.-P., "An Upper Bound on Bit Error Rate for a Single User of a Two-User System as a Function of the Interfering User's Signal Strength", *Proceedings of IEEE MILCOM*, Vol. 1, pgs. 362-367, Los Angeles, CA, Oct. 21-26, 2000.

[85] Tanabe, Y., Fujishima, K., Ogawa, Y., and Ohgane, T., "A Spatial-Domain RAKE Receiver Using a Super-Resolution Technique", *IEICE Transactions on Communications*, Vol. E83-B, No. 8, pgs. 1664-1670, Aug. 2000.

[86] Tarokh, V., Jafarkhani, H., and Calderbank, A.R., "Space-Time Block Codes from Orthogonal Designs", *IEEE Transactions on Information Theory*, Vol. 45, No. 5, pgs. 1456-1467, Jul. 1999.

[87] Tarokh, V., Jafarkhani, H., and Calderbank, A.R., "Space-Time Block Coding for Wireless Communications: Performance Results", *IEEE Journal on Selected Areas in Communications*, Vol. 17, No. 3, pgs. 451-460, Mar. 1999.

[88] Tarokh, V., Seshadri, N., and Calderbank, A.R., "Space-Time Codes for High Data Rate Wireless Communication: Performance Criterion and Code Construction", *IEEE Transactions on Information Theory*, pgs. 744-765, Mar. 1998.

[89] Tarokh, V., Seshadri, N., and Calderbank, A.R., "Space-Time Codes for High Data Rate Wireless Communications: Performance Criteria in the Presence of Channel Estimation Errors, Mobility, and Multiple Paths", *IEEE Transactions on Communications*, Vol. 47, pgs. 199-207, Feb. 1999.

[90] TIA 45.5 Subcommittee, "The CDMA 2000 Candidate Submission", June, 1998.

[91] Tufts, D.W., Kumaresan, R., and Kirsteins, I., "Data Adaptive Signal Estimation by Singular Value Decomposition of a Data Matrix", *Proceedings of the IEEE*, Vol. 70, No. 6, pgs. 684-685, Jun. 1982.

[92] Van Trees, H.L., "Detection, Estimation, and Modulation Theory", New York: Wiley and Sons, 1968.

[93] Varanasi, M.K., and Aazhang, B., "Multistage Detection in Asynchronous Code-Division Multiple-Access Communications", *IEEE Transactions on Communications*, Vol. 38, No. 4, pgs. 509-519, Apr. 1990.

[94] Varanasi, M.K., and Aazhang, B., "Near-Optimum Detection in Synchronous Code Division Multiple Access Systems", *IEEE Transactions on Communications*, Vol. 39, pgs. 825-836, May 1991.

[95] Verdú, S., "Multiuser Detection", Cambridge University Press, 1998.

[96] Viterbi, A.J., "CDMA: Principles of Spread Spectrum Communications", Addison-Wesley Publishing Co., Massachusetts, 1995.

[97] Wang, X., and Poor, V., "Blind Multiuser Detection: A Subspace Approach", *IEEE Transactions on Information Theory*, Vol. 44, pgs. 677-690, Mar. 1998.

[98] Wicker, S.B., "Error Control Systems for Digital Communication and Storage", Englewood Cliffs, New Jersey: Prentice Hall, 1995.

[99] Wilson, S.G., "Digital Modulation and Coding", Prentice Hall, 1996.

[100] Winters, J.H., Salz, J., and Gitlin, R.D., "The Impact of Antenna Diversity on the Capacity of Wireless Communication Systems", *IEEE Transactions on Communications*, Vol. 42, No. 2/3/4, pgs. 1740-1751, Feb./Mar./Apr. 1994.

[101] Wozencraft, J.M., and Jacobs, I.M., "Principles of Communication Engineering", Second Edition, Prospect Heights, Illinois: Waveland Press, Inc., 1990.

[102] Xie, Z., Rushforth, C.K., Short, R.T., and Moon, T.K., "Joint Signal Detection and Parameter Estimation in Multiuser Communications", em IEEE Transactions on Communications, Vol. 41, No. 7, pgs. 1208-1216, Aug. 1993.

[103] Zhang, Y., and Blum, R.S. "Multistage Multiuser Detection for CDMA with Space-Time Coding", *IEEE 10th Workshop on Statistical Signal and Array Processing*, Pocono Manor, PA, Aug. 14-16, 2000.

[104] Zheng, F.C., and Barton, S.K., "On the Performance of Near-Far Resistant CDMA Detectors in the Presence of Synchronization Errors", *IEEE Transactions on Communications*, Vol. 43, No. 12, pgs. 3037-3045, Dec. 1995.

[105] Zoltowski, M.D., Krauss, T.P., and Chowdhury, S., "Chip-level MMSE Equalization for High-Speed Synchronous CDMA in Frequency Selective Multipath", *Proceedings of SPIE*, Apr. 2000.

[106] Zronar, Z., and Brady, D., "Multiuser Detection in Single-Path Fading Channels", em IEEE Transactions on Communications, Vol. 42, No. 2/3/4, Feb./Mar./Apr. 1994.

# Vita

Seema Sud was born in Birmingham, England, on January 31, 1971. She has been a senior staff member of the Adaptive Signal Exploitation Branch of Science Applications International Corporation (SAIC) since May, 2000. Her work has focused on the research of adaptive signal processing algorithms for equalization of CDMA, AMPS, and GSM signals. Prior to working at SAIC, she worked at Stanford Telecommunications (now ITT Industries) as a senior engineer and staff member for nearly seven years in the area of design and analysis of satellite communications systems and optical cellular systems. She received the B.S. degree in electrical engineering from the University of Maryland at College Park in 1992 and the M.S. degree in electrical engineering from George Mason University in 1998, graduating from both with high honors. She is a member of the Phi Kappa Phi, Tau Beta Pi, Eta Kappa Nu, and Golden Key honor societies. She received a three year Bradley research fellowship in 1999 to pursue the Ph.D. degree at Virginia Tech. Her research interests include adaptive signal processing, coding, equalization, and multiuser detection/interference suppression for wireless RF communications.